Application of Hydro-acoustic techniques for the shallow water environmental studies off Goa

Thesis submitted to

Goa University

for the degree of

DOCTOR OF PHILOSOPHY

in

MARINE SCIENCES

By

Kranthikumar Chanda
Registration Number: 201409075

Research guide:

Dr. Bishwajit Chakraborty

Research Co-guide

Dr. Yatheesh Vadakkeyakath

School of Earth, Ocean, and Atmospheric Sciences,
Goa University
Taleigao, Goa

2019

Dedicated

To:

My parents & my family members

Statement

I state that this thesis entitled "**Applications of hydro-acoustics techniques for the shallow water environmental studies off Goa**" is my original contribution and it has not been submitted on any previous occasion. The literature related to the problem investigated has been cited. Due acknowledgements have been made wherever facilities and suggestions have been benefit.

.

Place: Goa University,
03 September 2019

Kranthikumar Chanda.
Reg.No 201409075

Certificate

This is to certify that the thesis entitled "**Applications of hydro-acoustic techniques for the shallow water environmental studies off Goa"** submitted by Kranthikumar Chanda to the Goa University for the degree of Doctor of Philosophy, is based on his original studies carried out under my supervision. The thesis or any part thereof has not been previously submitted for any other degree or diploma in any university or institution.

Dr. Bishwajit Chakraborty
Emeritus Scientist
Geological Oceanography Division
CSIR-National Institute of Oceanography
Dona Paula- 403004
Goa

Dr. Yatheesh Vadakkeyakath
Senior Scientist
Geological Oceanography Division
CSIR-National Institute of Oceanography
Dona Paula- 403004
Goa

Place: Goa University

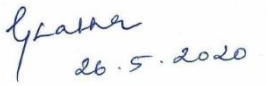

(Bishwajit Chakraborty) (BOE Chairman)

(Dr.G.Latha
Scientist-G
Group Head, Ocean Acoustics
National Institute of Ocean Technology
Pallikaranai
Chennai - 600100)

Acknowledgements

I would like to express my sincere gratitude to my advisor Dr Bishwajit Chakraborty, who has given me an opportunity to work with him for my PhD. His patience, motivation, and immense knowledge helped me to complete this work successfully.

I am also grateful to Dr Yatheesh Vadakkeyakath for providing valuable guidance as a Co-guide.

I would like to thank Prof. Harilal Menon, Member of the Faculty Research Committee and Dean, School of Earth, Ocean and Atmospheric Sciences, Goa University, for his constructive comments that helped me to improve the quality of my PhD thesis.

I am grateful to the present and former Directors of CSIR-NIO. Prof Sunil Kumar Singh, Director, for providing all the necessary infrastructure and facilities to carry out this study. I am also thankful to Dr. Shetye S. R and Dr. S. W. A. Naqvi for providing infrastructure and scientific facilities during initial period.

I am thankful to Dr V. V. Gopalakrishna who introduced me to the oceanography research at CSIR-NIO.

I am grateful to Dr. Andrew Menezes, for his valuable suggestions during thesis correction. I would like to thank Mr. William Fernandes for designing Hydrophone array and MCDL systems. I am thankful to Mr. Vasudev Mahale, for providing all the lab facilities. I am thankful to Dr Haris for his valuable suggestions and support in data analysis.

I am thankful to the Head, Ocean Acoustic Group at National Institute of Ocean Technology (NIOT) and their team (Dr M.C Sanjana, Mrs Malarkodi, Dr M.M Mhanty Mr Najeem Shajahan, Noufal K.K and Dr Ashokan) for helping me in validation and calibration of hydrophones and Tank facility.

I thank Desmond Gracias, Vijaykumar Kanojia, Narayan Satelkar and Yogesh Agarvadekar for their help during data collection on board Jesus King at Grande Island. I also thank Sundar Damodaran and Ashok Kankonkar for their help in providing current meters system during our research experimental period. I am also

thankful to Dr Pratima Kessarkar and Dr Lina Fernanades for providing facilities in sedimentology lab.

All the work consolidated in this thesis was carried out at CSIR-NIO, Goa and I sincerely express my gratitude for the support received from the various departments especially HRM, Library, Admin, Accounts, and ITG. I duly acknowledge with much gratefulness the Jawaharlal Nehru Memorial Fund (JNF, Delhi) for providing me the Jawaharlal Nehru Scholarship to carry out my PhD study at CSIR-NIO. Financial support for the research project was provided by the National Institute of Ocean Technology (NIOT), Ministry of Earth Sciences (MoES), Government of India.

I am grateful to Prof. D. Cato personal communication with Dr Bishwajit Chakraborty for his valuable help towards conformation of fish family. Special Thanks to, Dr Akamatsu Tomonari, Prof. Raquel Vaconcelos, Dr Sandor, Dr ShyamKumar Madhusudhana Mr Tomas for their valuable suggestions in improving the thesis research work.

I am also thankful to Prof. SSVS Ramakrishna, Dr R. R. Rao, and Dr Ramalingeswara Rao for their moral support.

I wish to offer my special thanks to Prof. C.U. Rivonkar and Prof Vishnu Murty Matta. I am also thankful to all Marine Science Department office especially Mr. Yashwant for helping in administration formalities in the Goa University.

Colleagues and friends have been generating good ambience around me always. I would like thank all my lab colleagues Mr Gautham S, Mr Vishnuvardan Yadati, Ms Afreen Hussian, Mr Shubham Shet , Mr Tejas Salkar, Mr Abhishek Shet, Dubay K, Miss Shivani M, Mr Girish, Mr Vishal Gupta, and Mr Ujjwal Anand. Dubay K. I would like to thank all my close friends Dr's Suryaprakash Lankalapalli, Aditya Peketi, Suneel Vasimalla, Sriram Gullapalli, DamodhraRao, Srinivas Rao Aravapalli, Ramakrishna Reddy T, Krishna Vudumala, Kartheek Chennuri and Rajkumar Mallela, AVS Chaitanya, Ratnakumar, KLMBR Ramakrishna, VenugopalReddy T, AVS Chandrashekar Rao, Mr Suresh Yenni, Mr Tulasiram .S, Mr Srinivasra Rao Darsipudi and Mr Trinadh for their support at various stages of my tenure in NIO.

Last, but not least my parents and family members, Mr NageswaraRao, Mrs Rajeswari, Mr Shyam Prasad Mrs Kanaka Durga, Ms Laya, Mr Gowatham Manikanta Swami, and sincerely appreciate their uplifting engagements.

Contents

List of Figures

List of Tables

Acronyms

ACI	Acoustic Complexity Index
AE	Acoustic Entropy
AN	Ambient Noise
AR	Acoustic richness
BW	Beam Width
CSIR	Council of Scientific Industrial Research
CSIR	CSIR-National Institute of Oceanography
DRDO	Defence Research and Development Organization
EEZ	Exclusive Economic Zone
GOD	Geological Oceanographic Group
GPS	Global Positioning System
HRM	Human Resource Management
ITG	Information Technology Group
MOES	Ministry of Earth Sciences
NIOT	National Institute of Ocean Technology
NPOL	Naval Physical and Oceanography Laboratory
NSTL	Naval Science and Technology Laboratory
NCPOR	National centre for Polar and Ocean Research
ONRG	Office of Naval Research Global
PCA	Principal Component Analysis
SONAR	Sound Navigation And Ranging
UWR	Underwater Range
WCMI	Western continental margin of India

Chapter 1

Introduction

1.1 Motivation

Hydroacoustics is the science of sound waves in the water that has become an important tool for underwater remote sensing (Balk, 2001; Shabangu *et al.*, 2014; Simpson, 2014). Hydroacoustics can be broadly classified as two disciplines: i) active and ii) passive acoustics. For an active acoustic system, acoustic pulses are transmitted into the water for producing backscatter echoes. By examining the received echoes, it is possible to estimate the range and in certain cases detecting the presence and bearing of an underwater target (Urick, 1983; Lurton, 2002). Active acoustic systems are widely used for many oceanographic applications (APL Handbook, 1994; Mann *et al*., 2008). However, the transmission of sound levels in the ocean for a prolonged duration may cause long-range effects on aquatic animal health (Popper and Hawkins, 2012). Active acoustic activities (for e.g. in marine protected areas) are now being subject to formal permission as emerged recently (Tyack *et al.*, 2015). Therefore, passive acoustic technique, a method for detecting and monitoring acoustic signals in an underwater environment is advancing as a vital tool for ocean soundscape studies.

The passive acoustic system transmits no signal, and it is designed to detect acoustic signals emanating from the original sources, including natural processes in the ocean, underwater noise sources of biological origin such as marine mammals

(Southhall *et. al.*, 2007), crustaceans or fish (Tavolga, 1971), and anthropogenic noise sources (Ainslie, 2012). By analyzing passive acoustic recordings, it is possible to discriminate and identify different animal species and to calculate the relative number of animals present within the measurement range. These key pieces of information can be complemented by ocean productivity or yearly migratory passage of animals such as great whales. A new application of passive acoustics involves awareness of environmental issues, which has spurred the development of passive acoustic techniques (Nystuen *et al.,* 2004). Progress in the field of passive acoustics has attracted researchers to investigate physical and biological processes such as oceanic features, seafloor habitats, and associated processes (Dahl *et al.,* 2007). There is a growing consensus that anthropogenic sound levels in oceans are increasing that can have adverse effects on marine life (Tyack, 2008).

Hitherto, most of the passive acoustic experiments such as propagation modeling and related geo-acoustic inversion studies have been carried out in deeper waters (Gervaise *et al*., 2007). However, the focus is needed for shallow water studies such as physical and biological characterization of a littoral environment (Pace and Jensen, 2002), especially in the reef and off reef regions (Bertucci *et al.,* 2016). Understanding the underwater environment is possible through ambient sound field measurement and "soundscape" studies (Pijanowski *et. al.,* 2011). The term "soundscape" has been used in many disciplines to describe the relationship between the waterscape (or landscape) and the relative composition of sound present.

Most of the fishes and invertebrates use sound for vital life functions. Based on a review of 115 primary studies encompassing various human-produced underwater noise sources, 66 species of fish and 36 species of invertebrates reveal noise impacts on development, including body malformations, higher egg or immature mortality, developmental delays, delays in metamorphosing and settling, and slower growth rates (Weilgart, 2018). Anatomical impacts from noise involve massive internal injuries, cellular damage, hearing loss, and even mortality (Hastings and Popper, 1996; Hawkins and Poppers, 2017). Ecological functions of invertebrates such as water filtration, mixing sediment layers, and bio-irrigation, which are key to nutrient cycling on the seabed, were adversely affected by noise. Once the population biology and ecology are impacted, it will have succeeding consequences on fisheries and even food security for humans.

Studies on population dynamics and related ecosystem function of non-migratory fishes and invertebrates are relatively easy to accomplish as compared to migratory marine mammal species. Many fish species rely on vocal signaling during their activities and produce sounds using sonic muscles that vibrate the swimbladder or bony elements (stridulation) (Fine and Parmentier, 2015; Parmentier *et al*., 2016). Fishes use sound to attract mates and defend their territory (Vasconcelos *et al*., 2010). In shallow water, the ambient sound field generally consists of various types of sound sources such as fish sounds (biophonies), wind and flow sounds (geophony), and boat sounds (anthrophony) (McWilliam and Hawkins, 2013).The spatial structure of the sound field is dependent on the nature of the waveguide comprising the multipath sound propagation between the sea surface and the seabed (Jensen *et al*., 2011). Therefore, the characteristics of any signal received at the recording location can be affected by the variability of environmental parameters (i.e. sound speed and absorption) in the medium. If these propagation features are characterized, it is possible to use the recorded soundscape and fish sound as an acoustic metric for studying ecosystem function (Rountree *et al*., 2006).

In this context, the research carried out here expounds passive acoustic (fish sound) data recorded using an autonomous wideband hydrophone system with an intention to understand shallow-water biodiversity of the study area (Au and Lammers, 2016). In general, the temporal and spectral characteristics of passive acoustic recordings such as "oscillogram", "spectrogram", and peak sound level of the "power spectral density" (PSD) are used for fish sound identification (Fish and Mowbray, 1970; Erbe *et al*., 2015). The power spectrum encompasses several dominant frequencies, which presumably represent major oscillation modes in the fish sound, but the amplitudes of these modes vary in a complex manner (Wilden *et al*., 1998; Chakraborty *et al*., 2014a). Non-linear studies involve characterization of the phase couplings across temporal scales in the data. The phase couplings generated by a nonlinear process can be fundamentally differentiated by estimating Lyapunov exponents (Politi *et al*., 2006) or fractal exponents (Loutridis, 2009). Considering the latter aspect, the present work involves MFDFA (multifractal detrended fluctuation analyses) (Kantelhardt *et al*., 2002; Ihlen, 2012) to characterize the phase couplings revealed in the fish sounds. The multifractal analysis is a robust technique to identify the scaling behavior (Haris *et al*., 2014) of the fish sounds.

Eco-acoustics studies using passive acoustic techniques are important for shallow water biodiversity assessment, characterization (Farina, 2014), and habitat monitoring, especially in reef areas (Harris *et al*., 2016). Major eco-acoustic studies have been carried out in terrestrial as well as underwater (Sueur *et al*., 2008), yet there is a lack of such studies in a shallow water environment. Accordingly, this research work attempts to improve understanding of the shallow water reef and off reef system (Bertucci *et al.,* 2016), and related biodiversity of the coastal environmental habitat.

In the mid-frequency band, shallow water ambient sound generally consists of surface-generated wind-driven signals with occasional contributions from shipping and biological activities (Wenz, 1962; Urick, 1984). The sound field is influenced by the sources and transmission medium which in turn is transformed by water column and interface properties (including bottom characteristics) (Buckingham and Jones, 1987; Harrison and Simons, 2002). Such sound field can vary spatially as well as temporarily, exhibiting site-specific characteristics (Kuperman and Lynch, 2004). In shallow water region, ambient noise in the mid-frequency band is dominated by wind-driven wave activity, and under suitable oceanographic conditions, shows a notch in the horizontal for the downward refracting environment (Rouseff and Tang, 2006; Clark, 2007; Sanjana and Latha, 2012). In this thesis, such ambient noise characteristics are investigated in Grande Island location, Goa, India.

1.2 Research objectives

The doctoral research reported here uses passive acoustics data acquired from the shallow water areas off Goa, west coast of India (WCI). The work aims to understand:

- To understand the effect of noise source generated through the physical and biological process in the shallow water area, off Goa. The study involves fish sound identification based on temporal and spectral methods and their characterization using nonlinear and eco-acoustic metrics.
- The influence of ambient noise in shallow water off Goa. The study includes the assessment of geo-acoustic parameters on account of passive acoustic data.
- Effect of fish sound data on ambient noise model to characterize the shallow water environment off Goa.

1.3 Thesis outline

The thesis is organized as follows:

Chapter 1: Introduction

The chapter on introduction provides an overview of background studies carried out and briefly describes the established methods using passive acoustics for fish sound identification, non-linear characterization of fish sound, and eco-acoustics studies. The chapter also includes a brief background of ambient noise studies in shallow water environment using an array of hydrophones for mapping vertical directionality pattern of sound signals.

Chapter 2: Study area, data acquisition, and methodology

Chapter 2 provides a description of the study area, passive acoustics data recordings using the Song Meter submersible system, and ancillary instruments used for current and wind measurements. Methods to carry out spectral and temporal analyses along with the computation of power spectral density (PSD), spectrogram and principal component analysis (PCA) is covered briefly. This chapter also covers the operational aspects of the Song Meter submersible mooring. The details of the hydrophone array system assembly to measure ambient noise for vertical directionality pattern are also covered.

Chapter 3: Soundscape and identification of fish sound

Chapter 3 describes fish sound identification in eight different locations off Goa: Britona, Grande Island and Betul, where sounds of *Terapon theraps*, Toadfish (Batrachodidae), Sciaenidae and Barred Grunt (*c. nobilis*) were recorded. The soundscape characterization involves analysis of the “waveform”, “spectrogram”, and the PSD of the recorded passive acoustic data. Similarly, the chorus of *Terapon theraps*, sparse calls of Carangidaealong with other unnamed fish species community from the Malvan, Maharashtra area is also reported.

Chapter 4: Fish sound characterization using Multifractal Detrended Fluctuation Analysis (MFDFA)

The work involving multifractal detrended fluctuation analysis (MFDFA) to describe the recorded fish sound data from the open water of two major estuarine systems are explained in chapter 4. Applying MFDFA, the second-order Hurst exponent ($h_q = 2$) values are found to characterize Toadfish and Sciaenidae fish families. The higher $\Delta h(q)$ (width of the generalized Hurst exponent) values for Toadfish and Sciaenidae vocalizations indicate higher multifractality, implying greater heterogeneity. The results illustrated in this chapter suggest that the Sciaenidae fish calls are comparatively smoother in comparison to that of the Toadfish.

Chapter 5: Influence of environmental parameters on fish sounds

In Chapter 5, the soundscape of the shallow water locations from three major estuarine systems of Goa are quantitatively characterized.To understand the relative contributions of biophonies (fish), geophonies (the wind and flow, etc.), and anthrophony (boats, etc.), cluster analyses (principal component analyses) were applied to the parameters [SPL_{rms} (root-mean-square sound pressure level), wind, water temperature, and water flow]. The analyses help in characterizing biotic and abiotic sound signals in the ecologically important regions off Goa.

Chapter 6: Estimation of the eco-acoustic metrics from Grande Island and Malvan reef systems.

Underwater soundscape monitoring is an effective method to understand the biodiversity of an ecosystem. The biodiversity assessment is a key step for habitat monitoring in shallow reef areas (Harris *et al*., 2016). In the soundscape ecology, the automatic processing technique and resulting metrics (Sueur *et al*., 2008a) provide promising results, particularly towards the understanding of complex acoustic signatures. In this context, quantitative characterization of shallow water soundscape of the *Burnt Island* located off the Malvan and Grande Island (a coral reef system off Goa), in the west coast of India (WCI) is carried out. Besides identifying the sound sources, three acoustic metrics namely acoustic entropy (H), acoustic richness (AR), and acoustic complexity index (ACI) of passive acoustic recordings are computed and analyzed to understand their role in relation to the fish chorus, wave-breaking, and

sparsely available fish sound through a box plot based study from Malvan location. Soundscape data for present investigation acquired simultaneously from two locations from the Grande Island coral reef as well as away from reef area.Comparative study of the eco-acoustic metrics data between the two locations emphasizes relevant characterization of ecologically important locations.

Chapter 7: Influence of environmental parameters on eco-acoustic metrics

Chapter 7 provides a description of the work carried out to quantitatively characterize soundscapes of the ecologically important area off Goa, Grande Island, which is situated away from a coral reef area at 20m water depth. The soundscape characterization involves evaluation of PSDs for fish sound identification. Three acoustic metrics namely acoustic entropy (H), acoustic richness (AR), and acoustic complexity index (ACI) and SPL_{rms} (root-mean-square sound pressure level) of passive acoustic recordings are computed and analyzed to understand the reef environment. Acquisition of the concurrent ancillary data such as wind speed, water temperature, and water flow from the site is made. Involving these variables along with the computed acoustic metrics, correlation analyses and related PCA clustering is carried out to infer the role of the environmental parameters on the acoustic metrics.

Chapter 8: Ambient noise study using time series measurements off Grande Island

Chapter 8 describes time-series measurements of ambient noise using short hydrophone array at 0.5–4kHz frequency band in the shallow waters off Goa, Grande Island. The vertical directionality pattern generally varies with time and influenced by the contributing noise sources and environmental conditions. Noise in the mid-frequency band has characteristics of wind-driven wave activity. Notch characteristics are useful in the operation of receiving sonar systems and accordingly notch width and depth has been investigated in 0.5-4 kHz band. The environment is characterized by the sound speed profile in the water column and sediment grab data. The directionality pattern is observed with respect to sound propagation, and the critical angle of the seabed has been computed both theoretically and on-site measurements. In this context, an attempt been made to estimate geo-acoustic parameters.

Chapter 9: Summary

The concluding chapter summarizes the salient findings of the thesis. Graphical abstract of chapters presented in this thesis is illustrated in Fig. 1.1.

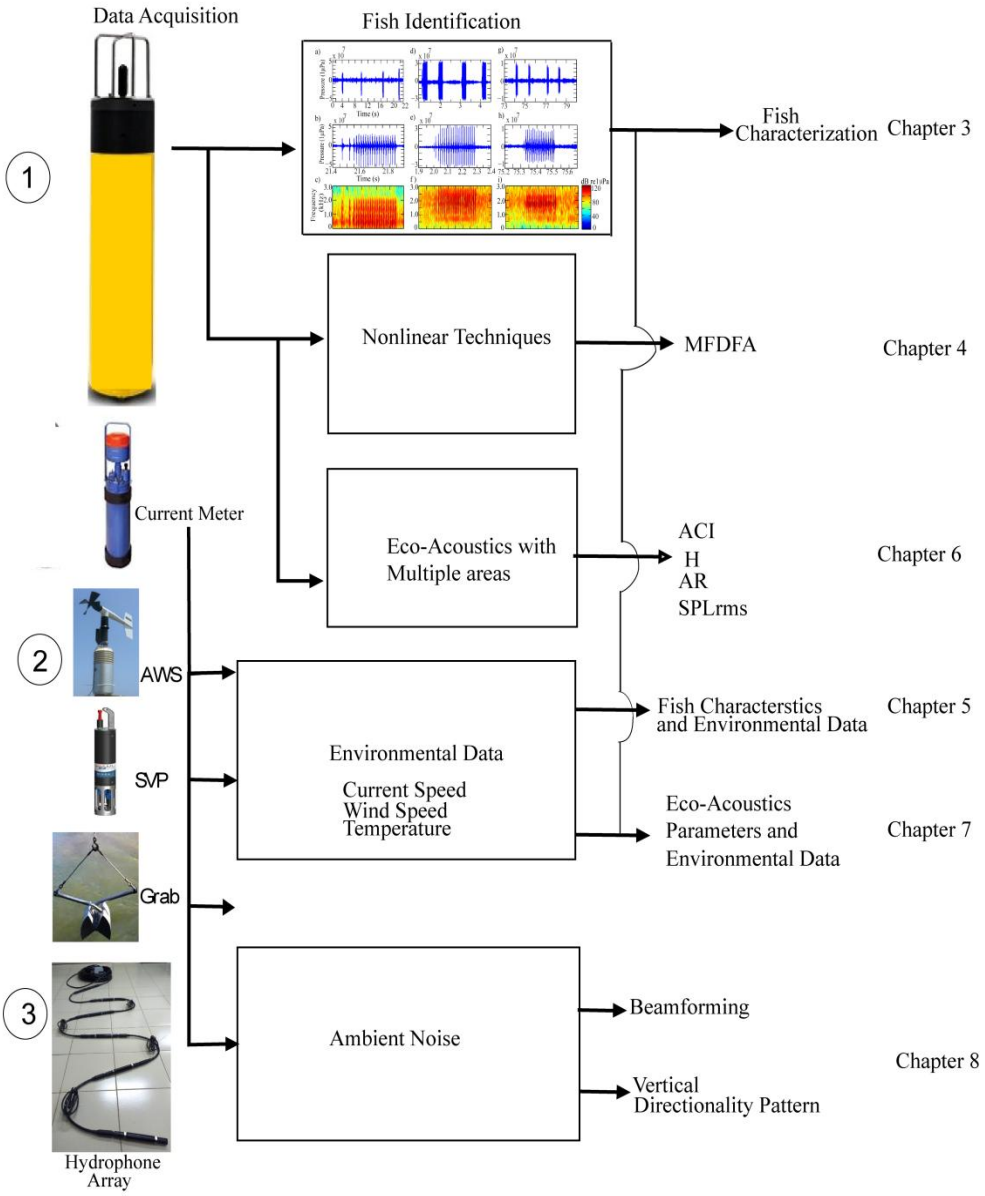

Fig. 1.1: Graphical abstract of chapters in the thesis.

Chapter 2

Study area, data acquisition and methodology

2.1 Introduction

Passive acoustic data for the present research were acquired from the shallow water locations off Goa and off Malvan in Maharastra district from the West Coast of India (WCI) (Table 2.1). Three major estuarine systems, off Goa, were selected for data acquisition for the present study. The mangrove and coral dominated areas are situated in Mandovi, Zuari and Sal estuaries. Among them extensive data acquisition was carried out for a couple of years around the Grande Island near the Zuari estuary. The present study also involves a reef system off Malvan, Maharashtra. Fishing boats were employed in the offshore data collection, and the experiments involved the deployment of passive acoustic systems such as SM2M+ and SM3M (M/s Wildlife Acoustics System) and other ancillary data acquisition systems. The ancillary systems used in this research are automatic weather system (AWS), current meter, sound velocity profiler and Van Veen grab. Besides using SM2M+ and SM3M systems, use of hydrophone array is employed to carry out an investigation on ambient noise vertical directionality. Therefore, the group of hydrophones [C55 series (M/s Cetacean Research)] system with built-in preamplifier was assembled to form a

hydrophone array system. The sampling and logging of the data from multiple hydrophone elements were accomplished by employing a "multi-channel data logger", which has been designed indigenously at CSIR-National Institute of Oceanography. A computer program was developed that could be run on a PC or laptop for the conversion of the acquired analog data to digital data as a component of hydrophone array system design. This was necessary to characterize the ambient noise environment in Grande Island area. Besides employing various techniques for passive acoustic data, temporal and spectral methods were used for identification of the fish sound. Fig. 1.1 of chapter 1 and Table 2.1 provide systematic chapter wise components of the study. Spectral techniques such as spectrogram utilizing short-time Fourier transform (STFT) as well as the power spectrum density (PSD) function was extensively used for fish sound identification, as elucidated in chapter 3. Besides, comparative studies between the estimated acoustic parameters and the environmental data have been comprehensively examined in this research. Taking into consideration that acoustic studies are characteristic of a large number of variables, principal component analyses (PCA) is employed for data reduction, reducing a large number of variables into a smaller number to make ecological assessment more practicable and assess the inter-relationship between the acoustic and environmental parameters. This chapter broadly covers study areas (Table 2.1 and Fig. 2.1). A complete elucidation of passive acoustic systems (SM2M+ and SM3M) made use of for fish sound data recording along with the ancillary systems has been provided. A concise description of the hydrophone array assembly utilized for ambient noise modeling is given as well. The methodology related to the employed spectral technique as well as PCA has also been explained here

2.2 Study area

The passive acoustic data were acquired from two selected study regions from WCI (Fig. 2.1). Detailed locations, date and time of data collection, equipment used and water depths etc are given in Table 2.1. Passive acoustic data along with the ancillary data were acquired from nine different spot locations at different times and

duration having different habitats are mentioned in Table 2.1 Description of locations in different areas and data details are given as follows:

Location 1 (15^0 30.587$^{'}$N 73^0 50.730$^{'}$ E) offBritona in Mandovi estuary is situated ~500 m away from the river bank close to the mangrove-dominated Chorao Island (Fig. 2.1) at a water depth of 7m (Uday Kumar *et al.*, 2013). Data were acquired utilizing SM2M+ system between 14:30 hr of 13 March 2014 to 13:30 hr of 14 March 2014 (Table 2.1). The water flow is dominant in this location due to the semidiurnal flood and ebb tides. The area has inland water navigation traffic with passenger vessels, fishing vessels and barges carrying iron ore. The data were acquired for a short duration from this mangrove dominated area. The results are presented in chapters 3 and 5.

The location 2 (15^0 20.682$^{'}$N 73^0 47.165$^{'}$ E) is situated towards the southern end of the Grande Island off Zuari estuary at a water depth of 20m (Fig. 2.1). The ship/boat movement is limited in the vicinity of the Grande Island as it is a protected area. Moderately higher live coral cover (8.05 ± 3.98 %) in the mid-shelf zone i.e., within the 5-8 m water depth has been reported from this location (Manikandan *et al.*, 2016). Location-wise data collection timings are also given (Table 2.1). This short time passive acoustic data is utilized to record fish sound as well so to compare with the fish sound and environmental data. The analyses are covered in chapters 3 and 5.

Location 3 (15^0 08.955$^{'}$N 73^0 55.483$^{'}$ E) is situated at a distance of 2.2 km off Betul from the Sal river mouth, which is also known for mangrove ecosystem as well as abundant finfish and shellfish resources (Fernandes and Achuthankutty,2010). This meandering Sal estuary runs parallel to the west coast geological fault, which follows a north-south direction before meeting the Arabian Sea at Betul. River Sal has been under stress due to siltation and pollution in the channel near Betul, where eco-restoration efforts have been undertaken recently (Ingole, 2016). The data was acquired from 14:30 hr of 20 March 2014 to 13:30 hr of 21 March 2014 (Table 2.1).The water depth at the study location is 11m. The short duration data analyses are covered in chapters 3 and 5.

Malvan is considered as one of the bio-rich coastal zones of the neighboring coastal state of Maharashtra (Anon, 2001). The present location 5 (15º 55.330’ N and

73º 26.500’ E) is situated off the western side of the Burnt Island (lighthouse) and 2.5 km away from the Malvan coast (Fig. 2.1 and Table 2.1). It is considered as an open ecosystem and has many submerged, exposed rocks that provide a perfect place for bio-organisms to thrive. Many crevices and cracks in the rocks serve as an ideal site for sheltering, feeding and breeding grounds for many invertebrates and also as an ideal substratum for harboring marine algae. It holds demersal fishery that provides for a credible proportion of demersal fish production. The water depth at the data acquisition location is 22m. The analyses of the acquired passive acoustic data are covered in chapters 3 and 6. Present analyses also cover abiotic sound recorded from this location.

From Grande Island, acquisitions of fish sound data were also made for multiple occasions at different spot locations. The data recorded (8-12 May 2015) from the deeper part at 30m water depth (Location 4: 15°18.544’ N 73°41.667’ E) are used for fish sound analyses (Fig. 2.1; Table 2.1). Similarly, long term data (14-23 May 2017) is being also acquired simultaneously from deeper part (~20m water depth) away from the coral reef area (Location 6: 15^0 20.686’ N 73^0 47.130’ E) as well as shallower part (~8m) in the coral reef area (Location 7: 15^0 47.954’ N 73^0 47.044’ E) for eco-acoustics study from Grande Island area (Manikandan *et al.*, 2016). Here, comparative studies based on the eco-acoustics parameters are covered in chapter 6. The study of the estimated eco-acoustic together with environmental parameters are covered utilizing location 8 (15°20.160’ N 73°45.277’ E) data (10-14 March 2016) at a 20m water depth and same is being covered in chapter 7. Fish identification studies utilizing fish sound analyses are presented in chapter 3 carried out at the above locations (4, 6, and 8) of Grande Island.

At location 9 (15^0 20.658’ N, 73^0 47.350’ E) of Grande Island (Fig. 2.1; Table 2.1), hydrophone array data were collected from 22-24 May 2018 at 20 m water depth. The location is away from the coral reef area near Grande Island. Ambient noise-related model studies were carried out using vertical directionality pattern (Harrison and Simons, 2002) and related geo-acoustics parameters, (Sanjana *et al.*, 2013), and the results are covered in chapter 8.

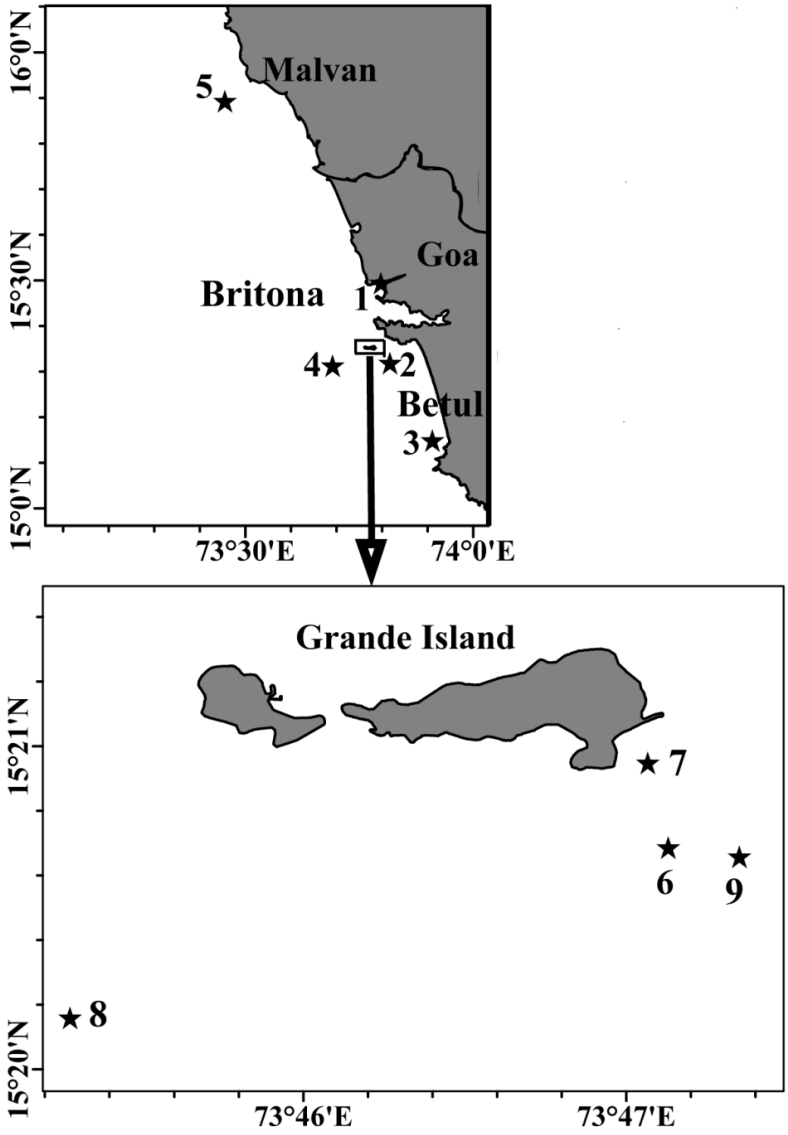

Fig. 2.**1: S**tudy locations where passive acoustic, environmental and sediment data acquired in the area off Goa and Malvan in the West Coast of India (detailed information is given in Table: 2.1). Locations 2 and 4 are off Goa Grande Island. Locations 6, 7, 8, 9 are also from Grande Island shown inside the box.

Table 2.1 Passive acoustic and environmental data acquisition details

Loc. No.	Locations	Position	Water Depth (m)	Equipment and Sampling frequency (Hz)	Experiment Date	Environmental data	Remarks data
1	Off Britona, Mandovi estuary	15º30.587' N 73º 50.730' E	7	SM2M+/44100	13-14 March 2014	Current Speed, Temperature and Sound speed	Covered in chapters 3 and 5
2	Grande Island off Zuari estuary	15º20.682' N 73º 47.165'E	20	SM2M+/44100	03-04 April 2014	Wind speed, Current Speed, and Temperature	
3	Betul off Sal estuary	15º08.955'N 73º 55.483'E	11	SM2M+/44100	21-22 March 2014	Wind speed, Current Speed, Temperature and Sound speed	
4	Grande Island off Zuari estuary	$15^0$18.544' N 73^0 41.667' E	30	SM2M+/44100	8-12 May 2015	Wind speed, Current Speed, Temperature and Sound speed	Chapter 3
5	Malvan off Maharastra coast	15º 55.33' N 73º 26.50' E	22	SM2M+/44100	18-20 May 2016	No environmental data	Chapters 3 and 6
6	Grande Island off Zuari	15º20.686'N 73º 47.130'E	20	SM3M/24000	14-23 March 2017	No environmental data	Chapters 3 and 6
7	Grande Island reef Zuari	15º20.954'N 73º 47.044'E	8	SM3M/24000	14-23 March 2017	No environmental data	Chapters 3 and 6
8	Grande Island off Zuari	15º 20.160'N 73º 45.277'E	20	SM3M/96000	10-14 March 2016	Current Speed and Temperature	Chapters 3 and 7
9	Grande Island off Zuari	15º20.658'N 73º 47.350'E	20	Hydro-phone array/48000, SM3M/48000	22-24 May 2018	Wind speed, Sound speed	Chapter 8

2.3 Data Acquisition

In this study, investigations making use of passive acoustic data is carried out. For this purpose, the Song Meter acoustic system for a marine application is extensively used for fish sound data acquisition. Apart from that, the hydrophone array has been specially designed to carry out the recording and processing for ambient noise data and modeling. Chapters 3, 4, 5, 6, and 7 illustrate how the passive acoustic data were acquired employing Song Meter (SM2M+ and SM3M). Using a hydrophone array, the ambient noise modeling studies that have been carried is covered in chapter 8. Acquisition of ancillary data such as wind, current, water temperature, sound velocity profiler data as well as surface sediment data is also a component of this work. The sediment sample data acquisition was utilized for grain size analyses as a part of ground-truthing. Here, the technical aspect of the Song Meter system is discussed

2.3.1 Song Meter

The Song Meter acoustic system (https://www.wildlifeacoustics.com)is a cost-effective, weatherproof marine recorder that can be used for underwater acoustic monitoring of fish. It has been effectively used during long-term bioacoustics monitoring of dolphins, whales and other marine life including fish as well as and anthropogenic noise in an underwater environment. Two models of the Song Meter systems i) SM2M+ and SM3M are used for present data acquisition activities. These recorders (SM2M+ and SM3M), are submersibles having a 16-bit analog to digital converter designed for short or long term deployment in fresh or saltwater. The unit is designed to allow quick refurbishment of the device along shipside for immediate redeployment. The batteries and SD flashcards can be easily swapped and the housing resealed for redeployment. The device can be anchored and recovered *via* tether, diver or by optional acoustic release. These systems are self buoyant submersible that uses a thick-walled PVC housing rated for deployment up to a depth of 150 m. The core electronic motherboard accommodates 32 D cell batteries which are installed on both sides of the board. Dimension wise, both the systems (SM2M+ and SM3M) are identically cylindrical shaped with a height 79.4 cm and 16.5 cm diameter, They can be fitted with a hydrophone with a length of 2.5 cm and 1.9 cm diameter. The systems

weigh around 9.5 kg in the air without batteries, and the buoyancy in saltwater is 5.5 kg (Fig. 2.2a, b).

The SM2M+ system consists of a single hydrophone having a frequencybandwidth of 2 Hz - 48 kHz. For SM3M system, two hydrophones one with standard acoustic and other with an ultrasonic frequency having a bandwidth of 2 Hz - 48 kHz and 2 Hz 192 kHz, respectively are housed. The systems record in audio (WAV) format files for predefined sampling interval. The sensitivity of each hydrophone is calibrated to 0.1 dB resolution. This calibrated value is taken as the average value over the band from 200 Hz to 1.6 kHz in 100 Hz interval, which needs to be applied during data processing (Fig. 2.3). From the frequency response the user can extrapolate sensitivity across the rest of the frequency range with some degree of accuracy, as they are quite consistent in response.

The SM2M+ and SM3M submersibles are powered through 32 D cells alkaline batteries. The recorder can accept 1.5V alkaline batteries, 1.2V NiMH batteries or 3V-3.3V lithium batteries. A board contains protection diodes that must be configured for the appropriate cell voltage (Fig. 2.2a). The SM2M+ is normally configured for 1.5 or 1.2 V cells. In this configuration the batteries are wired in parallel groups of 4 in series (Fig. 2.2b). Two AA batteries run the SM2M+ and SM3M clock. The SM3M has the battery life and memory capacity to record for hundreds of hours. The Song Meter systems were calibrated at ESSO-National Institute of Ocean Technology (NIOT) calibration facility (http://www.niot.res.in/ATF/). Operational deployment of SM2M+ and SM3M including schematic diagram of the mooring system is displayed (Fig. 2.4) along with the deployment photographs of the Song Meter (SM2M+ and SM3M).

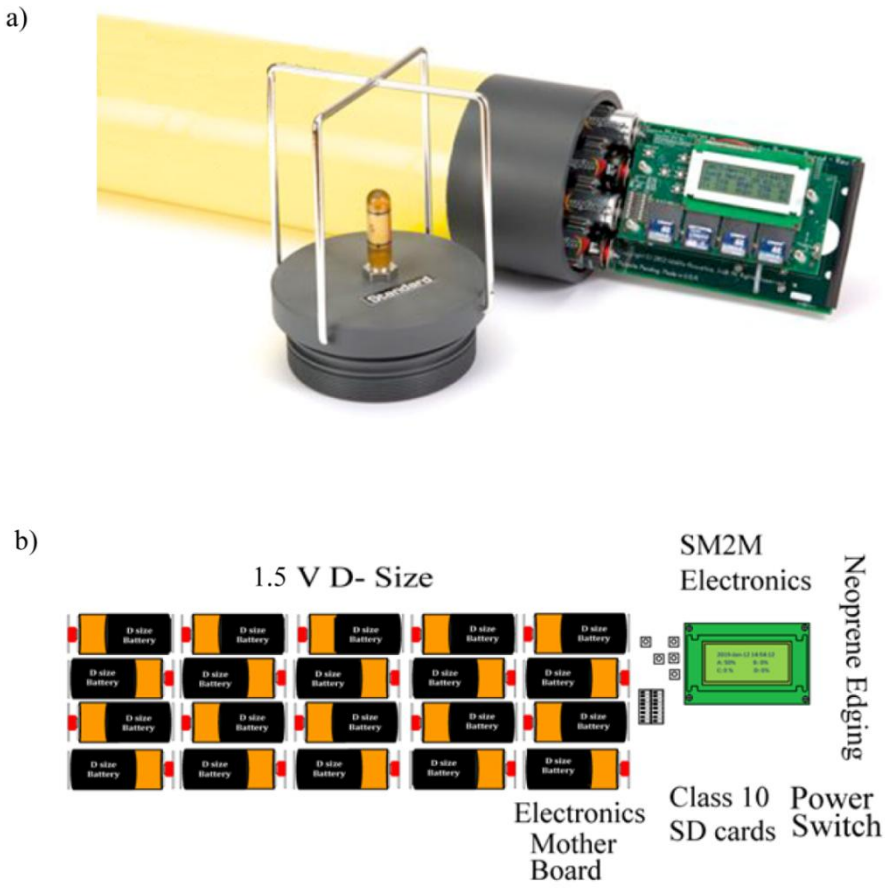

Fig. 2.2 (a) From left: Standard hydrophone on top cap of the SM2M+, and towards right: Board having electronic and storage unit of the digital recorder, (b) Photo of the motherboard that accepts 32 D cell batteries as shown (more batteries are installed on the back of the board modified from SM2M User Manual 2013061313.doc, www.wildlifeacoustics.com).

Both the systems have four SDHC/SDXC cards slots that may be utilized for recording data on to the SD cards. The SM2M+ and SM3M data recording capacity for SDHC cards is up to 32 GB and SDXC cards are up to 128 GB. Before every experiment these cards should be formatted to a FAT32 file system

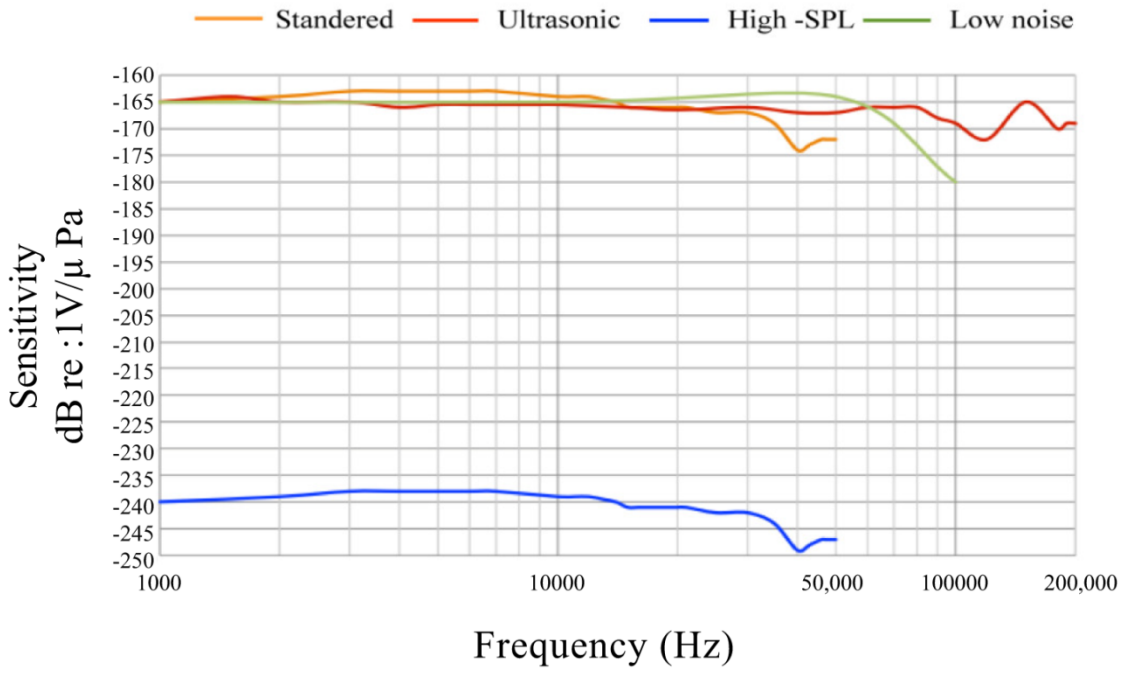

Fig. 2.3 Sensitivity response of the standard hydrophone used in the present study; Ultrasonic hydrophone increased recording bandwidth of the system; the low-noise hydrophone is for recording ultra-quiet environment; High SPL specifically to record and quantify high-pressure level (modified from SM2M User Manual 2013061313.doc_www.wildlifeacoustics.com).

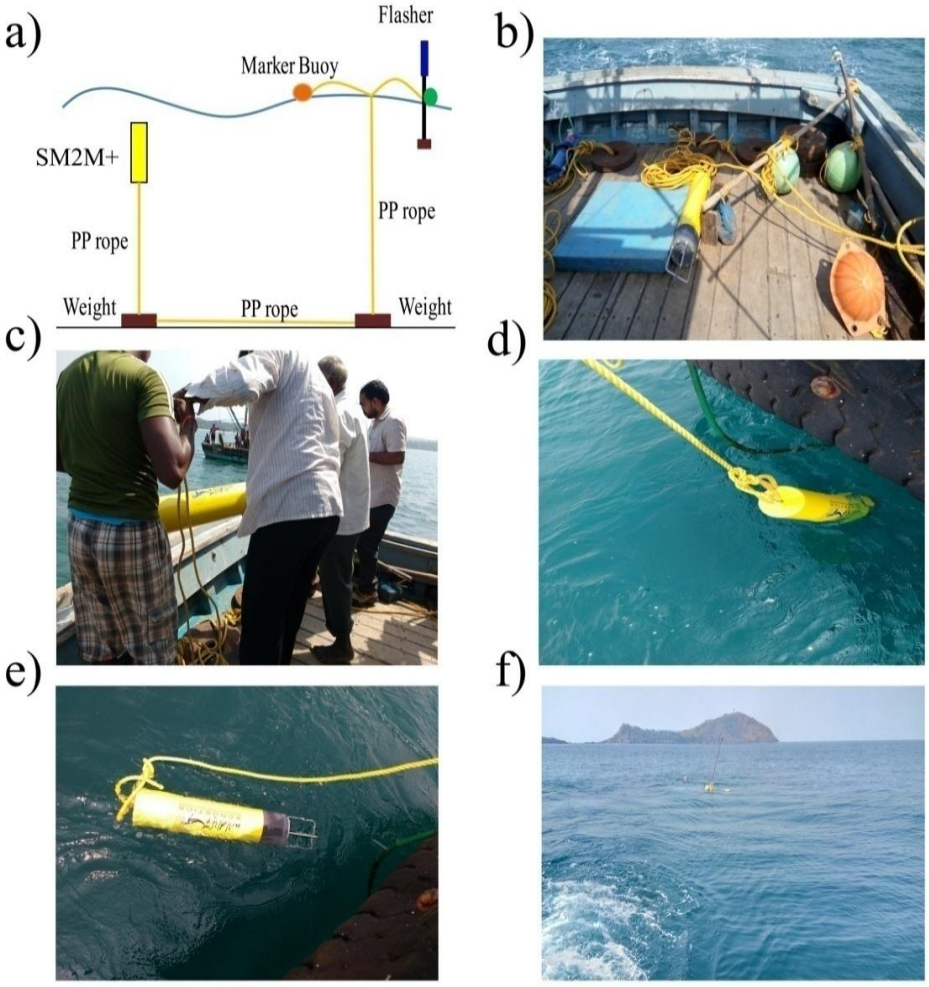

Fig. 2.4 Operational deployment of SM2M+ and SM3M: (a) schematic diagram of the mooring system is given along with the deployment photographs of the Song Meter (SM2M+ and SM3M) [Fig. 2 (b-f)]. The Song Meter system is programmed at the shore to finalize the data acquisition timings. The equipment is synchronized with the current meter where acoustic Doppler technique is used. This is necessary to avoid recording acoustic signal emanating from ADCP based current meter. U shaped moorings having positively buoyant Song Meter submersible (SM2M+) tied to a 40kg dead weight, which is lying on the seafloor, is employed here. The same deadweight is tied to another deadweight which is lying on the seafloor by a twenty-meter long rope. 2-3 glass floats where each float weighs around 20 kg to another mooring where beacon lights are attached to the floats to maintain the lights above the surface are used. For the Song Meter system, beacon light is important from the safety and navigational aspects.

2.4 Hydrophone array

The CETACEAN RESEARCH ™ (www.cetaceanresearch.com), C55 hydrophone is used as a single element in the hydrophone array system. This has preamplifier (20dB) possessing sensitivity of -165 (dB re1µPa) and having a useful frequency range of (8Hz to 100 kHz), and the 460 m depth range (Fig. 2.5a). Each element of hydrophones arrays are wired together and connected to a data logger to record wide-band sound signals. A self-contained battery operated autonomous multichannel data logger built around cortex-M3 arm microcontroller STM32F407 was used for simultaneous acquisition of acoustic (analog) signals from multiple hydrophones in a vertical array. The recorded signals are sampled, digitized and stored on solid-state media. A preamplifier gain of 20 dB was used to enhance the electrical signal and reduce the possibility of noise contamination from additional environmental factors for each element of the six elements hydrophone array having an inter-element spacing of 0.15m with a design frequency equivalent to 5 kHz. The array having an aperture length of 0.75m was moored from the water surface (Fig. 2.5b). The passivebeamformed data (azimuth angle versus operating frequency) is being computed offline at frequencies between 0.5-5.0 kHz employing delay and sum method. The beam width is found to be ~17º at 5kHz design frequency. The array pattern degradations are not unknown especially when limited array lengths are used. Therefore, spatial taper (Chakraborty, 1988) or adaptive beamforming techniques are generally preferred. However, in order to enhance the resolution using limited array length, the concept of the super-gain array has been employed in this study incorporating delay and sum beamforming methods (Siderius, 2012). In the present study, for improved beamforming, a spatially interpolated virtual element is introduced within the existing 6-element array to enhance the numbers element (i.e., total eleven elements) by reducing the inter-element spacing to 0.075m. The hydrophone array data areused to carry out ambient noise studies through vertical directionality pattern using a beamforming technique. Vertical linear hydrophone array was deployed for time series measurements in shallow water for ambient noise modeling. Time series noise data was acquired successfully. Data weresampled at 48 kHz, for the duration of the 60s at every 30 minutes interval. The hydrophone array

was deployed near the Grande Island at 20 m water depth (Location 9) during 22-24 May 2018 to record the ambient noise (Table 2.1), and the results have been described in chapter 8.

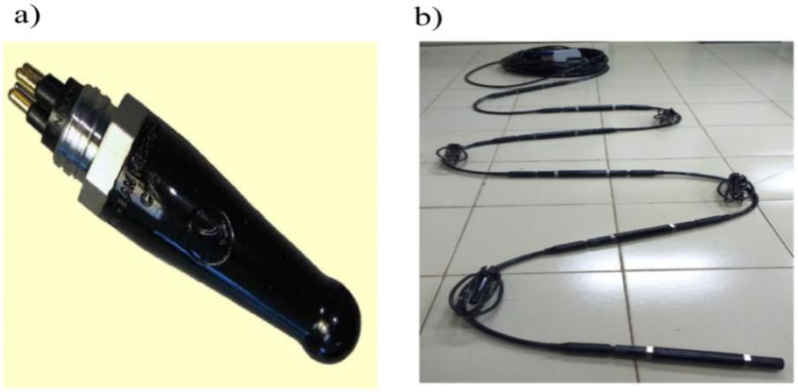

Fig. 2.5 a) C55 Single hydrophone, b) Hydrophone array

2.4.1 Multi-Channel Data Logger

Recording of passive acoustic data involves a listening device along with the instrumentation system. The passive listening device transforms mechanical disturbance to electrical signals. The subsequent sampling and logging of the transformed data are accomplished by employing the instrumentation system. One such system is the "multi-channel data logger", which has been designed indigenously at CSIR-National Institute of Oceanography with the capability to record 8-channels of passive acoustic data simultaneously (Fernandes *et al.,* 2018).

Beside hydrophone array, use of data logger system for recording the ambient noise data is employed. At the time ofacquisition every sample ensemble of 6-channels (out of 8 channels), 16 bytes are transferred from ADC to a microcontroller. Inthis mode a sampling rate of 48 kHz was obtained. The MCDL block diagram demonstrates thetotal system functioning protocol (Fig. 2.6). The system is powered through 8D cells each of 1.5V alkaline batterieshaving a total capacity of 7.2AH, to provide approximately 40 hours of continuous sampling of 6 channelsat a maximum sampling rate of 48 kHz. In active mode, it consumes a maximum of 150 mA, while the sleepmode consumption is less than 0.5 mA approximately.The C program

compiled either on Linux using GNU gcc compileror Windows is utilized to convert the recorded binary formatted data to ASCII file format. Themicrocontroller is interfaced with 8- channel Successive Approximation Register (SAR) - Analog to DigitalConverter (ADC) using a byte transfer mode that transfers data from ADC to the microcontroller.

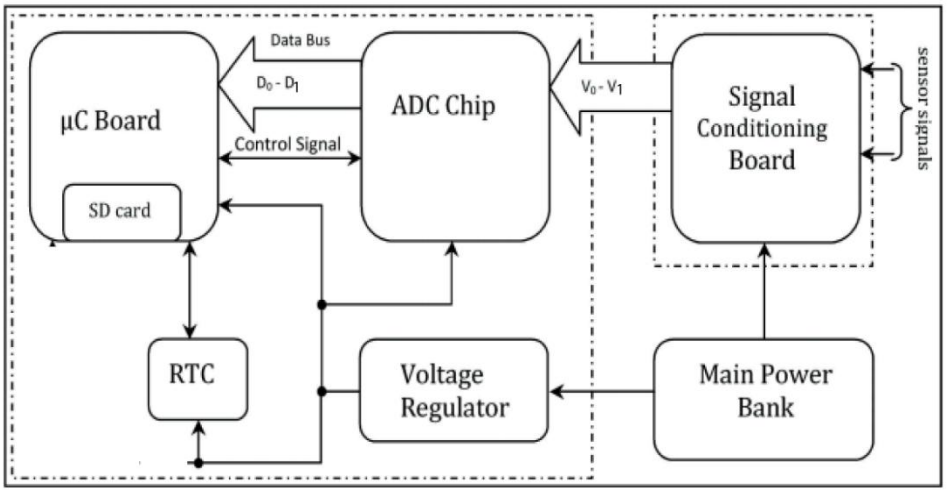

Fig. 2.6 Data acquisition functional block diagram

2.4.2 Beamforming technique

Beamforming technique has been employed to determine the directionality of the recorded signal acquired using passive hydrophone elements array (Sanjana and Latha, 2012)**.** The beamformed output of the six elements array as well as element super gain array data are explained in the ambient noise model study in chapter 8.

2.5 Ancillary Instruments

Besides passive acoustics systems such as SM2M+ and SM3M and Hydrophone array, ancillary data were simultaneously acquired to carry out the analyses in order to interrelate the acoustic parameters with respect to environmental data (Table 2.1). The equipment details are discussed below:

2.5.1 Current meter

SEAGUARD® RCM series is a new generation of current meters based on the SEAGUARD® data logger platform and the ZPulse™ multi-frequency Doppler current sensor. A mooring system is used to acquire the current meter (Fig. 2.7) data. The current sensor comprises acoustic pulses of several frequency components to lower the statistical variance in the Doppler shift estimate (Sundar *et al*., 2015). The advantage of this is to reduce statistical error with few pings, providing increased sampling speed and lower power consumption. The presently used current meter is an intermediate 2000 m depth rating having weights 14.8 kg in air and 8.5 kg in water. The battery required is Alkaline 9 volt, 15 Ah or Lithium 7 volt, 30 Ah. The resolution of RCM (ranged between 0-300 cm/s) is 0.1mm/s with mean accuracy ± 0.15 cm/s. Statistical variance (std.) of 0.3 cm/s, resolution of current direction is 0.01° with mean accuracy ±5° for 0-15° and ±7.5° for 15-35° respectively. The resolutions of the optional systems such as temperature (ranged between -4 to +36°C) and conductivity sensors (ranged between: 0 - 7.5 S/m) are 0.001°C and 0.0002 S/m.

Fig. 2.7 Current meter

2.5.2 Autonomous Weather Station (AWS)

Wind speed and related measurements were carried out using autonomous weather station (AWS) (Vijaykumar, 2017). The AWS (Fig. 2.8) is installed onboard fishing vessel with its sensors, and the vessel anchored near the locations during the data

acquisition time. The AWS is designed and developed at the Marine Instrumentation Division of the CSIR-National Institute of Oceanography, Goa. It provides data in digital format. The data collected by the AWS are true wind speed and direction, atmospheric pressure, air temperature, relative humidity, rainfall, GPS speed, GPS course, and the ship heading along with latitude and longitude of the ship position. Each data string is recorded with date and time. To account for the ship motion, the AWS is provided with GPS and compass, which are used to compute true wind speed and direction. All the sensors are sampled at 10s interval. The sampled values are averaged over 1-minutes, and the averaged values are stored in a data logger with corresponding time stamps. The wind speed and wind direction averaging are carried out using the vector method before storing in the data logger. The stored wind is thus a vector-averaged true wind that has been compensated for ship motion using GPS and compass. The specifications of AWS, the range of wind speed is 0-60 m/s with an accuracy of 0.2 m/s, wind directions $0\text{-}360^0$ with accuracy3^0, similarlythe range of air temperature $0\text{-}45^0$ C with accuracy $\pm$ 0.15^0C, and barometric pressure 800-1060 mb with accuracy 0.4 mb respectively.

Fig. 2.8 Autonomous Weather Station (AWS)

2.5.3 Sound Velocity Profiler

Sound velocity profiler (SVP) model SV Plus v2 (M/s AML Oceanographic) was used in the present study (Fig. 2.9). It can measure up to a depth of 2000 m. It has a sampling speed of 25 Hz. The accuracy of sound velocity is ± 0.05 m/s. It needs 9 D alkaline cells, 9 D cell Ni-Cd rechargeable batteries. For profiling, it is utilized

through a sensor cage to protect the instrument. The system can provide water column temperature with respect to the depth and sound speed data.

Fig. 2.9 Sound Velocity Profiler (SVP)

2.5.4 Sediment Sampling

Van-Veen Grab (stainless steel) of size 25x25 cm and depth of cut 15 cm was used for sediment collection (Fig. 2.10). For the present study the sediment data were collected using a Van-Veen grab, covering an area of 0.0625 m^2 and penetration of 10 cm, following a standard protocol. About 20 g sediment was taken from each grab sample to carry out the textural analyses using a 4.0 cm diameter core tube. The sediment was repeatedly washed in distilled water until all the chloride ions detectable with 4 % silver nitrate were removed. These samples are then treated with 10 % sodium hexameta phosphate and kept overnight fordispersion before being subjected to the grain size analyses (Ingole *et al.*, 2002). The acquired sediment samples were subjected to wet sieving using a 62 μm sieve to separate the sand from the mud fraction. The size distribution of the mud fraction (< 62 μm) was measured with an LDPSA (Laser diffraction partial size analyzer). The size distribution of the sand fraction was determined using a standard dry sieving method as it was difficult to maintain uniform suspension of sandy material within the laser particle analyzer. The shelf sediments normally contain shelly material, which had to be sieved prior to

measurement by laser diffraction. The mean grain size M_{φ}= - $\log_2 U_g/U_0$ (where U_0 = 1 mm) was then calculated for each of the sediment data locations.

Fig. 2.10 Van-Veen Grab

2.6 Spectral and clustering methods

In this section spectral techniques such as spectrogram for visualization of segmented fish sound data is made. Similarly, power spectral density is applied to estimate the frequency peak of the fish calls and for the identification of fish calls. These two techniques are extensively used in chapter 3. Principal component analysis (PCA) is applied to understand the interrelationship among the environmental parameters with respect to the fish call.

2.6.1 Spectrogram

It provides the time localized frequency information for situations in which frequency components of a signal vary over time. The spectrogram is a visualization of time series to understand the frequency pattern of the recorded signal. The spectrogram is a linear time-frequency representation of the pre-windowing of the fish sound signal, and calculating its Fourier transform. This transform is known as a Short Time-Fourier Transform and referred to as STFT (t, f) where t is the time variable and f the frequency. A quadratic form related to the Short Time Fourier

Transform can be obtained by taking the square of this transform. The spectrograms provide the spectral energy density of the signal in the time-frequency domain. The spectrogram of a signal x(t) is referred to as SPECT(t, f) (Padovese et al., 2009)

$$\text{SPECT}(t, f) = \left| \int x(\tau)\, h^*(\tau - t)\, e^{-2j\pi f\tau}\, d\tau \right|^2 \qquad (2.5)$$

where h (t) is a sliding window weight, and the superscript * denotes conjugate. Matlab (www. mathwork.com) was employedfunctions are given in details (Table 3.1).

2.6.2 Power Spectral Density (PSD)

Power spectral density is the measure of signal power content versus frequency. The power spectral density is typically used to characterize the peak frequency of the signal. The power spectrum is defined as the square of the amplitude of the Fourier transform of a time series and can thus be regarded as an expression of the variance of the underlying process. Power spectral density function (PSD) shows the strength of the variations (energy) as a function of frequency. In other words, it shows at which frequenciesvariations are strong and at which frequencies variations are weak. The unit of PSD is energy per frequency (width) and energy can be obtained within a specificfrequency range by integrating PSD within that frequency range. Computation ofPSD is done directly by the method called FFT or computing autocorrelation function and then transforming it.

Welch's averaged, modified periodogramis implemented in the MATLAB toolbox (www.mathwork.com) by the pwelch function (Table 3.1) in chapter 3. A Hanning window is used to compute the modifiedperiodogram of each segment. The voltage level of the hydrophone is observed throughthe data acquisition system during the initial stage of the data collection. Once the signal is recorded then it is converted from voltage to pressure in terms of Pascal.Then the PSD is estimated by using the Welch method (Welch, 1967).

2.6.3 Principal Component Analysis (PCA)

PCA is a statistical procedure that uses an orthogonal transformation to convert a set of observation of possibly correlated variables into a set of values of linearly uncorrelated variables called principal components (Hoppe and Roan, 2011). In order to implement PCA,Pearson's correlation coefficient (the covariance of the two variables divided by the product of their standard deviations)of the datasets is computed.Thereafter eigenvalues and eigenvectors that form a feature vector using the correlation matrix of the variables are computed. The principal components are determined through the use of the eigenvector corresponding to the highest eigenvalues. PCA orders the resulting orthogonal components (PCs) so that those with the largest variation come first, and eliminates those components that contribute the least to variation in the dataset.

Chapter 3

Soundscape and identification of fish sound

3.1 Introduction

Marine biologists have been conducting specialized studies in ecological systems, food chains and marine population dynamics (Levington, 1995). They attempt to describe different species of animals and plants, their distributions, size and their relationships and sustainability in the oceanic environment (Hughes *et al*., 2013). Traditionally, marine biologists have used nets to sample the fish. Nets are biological tools that have become more sophisticated. However, they are constrained by operational limitations in terms of obtaining information regarding swimming fish species. The fish species in tropical waters are an important part of the biomass, and a few of them generate sound which can be made use of to identify it (Fish *et al*., 1952).

In the underwaterenvironment, marine animals use sound signals to communicate (Ladich, 2015; Bass and Ladich2008). Many fish species rely on vocal signaling during their activities, and produce sounds using sonic muscles that vibrate the swimbladder or the bony elements (stridulation) (Parmentier and Fine2016). Generally fish use sound signals for attracting mates and defending its territory. In addition, there is recent evidence that fish may also use sound as a contact call of conspecifics to let know where they are (https://www.the-scientist.com). Passive acoustic techniques, to identify fish sound patterns in the ocean are being utilized for research in ocean acoustics since the 1950s (Wood and Parrish, 1950; Bardyshev, 2007). Many fish species are known to make sound associated with a variety of

situations, such as courtship, spawning, mating, territory defense, competition for food and to signal alarm. Studies also involve the behavioral significance of sounds from tropical fish species. During spawning season, large active calling from specific fish is globally used by fisherman to locate fish aggregations. The noise consists of large numbers of sounds from conspecifics produce a masking effect to another sound. Reproductions related fish "chorus" are common with calling as a group acting to mediate partner selection and release gamete at night time. The characteristics of a sound, including a series of pulses and duration can be important to its communicative value and behavioral studies (Amorim, 2006).

The characterizations of the sound signals produced by marine animal and fish are ongoing investigations that were initiated long ago (Fish and Mowbray 1970) and are continuing to date (Towsey *et al*., 2012). Moreover, relating such sound signals with respect to the skeletal and muscular details of the animals is also an important research subject (Au and Banks, 1998; Kasumyan, 2008). Passive acoustics provide a near-perfect ocean observatory sensor for the biological activity of the fish. Besides, passive acoustic recorded data is also used to learn about their ecology. Many fish species have been known to make sounds ever since humans started exploiting them. In this chapter, a focus on the recent advances in the use of passive acoustics to identify the fish family or the species using autonomous acoustic recorders (Lammers *et al.*, 2008) is presented. Fish sound monitoring using passive acoustic data is in a rapid stage of development as an additional tool in fisheries research (Rountree *et al*., 2006; Luczkovich *et al*., 2008). Recent developments in fish passive acoustics are based on the results of decades of research into the mechanisms and physiology of fish sound production and hearing. Several excellent texts and thoroughly reviewed articles on mechanisms of fish sound production, hearing, and acoustic communication (Popper and Fay, 1999; Ladich and Myrberg, 2006; Webb *et al*., 2008) have been made available. Fish sounds are of generally low frequency, with some large fish species, like the goliath grouper producing sounds as low as 60 Hz (Mann *et al*., 2009). The acoustic characteristics of fish sounds are directly tied to the mechanisms of sound production (Parmentier and Fine, 2016). In this study, passive acoustic data was acquired using autonomous systems with broadband hydrophones

used for fish sound recordings.Fish sound identification methods employed at different study locations (within Goa and Malvan, Maharashtra, India) has been reported here. In the next section a brief note describes the sound-producing mechanisms of the fish species. Thereafter, a method related to the fish sound identification and characterizations in the laboratory and field is elucidated.

3.2 Sonic Mechanisms in Fishes

Three general types of sound production mechanisms (Fish, 1954) in the fish have been identified such as: i) swimbladder, ii) stridulatory and iii) hydrodynamic.

i) Swimbladder mechanism: The swimbladder of the fish acts as a resonator and can change the quality of the observed sound (Ladich and Fine, 1994). Swimbladder mechanism is also known to function analogous to a drum. In some fish species the pneumatic duct between the swimbladder and esophagus may play an important role in sound production as a resonator, and the generated sounds are detected when the air bubbles are ejected. The bladder sound has short pulse characteristics.

ii) Stridulatory mechanism: Most of the fish posses opposing pair of denticles in the pharynx, which leads to sound production during feeding. Feeding seahorse makes clicks, and these clicks are produced by the cavitations sound due to the collapse of vapor bubbles in the fluid which may be caused by rapid pressure changes within the buccal cavity. Incisor teeth help in biting through the exoskeleton, which produces strong metallic sounds. The frequency generated out of these activities ranges from 100 to 8000 Hz predominantly from 1000-4000Hz (Ladich and Bass, 2003).

iii) Hydrodynamic or swimming sounds: The movement of an object through water creates displacement. This displacement can lead to the harmonic vibrations which can be produced by the fins and the body of a swimming fish. These types of sounds are produced due to a sudden change in direction while swimming. These sounds are represented mainly by low-frequency nonharmonic oscillations with frequencies less than 100 Hz. (Moulton, 1960; Demski *et al*., 1973).

3.3 Laboratory experiments and field data recordings

In order to understand the role of fish sounds in the overall behavioral repertoires of a species, accurate measurement of sound characteristics as well as concurrent behavioral observations is necessary. To minimize distortions due to reverberation, sound recordings are conducted ideally in an open body of water with a depth and width exceeding the wavelength of the targeted sound. The open-water environment is readily available, although various experimental conditions (e.g., water temperature, ambient noise) are hard or impossible to control, and the turbidity may render behavioral observations difficult. Recording fish sounds in a small tank allow precise behavioral observation and better control of environmental factors than in the natural environment. However, due to the physical limitations of small tanks, the true characteristics of sounds are hard to assess due to many physical constraints of small tanks (Parvalescu, 1967). For example, the duration of fish sounds usually exceeds 2 ms (Fish and Mowbray, 1970), during which the sound travels about 3 m, but most commonly used glass aquaria in a laboratory (Fig. 3.1) are rarely over 2 m in length. Therefore, even a short-duration sound could result in reverberation, defined as the persistence of sound in an enclosed space as a result of multiple reflections after sound generation has stopped (Yost and Dye, 1997). Hence, it is impossible to separate the original sound from the reflected sound in the time domain when the sounds are recorded in small tanks. Tank resonance can also cause other problems. In a closed-boundary system, standing waves persist after cessation of sound generation. Thus, the frequency recorded may be the resonant frequency of the standing wave due to its longer duration than the original fish sound. If the resonant frequency of the tank happens to be close to the frequency of the sounds produced by the fish, the original spectrum will be seriously distorted, thereby prohibiting an accurate characterization of the original sounds (Akamatsu *et al*., 1998). Additionally, the fish sound data acquisition at the laboratory level is also problematic due to the sound generated by the pump. Pump generated sound works as a masker for the actual fish sound and contaminates the original sound generated by the fish. Pumps are normally used in the tank for oxygen supply, as without oxygen supply the animal becomes stressed. These

are some of the practical difficulties in the laboratory level analyses (Chakraborty *et al*., 2014a; Haris *et al*., 2014).

Although the constraints of a small tank have been known for more than 30 years (Parvulescu, 1967), the acoustics experiments in the small tank have received little attention due to extremely limited investigations, and the potential problems remain unaddressed in most studies analyzing fish sounds (Akamatsu *et al*., 2002). In this research, passive acoustic recordings from eight locations in the open waters along the Goa coast, such as, off Britona in the Mandovi estuary, off Betul in the Sal estuary and off Grande Island in the Zuari estuary as well as from the Malvan reef area, off the Maharashtra coast, were acquired. Fisheries boats (M/s Jesus King I and Jesus King II) were deployed for data acquisition from a survey site. The boats were anchored and kept far away from the mooring system setup for data collection. The boat motors were switched off at the time of collection of environmental data and passive acoustical data as well.

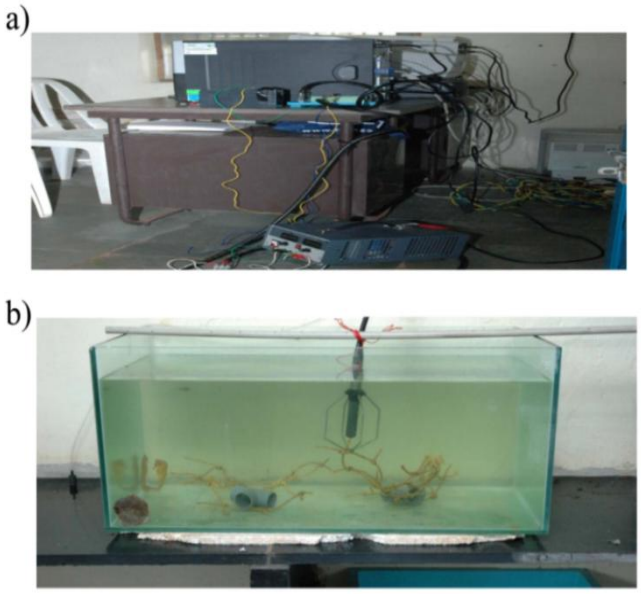

Fig. 3.1 Seahorse sound data recording system: a) Electronic devices including personal computer, b) Glass Tank and Hydrophone

3.1.1 Spectral Analyses

Spectral analyses of 1 to 2 minutes of data acquired at the 15-minute interval were used to calculate power spectral density (PSD). Concatenated PSDs were generated on the time-frequency axis for location soundscape. Such soundscape plots indicating the duration of data acquisition, and intensity depicted by the color bar are presented, exemplifying the eight locations (Table 2.1). Thereafter, the recorded sounds were analyzed using an algorithm developed for the purpose (Fig. 3.2), waveforms, spectrograms and power spectral density (PSD) applied to the segmented signals of individual fish calls. Spectrograms visualize the time-frequency content of the signal, and are commonly used to analyze animal vocalizations. More details of animal vocalization have been covered in this chapter. PSD has been used to estimate peak frequency. For estimation of the PSD and spectrogram, Matlab (www. mathwork.com) related functions were used (Table 3.1). We used window sizes for locations concatenated PSD (2048) and PSD (1024) of single call to achieve frequency resolution. For spectrogram of the single call, the window size of 256 was used to increase time resolution to identify the animal/species. Increasing the window size for spectrogram will reduce the temporal resolution of the call. Furthermore, temporal call parameters such as call duration, the number of pulses and inter-cell separation of the fish calls were made use of to identify the fish sound (Table 3.2). In order to corroborate the fish sounds, available data of fish sound files accessible on the websites i) Discovery of Sound in the Sea (https://dosits.org), ii) The Fish Base project (http://www.fishbase.org/) and iii) Mc Cauley library (https://soundcloud.com/ab cscience/sounds-of-science-teraponsspawning) were utilized. Besides, the seminal work on biological underwater sounds for fish sound identification (Fish and Mowbray, 1970) was extensively made use of.

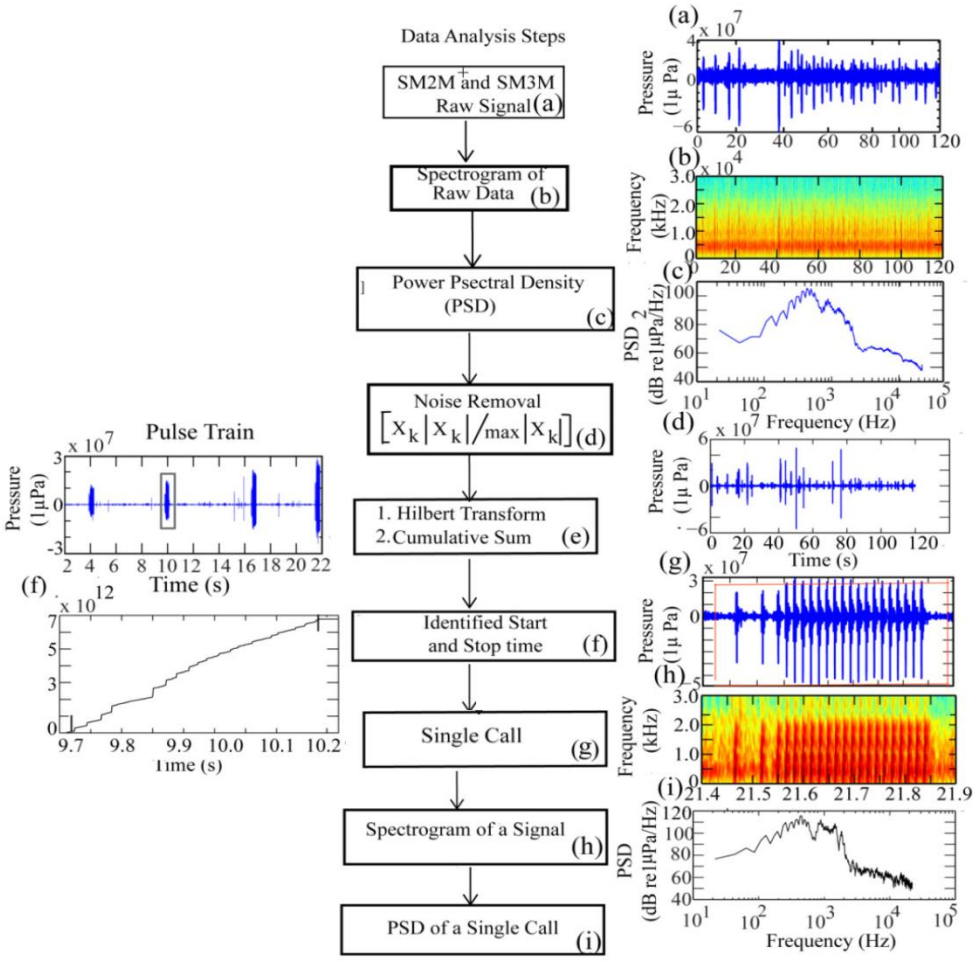

Fig. 3.2 Fish sound segmentation flow chart employed in this work

Table 3.1 Matlab functions use and details for spectral calculations

Study Areas	**Type of fish**	**Concatenated PSD[1]: Hanning window size; overlap; nfft**	**Spectrogram[2] (single call): Hanning window size; overlap; nfft**	**PSD (single call)[3]: Hanning window size; overlap; nfft**
Location 1 Off Britona	Toadfish	2048,1024, 2048	256,128,1024	1024,512,1024
Location 2 Off Grande Island	*Terapon theraps*			
Location 3 Betul	*Terapon theraps*			
Location 4 Off Grande Island	Barred grunt			
Location 5 Off Malvan	*Terapon theraps*			
	Carangidae			
	Malvan Type A			
Location 6 Off Grande Island	*Terapon theraps*		2048,2000,2048	2048,1024,2048
	Toadfish		256,200,1024	
	Grande Type A			
	Grande Type B			
Location 8 Off Grande Island (~ 20m water depth)	*Terapon theraps*		2048,2000, 4096	
	Sciaenidae		256, 200, 1024	
	Grande Type A			
Location 9 Off Grande Island	------		--	----

[1]Computed power spectral density using pwelch function, [Pxx,f] = (x, window size, overlap, number of fast Fourier transform (nfft), fs)'Pxx'is PSD estimate matrix, f is cyclic frequency vector x is input data fs is sampling frequency of the signal.

[2] Computed spectrogram based on [S, F, T, P] is 'S' is Short-time Fourier Transform estimate matrix, F is cyclic frequency vector and 'T' is time instant vector and 'P' is power spectral density estimate vector.

[3]Computed power spectral density for the single call using pwelch function having window size overlap and nfft and sampling frequency (fs).

Note : The sampling rate of all the locations was given in Table 2.1.

3.4 Fish call parameters

The procedure to determine fish sound parameters requires noise reduction, segmentation and classification (Fig. 3.2). Therefore, to understand the nature of the biological sound present, the spectrogram (b in Fig. 3.2), of the raw 60/120s data is generated. A large spurt of signals is observed close to the lower frequencies. The PSD of the entire data has been depicted in Fig. 3.2 (c). Thereafter, an application of the noise reduction method is employed (Zimmer, 2011). The extraction of noise-free fish sound is imperative before data processing. In order to identify the start and stop point of the individual fish call, an enhancement of the contrast between signal and background noise in the data stream is required. Therefore, noise level reduction is carried out by multiplying the time series x_k with ratios of its corresponding absolute $|x_k|$ to the maximum absolute value$[x_k|x_k|/\max(x_k)]$ (d in Fig. 3.2) (Haris *et al*., 2014). In the next step, Hilbert transform based envelope detection procedure is applied. Data segmentation is implemented in two steps. At first the coarse segmenting each call is visually completed. Next, a cumulative sum is employed across the individual data to determine the exact start and stop time. A sharp rise in the slope of the cumulative sum marks the beginning of a sound event. The flat or saturated part of the curve corresponds to the end of a sound event (e & f in Fig. 3.2). After segmenting the signals, to identify the fish family/species, the spectrogram of the each call signal is generated (g in Fig. 3.2). Each fish family/species produces a sound that will have a peak frequency which is distinct, and can be used to distinguish the species. To determine the peak frequency, the PSD plots of all the call signals, (h in Fig. 3.2), are compared with the peak frequencies of the segmented call signal and those given in the referenced works. Thereafter, the determination of temporal parameters such as call duration, number of pulses within the calls, and inter-call durations are made. Detailed temporal and spectral parameters are shown (Fig. 3.3):

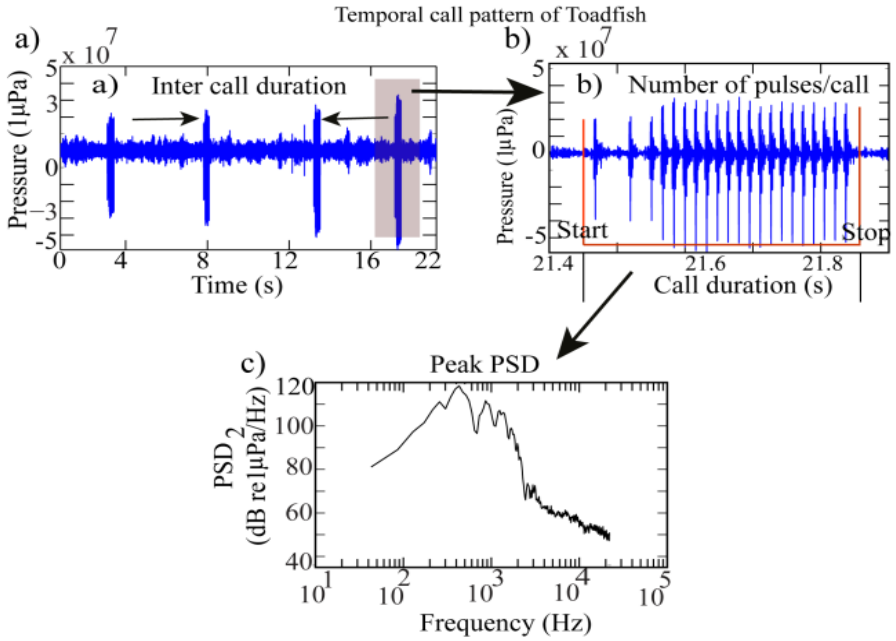

Fig. 3.3 Temporal and spatial parameters of the fish sound data

3.5 Location-wise soundscape and fish sound analyses

The term ‘soundscape’ has been used by a variety of disciplines to describe the relationship between the landscape (or waterscape) and the relative composition of all sounds present therein (Pijanowski *et al.*, 2011; McWilliam and Hawkins, 2013).In shallow water, the ambient sound field generally consists of various types of sound sources such as biophony, anthrophony as well as the geophony. Here, the analysis of fish sounds (biophonies) and abiotic sounds such as windand flow sound (geophony) and sounds of the boat (anthrophony) are carried out. The spatial structure of the sound field is dependent on the nature of the waveguide which forms due to the multipath propagation between the sea surface and seabed (Jensen *et al.*, 2011). Therefore, the characteristics of any signal received at a recorder’s location can be affected by the variability in environmental parameters. While these propagation features are acknowledged, this research aims to quantify the soundscape and fish acoustic signals as received at the recorders to serve as a representation of what others may receive from their environment in their given locations. The study locations are

well-known for tidal-stream influence such as seawater inflow, freshwater runoff, and salinity variations mainly during the southwest monsoon seasons (Manikandan *et al*., 2016; Singh *et al*., 2004; Sreekanth *et al*., 2015; Fernandes and Achuthankutty, 2010). Moreover, the variability in the soundscape arises from the bathymetric relief, an active shipping channel, frequent small boat transits and biological sounds. The study objectives will include identification of fish species using their vocalizations, andcharacterization of recorded biophony to understand their relationships using passive acoustic data from ecologically important shallow water regions off Goa and Malvan (Maharashtra) from West Coast of India (WCI).

For identification of the fish species, calculations for estimation of the spectrograms and PSDs of an individual call are made. For spectrogram, the 'pwelch' function (Table 3.1) is used. For species identification, temporal and spectral parameters of the fish calls (Table 3.2) are determined and compared with available information (Fish and Mowbray, 1970). The inter-call interval (from the end of one call to start of next call), single call duration and the number of pulses per bout were estimated. The spectral parameters such as PSD of single call are also calculated using 'pwelch' function(Table 3.1), and the frequency peaks are estimated.

3.5.1 Fish sound characterization off Britona near Chorao Island (Location 1)

The investigation here has been carried out in a shallow littoral environment offBritona,amangrove-dominated site near the Chorao Island (Singh *et al*., 2004) in the Mandovi estuary (Location 1) (Fig. 2.1; Fig. 3.4) as indicated earlier in chapter 2. Mandovi is one of the important estuaries sustaining the breeding and nursery grounds for many a species. It encompasses mangrove and mudflats dominated areas, which provide important shellfish resources to the local community (Udaykumar *et al*., 2013). Location 1 is well known for marine traffic of small passenger vessels and iron ore barges, and the frequent presence of anthrophony (boat sound) is indicative (Fig. 3.5a). The passive acoustic data was acquired using SM2M+ system at 07m water depth.

In order to understand area soundscape, the PSDs in time and frequency axes (Fig. 3.5a) of the wideband data of location 1 is presented. The figures depict the

concatenated power spectral densities (PSDs) plot, of 120s passive acoustic data records, acquired at 15-minute intervals, obtained using the Matlab function (www. math work.com) (Table 3.1). The analyses of the concatenated PSD data revealed fish choruses from 21:30 to 23:00 hrs. The highest peak of the PSDs for 120s recorded data reveal (100.0 ± 3.0 dB re1µPa^2/Hz) at (470±52 Hz) frequency suggesting fishsound (indicated as 1 in Fig. 3.5a). Interestingly, such sound was absent during the rest of the time. During the period of 02:15 to 03:15 hrs, the estimated peak PSD values (71. 2 ± 4.1 dB re1µPa^2/Hz) could be attributed to boat sounds when the fish sound is absent (Fig. 3.5a).

Notably, Toadfish call trains from location 1 (Britona) (Fig. 3.6 a-c) matches well with the reported Toadfish sound (*.wav format) of archived data [www.dosit.org]. The PSD of a single call was also calculated using "pwelch" function (Table 3.1). Though identification of 600 Toadfish calls from this location was made, however, calculations of the frequency peaks were estimated for fifty calls. The peak frequency of Toadfish was found to be (448.96±40.30 Hz) (Fig. 3.7a). Fish sounds are usually not sharply tuned, and the difference in amplitude at different frequency peaks due to the potential addition of spurious variability to a dataset is quite likely. Moreover, the fish sound recorded with varying distances from the hydrophones could connote that farther signals could have their frequencies dispersed relatively more than the signals emitted closer to the hydrophones. The peak frequencies of a single call PSDs shows consistent peak level (110-115 dB re 1µPa^2/Hz) taken from the four representative calls within the chorusing time. The representation of the PSD of the waveform of the data recorded at the 06:00 hr is the representative of the background noise here. An increase of 40-45 dB above the background sound caused by the Toadfish chorusing is observed (Fig. 3.7a). Often there are intricacies involved in acquiring specific fish sound to confirm the identity of the species due to water turbidity. However, from the available information and inferences from other researchers, it is suggestive of toadfish of Batrachoididae family found in the Arabian Sea (Mahanty *et al*., 2013; Greenfield, 2012). Interestingly the local fishermen are also lending support to this plausible observation. The inter-call interval (from the end of one call to start of next call), represents a single call duration (0.45± 0.05 s), and the number of pulses per

bout is observed to be (17.80 ±3.17) (Table 3.2), indicative of a toadfish boatwhistlesound (Vasconcelos *et al*., 2010; Mensinger, 2014). The scatter plot (Fig. 3.8) provides the distinct characteristics of Toadfish sound.

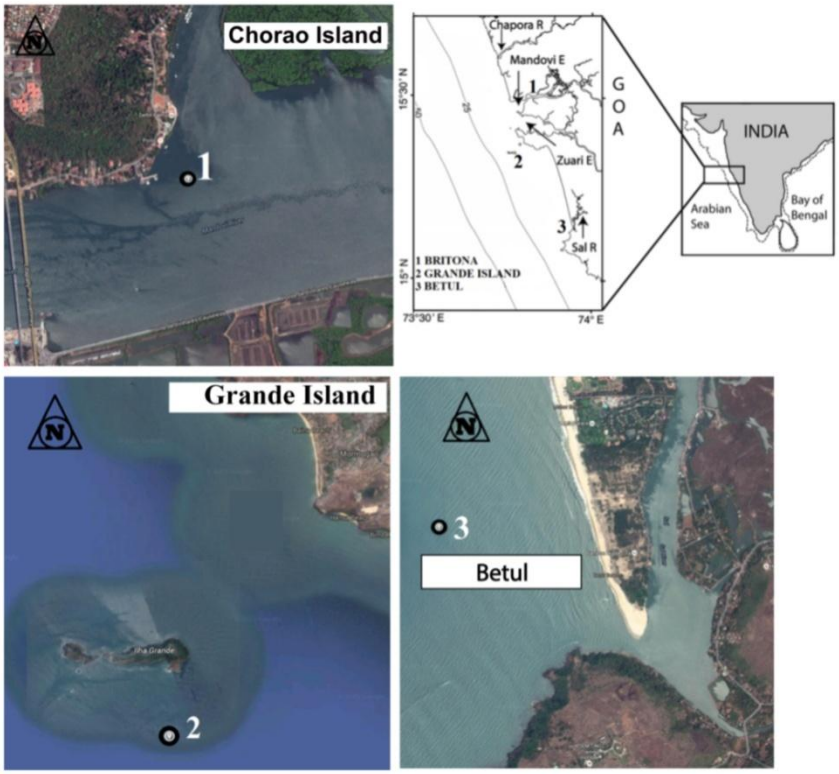

Fig. 3.4 Three study locations off Britona in Mandovi estuary (Location1), off Grande Island in Zuari estuary (Location 2), and off Betul (Location 3) in Sal estuary adapted from (www.google.com).

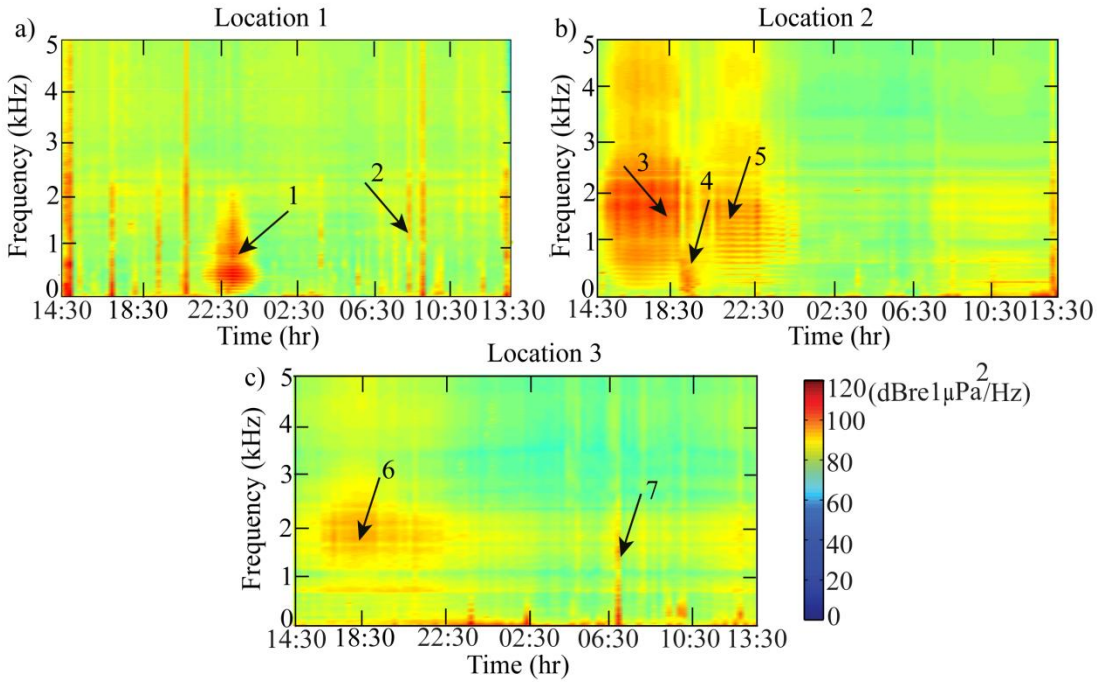

Fig. 3.5 Concatenated power spectral density (PSD) in dB re 1µPa^2/Hzconcerning the time in hr at an interval of 15 min: (a) Location 1; (b) Location 2; (c) Location 3. In Location 1, Arrows 1 and 2 indicate toadfish and boat sound respectively. In Location 2, Arrows 3 and 5 indicate the *Terapon theraps* sound and Arrow 4 shows boat sound. In Location 3, Arrows 5 and 6 show *Terapon theraps*and boat sound respectively.

3.5.2 Fish sound characterization off Grande Island (Location 2)

The Grande Island is surrounded by coral reef habitat having diverse flora and fauna, which are specific to coral reef habitat (Manikandan *et al*., 2016). The present location 2 is situated away from the coral reef system with 20 m water depth. The analyses of the concatenated PSD data i.e., soundscape data revealed fish choruses. Analyses of the passive acoustic time series and the corresponding PSD data substantiate the presence of the fish sound (during 14:30 to 00:30 hrs) at location 2 (Fig. 3.4b). The PSD peaks analyzed for fish chorus sound is found to be within the 15:00 to 18:30 hr (96.7±2.6 dB re1µPa^2/Hz) (indicated as 3 in Figure 3.5b). Due to the occurrence of boat sound during the 18:45 to 19:30 hr period, the PSD peaks of the fish chorus sounds varied significantly. The PSD peaks of the boat sound were estimated to be (89.1 ±3.9 dB re1µPa^2/Hz) for boat sound frequencies (188.0 ±53.6 Hz) (indicated as 4 in Fig. 3.5b) and (80.3 ± 6.2 dB re1µPa^2/Hz) at fish sound

frequencies (1749±11 Hz). Reduction in (16.4 ± 3.6 dB re1µPa^2/Hz) from the peak PSD level of the fish sound was observed with respect to the PSD peak fish sounds prior to the boat sound occurrence in the area. During the observation period (20:15 to 23:00 hrs), with absolutely no boat sound in the vicinity, an increase (4.7±2.6 dB re1µPa^2/Hz) in the peak PSD level was observed for fish sound(indicated as 5 in Fig. 3.5b), signifying upturn of the fish chorus sound.

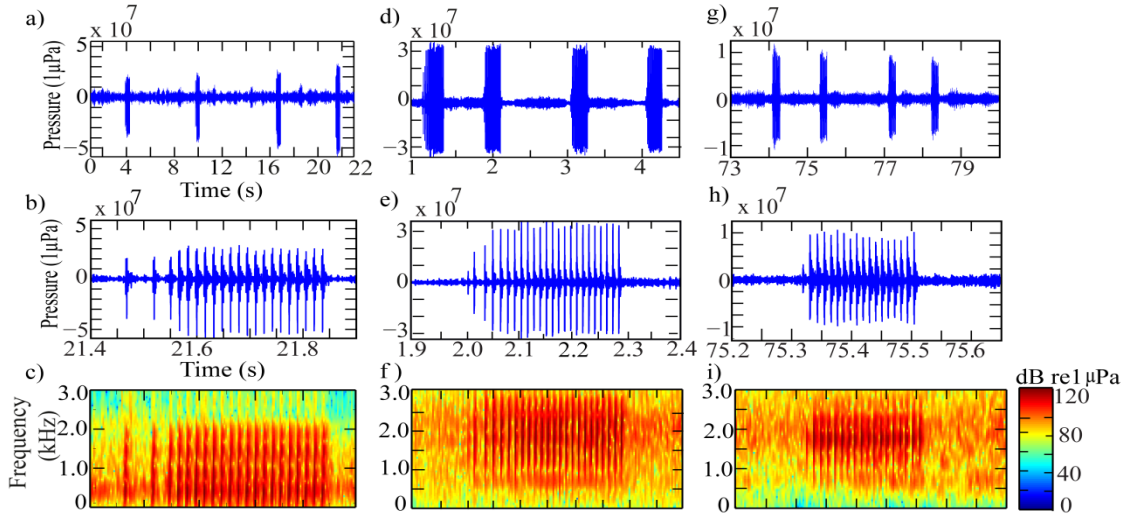

Fig. 3.6 a) Call pattern, b) waveform (1 µ Pa) versus time (s) and c) spectrogram fortoadfish species from Location 1; d) Call pattern, e) waveform (1 µ Pa) versus time (s) and f) spectrogram for *Terapon theraps* fish from Location 2; and g) Call pattern, h) waveform (1 µ Pa) versus time (s) and i) spectrogram for *Terapon theraps* fish species from Location 3.

At location 2, during the call interval (0.59± 0.08), thesingle call duration and the number of pulses per bouts were observed to be (0.26± 0.03 s) and (22.00±2.50) respectively (Table 3.2). Moreover, the spectrogram (Fig. 3.6f) of a single call from Grande Island(location 2) confirms that the sounds were from the fish belonging to the Terapontidae family (Cato, 2017)(Fig. 3.6 d-f). Near the Grande Island of Zuari estuary, the PSD of the single call shows frequency peak at (1765.00±14.90 Hz) with PSD levels within the (100-108 dB re 1µPa^2/Hz) levels (Fig. 3.7b) indicating *Terapon theraps* fish chorus due to the similarity in their 'trumpet' like-sounding mostly during the dusk period. The sound level in the shallow waterswas reported to be ~40 dB above the quieter ambient noise level. The energy levels of Terapontidae fish

chorus observed in the shallow waters off Kochi, Kerala was also reported to be ~40 dB above the background sound levels (Mahanty *et al*., 2015). The scatter plots (Fig. 3.8 a-f) reveal distinct fish call sound characteristics of *Terapon theraps* species recorded at location 2.

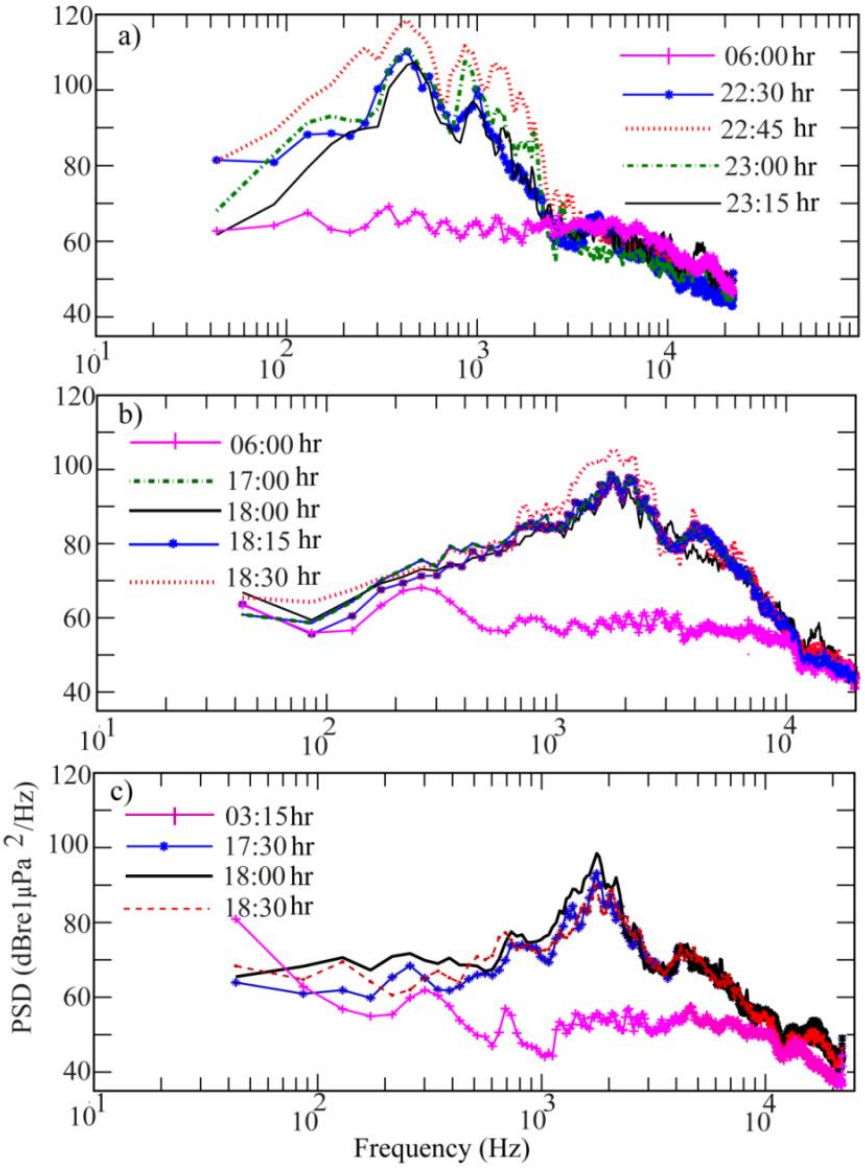

Fig. 3.7 Power spectral density in (dB re 1µPa^2/Hz for a) Location 1, b) Location 2 and c) Location 3

Table 3.2 Estimated fish sound parameters from study locations

Location	**Type of fish**	**Total Calls**	**Call duration (s)**	**Number of pulses/call**	**Peak frequency (Hz)**	**Inter call duration (s)**
Britona (Location1)	Toadfish	600	0.45±0.05	17.80±3.17	448.96±40.30	4.97±1.05
Grande Island (Location 2)	*Terapon theraps*	1773	0.26±0.03	22.00±2.77	1765.00±14.90	0.59±0.08
Betul (Location 3)	*Terapon theraps*	670	0.25±0.05	21.55±2.72	1779.00±51.08	1.11±0.54
Grande Island (Location 4)	Barred grunt	1726	0.85±0.12	10.20±1.82	289.06±74.93	2.36±1.08
Malvan (Location 5)	*Terapon theraps*	644	0.25±0.03	19.50±2.50	1768±73.68	0.68±0.29
	Carangidae	74	0.09±0.02	7.60±1.520	947.46±21.53	--------
	Malvan Type A	3	0.04±0.01	5.35±1.84	1735±45.63	0.10±0.03
Grande Island (Location 6)	*Terapon theraps*	2650	0.23±0.040	24.50± 3.28	1545.21±75.43	0.62±0.53
	Toadfish	115	0.39±0.06	20.20± 2.82	343.10±60.22	1.06±0.37
	Grande Type A	5250	0.17±0.02	16.35± 2.25	1005.00±122.82	1.45±0.59
	Grande Type B	240	0.39±0.01	22.10± 3.05	829.28±102.16	2.21±0.91
Grande Island (Location 8)	Sciaenidae	940	0.125±0.025	7.20± 1.70	708.50±49.44	1.76±0.40
	Terapon theraps	2115	0.24± 0.023	21.40± 3.78	1523±26.42	1.09±0.63
	Grande Type A	1850	0.167±0.020	18.20± 2.11	1028±84.41	0.49±0.40

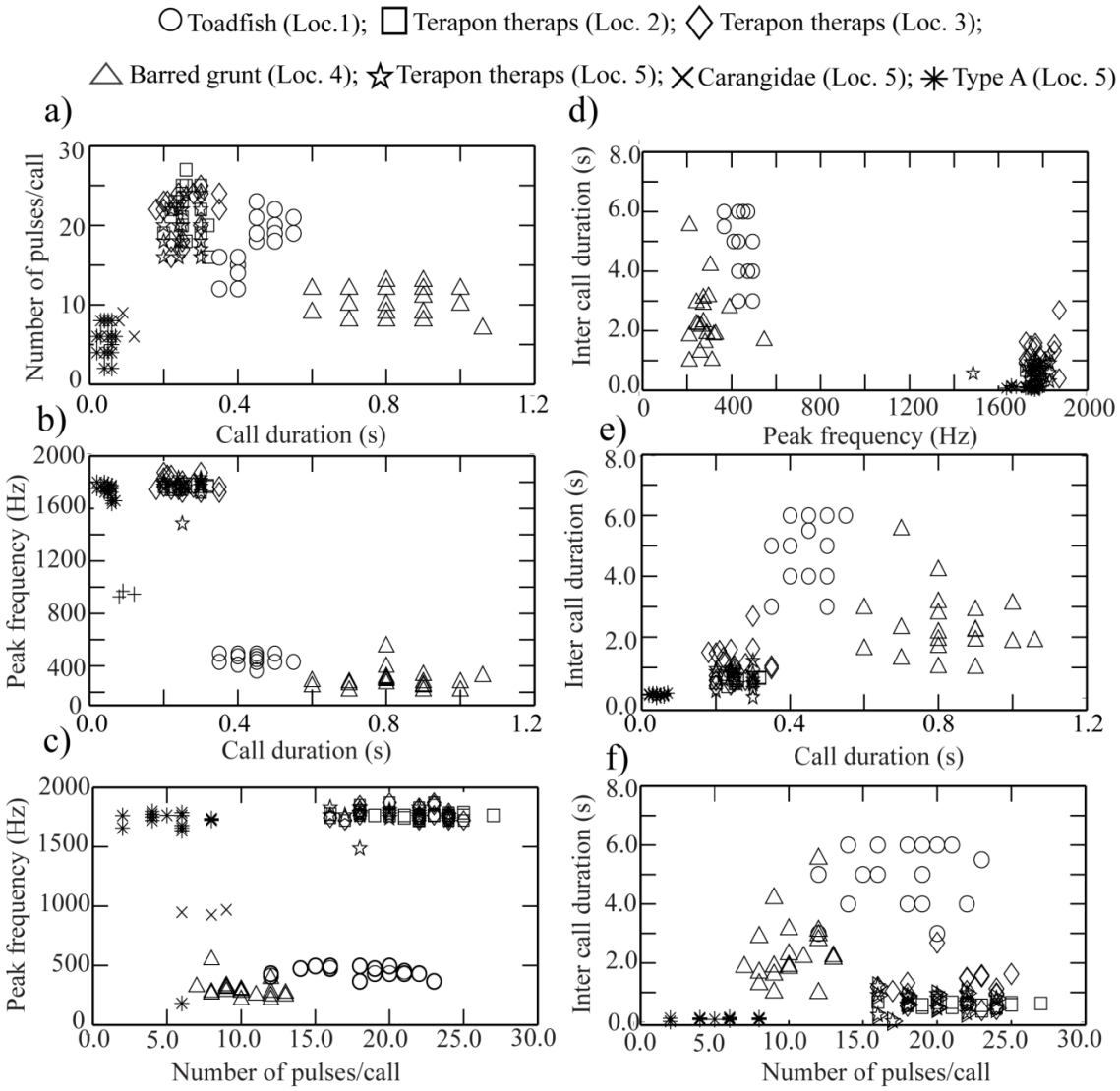

Fig. 3.8 (a-f) Scatter plots between the temporal parameters [call duration (s); no. of pulses/call; inter-call-duration (s) and spectral parameter (PSD peak frequency)] for single calls for identified fishes from Location 1-5.

3.5.3 Fish sound characterization off Betul from Sal estuary (Location 3)

Like Mandovi, Sal is also a mangrove-dominated estuary (particularly the *Avicennia* species), having backwater fishery and Molluscan resources (Fernandes and Achuthankutty, 2010). River Sal was under stress due to siltation and pollution along the marine traffic channel near Betul, where eco-restoration efforts have begun recently (Ingole, 2016). This ecologically significant site can provide a spectrum of baseline soundscape knowledge to carry out future research as anthropogenic changes

take place. SM2M+ passive acoustic data acquisition was moored at 11m water depth to acquire the data. The analyses of the data acquired fromBetularea(location 3)in the Sal estuary revealed fish chorus sound that also belongs to the Terapontidae family. The PSD peak levels of the single call waveform data (Fig. 3.7c) were found to be (95-100 dB re 1µPa^2/Hz), which is comparatively less than the level observed in location 2 for similar fish species. At the Betul location, the single call duration and pulses per call of the *Terapon theraps*were observed to be (0.25± 0.05 s) and (21.55±2.72) respectively(Fig. 3.6 g-i and Table 3.2). Similar to the *Grande Island* (location 2), the peak of the wideband PSD levels were found to be ~40 dB higher (Fig. 3.7c). Interestingly, clear-cut overlapping sound characteristics of *Terapon theraps* fish were observed for locations 2 and 3 (Fig. 3.8 a-f).

3.5.4 Fish sound characterization off Grande Island (Location 4)

Location 4 is situated towards the deeper end at 30 m water depth, away from the coral reef system near the Grande Island. SM2M+ - a passive acoustic data acquisition system was moored midway in the water column. The passive acoustic data acquisition was carried out from 07-12 May 2015 (Table 2.1). The analyses of the concatenated PSD data reveal three types of sounds i.e., fish sound (indicated as 2 in Fig. 3.9a), the anthropogenic sound (boat sound indicated as 1), and another type of sound probably from metal chains used by boats to anchor during the period starting from 07:00 hrs (on 11 May 2015) to 03:00 hrs (of 12 May 2015) (indicated as 3). The wind data reveal high-speed winds due to the pre-monsoon session, especially during the period 11-12 May 2015, having an average value of 4.20 m/s [0.5 (min.) 9.25 (max.) m/s]. The analysis of time series data indicates a daily fish chorus from the early hours of dawn (02:30-06:00 hr) (Fig. 3.9a). The grunting fish sound signatures are symptomatic that are also observed in the data. The waveform, spectrogram and peak PSD of single fish call have been depicted (Fig. 3.9 b-d). The PSD of the sound data substantiates the presence of the fish sound (Location 4) near Grande Island. The peak level of the PSD for fish chorus sound is found to be within the (95.0±2.6 dB re1µPa^2/Hz) (Fig. 3.9d), and the peak frequency of the PSDs of the fish chorus sounds is noted (289.06±74.93 Hz). The fish sound signals were identifiedas the grunting

sound of the "Barred grunt" using the waveforms (Fish and Mowbray, 1970). The temporal call parameters such as call duration, the number of pulses per call and inter-call duration determined from waveforms along with the spectral peak of the PSD are also estimated (Table 3.2). The single call parameters including peak frequency are found to corroborate with the fish species *Conodon nobilis* (Pombo *et al*., 2014; Fish and Mowbray 1970) having a family name: Haemulidae, popularly called as a "Barred Grunt". This fish uses stridulation mechanisms to produce sound (pharyngeal teeth), which is then amplified using swimbladder (http://www.fishbase.org/). These sounds may be associated with feeding. Both males and females produce soundswhen the fish is in distressed. Barred Grunt call parameters are observed to be distinct as shown in the scatter plot (Fig. 3.8 a-f).

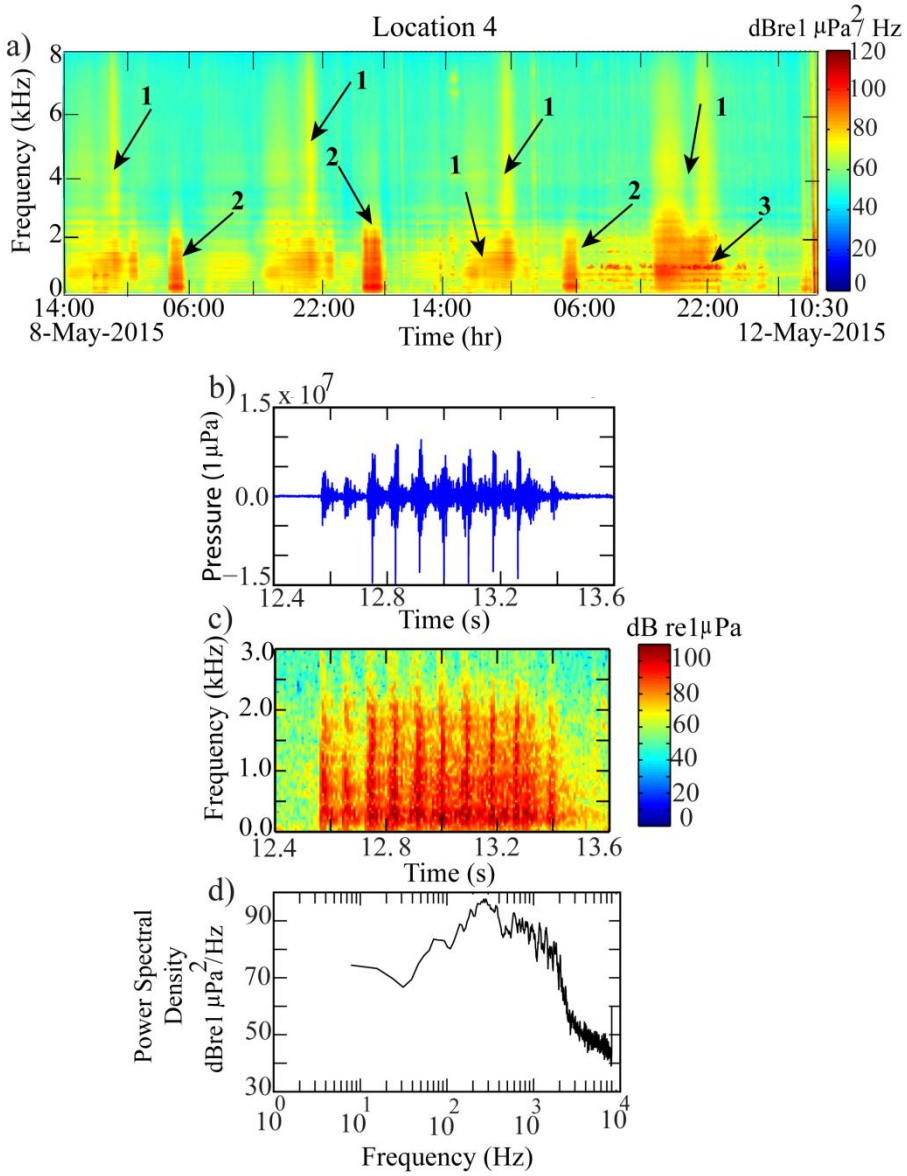

Fig. 3.9 a) Concatenated power spectral density (PSD) in dB re 1µPa^2/Hzconcerning the time in hr at an interval of 15 min, b) waveform (1 µ Pa) versus time (s), c) spectrogram and d*)* Power spectral density in (dB re 1µPa^2/Hz) forBarred Grunt (*Conodon Nobilis*). Fish sound indicated as 2), the anthropogenic sound (boat sound indicated as 1), and another type of sound probably from metal chains used by boats to anchor during the period as 3).

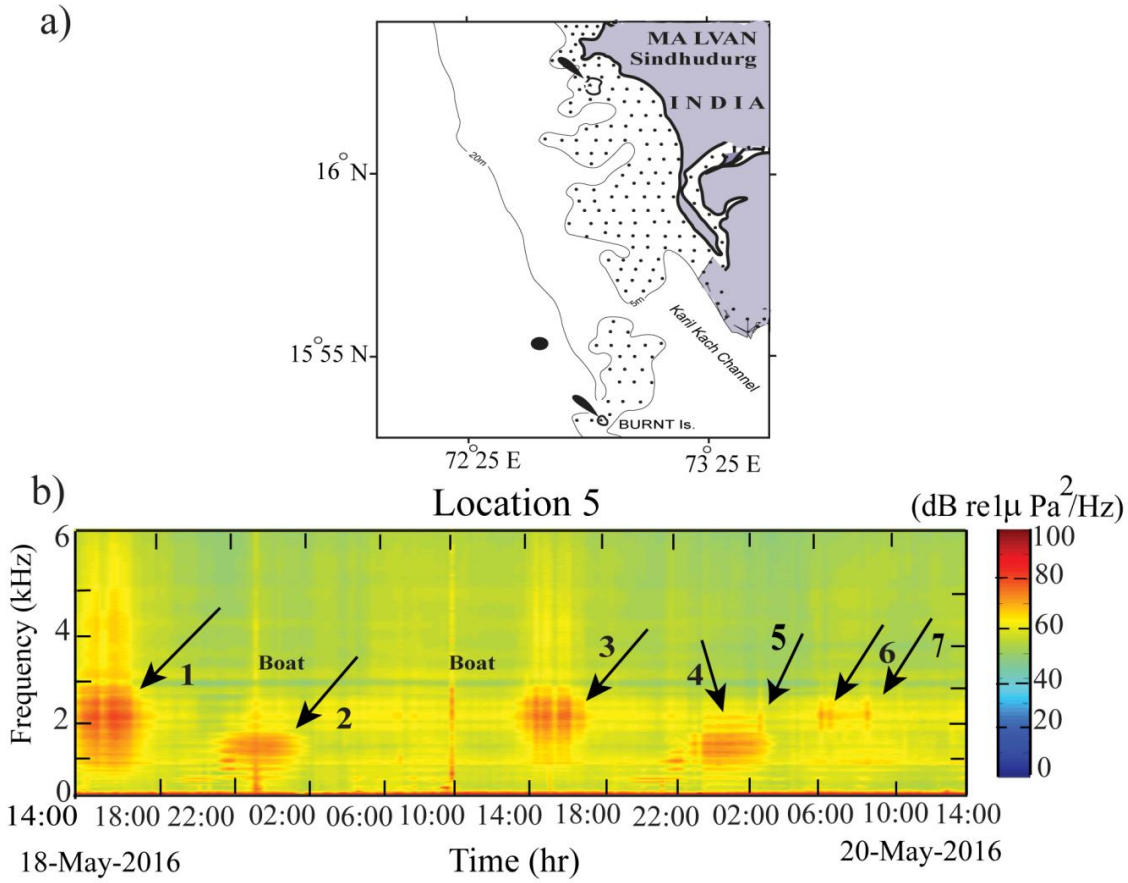

Fig. 3.10 a) Study location off the Malvan Coast (west of Burnt Island) in the west coast of India, b) Concatenated power spectral density (PSD) in dB re 1µPa^2/Hzconcerning the time in hr at an interval of 15 min from Malvan area, Maharashtra (given arrows are discussed in the text).

3.5.5 Fish sound characterization off Malvan reef system (Location 5)

Malvan is considered as one of the bio-rich coastal zones in Maharashtra, India (www.icmam.gov.in/MAL.PDF, 2001). The present study location (Location 5) is situated off the western side of the Burnt Island (lighthouse) and 2.5 km away from the Malvan coast (details are given in chapter 2) (Fig. 3.10a). Passive acoustic data were recorded using SM2M+ system. The water depth of the area is 22.5m, and the recorder was moored half way down the water column. The concatenated plot of the PSD in time and frequency axes of broadband data is presented for the study area (Fig. 3.10b) (Kranthikumar *et al.,* 2019). The data were analyzed for the entire recordings. At this location, the analogousfish choruswas acquired as on (18 May 2016; 14:00 to 17:30 hr) and (19 May 2017; 14:00 to 17:30 hr) with the broadband

hydrophones, the recorded sound (indicated as 1 and 3 in Fig. 3.10b). Thereafter, symptomatic type abiotic sound was detected which is depicted as 2 and 4 (Fig. 3.10b) for 18 and 19 May 2016 (21:30 to 01:45 hrs) and 20 May 2016 (00:00 to 02:30 hrs). On 20 May 2016, sporadic sounds of exiguous unnamed fish species (indicated as 6 and 7) were recorded between 02:45 to 08:00 hr.

Prominent biotic sounds due to the acoustic activity, denoted as 1, 3, 5, 6 and 7 (Fig. 3.10b), for further investigation and identification of fish sounds has been marked out. The chorus observed in the present study can possibly be ascribed to Terapontidaefamily due to the similarity in their 'trumpet' like sound (McCauley, 2012; Mahanty *et al.*, 2015; Mahanty *et al.*, 2018). Soundscapefor*Terapon theraps* representative call data acquired on 18 May 2016 (14:00 to 17:30 hr) and on 19 May 2016 (14:00 to 17:30 hr) is indicated as 1 and 3 (Fig. 3.10b). The spectral frequency peak of a representative single call at (1758±29 Hz)has a PSD level variation from (78 - 90 dB re1µPa^2/Hz) (Fig. 3.11 a-c) for 18 May 2016 data. Similarly, the waveform, spectrogram and peak PSD of single call recorded on 19 May 2016 (at 16: 15 hr) are also depicted (Fig. 3.11 d-f). A comparison between the peak PSD levels excluding the chorus i.e., in the absenceof*Terapontheraps* fish sound is carried out. The peak PSD level is observed to be (~40 dB re1µPa^2/Hz) lower as compared to the chorus. The time interval between (15-21) pulses per call is found to be varying (0.25±0.03 s) (Table 3.2). The peak level of the PSDs of the single call from the chorus is high as depicted (Fig 3.11c). Table 3.2, further provides temporalcharacteristicsof the *Terapontheraps*fish calls(McCauley and Cato, 2000).

Soundscape data (Fig.3.10b) shows the biotic sound (fish chorus as well as sparsely available fish family) i.e., areas are marked as 1, 3, 5, 6, and 7. The abiotic sounds (2 and 4) are found to have estimated peak PSDs of the abiotic sounds such as wave-breaking sound indicating peak level (~75 dB re1µPa^2/Hz) at frequencies (1142±23Hz).

Analyses of the limited number of waveforms, spectrogram and PSDs of the time series data of 20 May 2016 at 07:00 hrs that producebiophonies like barks and scratchy burst [marked as '6' (Fig. 3.10b)]. The spectral analyses results of the singlecall are depicted (Fig. 3.11g-i). The peak frequency of PSDs (947.46 ±21.53

Hz) indicates that the sound is produced by fish belonging to the family of Carangidae (Fish and Mowbray, 1970). They are marine fish family found in the tropical Indian Ocean. More details of the call signals are tabulated (Table 3.2). The limited recordings of Carangidae data show that the call signals with a duration of (0.09±0.02 s) have (7.61±1.52) pulses per call (Table 3.2). The family Carangidae is a pelagic fish (Clarke and Privitera, 1995) community with diverse names like jacks, amberjacks, pompanos, scads, pilot fish, etc. Also, the presence of *Carangidae* inthe WCI has been reported earlier (www.fishbase.org).

The concatenated PSDs of the time series data during 20 May 2016 during 02:45 to 08:00 hr) (indicated as 5 and 6) is depicted (Fig. 3.10b). The fish sounds observed in the present context does not reveal any particular family or species. The waveform, spectrogram and peak of the PSD are depicted in (Fig. 3.11j-l). The call duration (0.04±0.01 s) and the number of pulses per call (5.35±1.84) for unidentified fish species have been tabulated (Table 3.2). The peak frequency of the PSD of a single call (Fig. 3.11 l) shows a peak at (1735.00± 45.63 Hz), and this unknown fish sound is referred to as a Malvan Type A in this study.

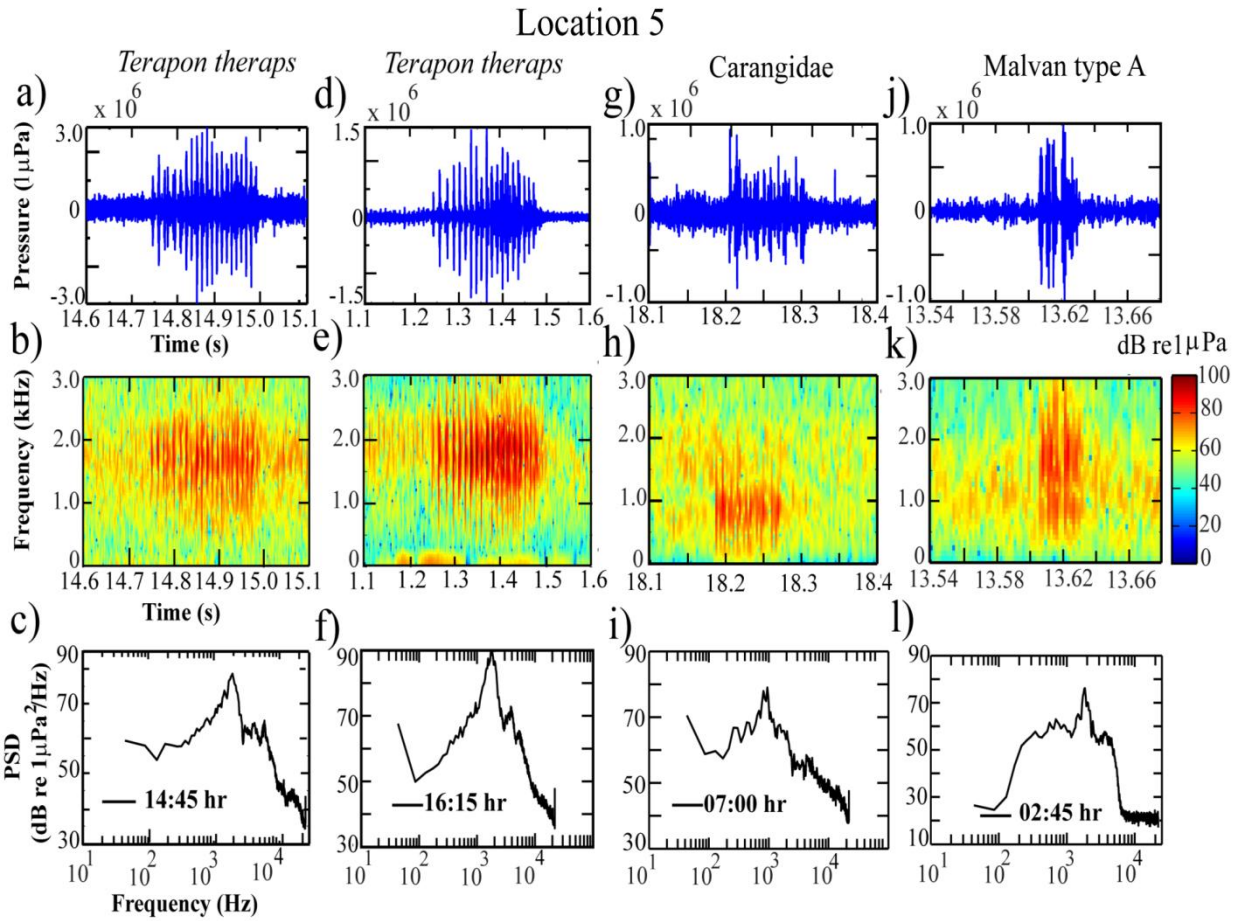

Fig. 3.11 Waveform, spectrogram and PSD of representative fish species calls: (a-c) *Terapontheraps* on 18 May 2016 @ 14:45 hr, (d-f) *Terapon theraps* on 19 May 2016@ 16:15 hr, (g-i) *Carangidae* on 20 May 2016 @ 07:00 hr, and (j-l) Unnamed fish (Malvan Type A) on 20 May 2016@ 02:45 hr from location 5.

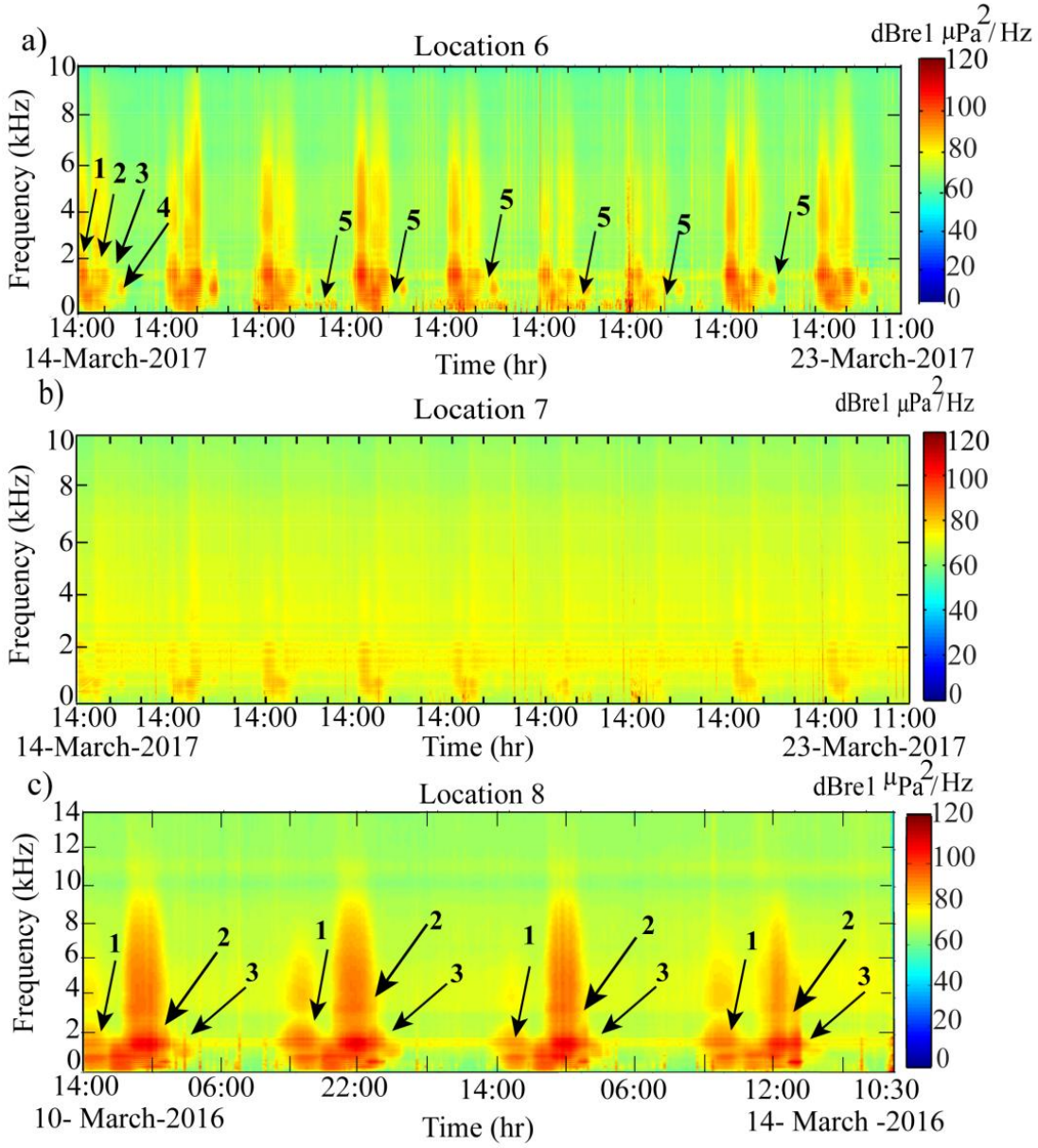

Fig. 3.12 a) Concatenated power spectral density (PSD) in dB re 1µPa^2/Hzconcerning the time in hr at an interval of 15 min from Grande Island (Location 6); b) Concatenated power spectral density (PSD) in dB re 1µPa^2/Hzconcerning the time in hr at an interval of 15 min from Grande Island (Location 7); c) Concatenated power spectral density (PSD) in dB re 1µPa^2/Hzconcerning the time in hr at an interval of 15 min from Grande Island (Location 8); (given arrows [1-4] are indicated as fishes and 5 indicated as humpback whale). Time axis of the plots is not to be scaled.

3.5.6 Fish sound characterization off Grande Island (Locations 6 and 7)

Prominent biotic sounds due to the acoustic activity are indicated as 1, 2, 3, 4 and 5 in location 6 from the concatenated PSDs (Fig. 3.12a) in time and frequency axes of broadband data acquired at 20m water depth away from the reef (Fig. 2.1) from 14-23 March 2017. In general, recorded data reveals fish sound during 14:00 - 03:00 hr as indicated (1 to 4 in in the figure). Humpback whale sound (indicated as 5) is also recorded in this location from 16-21 March 2017 (Madhusudhana *et al*., 2019). The analysis suggests that the recorded biophonies also include Humpback whale sound along with the fish sound. The Humpback whale sounds are recorded dominantly within the timings 12:00-15:30hr and 00:00-04:30hr. Occasional whale sounds are also recorded within the 18:00-22:00hr.

At location 6, *Terapon theraps* fish sounds (indicated as 1 in Fig. 3.12a) are recorded within the 14:00 – 19:30 hr and 21:30-22:30 hr of each day from 14-23 March 2017 (Table 3.2). The chorus observed in the present study ascribes to Terapontidaespecies due to the similarity in their 'trumpet' like-sounding (Mc Cauley and Cato, 2000; Mahanty *et al*., 2015). Waveform, spectrograms for *Terapon theraps* representative call data, and corresponding spectral frequency peak of the call provide 1545.21±75.43 Hz (Fig. 3.13c). Similarly, the fish sound of Toadfish i.e., Batrachodidae family is also identified based on the data recorded during 19:30-21:00 hr of each day from location 6 (indicated as 2 in Fig. 3.12a). The spectral analyses results for a single Toadfish call are depicted (Fig. 3.13d-f).The peak frequency of PSDs (343.10±60.22 Hz) indicates that the sound produced by fish belonging to the family of Toadfish (Batrachoidae). Further details of the call signal are tabulated (Table 3.2). The presence of Toadfish inthe WCI is reported in (Mahanty *et al*., 2013), and (https://dosits.org) has been further validated.

Identification of a fish family of two other types of fishes based on their temporal and frequency peak PSDs could not beencarried out even though recorded calls are distinctly observed within the call time.This is due to the unavilibility of similar fish sound record in the known archive. Their presence was observed within the 20:30-21:30 hr and 00:30-03:00 hr for Grande Type B and Grande Type A respectively. Interestingly, there is an overlapping between the Grande Type B and Toadfish is seen

through spectral peaks within the 20:30-21:00hr for each day datasets. Again within the 21:30-22:30 hr, *Terapon threaps* fish species is identified. Similarly, another unidentified fish sound referred to as Grande Type A within the (00:30-03:00 hr) is analyzed (details posted in Table 3.2). Representative waveform, spectrogram and peak frequency is presented (Fig. 3.13 g-i). The peak frequency of the PSD of a single call shows a peak at (829.28±102.16). The single calls duration (0.39±0.01 s) and the number of pulses per call (22.10±3.05) are tabulated (Table 3.2). Temporal and spectral parameters for location 6 are presented in Fig. 3.16 (a-f). Distinct clustering for Toadfish family, *Terapon theraps* species and Grande Type A is observed in the scatter plot. In location 6, recording of the 5424 calls of the Humpback whales are recorded (Madhusudhana *et al*., 2019). Besides that, recordings of 2650, 115, 5250 and 240 call signals from *Terapon threaps*, toadfish, Grande Type A and Grande Type B respectively are made.

The concatenated PSDs in time and frequency axes of wideband data is presented for 20m water depth area (Location 6) away from the reef (Fig. 3.12a), and 8m water depth (Location 7) close to the reef (Fig. 3.12b).The distance between the locations are around 500m. From location 7, fish sound identification based on the peak frequency of the PSD does not provide clear cut frequency peaks. The background sounds are found to be dominant as shown Fig. (3.12b) probably due to the different habitat (8m water depth). A comparison between the levels of the peak PSDs (Fig. 3.14) of the simultaneously acquired time-series data through SM3M systems deployed at locations 6 and 7 reveal useful information. Identifiable animal sounds of location 6 are recorded at location 7 too. Significantly low PSD levels in location 7 are found in comparison with PSDs from location 6. Maximum fall (12-35 dB) in PSD level of location 7 is observed with respect to the location 6 as shown in the PSD plots for a time-series data acquired at the same time in both the locations 6 and 7 hydrophones. A critical observation of Fig. 3.14 suggest, a transmission loss of 35dB, 12dB, 22dB, 12 dB and 27 dB for *Terapon threaps*, toadfish, Grande Type B, Grande Type A and Humpback whale sounds respectively. Recorded data and their analyses suggest that the level of the peak PSDs received at location 6 is much clearer. However, such distinctness in the fish signals calls is not seen in location 7.

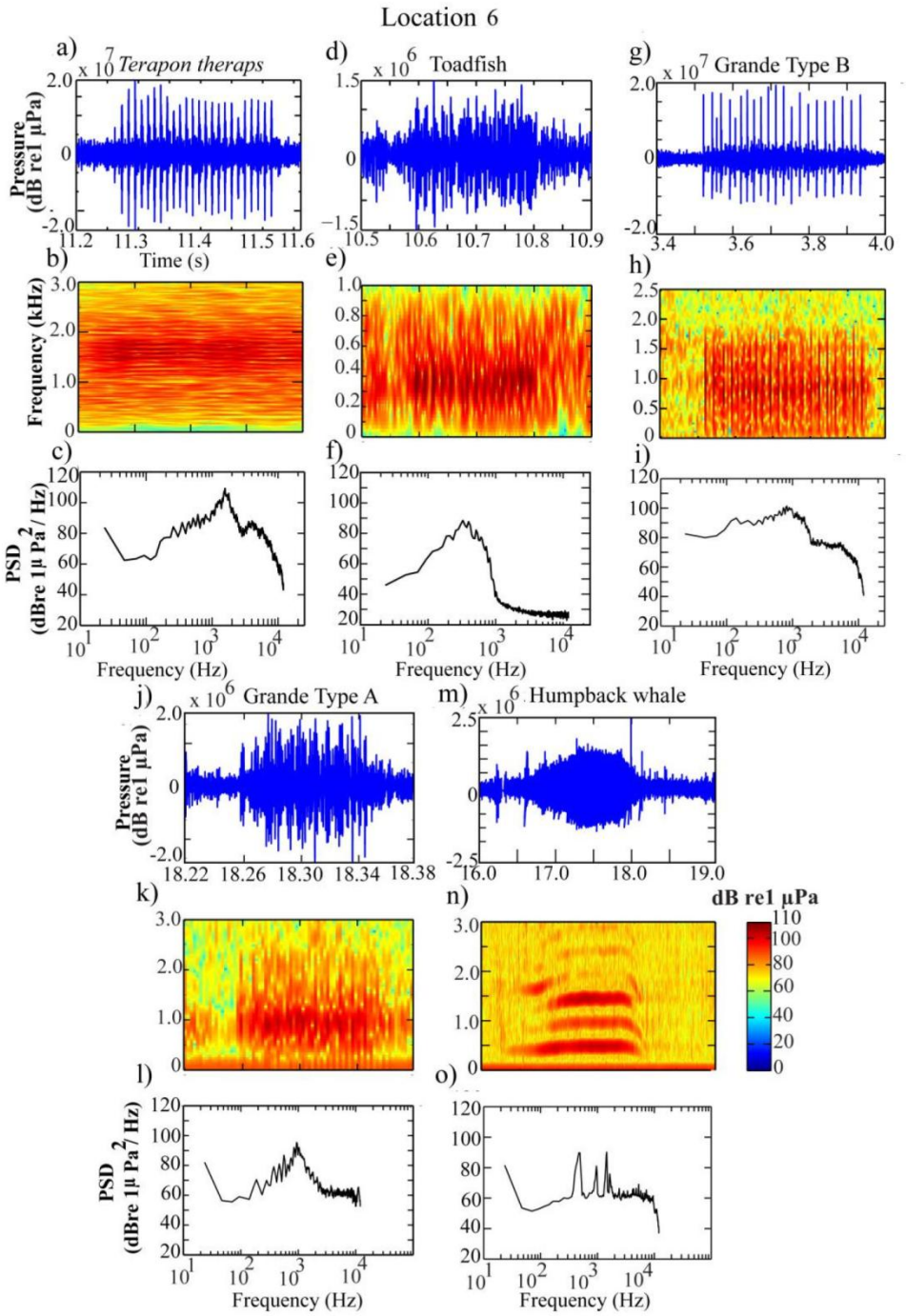

Fig. 3.13 Waveform, spectrogram and PSD of individual representative fish call: *Terapon theraps* (a-c); Toadfish (d-f); Grande Type B (g-i); Grande Type A (j-l), and Humpback whale (m-o) from location 6.

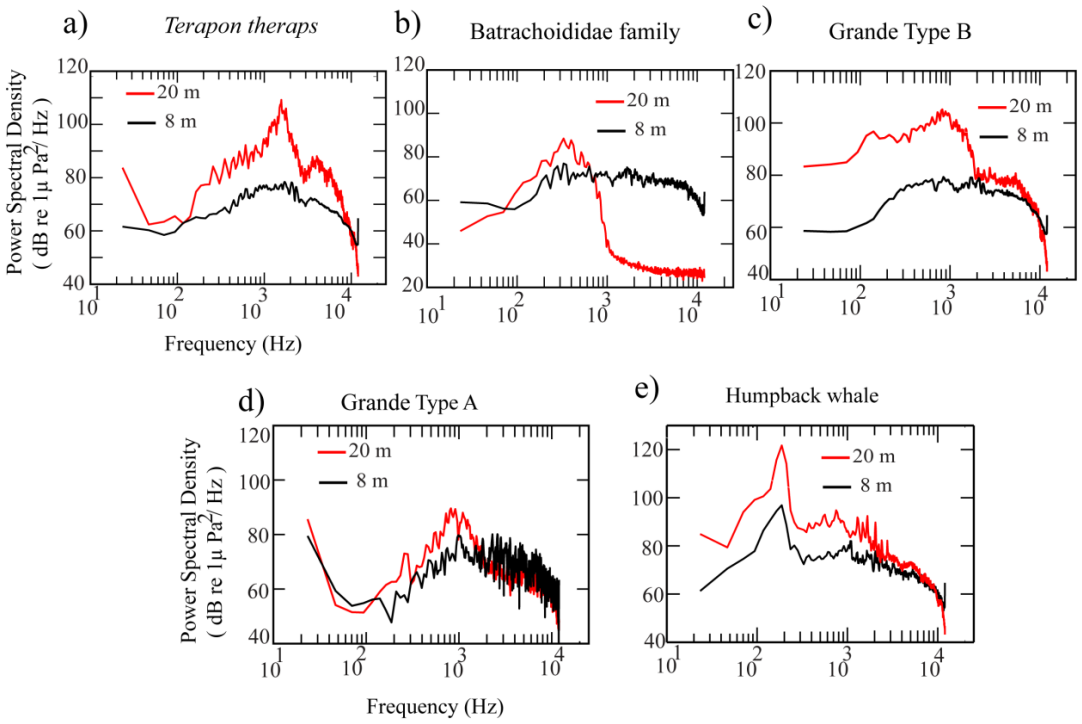

Fig. 3.14 PSD of the time series data of different fish sound acquired simultaneously using two SM3M systems moored at locations 6 and 7 at the water depth of 20m and 8m respectively. The frequency peaks are found to be higher for *Terapon theraps*, Grande Type A and Humpback whale sound for locations 6 in comparison with 7. The peaks are indistinct for Batrachoididae (Toadfish) and Grande Type A for location 7 though the frequency peak PSDs are comparable.

3.5.7 Fish sound characterization off Grande Island in 2016 (Location 8)

The concatenated PSD plots in time and frequency axes of broadband passive acoustic data for Grande Island location (Fig. 2.1) off the reef at 20m water depths are depicted (Fig. 3.12 c). The soundscape data reveals fish choruses from 14:00 to 03:00 hr of 10-14 March 2016. Three different sound regions within concatenated PSDs starting from (16:00 to 18:00 hr), (19:00 to 22:00 hr) and (00:30 to 02:00 hr) are observed attributed to three different fish sound types. The call patterns are repetitive for every day, and timings are routinely observed. No fish sounds are observed within the (03:00 to 11:00 hr) as depicted (Fig. 3.12a). Off reef Grande Island at 20m water depth from location 8 provides, nine hundred forty fish calls (Table 3.2) of Sciaenidae (common name: croakers and drums), which is indicated as '1' are recorded (Fig. 3.12c) (Ramcharitar *et al* 2006). The waveform, spectrogram, and PSD ofa single

call (Fig. 3.16a-c) reveal that the peak PSD of a single call (708.50±49.44)Hz. The callduration (0.125± 0.025 s) and a number of pulsespercall (7.20±1.70) are also tabulated (Table 3.2).

Recording of 'trumpet' like sound mostly during the period(19:00 – 22:00 hr) indicated as '2' depicted (Fig. 3.12c). Inter-call-duration (1.09±0.63 s), and single call duration and numbers of pulses per bouts were observed to be (0.240± 0.023 s) and (21.40±3.78) respectively (Table 3.2). The waveform, spectrogram, and PSD of calls from recording near Grande Island (Fig. 3.16d-f) confirm the sounds were from *Terapon theraps* fish species (McCauley and Cato 2000; Mahanty *et al*., 2015).The PSD of the calls shows a frequency peak at (1523.00±26.42 Hz). *Terapon threaps* call signals of 2115 are recorded from this location in four days in comparison with the recorded calls of 2650 from location 6 during 2017 for nine days.

The concatenated PSDs of time series within 00:30 to 02:30 hr also show (Fig. 3.12c) fish sounds which are indicated as '3'. Family or species of this fish based on the sound could not be identified. However the dominant presence of this species could be established from the analysis of the present data (total calls of 1850). The waveform, spectrograms, and PSD are also presented for the representative single call (Fig. 3.16g-i). The PSD of the single call shows a frequency peak at (1028.00±84.41Hz). Single call duration and numbers of pulses per bouts were observed to be (0.167± 0.020 s) and (18.20±2.11) respectively. This type of fish sound is mentioned as a Grande Type A (Table 3.2) also in location 6 where 5250 calls were reported for nine days. The selected fish call parameters from location 8 are presented (Fig. 3.16a-f). Distinct patterns for Sciaenidae, *Terapon theraps* and unknown fish family/species of Grande Type A for chosen parameters are shown in the scatter plot.

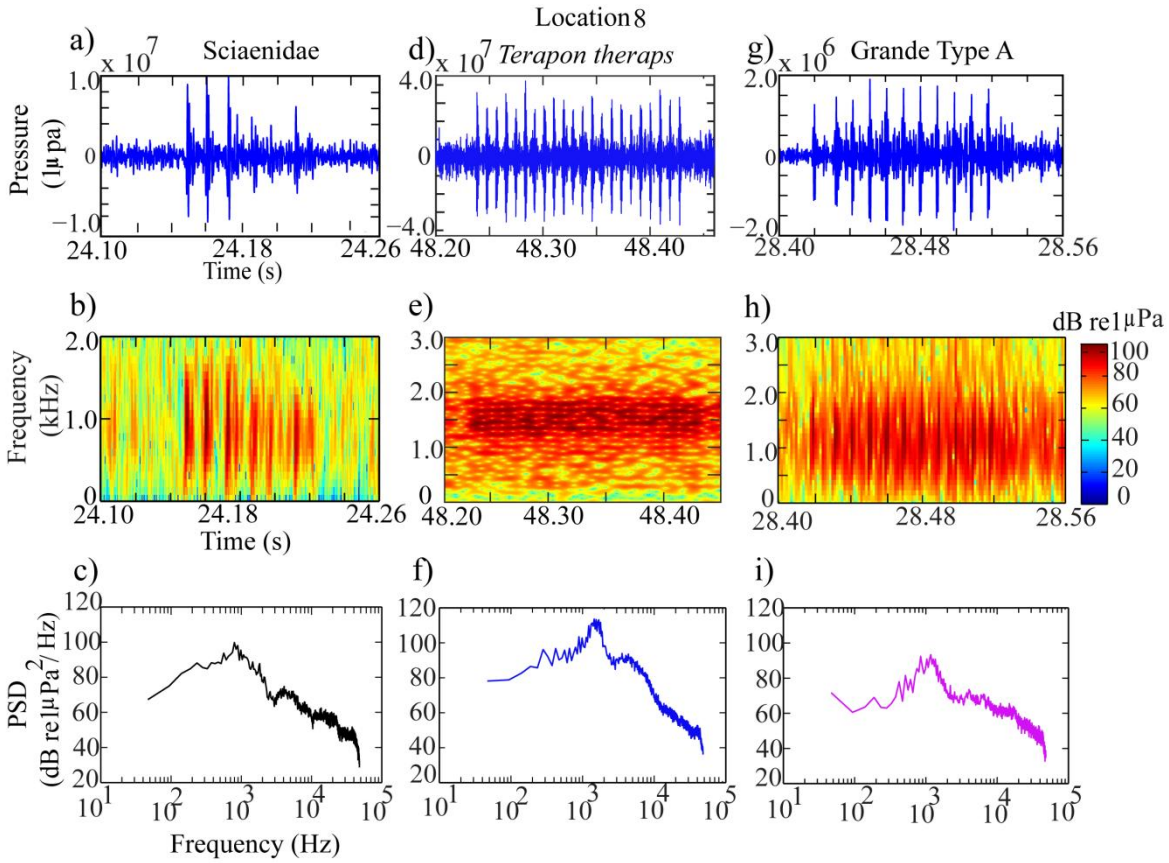

Fig. 3.15 Waveform, spectrogram and PSD of representative individual fish call: (a-c) Sciaenidae , (d-f) *Terapon theraps*, (g-i) Grande Type A from location 8.

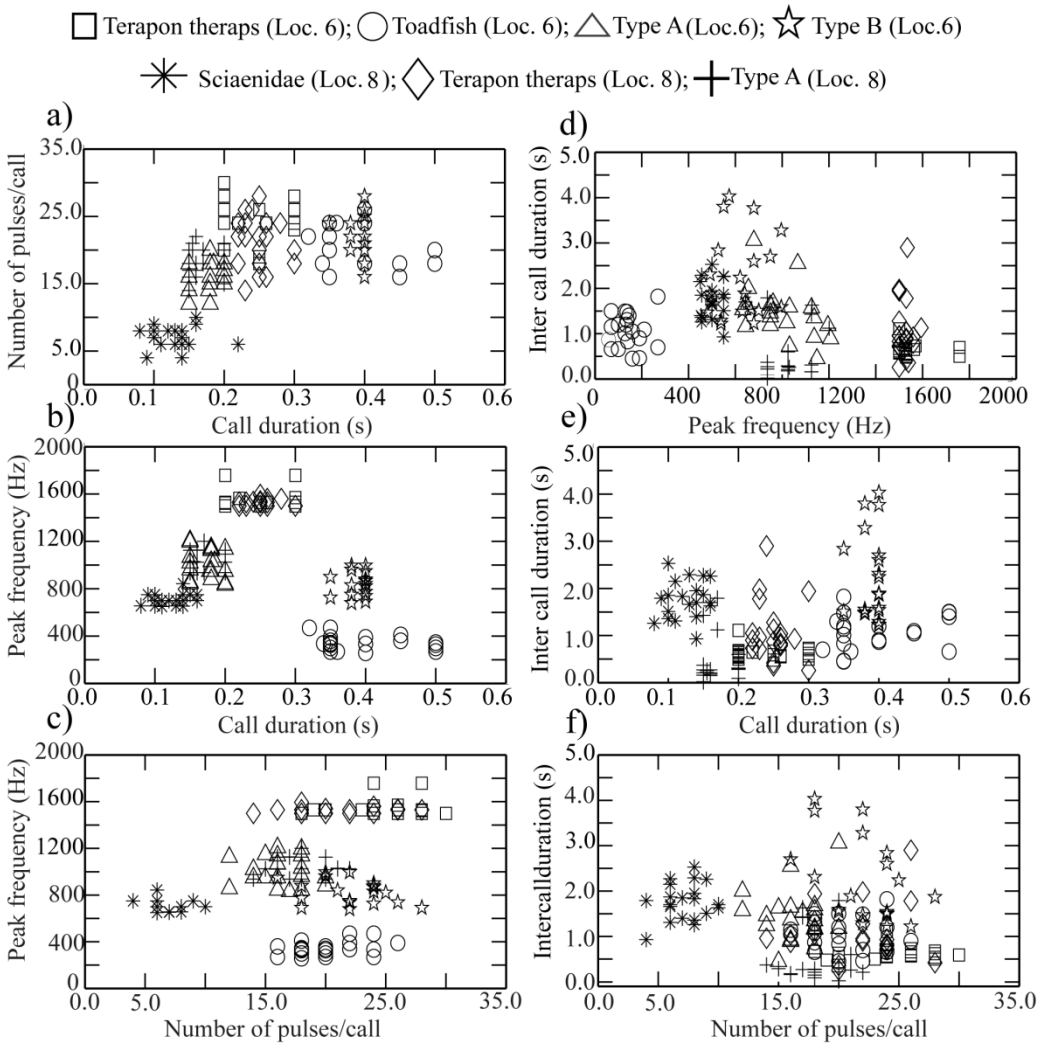

Fig. 3.16 (a-f) Scatter plots between the temporal parameters [call duration (s); no. of pulses/call; inter-call-duration (s) and spectral parameter (PSD peak frequency)] for single calls for identified fishes from locations 6 and 8.

3.6 Conclusions

Here, the underwater soundscape of the eight locations from the Goa and Malvan, Maharashtra are presented. Besides soundscape, calls of individual fishes are segmented using a semi-quantitative technique which is shown (Fig. 3.2). Peak PSD of each fish call from eight locations was estimated. Besides that, the temporal parameters of the fish calls are calculated. Scatter plots between the parameters of the call signals also show a pattern, which helps in identifying the fish sound.

Identification of the Toadfish calls from mangrove dominated Mandovi estuary (Location 1) is made. *Terapon theraps* fish species sounds are reported from the Grande Island of Zuari estuary (Location 2) and Sal estuary (Location 3) off Betul. Along with the short term biophony data from these three locations, recording of the wind, current speed and water temperature data are made.

Towards the deeper part of the Grande Island at 30 m water depth (Location 4), "Barred Grunt" (*c.nobilis*) fish sound is reported, and their characteristics are presented. Report on the recorded fish sound from Malvan, Maharastra includes: Terapontdie (*Terapon theraps)* fish chorus producing trumpet-like sound as well as very limited fish sound data from Carangidae. Besides these two fish families, the recorded fish sounds are not identifiable, which is mentioned as Malvan Type A. For this fish type data, peak PSD of call signals suggest Terapontidae fish family, however, temporal call parameters are not identifiable as depicted in scatter plot [Fig. 3.8 (a-f)].

For location 6, the data are recorded for nine days from 14-23 March 2017. Two identified fish families are Terapontidae *(Terapon theraps)* and Toadfish. Though, calculation of the temporal and spectral parameters from recorded data is carried out for other two fish sounds, identification of the fish family/ species is incomplete. These two fish types are mentioned as Grande Type A and Grande Type B from this location 6.

Call signals recorded from 1-14 March 2016 (for four days) having 20m water depth from Grande Island (Location 8) reveal two fish species/family: *Terapon theraps* and Sciaenidae. The third type of fish sound records from this location is mentioned as Grande Type A. Interestingly, a clear look at the spectral and temporal parameters of Grande Type A of location 6 and Grande Type A of location 8 is found to be overlapping in the scatter plot [Fig. 3.16 (a-f)], which suggest that both the fish families are similar.

Chapter 4

Fish sound characterization using Multifractal Detrended Fluctuation Analysis

4.1 Introduction

Many fish family uses vocal signal during their activities and produce sounds using sonic muscles that vibrate the swimbladder or rubbing of bony elements (stridulation) (Fine and Parmentier, 2015). The passive acoustic data recording using an autonomous system with wideband hydrophones are imperative for fish sound data recording (Au and Lammers, 2016). In this study,fish vocalizations are recorded using a passive acoustic device from the shallow water locations of two major estuarine systems. Fish sound identification under captive conditions and related difficulties are not unknown and discussed elaborately in chapter 3 (Akamatsu *et al*., 2002). The tank dimension, maintenance of oxygen level and effect of chronic aquarium noise exposure to fish health within the tank are major hindrances to study the fish behavior under captive environment. Therefore, in recent years *in situ* passive acoustic data recordings and analyses became increasingly popular (Mahanty *et al*., 2018).

In general, the temporal and spectral characteristics of fish calls such as oscillogram, spectrogram, and peak sound level of the power spectral density (PSD) (Table 4.1a) allow fish family identification (Fish and Mowbray, 1970). The power spectrum encompasses several dominant frequencies, which presumably represent major oscillation modes in the fish sound, but the amplitudes of these modes may vary in a complex manner **(**Chakraborty *et al*., 2014a**).** The animal vocalizations are frequently characterized by two basic parameters, namely, the dominant and peak frequency (Tricas and Boyle, 2014). Colson *et al*., (1998) compared the peak frequency derived from the fish vocalization. However, the peak frequency is found to be fluctuating, which may be ascribable to the phase couplings observed across temporal scales in the fish call train (Haris *et al*., 2014), for example the Toadfish and Sciaenidae studied here (Fig. 4.1a, b). The insets in panels (a) and (b) show temporal variation of the local Hurst exponent $H_t$in call signals. The computation of H_t is advantageous to identify the time instant of structural changes within the time series (Ihlen, 2012). The standard second-order spectral analyses (power spectrum and spectrogram) are 'phase blind', (Higuchi *et al*., 1990) and we need bispectral or higher-order statistical methods to identify phase coupling. The power spectral density based analyses are not effective for such nonlinear signals due to the presence of large fluctuations, especially at high-frequencies and the use of a nonlinear technique to characterize recorded fish sound data (Rice *et al*., 2011) is a necessity. Therefore, here we investigated "nonlinearities" in fish sound by MFDFA. We include surrogate and shuffled series tests to make sure that the multifractal spectrum width is generated by "nonlinearities" and not from multifractal noise. We found shuffled series provides smaller multifractal spectrum width in comparison with the original time series. This suggests a significant influence of "nonlinearities" in the fish sound. The combined use of the MFDFA and surrogate/ shuffled series test can detect the considerable influence of phase couplings across temporal scales that generate the intermittency (i.e., burstiness) in the fish sounds studied here. Previous studies have reported such complexities in seahorse (*Hippocampus Kuda*) feeding clicks due to nonlinearities in the sound production system (Chakraborty *et al*., 2014a).

The nonlinear phenomena in animal vocalizations are common, and now being used to understand the bioacoustics observations including family description (Tokuda *et al*., 2002). Therefore, the application of nonlinear signal processing techniques is important to describe complexities of animal vocalizations, and have been hypothesized to take an important role in individual identification. Multifractal system (Mandelbrot, 1989; Ivanov *et al*., 1999), is a generalization of a fractal system in which a single scaling exponent is not enough to describe its dynamics. Instead, a continuous spectrum of exponents (so-called singularity spectrum) is needed. The MFDFA was first conceived by Kantelhardt *et al*., (2002). This method has been applied to study the multifractal scaling behavior in feeding clicks of seahorse (*Hippocampus Kuda*) (Haris *et al*., 2014). Accordingly, in this work, the MFDFA is used to evaluate its effectiveness in distinguishing two fish family vocalizations (Toadfish and Sciaenidae).

Toadfish produce sounds by contracting its fast intrinsic sonic muscles attached to large areas of the swimbladder. Sounds include boatwhistles (produced by rapid, sustained sonic muscle contraction), and grunts (agonistics sounds) (Tower, 1908). The members of the Batrachoididae family such as *Colletteichthys occidentalis* are usually called Toadfishes (Greenfield, 2012), which have been reported in the Arabian Sea. Sciaenidae is a family of fishes commonly called drums or croakers. Sciaenidae have extrinsic sonic muscles originate on other muscles which are superficially attached to the swimbladder. Sciaenidae sounds range from pulsed to tonal produced by a rapid contraction of the sonic musculature. Both the fish family produces sound using sonic muscles that vibrate the swimbladder. There is a long history of many elegant studies of fish sound generation involving neural, muscular and hormonal mechanisms (Bass and Ladich, 2008).

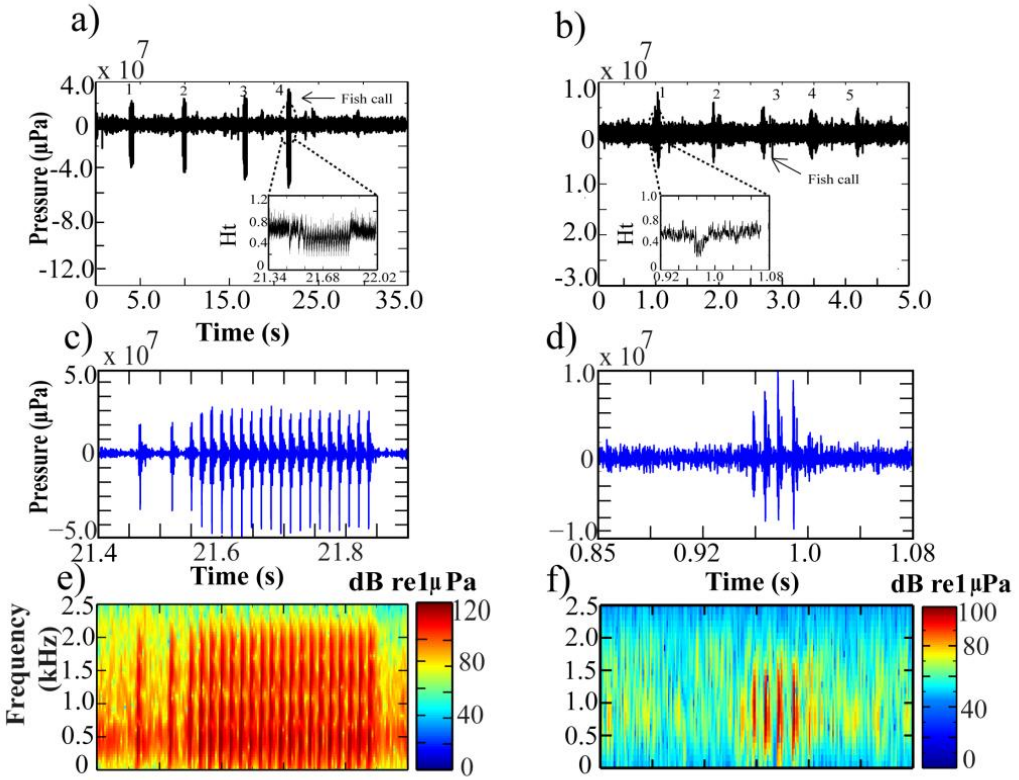

Fig. 4.1 (Color online) Example oscillogram of Toadfish and Sciaenidae are depicted in panel (a) and (b). The inset in panels shows an example for temporal variation of the local Hurst exponent H_t in the respective fish calls, highlighting the time instant of structural changes. The spectrogram analyses show undulation in the signal (c and d) with several dominant frequencies ranging between: (e) 0.1 – 2.5 kHz for Toadfish and (f) 0.5 – 1.5 kHz for Sciaenidae (see introduction section for more details).

Table 4.1(a). Details of fish calls and corresponding peak frequencies.

Duration of deployment	**Deploy-ment depth (m)**	**Fish type**	**Indivi-dual call duration (s)**	**Number of pulses per call**	**Peak frequency (Hz)**
13-14 March 2014 (14:00 - 13:30)	5	Batrachoi-didae (Toadfish)	0.25-0.60	10-38	470±52
10-11 March 2016 (14:00 -10:30) hr	10	Sciaenidae	0.04-0.10	4-10	700±54

4.2 Materials and Methods

The present study utilizes passive acoustics data acquired from two shallow and littoral environments in Goa, India: i) off *Britona* near *Chorao Island* in the Mandovi estuary (Location 1), and ii) the *Grande Island* in the Zuari estuary (Location 6), two major estuarine systems in Goa, India. The study location details can be seen in chapter 2 (Fig. 2.1) (Sreekanth *et al*., 2015). The Toadfish sounds were recorded off *Chorao Island* at 7m water depth. The Sciaenidae sounds were recorded off *Grande Island* at 20m water depth.

Modern autonomous underwater acoustic recorders, the Song Meter systems (www.wildlifeacoustics.com) (SM2M+) were used for the experiments conducted to acquire fish sound data for this study. The data was recorded with sampling frequencies of 44100 and 96000 Hz, respectively for deployments off *Chorao Island* and *Grande Islands*. The Song Meter hydrophones (standard acoustic type) possess bandwidth of 2-48000 Hz, and the details are provided in chapter 2.

The spectral characteristics of fish calls were calculated by applying spectrogram and PSD analyses. Individual call details of both fish families are given (Table 4.1a). The PSD analysis for peak frequency estimation was performed using Matlab and temporal details of the waveforms are provided in chapter 3 (Table 3.1). The extraction of noise-free fish sound is needed before applying the MFDFA, and the same is also covered (section 3.4 of chapter 3).

The fish sound may exhibit a broad power spectrum with many subsidiary peaks. The phase coupling behavior complicates the detection of peak frequencies in the data. This can be corroborated by the spectrogram analyses provided (Fig. 4.1e, f). MFDFA can provide satisfactorily good results when the input signals (fish sounds) are noise-like time series. The time series can be realized as noiseas if the Hurst exponent H_t in the standard detrended fluctuation analysis (DFA) varies between 0.2–0.8. The MFDFA can be employed directly in such instances without transforming the signal (Ihlen, 2012). The local Hurst exponent H_t values of Toadfish and Sciaenidae analyzed in the present study were restricted within 0.2 to 0.9 (see the inset in Fig. 4.1a and b). Therefore, as suggested by Ihlen (Ihlen, 2012), the time series does not require any mathematical operation before performing MFDFA. The MFDFA followed herein has several advantages over the standard power spectral density (PSD) analyses. Previous analyses (Chakraborty *et al*., 2014a) using PSD has focused on the quantification of the single power-law exponent β(i.e. monofractal feature) to study the seahorse clicks. However, the results of the further study (Haris *et al*., 2014) affirm that the fish sounds are intrinsically complex and require multiple exponents for its characterization.

4.3 MFDFA Technique

In this section, the MFDFA technique (Kantelhardt *et al*., 2002) is briefly presented. In general, the MFDFA comprised of five major steps. The first step involves the subtraction of the mean $< x >$ from the fish sound time series x_k of length N to determine the cumulated data series $Y(i)$. In the second step the resulting profile $Y(i)$ was divided into non-overlapping segments $\left[N_s \equiv int\left({}^{N}/_{s}\right)\right]$ of equal length , and the local linear trend for each of the segment was calculated in the third step by a least-square fit of the series to determine the variance

$$F^2(s,v) \equiv \frac{1}{s}\sum_{i=1}^{s}\{Y[(v-1)s+i]-y_v(i)\}^2, \qquad (4.1)$$

for each segment $v = 1, \ldots, N_s$, where $y_v(i)$ is the fitting polynomial in the segment$v$. In the fourth step, the average overall segments were computed to obtain the q^{th} order fluctuation function

$$F_q(s) \equiv \left\{ \frac{1}{N_s} \sum_{v=1}^{N_s} [F^2(s,v)]^{q/2} \right\}^{1/q}, \qquad (4.2)$$

where the index variable q can take any real value except zero. These fluctuation functions depend on the time scales s for different values of $q[-5\ to\ 5]$. In the fifth step, from the slopes of the plot between $log_2[F_q(s)]$and $log_2(s)$for a range of $q$the scaling behavior of the fluctuation function was determined. If the series x_k has long-range power-law correlations, $F_q(s)$ scales with s as

$$F_q(s) \sim s^{h(q)}. \qquad (4.3)$$

The function $h(s)$is a generalized Hurst exponent. Another way to characterize a multifractal series is the calculation of the singularity spectrum $f(\propto)$, which is related to the classical multifractal scaling exponents $\tau(q)$ via a Legendre transform as $\propto = \tau'(q)$ and $f(\propto) = q \propto -\tau(\propto)$. Here, $\propto$is the singularity strength or Holder exponent, while $f(\propto)$ denotes the dimension of the subset of the series characterized by $\propto$. Referring to Eq. (13) of (Kantelhardt *et al*., 2002), $\propto$ and $f(\propto)$ can be directly related to $h(q)$ as

$$\propto = h(q) + q\big(h'(q)\big) \text{ and } f(\propto) = q[\propto -h(q)] + 1 \qquad (4.4)$$

In a multifractal formalism, the Hurst exponents provide information on the degree of call smoothness (or roughness). Twenty representative calls were used from each fish family for the MFDFA. From Table (4.1a), the fish call durations are observed to be in the range of 0.25 to 0.6 s (for Toadfish) and 0.04 to 0.10 s (for Sciaenidae). With sampling frequencies of 44100 and 96000 Hz used during data acquisition, the average data sample numbers *N* (within the call duration) of Toadfish and Sciaenidae were 17200 and 12384 respectively. Due to the different sampling frequencies used, the data sample numbers extracted for analyses are also different. A local slope computation was necessary (Green *et al*., 2014) to identify the equal scaling range between these two data sets. For local slope computation, suitable segment size (s)

was chosen from minimum (16) to maximum $\left({}^{N}/_{4}\right)$ i.e., 3121 and 4300 for Sciaenidae and Toadfish respectively. The computed local slopes are found to be reasonably constant up to $s = 256$ for three values of q ($q = -5, q = 0, q = +5$). The range of scales (s) for the computation of $F_q(s)$presented in this work is chosen within 16 - 256. This range of scaling was then used to calculate the multifractal spectrum with the polynomial order (*m=1*).

4.3.1 Generalized Hurst Exponent $h(q)$ and Singularity Spectrum $f(\propto)$

The understanding of fish sounds using MFDFA is practicable by analyzing the graph of $q$versus $h(q)$. The fish calls would be a monofractal if $h(q)$is constant for all values of q (Kantelhardt *et al*., 2002). The width of $h(q)$ the curve$[\Delta h(q) = hqmax - hqmin$ shows a measure of the multifractality and indicates the deviation from monofractal behavior. Similarly, $\propto$ versus $f(\propto)$ (multifractal spectrum) can also provide information about the multifractality. If the $f(\propto)$curve (i.e. multifractal spectrum) of fish call converges to a single point, it can be a monofractal. The width of $f(\propto)$ the curve$[W = \propto_2 - \propto_1]$ also underlines a measure of multifractality and indicates the deviation from monofractal behavior. The width W would be small (e.g. background signal) and tend to zero in the case of a monofractal series. The unvarying $h(q)$reduces $f(\propto)$ spectrum to a narrow width and considered as monofractal series. Computation of an additional parameter $(B) = \left[\frac{(\propto_2 - \propto_1) - (\propto_0 - \propto_1)}{(\propto_2 - \propto_1)}\right]$, which measures the degree of asymmetry of the multifractal spectrum is carried out (Chakraborty *et al*., 2014b).'B' value indicates the dominance of low or high fractal exponents and $\propto_0$ denotes maximum singularity. The value B is zero for symmetric shapes and positive and negative for right or left-skewed shapes respectively. A left-skewed spectrum denotes dominant low fractal exponent distributions, while the right-skewed spectrum implies the dominance of high fractal exponents.

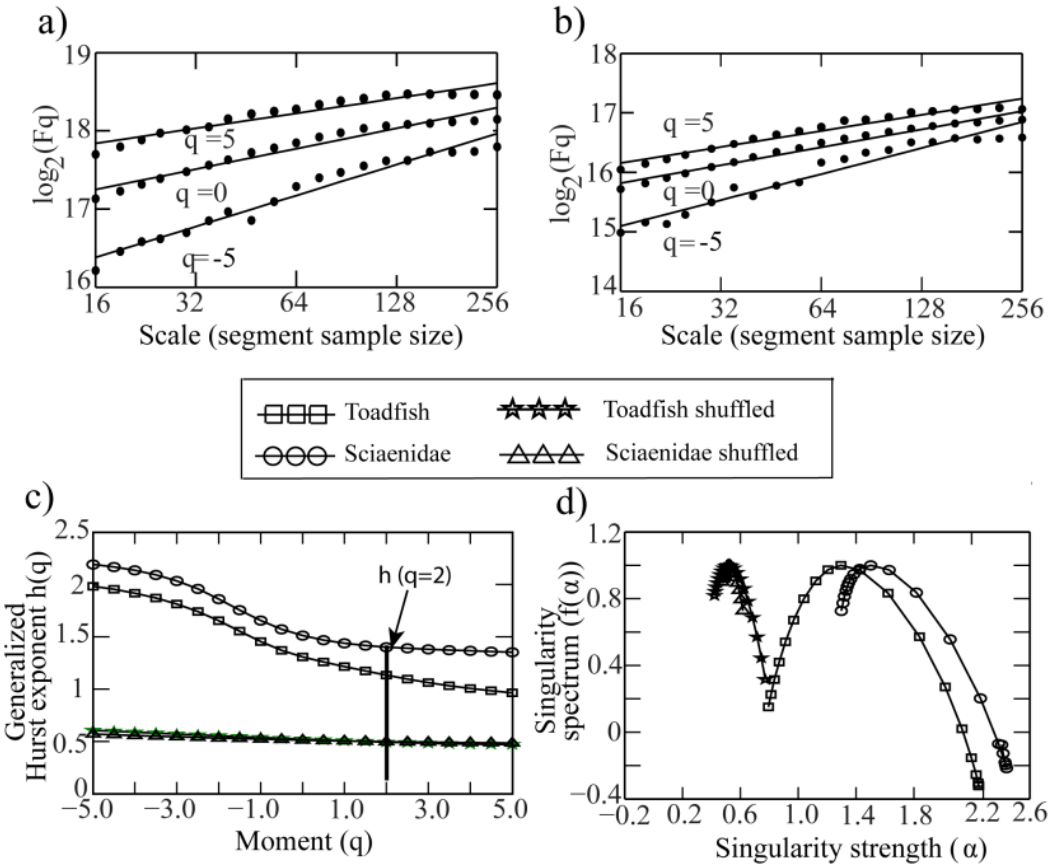

Fig. 4.2 Panels (a) and (b) represent Log-log plot of the fluctuation function $F_q(s)$ versus scale s for Toadfish and Sciaenidae respectively. Panel (c) and (d) depict generalized Hurst exponent $h(q)$ curve and singularity spectrum for a representative call of Toadfish, Sciaenidae, and corresponding shuffled signals.

4.4 Results and Discussion

Notably, the characteristics of Toadfish representative call train (Fig. 4.1a), single call (Fig. 4.1c), and related spectrogram (Fig. 4.1e) off *Britona* location are found to be matching well with the archived Toadfish sound (*.wav format) available at the Discovery of Sound in the Sea (DOSITS) website (www.dosits.org). Given the call interval of ~5 s (Fig. 4.1a), the recorded call duration and a number of pulses per call are observed to be 0.25-0.60 s and 10-38 respectively (Table 4.1a), indicating Toadfish boatwhistle sound (Mensinger, 2014). The PSD analyses of individual calls show a peak frequency of 470±52 Hz in comparison with the DOSITS archives (450 Hz). Fish sounds are usually not sharply tuned, therefore the difference in amplitude

at different peak frequency is quite likely due to the potential addition of spurious variability in the dataset. Call pattern (Fig. 4.1b) from the *Grande Island* location and the spectrogram of a single call confirms Sciaenidae sound (Fig. 4.1f) (Fish and Mowbray, 1970; Ramcharitar *et al.*, 2006). The PSD analyses of individual call show a peak frequency of 700±54 Hz. The call duration and a number of pulses per call for Sciaenidae are observed to be 0.04-0.10 s and 4-11 respectively (Table 4.1a).

4.4.1 Application of MFDFA

The log-log plots of $F_q(s)$versus s and corresponding regression slopes for the Toadfish (Fig. 4.2a) and Sciaenidae (Fig. 4.2b) are q-dependent (between -5 to 5), indicating multifractality and scaling behavior. The second-order Hurst exponent account for the overall root-mean-square (RMS) fluctuation in the data (Haris *et al*., 2014). The average $h(q = 2)$values for Toadfish and Sciaenidae are found to be 1.10±0.03 and 1.43±0.02 respectively (Table 4.1b). Mean values of the estimated parameters are presented along with the standard deviation in the table. Low standard deviation value suggests that the data points are closed to mean values. Similar lower values of the estimated MFDFA parameters are also depicted (Movahed *et al*., 2006). The $\Delta h(q)$ values can be used to describe the multifractality of representative fish calls (Fig. 4.2c). Greater multifractality [i.e. higher $\Delta h(q)$] were observed for Toadfish (1.05±0.08) in comparison with Sciaenidae (0.94±0.06) fish sounds. The shape parameters estimated from the $f(\propto)$ singularity spectrum also corroborates with this interpretation. The Wvalues of Toadfish and Sciaenidae show a higher degree of multifractality (Fig. 4.2d). Wvalues are significant for both Toadfish (1.55±0.08) and Sciaenidae (1.20±0.09) (Table 4.1b). The estimated B values for Sciaenidae and Toadfish are positive, highlighting the right-skewed multifractal spectrum. In comparison, the Sciaenidae possess higher B values (0.65±0.08), indicating high fractal exponents dominating the distribution as compared to Toadfish sound (0.22±0.07) (Fig. 4.3a).

The origin of multifractality in a time-series needs to be validated. Two basic sources of multifractality in the time-series are (i) multifractality due to long-range correlations of the small and large fluctuations and (ii) multifractality due to broad

probability density function (Kantelhardt *et al*., 2002; Chakraborty *et al*., 2016). Therefore, there is a need to verify the multifractality of fish calls analyzed in this study. The shuffled series for the individual call pattern is generated by applying a shuffling procedure that eliminates (Theiler *et al*., 1992) long-range correlations in the data. The $\Delta h(q)$ values computed with these shuffled series are 0.16±0.03 and 0.16±0.05, respectively, for Toadfish and Sciaenidae (Table 4.1b). Similarly, the estimated average $W$for Toadfish and Sciaenidae are (0.32±0.06) and (0.17±0.05) respectively (Table 4.1b). The validation process indicates that the shuffled series of fish calls show monofractal behavior. The $h(q=2)$ values of shuffled series are found to be 0.51±0.01 for both the fish family representative calls (Fig. 4.3c; Table 4.1b) . The origin of multifractality in a time-series can be attributed to broad probability density function if $h(q)$values does not change with the shuffling procedure, i.e. $\left[h_{original}\ (q) = h_{shuffle\,d}(q)\right]$. In this study, applying the shuffling and surrogate procedures to both the fish sound, it is found in the study that the recorded fish sounds (Toadfish and Sciaenidae) exhibit long-range correlation because the magnitudes of $h(q)$ and $h_{shuffled}\ (q)$ show significant differences (Fig. 4.2c) (Kranthikumar *et al*., 2019).

4.4.2 Characterization of Fish Sound Data Using MFDFA

Fig. 4.3(b-d) presents scatter plots of $\Delta h(q)$, W, and $B$with respect to the call duration (s) of two families, showing clustering pattern. For a non-stationary time series, the $h(q=2)$ values are greater than unity (Movahed *et al*., 2006) as observed in both fish families (Table 4.1b). In that case, the relation between h $(q=2)$and Hurst exponent (H) is given by $[H = h(q = 2) - 1]$. Accordingly, the Hurst exponent (H) is found to be 0.10±0.08 for Toadfish and 0.43±0.02 for Sciaenidae sounds, indicating anti-persistence Hurst exponent $H < 0.5$. Under such condition, the autocorrelation exponent γ and power spectrum scaling βcan be estimated using the relation: $[\gamma = -2H]$and $\beta = 2H + 1$. As shown in Table 4.1(b), for Toadfish, β and γ are (1.20±0.08) and (-0.20±0.09) respectively. Similarly, for Sciaenidae $\beta$and γ are (1.86±0.04) and (-0.86±0.04) respectively. These suggest that both Toadfish and

Sciaenidae fish sounds are long-range anti-correlated time series (Yu et al., 2011; Marmelat *et al*., 2012). Also, a higher β value for Sciaenidae indicates the series is comparatively smooth.

Recently, tremendous improvement is observed in the application of the statistical mechanics particularly to understand biological systems (Stanley *et al*., 1994). Long-range correlations appear as a ubiquitous phenomenon. Long-term data of healthy human heartbeats display scale-invariant long-range "anti-correlation" (a tendency to beat faster is balanced by a tendency to beat slower later on).More specifically, the appearance of long-range correlations in the healthy and young system and disappearance in the series produced by the aged and diseased system provide better understanding. Interestingly from the present study results, the long-range anti-correlation for Sciaenidae and Toadfish sound were observed. Besides the physiological aspect, one needs to understand the detailed sound generation mechanism of these fishes. In general, Toadfish generates few grunting sounds in association with the “boatwhistle” (Mensinger, 2014). Grunting sounds are considered as agonistic sound while the “boatwhistle” is known for courtship. A possible reason for observed anti-correlation for Toadfish sound may be related to the hybrid call type.

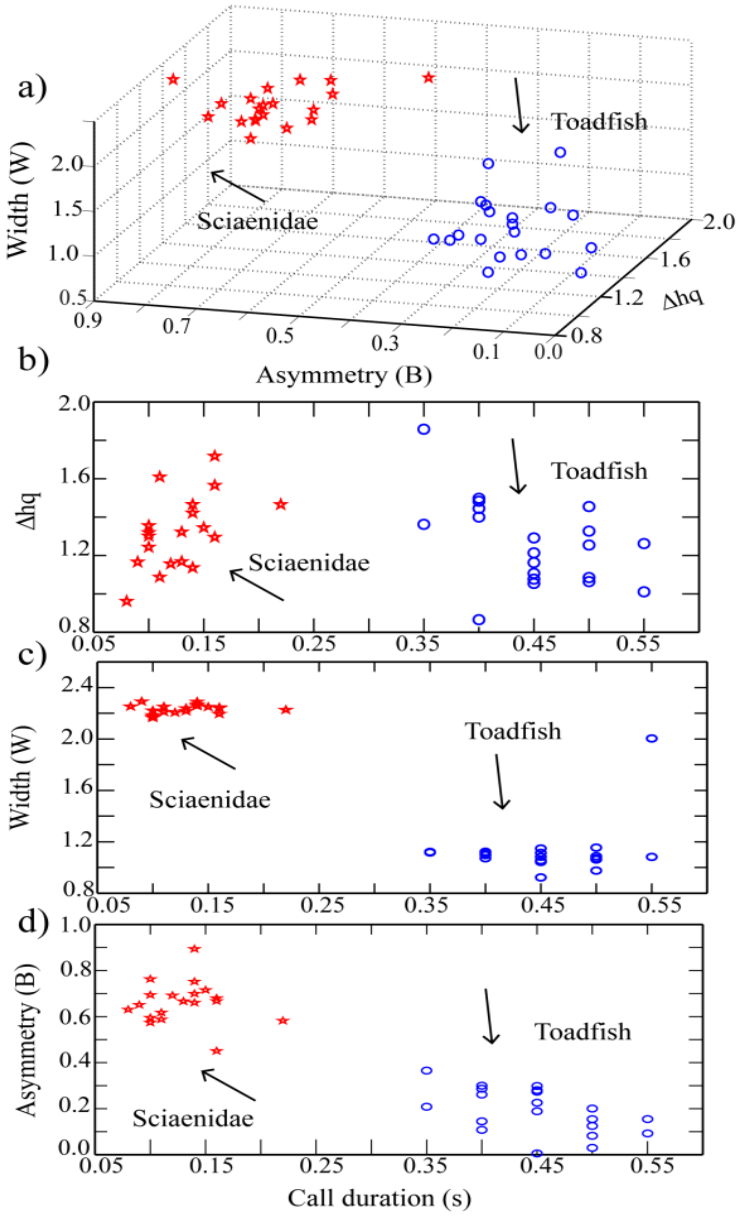

Fig. 4.3 Scatter plots of a) $\Delta h(q)$, W, and B for Toadfish, Sciaenidae; b) $\Delta h(q)$ versus call duration (s), c) W versus call duration (s), and d) B versus call duration (s). Plots are presented for the estimated parameters employing original signals.

Table 4.1(b) MFDA parameters calculated for original fish sound, shuffled, and surrogate data.

Time series type	$h(q=2)$	Δhq	w	B	H	β	γ
Batrachoididae (Toadfish)	1.10± 0.03	1.05± 0.08	1.55± 0.08	0.22± 0.07	0.10± 0.05	1.20± 0.08	-0.20± 0.09
Batrachoididae (Toadfish) Shuffled	0.51± 0.01	0.16± 0.03	0.32± 0.06	0.25± 0.05	0.51± 0.01	0.02± 0.03	0.98± 0.02
Batrachoididae (Toadfish) Surrogate	1.07± 0.04	0.80± 0.07	1.10± 0.08	0.33± 0.09	0.07± 0.04	1.14± 0.06	-0.14± 0.09
Sciaenidae	1.43± 0.02	0.94± 0.06	1.20± 0.09	0.65± 0.08	0.43± 0.02	1.86± 0.04	-0.86± 0.04
Sciaenidae Shuffled	0.51± 0.01	0.16± 0.05	0.17± 0.05	0.25± 0.08	0.51± 0.01	0.02± 0.02	0.98± 0.02
Sciaenidae Surrogate	1.38± 0.02	0.84± 0.08	1.14± 0.09	0.44± 0.08	0.38± 0.03	1.76± 0.04	-0.76± 0.05

4.5 Conclusions

The log-log plots of $F_q(s)$versus s and corresponding regression slopes for the Toadfish and Sciaenidae are -dependent (between -5 to 5), indicating multifractality.Toadfish and Sciaenidae fish indicate scaling behavior and small variance dominates the average $F_q(s)$. Second-order generalized Hurst exponent $[h(q=2)]$ values are found to be 1.10±0.03 and 1.43±0.02 for Toadfish and Sciaenidae respectively. Estimated values suggest that the Sciaenidae fish calls are comparatively smoother than the Toadfish.The smoothness observed here are due to the time series of the waveform data. Estimated Hurst exponents decide the smoothness of time series (Table 4.1b). The average value of the shape parameter $\Delta h(q)$ related to the $h(q)$ spectrum confirms the multifractal character of the Toadfish (1.05±0.08) and Sciaenidae (0.94±0.06). The average value of the W width of the multifractal spectrum) for both the fish sounds along with the degree of asymmetry (B) parameter also supports our multifractality observation. The high $\Delta h(q)$ and W values for both the fish family signify greater heterogeneity and multifractality.

Chapter 5

Influence of environmental parameters on fish sounds

5.1 Introduction

It is now possible to learn about the underwater environment through the measurement and evaluation of its ambient sound field (Lammers and Au, 2016). The term "soundscape" has been used by a variety of disciplines to describe the relationship between the landscape (or waterscape) and the relative composition of sound from various sources present therein (Pijanowski *et al*., 2011; McWilliam and Hawkins, 2013; Farina, 2014). It is important to investigate the variation in the sound field, which is comprised of biophony (e.g., fish chorusing), geophony (e.g., wind, waves breaking, tidal currents), and anthrophony (e.g., vessel sounds, etc.) (Erbe *et al*., 2015).

In shallow water, the ambient sound field generally consists of various types of sound sources such as biophony, anthrophony as well as the geophony. Here, fish sounds (biophonies), windand flow sounds (geophony), and boat sounds (anthrophony) are analyzed. The spatial structure of the sound field is dependent on the nature of the waveguide which is formed due to the multipath propagation between the sea surface and seabed (Jensen *et al*., 2011). Therefore, the characteristics of any signal received at a recorder's location can be affected by the variability in environmental parameters. While these propagation features are well recognized, this chapter is aimed at quantification of the soundscape and the fish sounds as received at

the recorders to serve as a representation in the experimental location, and for comparison of what others may receive from their environment in those locations.

The study locations here are well-known for tidal-stream influence such as seawater inflow, freshwater runoff, and salinity variations mainly during the southwest monsoon season (Singh *et al*., 2004; Fernandes and Achuthankutty, 2010). Moreover, the variability in the soundscape arises from bathymetric relief, proximity to an active shipping channel, frequent transits of small boat, and biological sounds. Therefore, the passive acoustic data collected by autonomous systems having hydrophones together with the ancillary data systems for wind, currents and water temperature. Knowing the cyclicity of these parameters can help eliminate diurnal signatures inherent to the soundscape. Water temperature is an important parameter for examination as the data collected currently have shown considerable variation at all the three study locations. Since the temperature affects sound speed, a correlation of sound pressure level and temperature may indicate a correlation with other variables that shift with temperature like salinity. Moreover, the temperature is a feature that animals respond to (Amron *et al*., 2017), hence if the sound pressure levels are driven by biotic signals, it would follow that a temperature change could affect a shift in overall sound pressure levels that could result in changes in the chorusing animals. Extensive analysis of the acquired dataset employing underwater active and passive acoustics (Haris *et al*., 2012; Nedelec *et al*., 2015) along with the wind, water temperature, and water flow of the locations has been carried out using Principal Component Analysis (PCA).

The study makes use of passive acoustic data from three ecologically important shallow water regions off Goa. The objective of the study includes fish species/ family identification making use of their vocalizations, andcharacterization of recorded biophony and geophony to understand the relationships.

5.2 Ancillary Data Acquisition

The studies related to fish sound identification has been explained in chapter 3. The present study investigates the influence of environmental data on time series data of fish sounds recorded from the three ecologically important sites (locations 1-3). The environmental conditions such as current speed, wind speed, temperature and tidal data were acquired from these locations. The flow measurement is important to determine the extent of ambient sound generation due to the water flow movement in the study areas. In addition to the deployment of Doppler current sensor, recordings of the sequential current velocity and temperature data using moored RCM (www.aanderaa. com) from all the three locations were carried out. The RCM has smart sensors for recording temperature, pressure, and conductivity. A delay interval of 300 s was enabled between the acoustic signal transmission/reception by RCM and the passive acoustic data acquisition system.The maximum current value measured was 0.40 m/s in the mangrove- dominated Britona (Location 1) in the Mandovi estuary (Fig. 5.1a). Interestingly, the magnitude of the measured current values was negligible (within the 0.20 m/s) in the other two locations (Fig. 5.1b, c). The mooring depth for the RCM system was fixed at 5 m, 17 m and 8 m for the locations 1, 2 and 3 respectively. Temperature measured using RCM at all the three locations is depicted in (Fig. 5.1d).

Furthermore, the meteorological parameters were measured using an autonomous weather station (AWS) (Mehra *et al*., 2010). The AWS provides digital data as 10-minute vector average of 60 samples recorded with 10-s intervals. The wind gust measurements are also recorded (i.e., the largest wind speed amongst an ensemble of 60 samples within the 10-minute sampling span). The wind data was acquired through the use of an AWS was installed on an anchored boat towards fore and aft direction. Wind data were acquired onlyfrom two sites, location 2 and location 3. The wind data collected from the two locations, Grande Island and Betul area are depicted in (Fig. 5.1b, c). Wind data from location 1 could not be collected due to unavailability of the AWS. The geographical position of the installed AWS was fixed using GPS.

5.3 Analyses of SPL_{rms} data

The root-mean-square sound pressure level (SPL_{rms}) were calculated for 2 minute-long files recorded every 15 minutes. The expression for SPL_{rms} in (dB re1µ Pa)is given below (Erbe, 2011):

$$SPL_{rms} = 20\log_{10}\left(\sqrt{\frac{1}{T}\int_t P(t)^2 dt}\right) \qquad (5.1)$$

Where P(t) is a root-mean-square (RMS) pressure level. Based on the published frequency ranges of the majority of fish calls, the frequency of snapping shrimp sound ranges from 100 to 20,000 Hz. Snapping shrimp sounds are usually above 3 kHz, while the fish sounds are much lower. Generally the two frequencies do not tend to overlap. The acoustic spectrum was partitioned into two frequency bands to focus on the dominant sound sources within each band (Kaplan *et al*., 2015). The low-frequency band (100 Hz to 2000 Hz) corresponds to the range in which most fish species vocalize. This band may also include noise generated by the winds (that can be higher) and waves. The high-frequency band (2000 to 20,000 Hz) encompasses the range (typically dominated) by the snapping shrimp. Boat noise covers a wide frequency band and may interfere with both the bands. Band-pass filtering involves the use of four-pole Butterworth filters in two frequency bands. The root-mean-square (RMS) of the sound pressure level (SPL_{rms}) was calculated at low-frequency (100 Hz to 2000 Hz) fish band, the high-frequency (2000 to 20,000 Hz) shrimp band, and the wideband (without filtering) for three locations is depicted in (Fig. 5.2a-c). Frequencies below 100 Hz represent mostly the flow noise (Bassett *et al*., 2014) that is highly interfering, and useful to isolate fish sound. However, the effect of flow noise may affect the RMS wideband sound pressure level.

At location 1, recordings of root-mean-square SPL_{rms} values of the wideband signal indicate variationsbetween 103-134 (dB re 1µPa) (excluding the sound impulses due to boat movement) (Fig. 5.2a). The SPL_{rms} (dB re 1µPa) is observed to have a maximum variation of 31dB re 1µPa. Due to the active flood and ebb tide in the river system near the mouth of the estuary, the SPL_{rms} is found to be periodically varying except during the slack tide period (Fig. 5.1a). Since the location is close to the mouth of river Mandovi, the effect of the water movement during the flood and ebb tide on the ambient sound is found to be contributing to an increased SPL_{rms} for

wideband signal, whereas the SPL_{rms} varies in the low-frequency fish band, and the high-frequency shrimp bands are absent (Fig. 5.2a). Occasionally sharp impulses are observed in the low-frequency fish band, but upon closer inspection, those are found to be due to boat movement. Besides the higher SPL_{rms} sound due to the toadfish sounds during the 21:30 - 00:30 hrs, the remaining part of the SPL_{rms} of the low-frequency fish band is nearly consistent (112.0±11.05 dBre 1µPa). A similar situation exists for high-frequency shrimp band where any traces of fish sound have not been identified (103.9±0.8 dBre 1µPa).

At location 2, Terapontidae chorus sound was recorded from 14:30 to 00:30 hrs (Fig. 5.2b) for SPL_{rms} of the wideband sound. Relatively quiet conditions were seen (SPL_{rms}= 103.9±0.8 dBre 1µPa) during 02:00 to 13:30 hrs, even during the higher wind speed (maximum 8 m/s) beyond 06:30-13:00 hr (Fig. 5.1b). Under these circumstances, a rise in SPL_{rms} (~29 dB re 1µPa) was observed between (101-130 dB re 1µPa). The SPL_{rms} due to the presence of fish species Terapontidae at location 2 for low-frequency fish band from Grande Island show comparatively higher (92-124 dB re 1µPa) values. Here, a rise in SPL_{rms} (32 dB re 1µPa)during the Terapontidae chorus period (Fig. 5.2b) was observed. Small differences (23 dB re 1µPa) in SPL_{rms} values were noted for high-frequency shrimp band.

In location 3, Terapontidae chorus sound was observed between15:30 to 23:00 hrs, and during the relatively quiet conditions between 01:30 to 13:30 hr (Fig. 5.2c). The variation in the SPL_{rms} is well within the (99-122 dBre1µPa) for wideband signal data. Excluding the boat noise, the maximum SPL_{rms} was found to be around 23 dB re 1µPa showing low ambient sound variation in Sal estuary. During 10:30-13:30 hr, the SPL_{rms} from Betul data shows a maximum difference of 19.0 dB re 1µPa among the Terapontidae chorusing time and bare fish calls of related species in the low-frequency fish band. A lesser amount of variation (~16.0 dB re 1µPa) in the SPL_{rms} values was noted in the case of the high-frequency shrimp band.

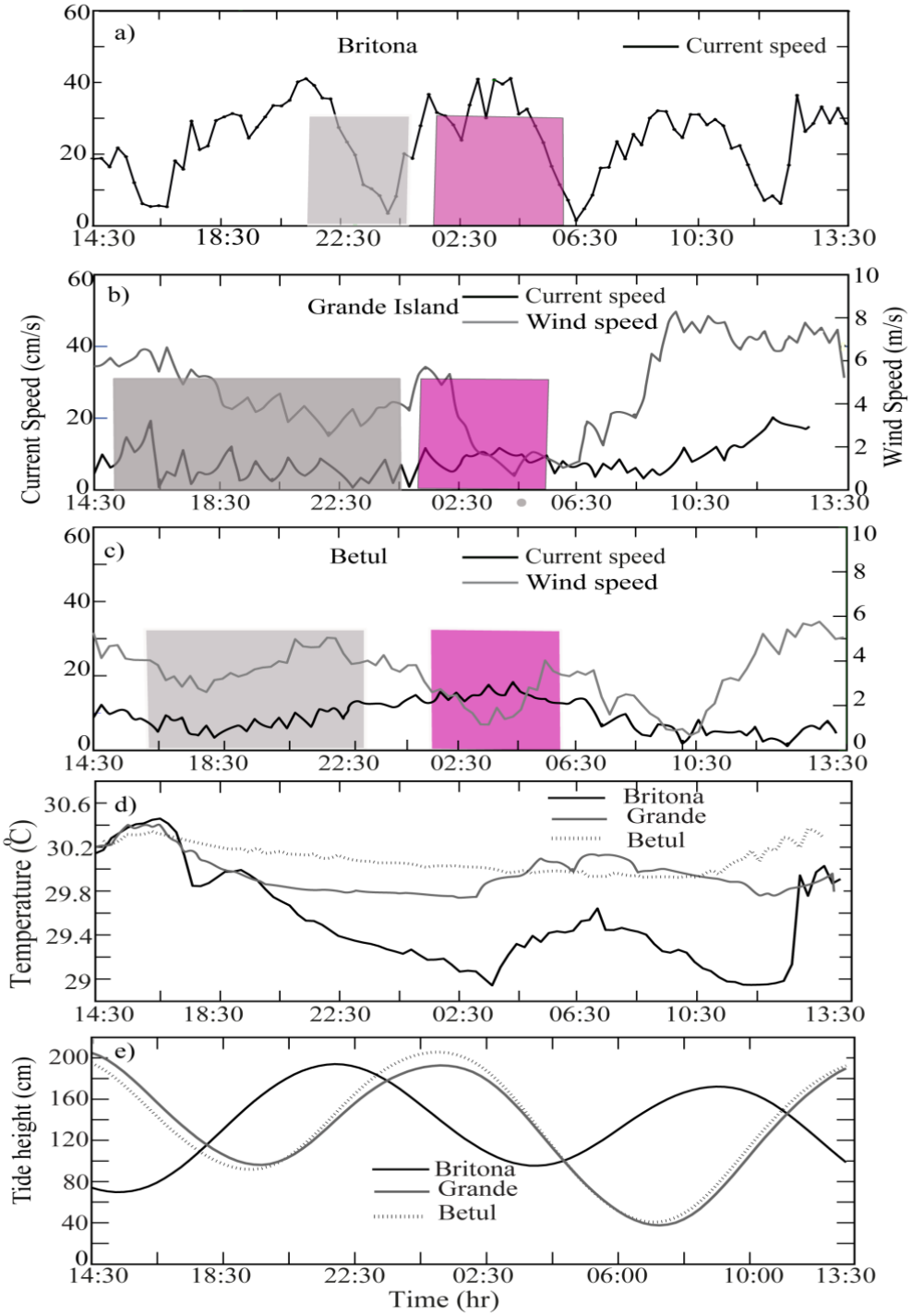

Fig. 5.1 Environmental parameters acquired at an interval of 15 min: a) current speed from Location 1; b) current and c) wind speed from Location 2 and Location 3 respectively (shaded areas in gray and magenta show fish and shrimp time segments respectively); d) measured temperature data from three locations; and e) predicted tide for the three locations. Tides are calculated based on the measured data from the Marmugao port area.

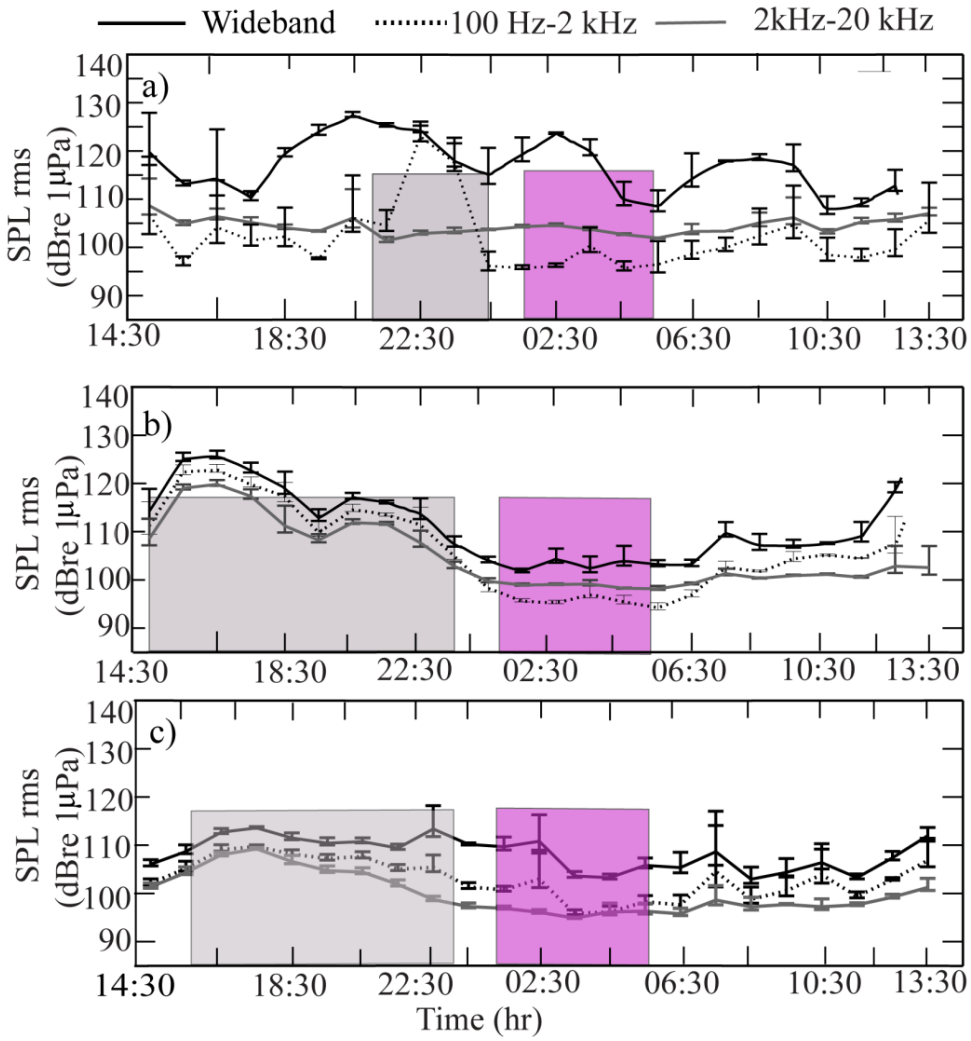

Fig. 5.2 Mean and standard deviations (with 25-75 percentiles) for each 15-minute interval passive acoustic data of 120 s SPL_{rms} (dB re 1µPa) concerning time (hr) for a) Location 1, b) Location 2, and c) Location 3.

5.4 Influence of environmental parameters on SPL_{rms} using cluster analyses

To characterize the relative contributions of biophonies (fish), geophonies (windand flow, etc.) and anthrophony (boats, etc.), cluster analyses were carried out with the application of principal component analysis (PCA). In the Mandovi estuary location, SPL_{rms} of wideband toadfish was observed to be a function of the water flow and temperature. In the Zuari estuary, the SPL_{rms} could be treated as a function of the

water temperature and wind. In the Sal estuary, the correlation coefficient of the SPL_{rms} and temperature was not significant enough, as compared to the other two locations. At location 3, it was the wind that largely influenced the SPL_{rms}. The present study reveals the relevant characteristics of biotic and abiotic sound signals in the ecologically important region off Goa.

Furthermore, to assess the influence exerted by the five (three of the Britona area) environmental parameters (current speed, current direction, wind speed, wind direction, and water temperature) vis-a-vis the SPL_{rms}, PCA was employed (Nedelec *et al.,* 2015). The present analyses involve the respective estimated SPL_{rms} and environmental datasets of the three locations. For each location, the environmental data was compared with three sets of SPL_{rms} - wideband, the low-frequency fish band (100-2000Hz), and high-frequency shrimp band (2000-20,000Hz) with respect to 1) fish time segment and 2) shrimp time segment. At first, the Pearsoncorrelation coefficient iscomputed of the measured parameters. Next, the PCA is carried out only for correlation matrices having 50 % components with good correlation coefficients (> 0.5) (Hristian *et al*., 2017). Based on that, nine sets of situations were found for the fish and the shrimp time segment data for the three locations and included those sets in the PCA (Table.5.1).

Location 1 of the tidal dominated Britona area showsthe highest correlation coefficient (0.668; p <0.0040), between the SPL_{rms} of the wideband signal and temperature during fish time segment between (21:30-00:30 hr), see (Table 5.1). SPL_{rms} is a measure of the overall recorded sound, which is used to observe the effect of environmental parameters from semidiurnal tide dominant sound in the shallow water depth (~7 m) of the estuary. Here, the PCA-based scatter plot (Fig. 5.3a) of thePC1 and PC2 suggests that the parameters e.g. SPL_{rms} (dB re 1µPa) and water temperature (Table 5.1) are controlling factors. The principal components (PC1 and PC2) together explain 92.97 % of the total variance in the data. This correlation could be ascertained through the evaluation of the time series data of the wideband signal (SPL_{rms}) (Fig. 5.2a) and temperature (Fig. 5.1d) data recorded during the fish time segment. A similar trend was also noticed in the measured current speed (Fig. 5.1a) and the predicted ebb tide (Fig. 5.3e) (based on the Marmagao harbor tide data). Interestingly, during that time period, the presence of toadfishsound could be detected

through SPL_{rms} of fish band data (Fig. 5.2a). At location 1, a conspicuous deviation in toadfish sound is observed during the ebb tide period where the water temperature also shows variation.

A strong correlation coefficient (0.669; p <0.0046) was obtained (Table 5.1) between the SPL_{rms} of the low-frequency fish band data with respect to the current direction during the fish time data segment. The principal components (PC1 and PC2) together could explain 90.07 % of the total variance in the data. PCA-based scatter plot between the PC1, and PC2 suggests that the parameters viz., SPL_{rms} (dB re 1µPa) and flow current directions are influencing factors (Fig. 5.3b). Prominentchanges in current direction occur during the flood or ebb tide due to thefresh and saline water movement along with the SPL_{rms} of low-frequency fish band data.

For the shrimp time segment, SPL_{rms} for wideband signal, show correlation coefficients (0.802; p $<5.3747e^{-06}$) with the current speed (Table 5.1). Similarly, principal components (PC1 and PC2) together explain 90.10 % of the total variance in the data. Within the same shrimp time segment, SPL_{rms} for high-frequency shrimp band also shows correlation coefficient (0.882; p $<5.7793e^{-05}$) with the current speed (Table 5.1). The principal components (PC1 and PC2) together explain 90.00 % of the total variance in the data. The first principal component accounts for 71.10% of the total variance. Variability of the current speed (Fig. 5.1a), the wideband sound signal as well as high-frequency shrimp band (Fig. 5.2a) contributes to better cohesion as compared to the low-frequency fish band data (Fig. 5.3 c, d).

From location 2, unlike location 1, wind-related data was acquired. Here, during the fish time segment, SPL_{rms} show good correlation coefficients with the temperature data for three situations. The correlation coefficients were found to be (0.802; p $<5.1822e^{-10}$), (0.762; p $<7.61e^{-09}$) and (0.774; p $<4.6684e^{-09}$) respectively for the wideband, the low-frequency fish and the high-frequency shrimp bands (Table 5.1). For the wideband sound data, the PCA-based scatter plot between the PC1 and PC2 suggests that the parameters viz., SPL_{rms} and temperature are influencing factors (Fig. 5.3 e). It was observed that the first two principal components (PC1 and PC2) together explain 68.35 % of the total variance in the data. The first principal component accounts for 49.50% of the total variance. Similarly, therelationship between the SPL_{rms} for low-frequency fish and high-frequency shrimp bands during the fish time

segment indicate similar processes in Grande Island. The PCA based scatter plot for low-frequency fish band within the fish time segment, PC1 and PC2 together explain 73.0% of the total variance (Fig. 5.3f). For high- frequency shrimp band, PC1 and PC2 together explain 73.48 % of the total variance in the data (Fig. 5.3g). In Grande Island, a higher correlation coefficient (0.703; $p < 0.0032$) between the wind directions with respect to the SPL_{rms} of the wideband signal during the shrimp time segment was also observed (Table 5.1). It was observed that the first two principal components (PC1 and PC2) together explain 65.5% of the total variance in the data (Fig. 5.3h). This phenomenon suggests the influence of wind data over the SPL_{rms} values of the wideband signal.

Location 3 from the Betul area of the Sal estuary shows a correlation coefficient (0.841; $p < 5.1247e^{-06}$) between the SPL_{rms} and wind speed for the shrimp time segment of the chosen high-frequency shrimp band (Table 5.1). It was observed that the first two principal components (PC1 and PC2) together explain 84.72% of the total variance in the data. The wind speed is fluctuating, i.e., varying between the 0.50 - 5.0 m/s. A clear-cut cluster between the SPL_{rms} and wind speed was observed in Betul location (Fig. 5.3i).

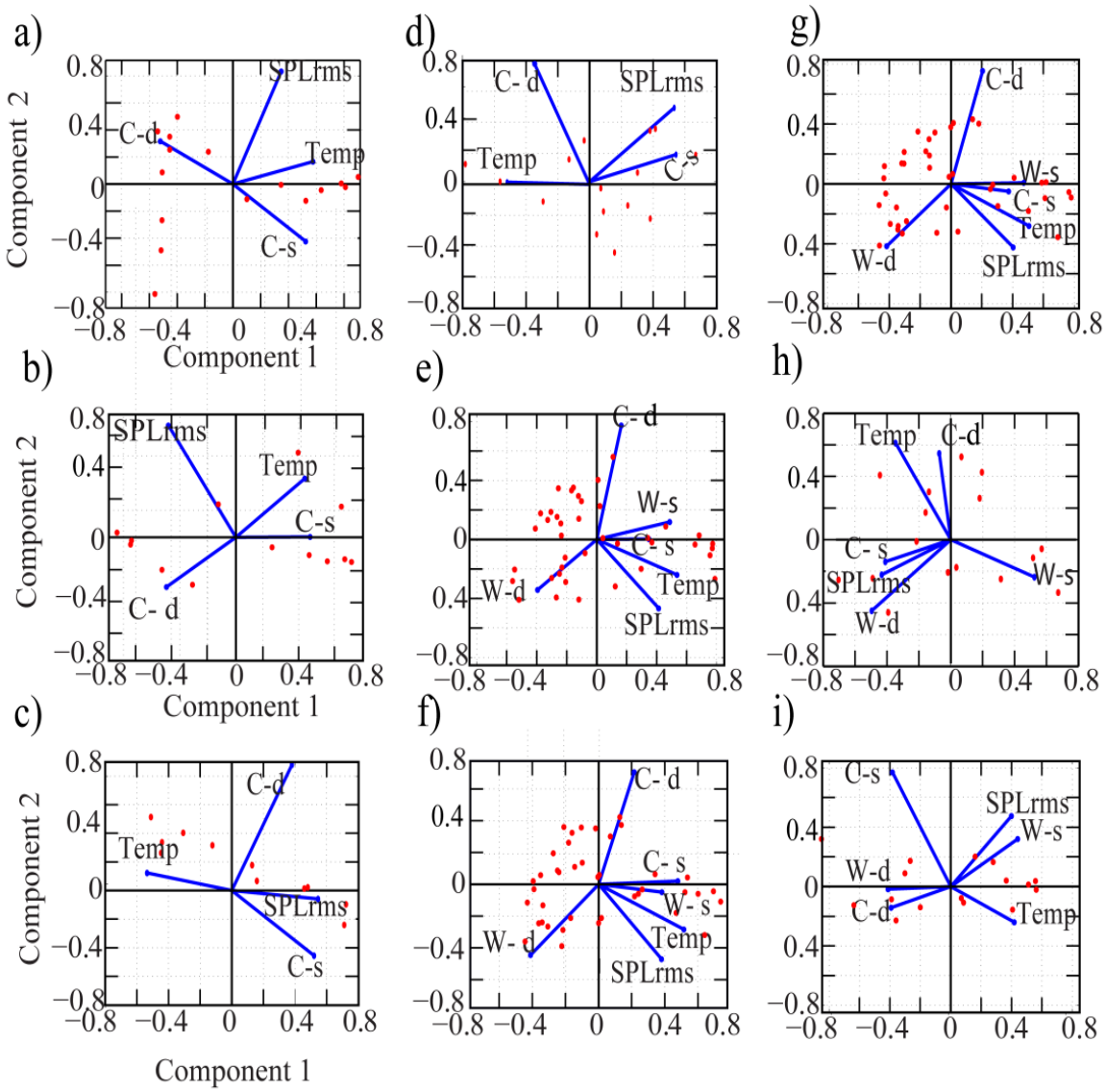

Fig. 5.3 Biplot of PCA for good correlation data with respect to the SPL_{rms}(dB re 1µPa) versus environmental parameters: PC1 versus PC2 for location 1: a) fish time segment for chosen original signal; b) fish time segment for chosen low-frequency fish band; c) shrimp time segment for chosen original signal; d) shrimp time segment for chosen high-frequency shrimp band. For location 2: e) fish time segment for a chosen original signal; f) fish time segment for chosen low-frequency fish band; g) fish time segment for chosen high-frequency shrimp band; h) shrimp time segment for chosen original signal. For location 3: i) shrimp time segment for chosen high-frequency shrimp band.

Table 5.1: Correlation Coefficient between the SPL_{rms} concerning the measured environmental parameters for three conditions of the sound signal during the fish and shrimp time segments

S No	**Loca-tion**	**Data time**	**Data type**	**Parameters**	**SPL_{rms} vs. Parameter having highest correlation**	***Correlation Coefficient**
1	Britona	Fish time segment (21:30-00:30)	Wideband	Current Speed; Current direction; Temperature	Temperature	r=0.668 p<0.0040
2		Fish time segment (21:30-00:30)	Low-frequency fish band		Current direct.	r=0.669 p<0.0046
3		Shrimp time segment (01:30-05:30)	Wideband		Current speed	r= 0.802 $p<5.3747e^{-06}$
4		Shrimp time segment (01:30-05:30)	High-frequency shrimp band		Current Speed	r=0.882 $p <5.7793e^{-05}$
5	Grande Island	Fish time segment (14:30- 00:30)	Wideband	Current Speed; Current direction; Wind speed; wind direction; Temperature	Temperature	r=0.802 $p<5.1822e^{-10}$
6		Fish time segment (14:30- 00:30)	Low-frequency fish band		Temperature	r=0.762 $p<7.61e^{-09}$
7		Fish time segment (14:30- 00:30)	High-frequency shrimp band		Temperature	r=0.774 $p<4.6684e^{-09}$
8		Shrimp time segment (01:30-05:30)	Wideband		Wind direct.	r=0.703 p<0.0032
9	Betul	Shrimptime segment (01:30-05:30)	High-frequency shrimp band	Current Speed; Current direction; wind speed; wind direction; Temperature	Wind speed	r=0.841 $p< 5.1247e^{-06}$

*'p' represents significance level. P<0.05 the correlation coefficient is called statistically significant.

5.5 Conclusions.

PCA based cluster analyses provide the number of variations that can be explained by sets of the auxiliary parameter for the recorded SPL_{rms}. In location 1 of a Mandovi estuary, SPL_{rms} was observed to be a function of the water flow and temperature. In location 2, SPL_{rms} was a function of the water temperature and wind data, whereas, for location 3, the correlation coefficient with the temperature was not that prominent as compared to the other two locations. In location 3, it was the wind that mainly influenced the SPL_{rms}.

Britona area (location 1) is close to the mouth of river Mandovi. The effect of the water movement during the flood and ebb tide on the ambient sound is found to be contributing to an increased SPLrms in low-frequency fish band data with respect to the current direction for fish time data segment. Prominent changes in current direction occur during the flood or ebb tide due to the fresh and saline water movement along with the SPLrms of low-frequency fish band data. Here, the flow noise may affect the wideband sound pressure level (Bassette *et al*., 2014).

In location 2, the temperature mainly influences on the *Terapon theraps* sound productivity, sound characteristics (intensity, frequency, and duration) were also changed along with the rise of water temperature and its impact on the existence of *Terapon jorbua* the changes in productivity and characteristics of sound that they produced (Amron *et al*., 2017). In Betul area (location 3), the correlation coefficient has been observed more due to local wind speed variation dominated over SPLrms(Mahanty *et al*., 2018)

These observations support the dominant relationship between the recorded SPL_{rms} and temperature especially from locations 1 and 2. The intensification of a sound generation with water temperature increases which influence the behavioral activity of marine animal (Putland *et al*., 2017; Farina, 2014). The study results suggest that passive acoustic is an important tool to understand the biological components in relation to the environmental variables.

Chapter 6

Estimation of Eco-acoustic Indices from Grande Island and Malvan reef systems

6.1 Introduction

In the underwater environment, the animal species use sound signal communication (Ladich, 2015). These aquatic animals utilise sound as their primary modality, whereas terrestrial animals use vision. Sound signals are produced by the fishes during their activities using the swimbladder or by rubbing its bony elements (stridulation) (Parmentier and Fine, 2016). The sound patterns created by the aquatic animals can be investigated through spectral analysis (Fish and Mowbray, 1970). Generally, employing power spectral density (PSD) analysis, the spectral peak frequency estimate is made use of to identify fish family/species.The waveform, spectrogram, and related spectral frequency peak are considered for the identification of species in a complex habitat environment (chapter 3).

Biodiversity assessment is a key step for habitat monitoring in shallow reef areas (Harris *et al*., 2016). Among the methods used in soundscape ecology, the automatic processing technique and the resulting metrics (Sueur *et al*., 2008a) provide promising results, particularly in the understanding of complex acoustic signatures. Acoustic complexity index (ACI)(Pieretti *et al*., 2011) is generally used to identify the temporal and spatial complexity of a soundscape. Similarly, acoustic entropy (H) based on the Shannon evenness index, is also utilized for examining the temporal and spectral

heterogeneity of the sound signal (Sueur *et al*., 2014). The acoustic richness index (AR) is modeled after H, but weights the signal by its median amplitude to account for background noise (Depraetere *et al.*, 2012). The ACI, H, and AR metrics are considered as suitable proxies for biodiversity estimation, presenting a fair estimation of acoustical characteristics with minimal post-processing of the recorded field data (Farina, 2014) if it can be appropriately ground-truthedto understand the role of fish behaviour in relation to the recorded fish sound. Investigation reported in the present chapter involves employment of eco-acoustic metrics (ACI, H, and AR) and SPL_{rms}.

In this chapter, the eco-acoustic analyses is carried out using soundscape data acquired using passive acoustics technique from location 5 (Malvan) and locations 6 and 7 (Grande Island) (Fig. 2.1). As indicated earlier, the Malvan site is located in the shallow and littoral environments, off the Sindhudurg district of the Maharastra state, on the west coast of India (WCI) (Anon, 2001). Here, the soundscape comprises of biotic and abiotic (wave-breaking sound) sounds (Fig. 3.10b), and the application of the eco-acoustic analysis is initiated to examine the acoustic signatures of entire recordings using the metrics ACI, H, and AR (Kranthikumar *et al.*, 2019). Detailed soundscape analysis and identification of fish families has been covered in the case of locations 5 (section 3.5.5 of chapter 3).

The present investigation also involves the eco-acoustic analyses from Grande Island, a coral reef system of Goa (Manikandan *et al.*, 2016). Recapping once again, the Grande Island is located at the central west coast of India, which is surrounded by coral reef habitat having diverse flora and fauna. The soundscape data in the present investigation has been simultaneously acquired from two locations: i) away from coral reef area at 20 m water depth (Location 6), ii) near coral reef area at 8 m water depth (Location 7). Correspondingly, the marine fish species/fish-families reported (in section 3.5.6 of chapter 3) correspond to location 6. At location 7, no distinct records of fish sound were recorded; however, the divers have observed a number of reef fishes (Hussain *et al*., 2016). Unlike location 6 (Fig. 3.12a), the soundscape record from location 7 reveals dominant background sound (Fig. 3.12b). The frequency peaks of the prominent PSDs from the time series data of locations 7 and 6 are found to be matching. However, the level of the spectral peaks (Fig. 3.14 in chapter 3) indicate decrease in peak levels for location 7 in comparison with the fish sound of

location 6. Employment of the acoustic metrics (ACI, H, and AR) is initiated to track the acoustic signatures of entire recordings from the two different locations i.e., the reef (location 7) and away from the reef (location 6). A presentation of the comparative study results, based on the eco-acoustic metrics of the two Grande Island regions along with the Malvan has been covered. Detailed soundscape analysis and identification of fish families found at location 6 is reported in section 3.5.6 of chapter 3.

6.2 Acoustic Metrics

In this section, three acoustic metrics are dealt along with the root-mean-square sound pressure level (SPL_{rms}). These three acoustic metrics are computed for three frequency bands (i.e. shrimp, fish, and wideband). In order to compute eco-acoustic indices, employment of soundscape ecology package *'Seawave'* (Sueur *et al.*, 2008b) has been resorted to for the R computing environment (https://cran.rproject.org/web/packages/seewave/index.html).

Besides the computation of acoustic metrics, the SPL_{rms} calculation is carried out using equation 5.1 (given in section 5.3 of chapter 5). The expression to compute SPL_{rms} into the frequency bandsfor 1 minute-long file recorded every 15 minutes interval is covered therein. As previoulsy mentioned in chapter five, the low-frequency band (100 Hz to 2000 Hz) corresponds to the range in which most fish species vocalize, also known as the 'fish band' (Kaplan *et al.*, 2015). This band may as well include noise generated by the wind (that can be rather high) and waves. Though these facts have been well covered in chapter 5, nevertheless it may be useful to have a brief review here. The sampling frequencies selected in the passive acoustic recorder systems (SM2M+) for the Malvan (Location 5) and (SM3M) for the Grande Island locations (6 and 7) are 44100 Hz and 24000 Hz respectively. In chapter 5, the high-frequency band (2000 to 20,000 Hz) encompasses the range of snapping shrimp. This range is applicable for Malvan data (Location 5) as the sampling frequency used is 44100 Hz. In the case of locations 6 and 7, for shrimp band data the frequency limits are (2000 to 12,000 Hz) as they were sampled at 24000 Hz. Boat noise include larger frequency band and may interfere with both the bands (mentioned above). RMS sound pressure level (SPL_{rms}) at low-frequency fish band (100 Hz to 2000 Hz), the

high-frequency shrimp band[2000 to 20,000 (location 5) /12,000 Hz (locations 6 and 7)], and 'wideband' (without filtering) are calculated. At lower frequency (below 100Hz), much of the component include the contamination of flow noise (Bassett *et al*., 2014) etc. The application of the bandpass filter within the range of 100 and 2000 Hz is used to isolate flow noise from fish and shrimp bands. Unlike the earlier findings in connection with the use of acoustic metrics for terrestrial and marine application, recent research is related to the computation of acoustic metrics for marine environments involving use of three different frequency bands (Kaplan *et al.,* 2015; Bertucci *et al.,* 2016; Bohnenstiehi *et al.,* 2018). This helps in data segregation and to comprehend the effect of biophonies (fish, shrimp), geophonies (wind, flow) and anthrophonies (pile driving) etc. In the present study, the soundscape complexity analysis was performed using H, AR and ACI metrics applicable for the acquired data. The complexities of the acoustic metrics are a function of species contribution, diversity in the community, time of day and the bottom characteristics (Sueur *et al.,* 2008a; Farina, 2014).

6.2.1 Acoustic Entropy Index (H)

In biodiversity, the Shannon evenness index (Sueur *et al*., 2008a) is generally used for the assessment of animal sounds in an environment. The acoustic entropy index (H) is composed of two sub-metrics H_t (temporal entropy index) and H_f (spectral entropy index). Temporal entropy (H_t) is computed by the application of the Hilbert transform of the signal and it is integrally scaled:

$$H_t = -\sum_{t=1}^{n} A\,(t) \times \frac{Log_2\left(A(t)\right)}{log_2(n)} \qquad (6.1)$$

where $A(t)$ - probability mass function of the amplitude envelope obtained through the Hilbert transform, and n the length of the signal, which was chosen to be 60s x sampling rate. Likewise, spectral entropy H_f is obtained from the integral of the mean spectrum:

$$H_f = -\sum_{t=1}^{N} s\,(f) \times \frac{Log_2\left(s(f)\right)}{log_2(N)} \qquad (6.2)$$

where, $s(f) -$ probability mass function of the mean spectrum calculated using a short term Fourier transform (STFT) along with the signal with a non-overlapping Hamming window of 1024 (N).Total entropy is the product of both temporal and spectral entropy ($H = H_t \times H_f$). However, making assumptions of independence is the easiest approach though the source is same, which is used to compute Hf and Ht. Conceptually, Hf indicates biodiversity because of recorded peak frequency, and Ht shows amplitude of the particular sound. We have applied the given computational method (Sueur et al. 2008), and details are given in the SEEWAVE software which is universally used.

6.2.2 Acoustic Richness Index (AR)

This index is the combination of the indices described for H index and median of the amplitude envelope M [= median A (t) x $2^{(1-\text{depth})}$] with 0 $0 \leq M \leq 1$ and depth is the digitization depth i.e., 16 bits. AR is ranked index calculated based on the rank of M and H_t indicies obtained with the functions M and H_t and n is number of objects used as input. We use following formula (Sueur *et al*., 2014; Gasc *et al*., 2015):

$$AR = \frac{(rank(H_t) \times rank(M))}{n^2} \qquad (6.3)$$

.

6.2.3 Acoustic Complexity Index (ACI)

ACI metric was calculated utilizing a Fast Fourier Transform (FFT) size of 1024 with sampling frequencies (44100 Hz and 24000 Hz for Malvan and Grande Island locations respectively) having bins (43.06 Hz and 23.44 Hz for Malvan and Grande Island locations respectively). The formula is given as (Pieretti *et al*., 2011):

$$ACI = \frac{\sum_{k=1}^{n} |I_k - I_{k+1}|}{\sum_{k=1}^{n} I_k} \qquad (6.4)$$

where $|I_k - I_{k+1}|$ is the absolute difference between two adjacent values of amplitude along with a frequency bin, n represents the total number of temporal steps (k), and the calculation is made at an interval of 1 s.

ACI was calculated using two-component such as $ACIt_f$ (spectral scale) and $ACIf_t$ (temporal scale) i.e. i) $ACIt_f$ of 1024 frequencies bins (43 Hz each for Malvan and 23.44 Hz for Grande Island locations) and ii) $ACIf_t$ of 60 temporal steps for a 1 s interval (for both the locations). An example of the calculation is provided for fish chorus acquired from Malvan location. ACI values are computed utilizing the combined values (Fig. 6.1a, b) for every 15-minute interval before the final presentation (Fig. 6.2 d). A similar method is adopted for computation of acoustic entropy (H) values (section 6.2.1).

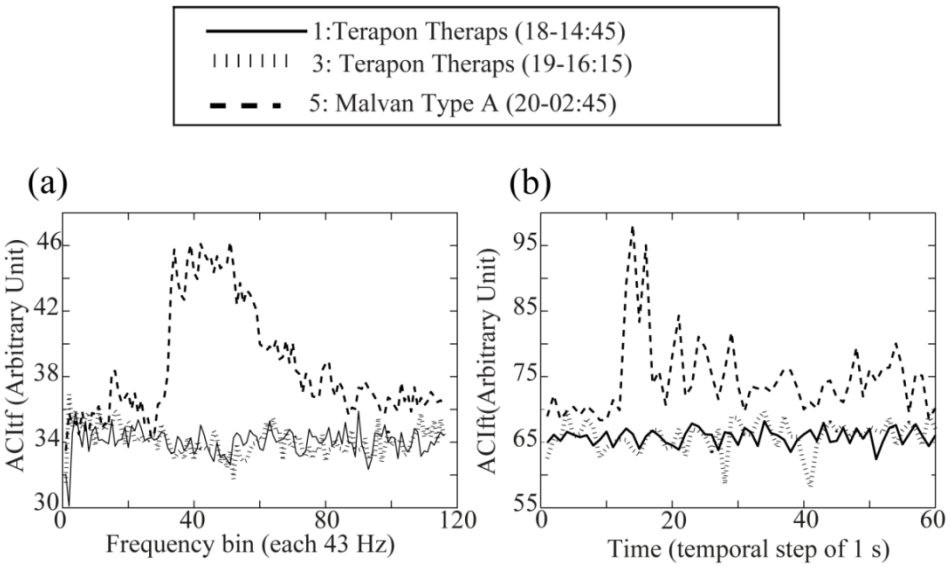

Fig. 6.1: The panel shows $ACIt_f$ versus frequency bin (each 43 Hz), bottom panel shows and ACIft versus time (1s steps): for *Terapon Theraps* (marked as '1' in Fig. 3.10b), *Terapon Theraps* (marked as 3 in Fig. 3.10b), and Grande Type A (marked as 5 in Fig. 3.10 b) (Please see chapter 3 of section 3.5.5)

6.3 Results

The calculation of the acoustic metrics using passive acoustic data from three locations has been carried out, and the time series along with the presentation of the box plots are presented here. For the box plot data, the mean values are tabulated (Table 6.1a-c) along with the H-spread and skewness parameters. The H-spread [the difference between the upper hinge (75^{th} percentile) and lower hinge (25^{th} percentile)] and skewness (the difference between the mean and median value of the data) are derived out of SPL_{rms}, H, AR and ACI time-series data (www.physics.csbsju.edu/stats/html.). In general, higher values of the H-spread show the variability of the computed metrics at the location, and the high skewed parameters indicatenon-normal distribution.

6.3.1 Performance study of acoustic metrics from Malvan (location 5)

Time-series plots for the entire data acquisition period (18-20 May 2016) from Malvan (Location 5) have been used to compute the acoustic metrics including SPL_{rms}:

SPL_{rms}

In addition to the identification of fish sounds, the SPL_{rms} values are examined to assess the general trends in the acoustic characteristics of the study site. Time series plots of SPL_{rms} values for the wideband, fish and shrimp bands are shown (Fig. 6.2a). The variations in SPL_{rms} values are higher during the fish chorus and abiotic sound period, notably for the wideband sound (indicated as 1 and 2 in Fig. 3.10b). Intermittent SPL_{rms} peaks due to boat generated sounds are also observed. Sharp peaks of the SPL_{rms} are observed for the sporadic fish calls that are indicated as 5, 6, and 7 (Fig. 3.10b). Box plots of the derived SPL_{rms} values for wideband, fish, and shrimp band signals are also presented (Fig. 6.3a). The mean SPL_{rms} value of the wideband data is observed to be higher (102.42 dB re 1µPa) as compared to the fish (94.62 dB re 1µPa) and shrimp (92.98 dB re 1µPa) bands (Table 6.1a). The distribution of fish band data shows more positive skewness followed by shrimp band data. Interestingly, the wideband data does not show such a skewed distribution. H-spread value of the SPL_{rms} is the highest for fish band data.

Acoustic Entropy Index (H)

The H metrics derived from the soundscape are considered as a suitable proxy to estimate the biodiversity of a reef system (Harris *et al.,* 2016; Sueur et al., 2008a). The H index is calculated based on the envelope and spectrum complexity of the recorded sound that varies between 0 and 1. The low values indicate pure tones and higher values signify numerous tones and even presence of frequency bands in the data. This metric is suitable for characterizing tropical region wherein the animal sound (biophony) dominates the background sound (geophony and anthrophony) (Gasc et al., 2015). Time series of H metrics calculated for wideband, fish and shrimp band sounds are presented (Fig. 6.2b). The level of the time series data of the fish band is found to be low due to the low bandwidth of the time series data, whereas higher H values are observed for shrimp band and wideband sounds due to the higher bandwidth of the chosen data.

Generally, the higher H values in the study area indicate prominent heterogeneity in the evenness of frequency and amplitude modulations.In this study, mean H value is the highest (0.888) along with the variability i.e., H-spread (0.039), as observed in the depicted box plot (Fig. 6.3b) for the wideband sounds. For the shrimp data, the highest mean H values (0.942) as well as the H-spread (0.008) have been noted. The mean H value calculated for fish band sounds is the lowest at 0.655 (H-spread: 0.020) (Harris et al., 2016; Bohnenstiehl *et al.,* 2018). Here, H values are low as observed during thefish chorus as well as during wave-breaking sounds (Fig 6.2b) (Kaplan *et al.,* 2015). Other than that, the H values do not offer substantial variation even for sporadic calls of Malvan Type A and *Carangidae* calls.

Acoustic Richness Index (AR)

The H metric has limitations for characterizing passive acoustic recordings in the temperate habitats wherein the background sound typically dominates the animal sound (Harris *et al.,* 2016). The AR metric, on the other hand, combines temporal entropy and amplitude instead of the spectral entropy as used by the H metric. The AR metric is derived based on the envelope complexity and intensity of the recorded data. Significant variation in the AR values (within the 0 and 1) is observed during the

presence of fish chorus and wave-breaking sound (Fig. 6.2c). It has been observed that the AR values are higher during the fish chorus and wave-breaking sound (indicated as 1, 3 and 2 and 4) (Fig. 3.10b). The AR values for the wideband data are also higher during the presence of a chorus. The box plots of AR metrics show similar variations for the wideband, fish band, and shrimp band signals (Fig. 6.3c). The mean AR values of the wideband, fish, and shrimp bands are found to be 0.309, 0.290 and 0.266 respectively. The distributions of AR metrics for the three bands show positive skewness, indicating non-normal data distribution (Table 6.1a). However, H-spread values are dominant for all the three frequency bands indicating high variability.

Acoustic Complexity Index (ACI)

The ACI was used for analyzing avian communities and measures the intensity variation of a given recording over changing frequencies (Pieretti *et al.*, 2011; Depraetere *et al.*, 2012; Sueur *et al.*, 2014; Farina, 2014; Harris *et al.*, 2016). The metric is particularly useful in areas affected by constant anthropogenic noise pollution and helps to identify diverse natural sounds despite the presence of human-generated background noise. The use of ACI metric was demonstrated in different Mediterranean soundscapes mainly composed of birds and cicada sounds (Depraetere *et al*., 2012). The time series plot of derived ACI metric for the wideband, fish and shrimp band sounds are presented (Fig. 6.2d). The magnitude of ACI values is highest for the wideband sound closely followed by shrimp band sounds. The magnitude of ACI values for the fish band sound is significantly low in comparison with the other two bands. During the dusk chorus and abiotic sound due to wave-breaking, there is a negligible variation in the ACI values for the three frequency bands. From the box plot data, the mean ACI values of the wideband, fish, and shrimp bands are found to be 1.7670×10^4, 0.1624×10^4 and 1.6080×10^4 respectively. The data distributions of the three bands are near normal, while all of them show low skewness values (Table 6.1a). The corresponding H-spread values were found to be negligible 681.79, 73.13 and 691.32 for the wideband, fish and shrimp bands respectively (Sueur *et al.*, 2008; Harris *et al*,. 2016; Bertucci et al., 2016).

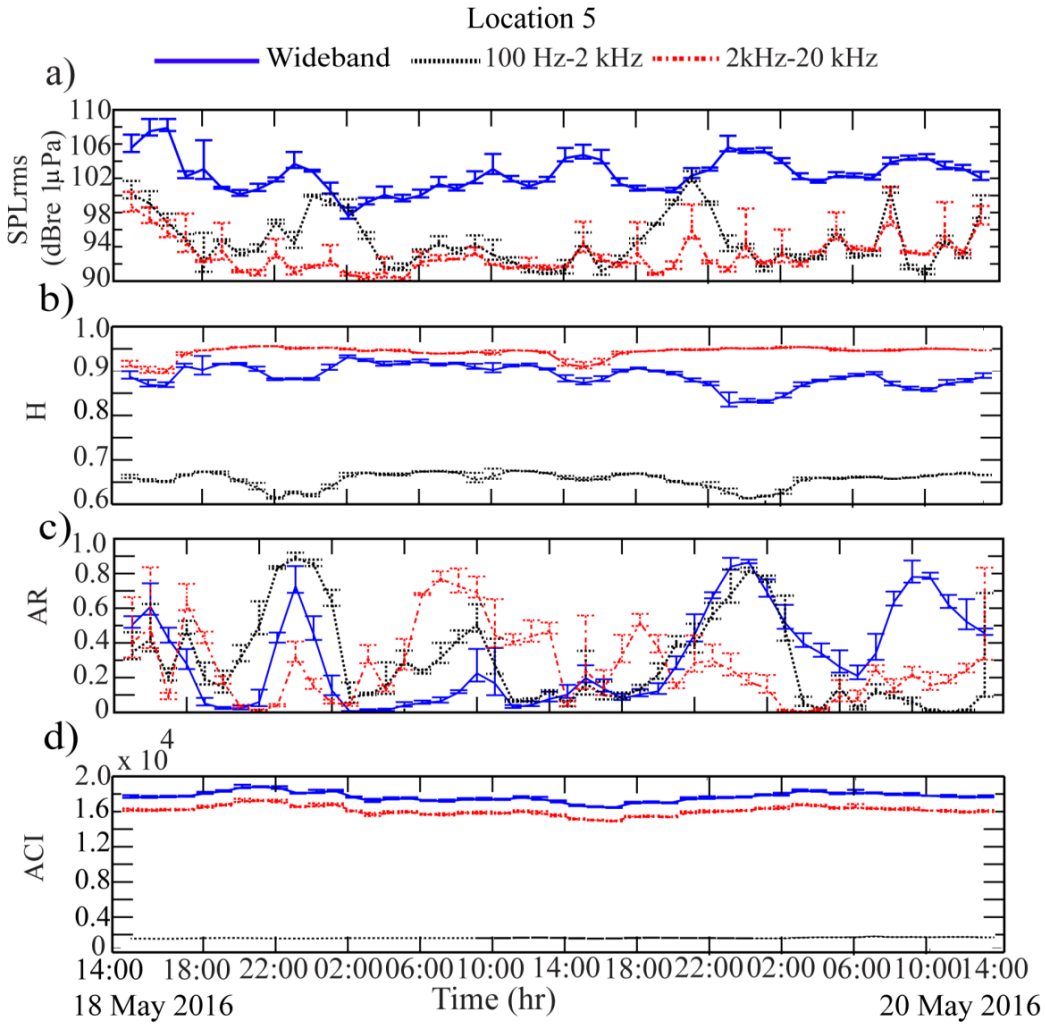

Fig. 6.2: (a) SPL_{rms} (dB re 1µPa), (b) Acoustic entropy (H), (c) Acoustic richness (AR), (d) Acoustic complexity index (ACI) for wideband, fish and shrimp bands for Location 5 (Malvan). H, AR and ACI are in arbitrary unit.

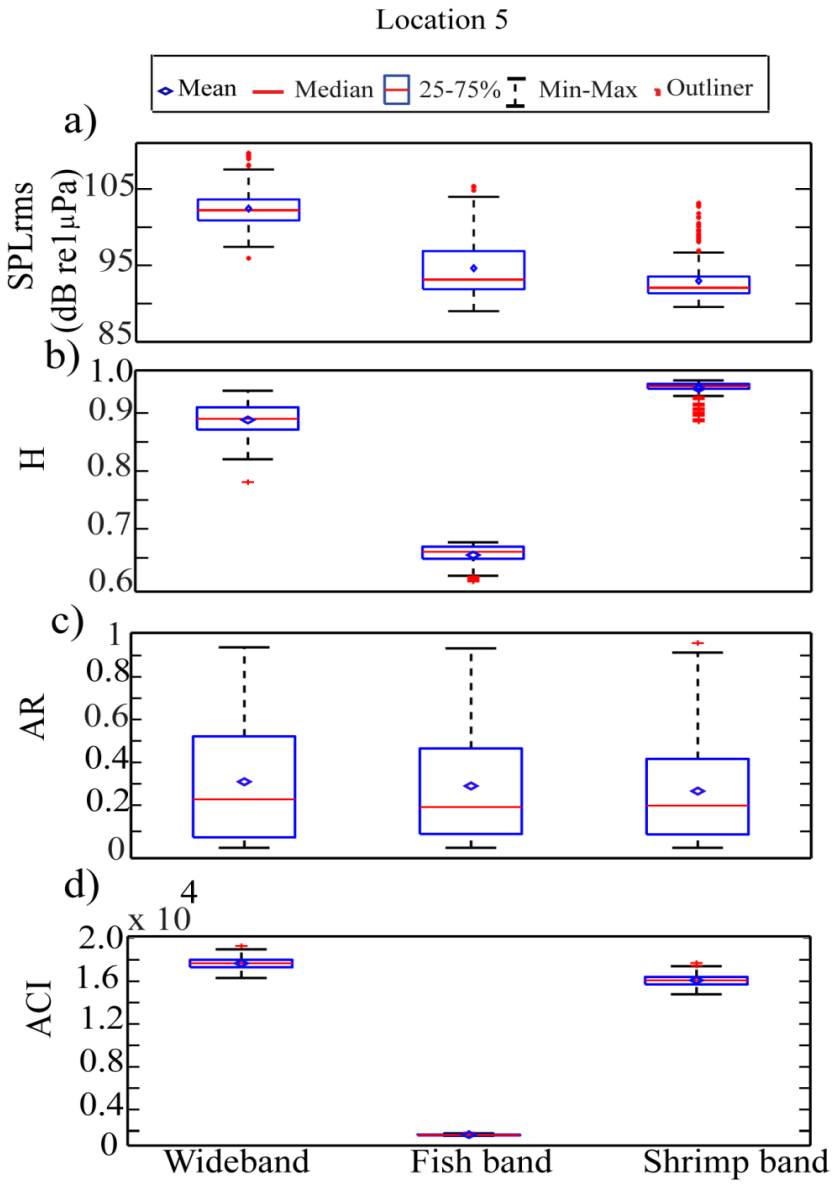

Fig. 6.3: Boxplots of the derived metrics for wideband, fish bands and shrimp bands: (a) SPL_{rms},(b) Acoustic entropy (H), (c) Acoustic richness (AR) and (d) Acoustic complexity index (ACI) for location 5 (Malvan Area). H, AR and ACI are in arbitrary unit.

Table 6.1 (a): Mean value of the acoustic metric and related H-spread and skewness values of entire data

Metrics	Frequency bands	Location 5			Location 6			Location 7		
SPL_{rms} (dBre1µPa)		Acoustic metric (Mean)	H-spread	Skewness	Acoustic metric (Mean)	H-spread	Skewness	Acoustic metric (Mean)	H-spread	Skewness
	Wideband	102.42	2.73	0.22	115.00	11.59	1.48	110.00	1.90	0.56
	Fish band	94.62	5.00	1.47	111.60	16.11	-0.21	105.90	3.88	1.24
	Shrimp band	92.98	2.21	0.90	107.60	8.64	2.66	108.40	1.20	0.14
H (arbit. unit)	Wideband	0.888	0.039	-0.001	0.929	0.060	-0.006	0.957	0.016	-0.006
	Fish band	0.655	0.020	-0.006	0.729	0.040	-0.003	0.761	0.002	0.000
	Shrimp band	0.942	0.008	-0.004	0.949	0.015	-0.006	0.949	0.003	0.000
AR (arbit. unit)	Wideband	0.309	0.471	0.082	0.227	0.266	0.056	0.314	0.484	0.098
	Fish band	0.290	0.310	0.010	0.275	0.422	0.073	0.315	0.489	0.091
	Shrimp band	0.266	0.354	0.068	0.289	0.457	0.093	0.316	0.473	0.089
ACI (arbit. unit)	Wideband	1.7670×10^4	681.79	-0.98	1.8330×10^4	1071.36	-40.62	2.0780×10^4	830.39	-48.04
	Fish band	0.1624×10^4	73.13	14.34	0.2944×10^4	259.31	23.42	0.3456×10^4	541.62	-65.17
	Shrimp band	1.6080×10^4	691.32	-0.47	1.5430×10^4	1003.87	-29.00	1.7370×10^4	580.87	-4.74

Table 6.1 (b): Mean value of the acoustic metric and related Location 6 'fish vocalization period'& 'no vocalization period'

Metrics	Time	Frequency band	Location 6 'fish vocalization period'			Location 6 'no vocalization period'		
SPL_{rms} dBre1µPa	Fish vocalization period 14:00-03:00 hr 15 /16 March 2017		**Acoustic metric (Mean)**	**H-spread**	**Skewness**	**Acoustic metric (Mean)**	**H-spread**	**Skewness**
		Wideband	119.90	7.32	-1.28	108.00	1.16	0.65
		Fish band	118.30	6.82	-2.337	101.10	3.54	1.63
		Shrimp band	113.30	13.33	2.343	103.80	1.59	0.70
H (arbit. unit)	Fish vocalization period 14:00-03:00 hr 15 /16 March 2017	Wideband	0.900	0.046	-0.013	0.965	0.002	-0.004
		Fish band	0.717	0.027	-0.010	0.762	0.015	-0.007
		Shrimp band	0.941	0.024	0.003	0.960	0.003	0.000
AR (arbit. unit)	Fish vocalization period 14:00-03:00 hr 15 /16 March 2017	Wideband	0.373	0.370	0.018	0.133	0.104	0.039
		Fish band	0.492	0.464	-0.102	0.130	0.084	0.060
		Shrimp band	0.400	0.590	0.048	0.214	0.196	0.060
ACI (arbit. unit)	Fish vocalization period 14:00-03:00 hr 15 /16 March 2017	Wideband	1.8100×10^4	1303.00	378.00	1.8760×10^4	905.00	87.00
		Fish band	0.2900×10^4	173.40	51.70	0.3073×10^4	247.500	-3.70
		Shrimp band	1.5230×10^4	1065.50	270.00	1.5730×10^4	540.00	12.00

Table 6.1 (c): Mean value of the acoustic metric and related Location 7 'fish vocalization period' & 'no vocalization period'

Metrics	Time	Frequency band	Location 7 'fish vocalization period'			Location 7 'no vocalization period'		
SPL_{rms} dBre1µPa	'No vocalization period' 03:00-11:00 hr 16 March 2017		**Acoustic metric (Mean)**	**H-spread**	**Skewness**	**Acoustic metric (Mean)**	**H-spread**	**Skewness**
		Wideband	111.8	2.187	0.224	109.00	0.99	-0.70
		Fish band	105.4	4.655	1.421	107.60	6.00	0.04
		Shrimp band	107.9	0.961	-2.727	109.30	1.87	0.41
H (arbit unit)	'No vocalization period' 03:00-11:00 hr 16 March 2017	Wideband	0.953	0.014	-0.000	0.956	0.002	0.007
		Fish band	0.750	0.029	0.000	0.767	0.003	-0.000
		Shrimp band	0.950	0.001	0.000	0.946	0.001	0.000
AR (arbit unit)	'No vocalization period' 03:00-11:00 hr 16 March 2017	Wideband	0.596	0.496	-0.070	0.057	0.050	0.043
		Fish band	0.300	0.634	0.227	0.601	0.485	-0.000
		Shrimp band	0.212	0.332	0.158	0.600	0.525	-0.018
ACI (arbit unit)	'No vocalization period' 03:00-11:00 hr 16 March 2017	Wideband	2.0280×10^4	772.00	-31.00	2.1410×10^4	361.00	-101.50
		Fish band	0.3208×10^4	372.65	74.30	0.3766×10^4	96.20	-24.00
		Shrimp band	1.7110×10^4	535.00	-7.500	1.7700×10^4	361.50	-92.00

6.3.2 Study of performance of acoustic metrics from Grande Island (locations 6 and 7) for the entire nine days data collection

Time-series plots for the entire data acquisition period (14-23 March 2017) from Grande Island (Locations 6 and 7) are being used to compute acoustic metrics including SPL_{rms}:

SPL_{rms}

The SPL_{rms} values were used to assess the general trends in the acoustic characteristics of the study site. Time series plots of the wideband, fish and shrimp bands for SPL_{rms} values are shown for locations 6 (Fig. 6.4a) and 7 (Fig. 6.5a). Box plots of the derived SPL_{rms} values for wideband, fish, and shrimp band data for the entire nine-days are presented for location 6 (Fig. 6.6a-d) and location 7 (Fig. 6.6e-h). The mean SPL_{rms} value of the wideband signals is observed to be the highest (115.00 dBre 1µPa)compared with the fish (111.60 dB re 1µPa) and shrimp (107.60 dB re 1µPa) bands for location 6. For wideband and fish band and shrimp bands, mean SPL_{rms} values for the location 7 are moderately higher i.e., (110.00 dBre 1µPa), (105.90 dBre 1µPa) and (108.40 dBre 1µPa) respectively (Fig. 6.6e). For fish band data of location 6, the higher variability (H-spread =16.11 dB re 1µPa) is observed in comparison with the location 7 SPL_{rms} data (H-spread = 3.88 dB re 1µPa) (Table 6.1a).

Acoustic Entropy Index (H)

Time series of H metrics calculated for wideband, fish and shrimp band sounds for location 6 and location 7 are presented in (Fig. 6.4b) and (Fig. 6.5b) respectively. For location 6, box plot data show the higher H value (Fig. 6.6b) for the shrimp band as well as the wideband sound and moderate values of the fish band. The level of the time series data are function of the signal bandwidth as seen in the Malvan (Location 5) data. The mean H values of the wideband, fish, and shrimp bands are found to be 0.930, 0.729 and 0.949 respectively. Similarly, for location 7, the mean H values of the wideband, fish,

andshrimp bands are found to be 0.957, 0.761 and 0.949 respectively (Fig. 6.5f). For three bands, the skewness and H-spread values are negligible for both the locations.

Acoustic Richness Index (AR)

Significant variation in the AR values (within the 0 and 1) is observed during the presence of fish chorus (Fig. 6.4c and 6.5c) for both the locations. It has been observed that the AR values of the time-series are higher during the fish chorus timings in locations 6 and 7 and generally follow trend of the SPL_{rms} data. The box plots of AR metrics for the wideband, fish and shrimp band data for locations 6 and 7 are presented (Fig. 6.6c and 6.6g). For location 6, the mean AR values of the wideband, fish and shrimp bands are found to be 0.227, 0.275 and 0.289 respectively. Comparatively higher mean AR values for the wideband, fish, and shrimp bands are found to be 0.314, 0.315 and 0.316 respectively for location 7. The H-spread values of both the locations are higher except for wideband data of the location 6 (Table 6.1a). For both the locations, moderate skewness values are observed for three frequency bands of both the locations.

Acoustic Complexity Index (ACI)

The time series plot of derived ACI metric for the wideband, fish and shrimp band sounds for locations 6 and 7 are presented in (Fig. 6.4d and 6.5d) respectively. Mean ACI value is the highest for the wideband sound followed by shrimp band sound for both the locations. From box plot data of location 6, the mean ACI values of the wideband, fish, and shrimp bands are found to be 1.8330×10^4, 0.2944×10^4 and 1.5430×10^4 respectively (Fig. 6.6d). The mean ACI values of the wideband, fish, and shrimp bands are found to be 2.0780×10^4, 0.3456×10^4 and 1.7370×10^4 respectively and can be observed for location 7 (Fig. 6.6h). The magnitude of mean ACI value of the fish band sound is significantly lower in comparison to the other two bands. For both the locations, the distributions based on the skewness and corresponding H-spread values are found to be the lowest for all the three bands (Table 6.1a).

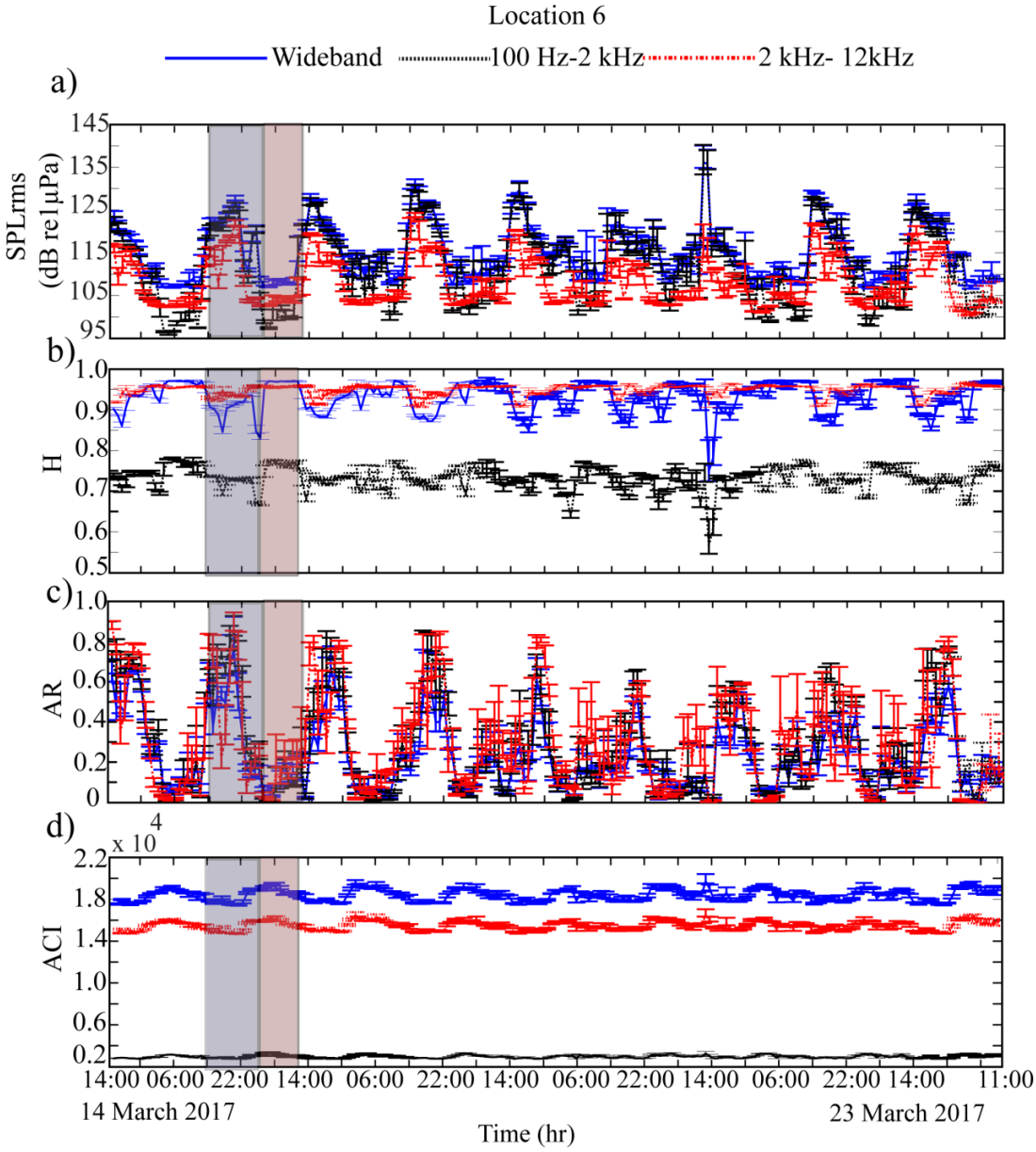

Fig. 6.4: (a) SPL_{rms} (dB re 1µPa), (b) Acoustic entropy (H), (c) Acoustic Richness (AR), (d) Acoustic complexity index (ACI) for wideband, fish and shrimp bands for location 6 (Grande Island 20m water depth area). Entire light gray color band depict twenty-four hr data. Data within the initial part of the gray and purple color bands indicate "fish vocalization period" and 'no vocalization period' for location 6. H, AR and ACI are in arbitrary unit.

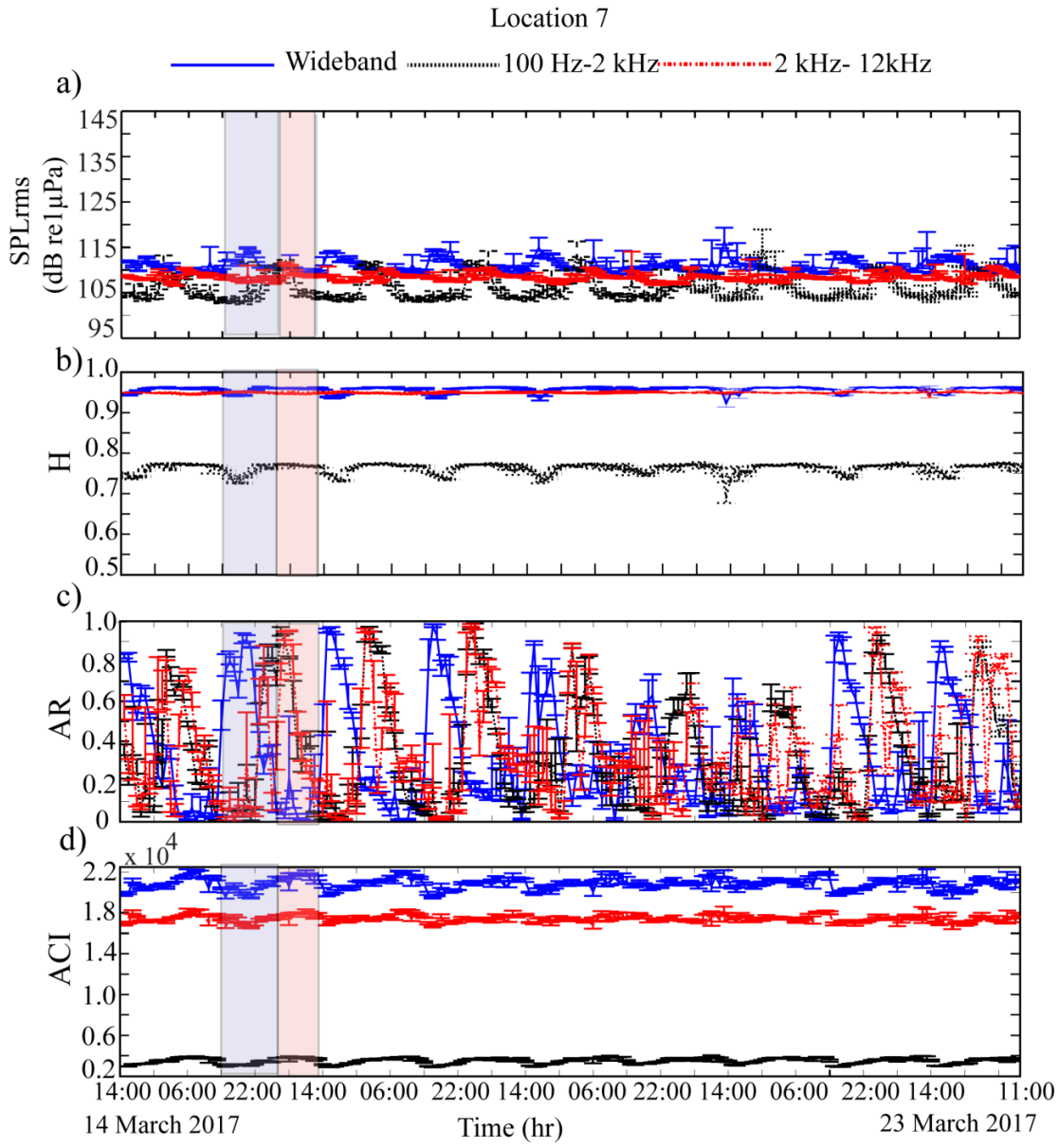

Fig. 6.5: (a) SPL_{rms} (dB re 1µPa), (b) Acoustic entropy (H), (c) Acoustic Richness (AR), (d) Acoustic complexity index (ACI) for wideband, fish and shrimp bands for location 7 (Grande Island reef area at 8m water depth). Entire light gray color band depict twenty-four hr data. Data within the initial part of the gray and purple color bands indicate "fish vocalization period" and 'no vocalization period' for location 7. H, AR and ACI are in arbitrary unit.

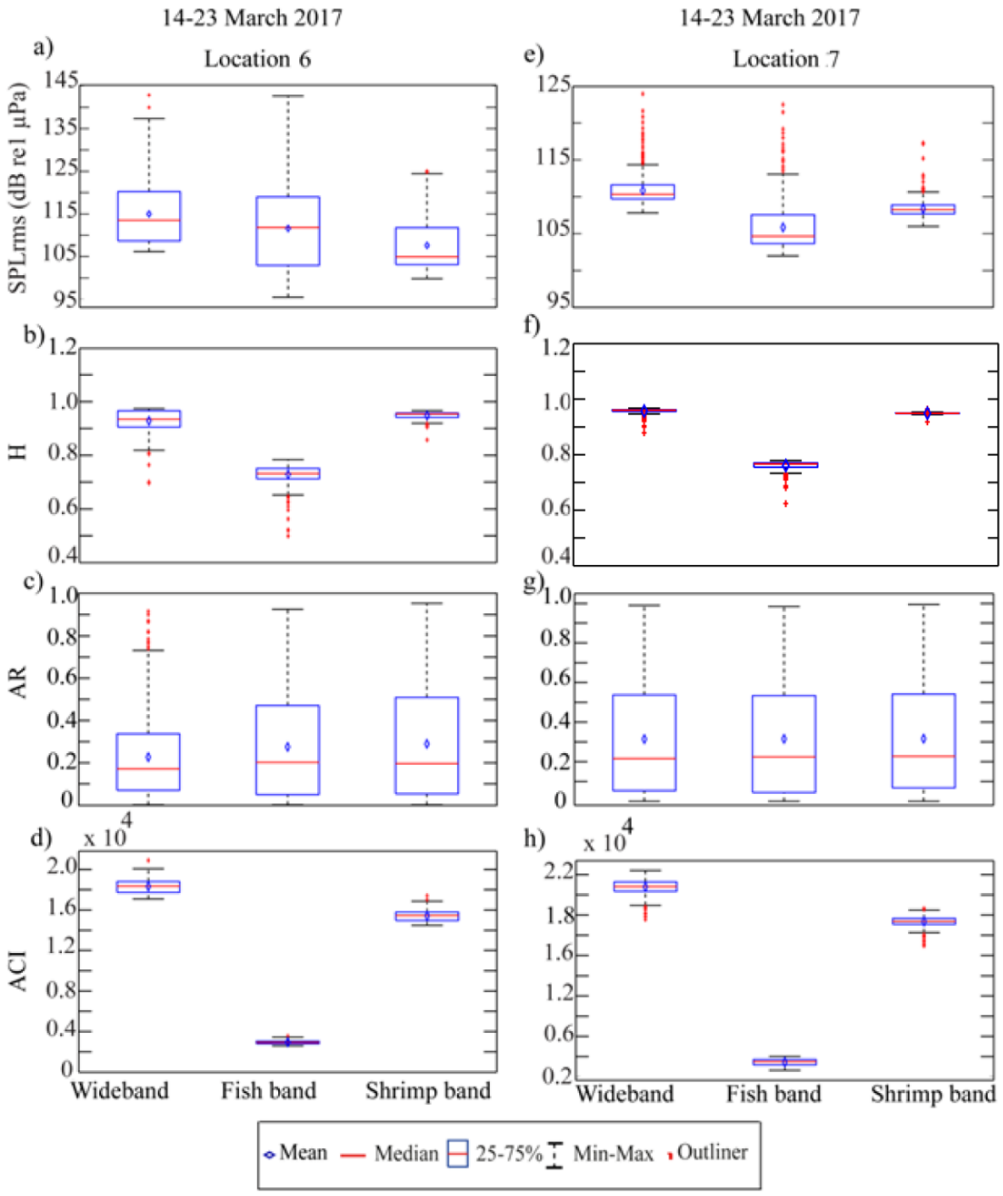

Fig. 6.6: Boxplots of the derived metrics for wideband, fish bands and shrimp bands for nine days data: (a) SPL_{rms},(b) Acoustic entropy (H), (c) Acoustic Richness (AR) and (d) Acoustic complexity index (ACI) for location 6, and (e) SPL_{rms},(f) Acoustic entropy (H), (g) Acoustic richness (AR) and (h) Acoustic complexity index (ACI) for location 7. H, AR and ACI are in arbitrary unit.

6.3.3 An analysis of the acoustic metrics and SPL_{rms} for 'fish vocalization period' and 'no vocalization (quite) period' for location 6:

In the previous section, the presentation of the acoustic metrics for the 9 days data was carried out. Further study is carried out to know the variability of these metrics with respect to the 'fish vocalization period' as well as ''no vocalization period'. Acoustic metrics during the 'fish vocalization period and ''no vocalization period' are examined to understand the situations in the presence or absence of fish sound. For location 6, the acoustic metrics for the representative 24 hr data within the 'fish vocalization period' [15 March 2017 (14:00 hr) to 16 March 2017 (03:00 hr)] and ''no vocalization period' [16 March 2017 (03:00 – 11:00 hr)] are computed. Light gray and purple colour bands are discernible for fish 'vocalization period' and 'no vocalization period' timings as depicted in Fig. 6.4. Four different fish sound types within the (14:00 to 22:30 hr), (19:30 to 21:30 hr), (20:00 to 21:00 hr) and (00:30 to 02:30 hr) have been identified as that of *Terapon Threaps*, Toadfish, unknown fishes noted earlier as Grande Type A and Grande Type B respectively (section 3.5.6, chapter 3). Humpback whale sounds (5424 calls) are also recorded from this location (Madhusudhana *et al.*, 2019) from 16 March 2017 afternoon up to 23 March 2017.

SPL_{rms}

Box plots of the derived SPL_{rms} values for the wideband, fish and shrimp bands are presented for 'fish vocalization period' (Fig. 6.7a) from location 6**.** The mean SPL_{rms} value of the wideband, fish and shrimp band data are found to be (119.9 dB re 1µPa), (118.3 dB re 1µPa), and (113.30 dB re 1µPa) (Table 6.1b). The SPL_{rms} values are higher in comparison with the mean values of nine days of data length (section 6.3.2). Moderate H-spread and skewness values are observed for wideband and fish band data except for shrimp band data where data variability is still higher. Within the 'no vocalization period', the mean SPL_{rms} value of the wideband, fish and shrimp band data are found to be (108.0 dB re 1µPa), (101.10 dB re 1µPa), and (103.80 dB re 1µPa) respectively (Table 6.1b) indicating lower values (Fig. 6.7e) in comparison with the 'fish vocalization period'

data. Fish band data show moderate to low data variability (H-spread) as well as non-normal distribution (skewness) for ‘fish vocalization period’ and ‘no vocalization period’. For the three frequency bands, SPL_{rms} values show a decreased in ‘no vocalization period’ data in comparison with the fish sound.

Acoustic Entropy Index (H)

Box plots indicate the mean H values for ‘fish vocalization period’ data of the wideband and shrimp bands, which are found to be 0.900 and 0.941 respectively (Fig. 6.7b). The mean H value for fish band data showsreduced value (0.717) due to its chosen bandwidth of limited size. For the H index, the H-spread and skewness values are found to be negligible for the three frequency bands (Table 6.1b). Similarly, for ‘no vocalization period’, the mean H values are found to be 0.965, 0.762, and 0.960 for wideband, fish and shrimp bands respectively (Fig. 6.7f). The H-spread and skewness values within the ‘no vocalization period’ are negligible for the three frequency bands (Table 6.1b). The H values are found to be higher during the ‘no vocalization period’ for the three frequency bands.

Acoustic Richness Index (AR)

Box plots of the AR values related to the wideband, fish bandand shrimp bands are presented for ‘fish vocalization period’ (Fig. 6.7c) from location 6. The mean AR values of the wideband, fish and shrimp band data are found to be 0.373, 0.492, and 0.400 respectively. H-spread and skewness parameters depicted in the box plot data show higher data variability and near-normal distribution (Table 6.1b). Within the ‘no vocalization period’ sound timings’, the mean AR value of the wideband, fish and shrimp band data are found to be 0.133, 0.130, and 0.214 respectively, indicating comparatively lower values (Fig. 6.7g). All the three-band data show limited data variability as well as non-normal distributions during ‘no vocalization period’ at location 6 (Table 6.1b). For ‘no vocalization period’, AR values are reduced considerably for the three frequency bands.

Acoustic Complexity Index (ACI)

For 'fish vocalization period' from location 6, the mean ACI value of the wideband, fish and shrimp band data are found to be 1.8100×10^4, 0.2900×10^4 and 1.5230×10^4 respectively (Fig. 6.7d). All the three band data show moderate data variability and near-normal distribution, only for the fish band. Within the 'no vocalization period', ACI values for the wideband, fish bandand shrimp bands are found to be 1.8760×10^4, 0.3073×10^4 and 1.5730×10^4 respectively (Fig. 6.7h). Study reveals similar variations in ACI box plot parameters for 'fish vocalization period' and 'no vocalization period' (Table 6.1b, c).

6.3.4 An analysis of the acoustic metrics and SPL_{rms} for 'fish vocalization period' and 'no vocalization period' for location 7:

For location 7, the box plots of acoustic metrics of fish sound for single representation of 24-hr data within the 'fish vocalization period', and 'no vocalization period' are elucidated here. The data recording timings are similar to the timings of location 6. Box plots of the derived acoustic metrics of the wideband, fish and shrimp bands are shown for 'fish vocalization period' and 'no vocalization period'(Fig. 6.8) related to location 7 having 8 m water depth. For location 7, acoustic metrics for 'fish sounds' within the 'fish vocalization period'.

SPL_{rms}

With respect to location 7, near the coral reef having water depth 8 m, the mean SPL_{rms} value of the wideband, fish and shrimp band data are found to be (111.80 dB re 1µPa), (105.40 dB re 1µPa), and (107.90 dB re 1µPa) respectively for 'fish vocalization period' (Fig. 6.8a). Within the 'no vocalization period', the mean SPL_{rms} value of the wideband, fish and shrimp band data are found to be (109.00 dB re 1µPa), (107.60 dB re 1µPa), and (109.30 dB re 1µPa) (Fig. 6.8e) indicating negligible differences in 'fish vocalization period' and 'no vocalization period' for all the three bands. Fish band data show

moderate data variability as well as non-normal distribution for 'fish vocalization period' (Table 6.1c). We could not synchronized the SM2M+/ SM3M systems during simultaneous data acquisition at locations 6 and 7, which is preventing us to estimate distance of the fish sound source. However, the distance between the sensor locations 6 and 7 is ~500m as we know from the position data.

Acoustic Entropy Index (H)

The mean H values for 'fish vocalization period' data from location 7 for wideband and shrimp band are observed to be 0.953 and 0.950 respectively (Fig. 6.8b). H values for fish band data showreduced values 0.750.For the H index, the H-spread and skewness values are found to be insignificant for three frequency bands (Table 6.1c). Similarly, for 'no vocalization period', mean H values are found to be 0.956, 0.767, and 0.946 for wideband, fish and shrimp bands respectively (Fig. 6.8f). The H-spread and skewness values within the 'no vocalization period' are negligible for the three frequency bands (Table 6.1c).

Acoustic Richness Index (AR)

The mean AR values of the wideband, fish and shrimp band data are found to be 0.596, 0.299, and 0.212 respectively for 'fish sound timings' (Fig. 6.8c)'. The data variability is higher for all the three frequency bands (Table 6.1c). However, skewness parameters also show higher values for 'fish vocalization period' and 'no vocalization period'. Within the 'no vocalization period', the mean AR value of the wideband, fish and shrimp band data are found to be 0.056, 0.602 and 0.595 respectively (Fig. 6.8g). Fish and shrimp band show moderate data variability as well as a normal distribution, whereas the data variability is limited in the case of wideband data (Table 6.1c).

Acoustic Complexity Index (ACI)

For ‘fish vocalization period’, the mean ACI value of the wideband, fish and shrimp band data are found to be 2.0280×10^4, 0.3208×10^4, and 1.7110×10^4 respectively (Fig. 6.8d). Within the ‘‘no vocalization period’, ACI values for the wideband, fish bandand shrimp bands are found to be 2.1410×10^4, 0.3763×10^4 and 1.7700×10^4 respectively. Fig. (6.8h) shows no differences in the box plot data for ‘no vocalization period’ in comparison to the ‘fish vocalization period’ (Fig. 6.8d). H-spread and skewness parameters of the box plot data for ‘fish vocalization period’ and ‘no vocalization period ‘show negligible variability for all the three frequency bands (Table 6.1c).

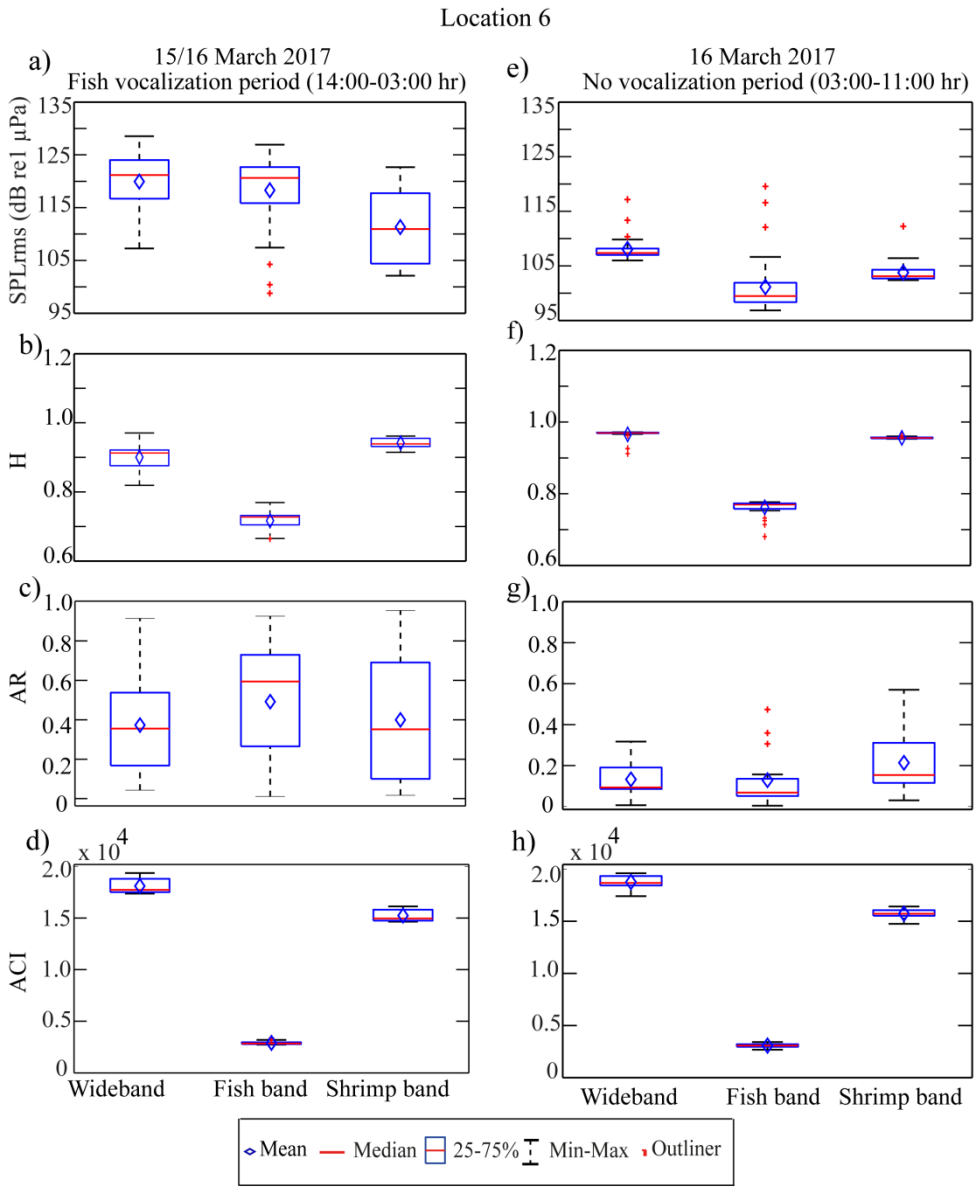

Fig. 6.7: Boxplots of the derived metrics for wideband, fish bands and shrimp bands for 'fish sound': (a) SPL_{rms},(b) Acoustic entropy (H), (c) Acoustic Richness (AR) and (d) Acoustic complexity index (ACI) for 'fish vocalization period', and 'no vocalization period' data (e) SPL_{rms},(f) Acoustic entropy (H), (g) Acoustic Richness (AR) and (h) Acoustic complexity index (ACI) for location 6. H, AR and ACI are in arbitrary unit.

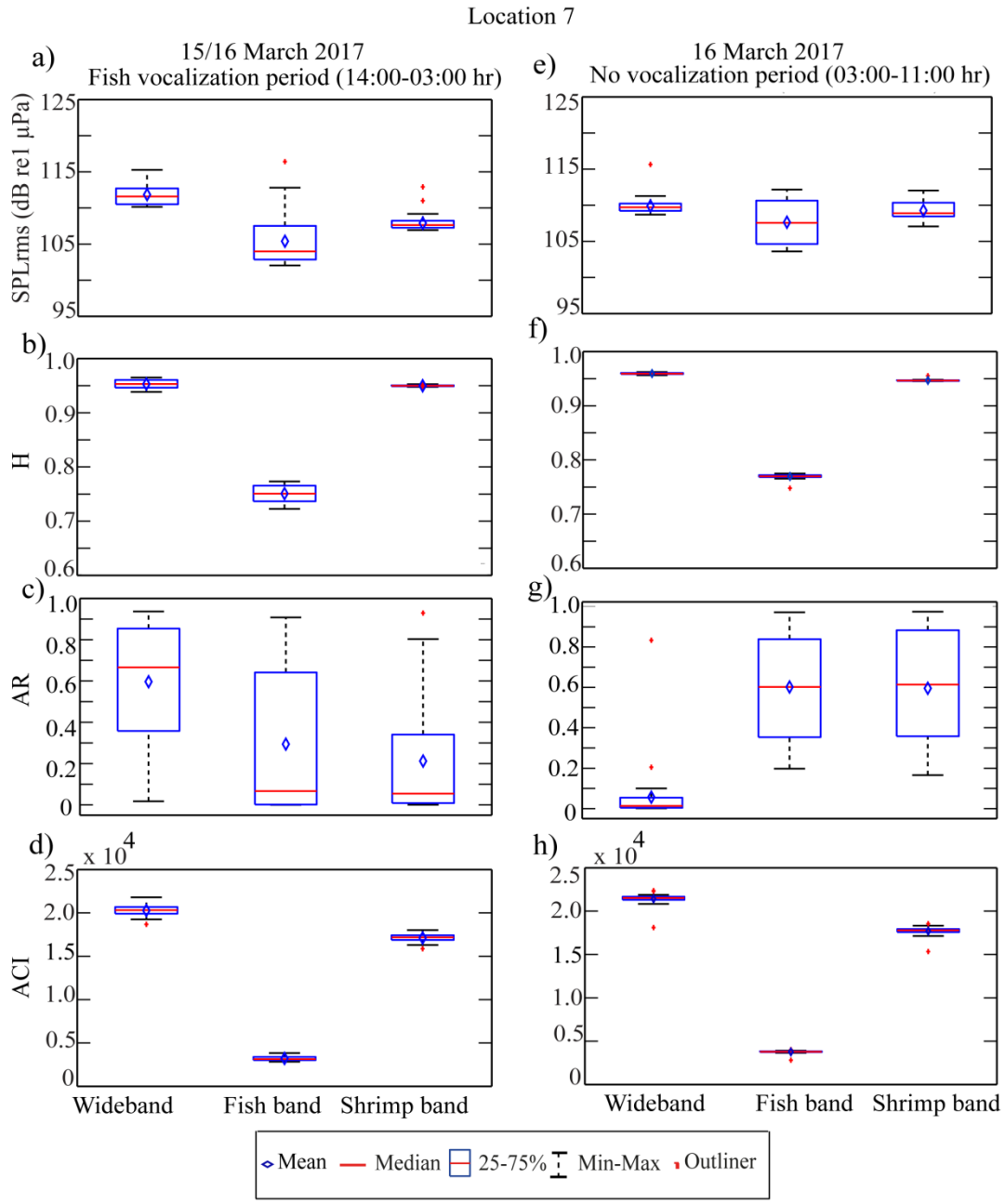

Fig. 6.8: Boxplots of the derived metrics for wideband, fish bands and shrimp bands for fish sound: (a) SPL_{rms},(b) Acoustic entropy (H), (c) Acoustic Richness (AR) and (d) Acoustic complexity index (ACI) for 'fish vocalization period' and 'no vocalization period' data (e) SPL_{rms},(f) Acoustic entropy (H), (g) Acoustic Richness (AR) and (h) Acoustic complexity index (ACI) for location 7.

6.4 Discussions

There are important issues to be considered before analyzing the acoustic metric of three locations (mentioned above):

Previous study results (Bertucci *et al*., 2016**)** highlighted that the intensity of fish vocalizations as well as the environments are the important components of SPL_{rms} parameters, and accordingly an analysis is presented here considering SPL_{rms} values acquired from the three different locations. Apart from wideband the two chosen frequency bands are known as fish and shrimp bands covering a frequency ranges (100-2000 Hz) and (2000 – 20,000 Hz) respectively (Kaplan *et al.,* 2015). Three study locations are involved with vocalization of *Terapon threaps* fish species, whose peak frequency is found to be varying around 1758±29 Hz. This allows selecting fish band up to 2000 Hz for the present analysis instead of the chosen 1000 Hz (Bertucci *et al*., 2016; Kaplan *et al.,* 2015).

For the three locations, the computation of H (acoustic entropy index) and ACI is carried out utilizing recorded time series data for the three frequency bands. Computed metrics for the three frequency bands show that both the indices are sensitive to the bandwidth selection. Computed time series data of the fish band (100-2000 Hz) shows a significant reduction in the H and ACI levels in comparison to the wideband and shrimp band (2000-20,000 Hz). For wideband and shrimp band, the higher H values and ACI are related to the chosen bandwidth.

Irrespective of the levels of the metrics (H and ACI), there is further reduction in the H and ACI values in the presence of fish chorus (Fig. 6.2b, d; 6.4b, d and 6.5b, d). For a particular band, the higher H values for three bands are related to the flat frequency spectrum along with the flat amplitude envelope (Sueur *et al.*, 2012), and for recordings having single peak frequency will have a lower H values. Bohnenstiehl *et al.,* (2018) have revealed that for soundscape dominated by impulses of wideband snapping shrimp sounds, the ACI increases with the snapping rate. Similarly, for soundscapes dominated

by harmonic fish calls led to a decrease in ACI. The acoustic metric, H also decreases in response to increasing rates of harmonic calls. Overall, variation in H and ACI can be modulated by variation in the acoustics of single sound-producing species. This explains the fact how H and ACI show low values during the presence of fish chorus, wave-breaking and sparse fishes. The biotic calls produced by the *Terapon threaps* (1758±29 Hz), Carangidae (947.46± 21.53 Hz), Sciaenidae (708.50±49.44) and many other fishes as well as abiotic sound (1142.00 ± 23.00 Hz) possesses the highest peak in their PSD values (section 3.5.5 of chapter 3), which suggests that, the biotic calls as well as abiotic wave-breaking sounds are generally harmonic in nature, and supports the reduction in H and ACI values for the three frequency bands when SPL_{rms} values are higher as shown in the time series plots.

Analysis of the three study locations:

In Malvan (Location 5), it was observed from time-series data that the SPL_{rms} values are higher during *Terapon threaps* fish chorus and abiotic (wave-breaking) sound and sporadic fish sounds of Malvan Type A and Carangidae, notably for the wideband sound in comparison to the other two bands. The variations of the SPL_{rms} of the fish and shrimp bands are similar except during the wave-breaking sound having peak PSD of (1142.00 ± 23.00 Hz) (Fig. 6.1a and chapter 3). The continuous high value of the wideband data suggests dominant sound having frequency <100 Hz. This low-frequency sound may be due to the flow **(**Bassett *et al.*, 2014), which is difficult to prove here in absence of current meter data. This suggests the dominance of the background sound. The box plot data (Fig. 6.3a) shows that higher variability of the fish band data (H-spread = 5.00 dB re 1μPa) along with the skewed distribution. However, the low values of SPL_{rms} (94.62 dB re 1μPa) at Malvan (location 5) for the fish band is observed among the three locations studied in this chapter.

Locations 6 of Grande Island possess 20 m water depth to show prominent time series for SPL_{rms} for the three frequency bands (Fig. 6.4a). Mean SPL_{rms} (111.60 dB re 1μPa) of the fish band data shows higher values along with the variability (H-spread = 16.11 dB re

1μPa). Four different fish sound types are recognized: *Terapon threaps*, Toadfish, and unknown fishes mentioned as Grande Type A and Grande Type B (section 3.5.6 of chapter 3). Location 7 is situated at 8 m water depth within the coral reef area, about 500 m distance from the location 6. In location 7, no significant difference in mean SPL_{rms} is observed for the three different bands (Fig. 6.5a). Moderate SPL_{rms} values are found to be within (105-110 dB re 1μPa) for location 7 (Table 6.1a). The low SPL_{rms} values as well as the identified fish (*Terapon threaps* etc.) sounds are similar to location 6, suggesting that due to the signal propagation from location 6 to the recording site of location 7, the signal levels are low. The causes of higher SPLrms for recorded fish and shrimp bands during non-vocalization periods are may be due to substrate vibration common in shallow depth (Hill, 2009). Sound often generated as a result of substrate vibration that can result from water flow, ground rumbling, and some anthropogenic sources. This suggests higher SPLrms due to closeness of the shallow location 7 during non-vocalization period due to dominant background sound (substrate vibration).

For Malvan (Location 5), H values of the fish band data are the lowest (0.655) in comparison with the other two bands as seen from the time series (Fig. 6.3b). Moreover, the time-series data of the H show moderate variations during the biotic (fish vocalization) and abiotic (wave-breaking) sounds for the three bands (Fig. 6.2b). Similar to H metric, the variations of ACI values for the fish band sound is significantly low ($0.16x10^4$) in comparison to the other two bands (Fig. 6.2d). During the dusk chorus and abiotic sound due to wave-breaking, there is a negligible fluctuation in the ACI values for the three bands, as observed in the time series data. Unlike H values, which is observed to be undulated (Fig. 6.2b) probably due to the background sound (Sueur *et al.*, 2008a), ACI time series data do not show such variations.

Similar to the Malvan location, the time series of the H values (average of nine days) for wideband and shrimp band data is higher than the fish band (0.729) for location 6 (Fig. 6.4b). A similar type of time series characteristics is also seen for ACI where fish band data are lower than the other two bands (Fig.6.4d). In general, the variation of the SPL_{rms} is found to be reciprocal with respect to the H and ACI in the presence of the fish

sound. Detailed analysis of the time series data suggests that the fluctuation of time series data of H is dominant even for the three bands in comparison to the ACI (Fig. 6.6 b, d). The observed characteristics of the H and ACI acoustic metrics for harmonic signals are already explained especially for understanding the biotic signals (Bohnenstiehl et al., 2018).

In the case of location 7, the mean H values calculated for the fish band is greater (0.761) in comparison to the other two locations (Table 6.1a). However, H is the lowest for the fish band in comparison to the other two bands of the same location 7 (Fig. 6.5b). This situation is similar to location 6. Even though signal levels are low (low SPL_{rms} values), the computed H metrics are found to be similar to location 6. Unlike Malvan (location 5), the variation of H values is found to be less undulating at location 7 (Fig. 6.6f).Like other locations, mean ACI values for the fish band sound is lower at location 7 (Fig. 6.5h). However, for fish band data it is higher among the three locations. As explained earlier, the reason for low values of H and ACI metrics for a particular band is due to harmonics. During the dusk chorus and abiotic sound due to wave-breaking, there is an insignificant variation in the ACI values for the three bands as observed in the time series data.

At location 5, the time-series data of AR values show significant variations among the three bands (Table 6.1a). For fish band data, the higher AR values during the fish chorus, wave-breaking as well as sparse fishes are observed (Fig. 6.2c). Comparable variability and distributions are seen in the box plots for the three bands (Fig. 6.3c). For location 6, AR values also show significant variations for the two bands (fish and shrimp), whereas there is relatively less variation for wideband sounds (Fig. 6.6c). For wideband, the overlapping of sounds is less than the fish and shrimp bands (Gasc *et al*., 2015). The variations between the SPL_{rms} and AR are found to be similar for this Grande Island location (Fig.6.4 a, c). The conditions are similarly for location 7, the highest mean values of AR are otained among the three locations (Table 6.1a). Again, for the three bands, the values of AR are similar (Fig.6.6 g). Incidentally, no difference is observed in

the variability of different bands. Here, the overlapping of fish sounds is moderate to alternating.

Besides, a comparative study is carried out based on the 24 hr data to observe the variation of the acoustic metrics during the presence and absence of fish vocalizations from the reef (Location 7) and off reef locations (Location 6). Study reveals higher SPL_{rms} (118.30 dB re 1µPa) and lower SPL_{rms} (101.10 dB re 1µPa.) during 'no fish vocalization period' in location 6 for fish band data (Table 6.1b). Similarly, at location 7 (near reef system) moderate mean SPL_{rms} value is 107.6 dB re 1µPa and SPL_{rms} (105.40 dB re 1µPa) is seen in the absence of fish vocalization (Table 6.1c). For the fish band, the SPL_{rms} is the highest at location 6, which suggest the presence of fish vocalization (Fig. 6.7a). The moderate values of SPL_{rms} in absence of fish vocalization suggest probable ambient sound due to geophoney.

The performance of H and ACI is similar, and in the presence of fish vocalization suggests low values (0.717) for fish band data at location 6 (Table 6.1b). Similarly, H value in the absence of fish vocalization is observed to be (0.762) (Table 6.1c). This suggests the variation of H values (0.762-0.717) for fish band data (Bohnenstiehl *et al*., 2018). Similar variations of H values are observed for wideband (0.965-0.900) and shrimp band (0.960-0.941) data. For location 7, the calculated variations of H values are observed to be within the (0.767-0.750) for the fish band (Table 6.1c). Similar variations of H values are observed for wideband (0.956-0.953) and shrimp band (0.950-0.946) data. For location 6, in the absence of fish sound the ACI value is observed to be $1.8760x10^4$, and in the presence of fish vocalization lower ACI value is found ($1.8100x10^4$). At location 6, ACI values are found to be varying within ($1.8760x10^4$-$1.8100x10^4$) for wideband. Similarly, for fish and shrimp bands the ACI values are found to be ($0.3073x10^4$ -$0.2900x10^4$) and ($1.5730x10^4$-$1.5230x10^4$) respectively.

In comparison to the H and ACI, acoustic metric AR is observed to be useful especially due to its higher variability as observed in the present study (Table 1b, c). At location 7, the performance of AR is different than the location 6. AR for fish and shrimp band is higher along with its variability, whereas for wideband data AR is low in the

absence of vocalization. Divers have reported a significant number of reef fishes in this location (Hussain *et al.,* 2016). However recording of the data as well as identification of reef fish sound from location 7 was not successful. The higher variability of AR may be due to the wind or any other environmental parameters such as bottom type. In the absence of the environmental data, it is difficult to identify the effect of environments (wind, current etc.) in the acoustic metrics. Next chapter covers the environmental data acquisition and their impact on the computed acoustic metrics.

6.5 Conclusions

Preseently the employment of the underwater passive acoustic data analyses technique is initiated for soundscape monitoring to understand the biodiversity of ecologically important locations from the west coast of India (WCI). The locations comprised of Malvan area off Maharashtra, and off Goa Grande Island region. Two locations of the Grande Island are selected where one is surrounded by coral reef habitat and having diverse flora and fauna, and the other location situated away from reef system at 20 m water depth. Three eco-acoustic indices namely H, AR, and ACI along with $SPL_{rms}$are computed for the three frequency bands viz., wideband, fish, and shrimp band. Computation of the acoustic metrics for the three locations reveals the characteristics of the study locations. In the absence of ground truth data acquired by the divers etc, the SPL_{rms} data is utilized. For fish band data, SPL_{rms} is the highest for location 6 of the Grande Island in comparison to the other two locations. The SPL_{rms} is the lowest in Malvan area.

Computed H and ACI for three frequency bands reveal a reciprocal relationship with the SPL_{rms} in the presence of fish vocalization. SPL_{rms} is higher in the presence of fish sound. These sounds are basically harmonics in nature, which provide lower values of H and ACI. The values of H and ACI are found to be dependent on the chosen bandwidth. For fish band data the magnitude of the H and ACI are found to be the lowest. H and ACI values are not always unique since they depend on the selection of sampling frequency as

well as bandwidth. However, they can be used as a good proxy to characterize the fish sound. SPL_{rms} and AR time series data reveal similar characteristics. During the highest intensity of the fish chorus, SPL_{rms} and AR levels also show higher values for the three frequency bands. The Box plot-based statistical parameters highlight the performance of the acoustic metrics more clearly indicating H-spread (data range) and skewness (data distribution). In general, H-spread of the H and ACI metrics is significantly low in comparison to AR and SPL_{rms}.

A study carried out based on the 24 hr data during the presence and absence of fish vocalization reveal significantly higher SPL_{rms} for location 6 in the presence of fish vocalization. Whereas moderate SPL_{rms} is observed at location 7 (reef system), is always available even during the absence of known fish sound from off reef location 6. In the presence of fish sound at location 6, those fish sounds are identified from the signal recorded at location 7. However the moderate sound recorded at location 7 could not be identified during the absence of the known fish sound of location 6. There lie three possibilities: i) sound from the reef fishes, ii) sound from geophonies especially wind, iii) sound related to habitat or bottom which is dominant in shallow water areas.

In general, the performance of H and ACI is similar, and in the presence of fish vocalization, low values (0.717) are obtained for fish band data at location 6. Similarly, H value in the absence of fish vocalization is observed to be (0.762) i.e., higher value for location 6. This suggests the variation of H values (0.762-0.717) for fish band data. Similarly, H values are observed for fish band for location 7 during fish vocalization and absence of fish vocalizations is found to be 0.750 and 0.767 respectively. Similarly, for location 7, the variations of H values are observed to be within the (0.767-0.750) for the fish band (Table 6.1c). For location 6, in absence of fish sound the ACI value is observed to be 1.8760×10^4, and in the presence of fish vocalization lower ACI value is found to be 1.8100×10^4. At location 6, ACI values are found to be varying within (1.8760×10^4-1.8100×10^4) for wideband. Similarly, for fish and shrimp bands the ACI values are found to be (0.3073×10^4 -0.2900×10^4) and (1.5730×10^4-1.5230×10^4) respectfully. In comparison with the H and ACI, acoustic metric, AR is least effected due to the chosen bandwidth.

AR values are observed to be higher in the presence of fish vocalization for both the locations as observed in the present study (Table 6.1b, c). At location 7, in the absence of fish vocalization mean AR values for fish and shrimp band is higher along with its variability, whereas for wideband data AR is low in the absence of vocalization. Under similar situation, AR values for all the three bands are lower for location 6.

Chapter 7

Eco-acoustic indices and analyses of the influence of environmental parameters

7.1 Introduction

In chapter 5, the influence of environmental parameters on fish sounds (SPL_{rms}) is ascertained and a comparative study is effectuated for three different locations. In this chapter, the eco-acoustics (Farina, 2014) parameter estimation is being carried out for passive acoustic data acquired at location 8 having a water depth of 20 m (Fig. 2.1; Table 2.1). Additionally, in this chapter, the influence of environmental parameters on the estimated eco-acoustics metrics related to the Grande Island location is being investigated.

The characteristics of fish vocalization can be affected by the variability of the environment (Bertucci *et al.,* 2016). The variability in the soundscape arises due to the environmental parameters such as wind, currents and water temperature (Vijay Kumar, 2017; Sundar *et al.,* 2015) etc. These are the parameters that animals respond to, so if the sound pressure levels are driven by biotic signals, it would follow that a change in the physical parameters would coincide with a shift in overall sound pressure levels that were a result of changes in chorusing animals. As mentioned, the biodiversity assessment is a key step for habitat monitoring in shallow reef areas (Harris *et al*., 2016), and the use of acoustic metrics such as ACI, H and AR (Sueur *et al.,* 2012) are being applied at locations 5, 6 and 7 (chapter 6). Lack of environmental data acquisition facility could not

allow carrying out investigations in connection with determining the influence of the environmental parameter. Therefore, an initiative has been taken for simultaneous acquisition of passive acoustic data along with the environmental data.

In this chapter, the investigations carried out using passive acoustics data analyses at location 8 near Grande Island (Fig. 2.1) from 10-14 March 2016 have been elucidated. Soundscape characteristics of this location, which is situated away from the coral reef area at 20 m water depth have been investigated. The spectral peaks of the animal vocalizations along with the temporal parameters (Luczkovich *et al*., 2008) are important subject matters in the soundscape studies. Fish sound identification carried out in this location has been covered in chapter 3. The two types of fishes were identified at location 8 such as i) Sciaenidae and ii) *Terapon theraps*. Another fish sound that could not be identified but whose spectral parameter (peak PSD) and temporal parameters were determined, has been referred to as the 'Grande Type A' in section 3.5.7 of chapter 3.

In addition to the utilization of the conventional spectral analyses for the identification of biotic signals (chapter 3), the investigations reported in this chapter involves the use of acoustic metrics (ACI, H, and AR) (Sueur *et al.,* 2012; Harris and Radford, 2014) and SPL_{rms} and their relationship with environmental parameters (wind, current, and temperature). This relationship can be deciphered through the estimation of correlation coefficients. The results of the principal component analysis (PCA) and the dendrogram of the twenty-four-hour data have also been presented (Nedelec *et al.,* 2015; Desjonqueres *et al.,* 2015). In order to identify the influence of the environmental parameters that could have affected fish sounds, further analyses of the recorded individual fish sounds such as Sciaenidae, Terapontdae (*Terapon threaps*) and the unnamed fish need to be carried out.

Information relating to Automatic Weather Station (AWS) and Current meter related to the environmental data are covered in chapter 2. The current meter system also acquires temperature data. Details of the mathematical expressions of the Acoustic Metrics are provided in chapter 6 and the same will not be repeated in this chapter.

7.2 Results

In this section three acoustic metrics were computed along with the root-mean-square sound pressure level (SPL_{rms}). The three acoustic metrics were computed in relation to the three frequency bands (i.e. shrimp, fish and wide-bands). In order to determine the eco-acoustics indices, utilization of soundscape ecology package *Seawave* (Sueur *et al.*, 2008b) developed for the R computing environment (https://cran.rproject.org/web/packages/seewave/index.html) has been used. The expressions to compute ACI, H and AR are dealt in chapter 6. Besides the computation of acoustic metrics, the SPL_{rms} calculation is also carried out using the equation (5.1) given in section 5.3 of chapter 5 for the three frequency bands. The sampling frequency to acquire the time series data for this location was 96000 Hz (Table 2.1).

7.2.1 Performance study of acoustic metrics including SPL_{rms}

Interestingly, the time series plots of the entire data recorded during the data acquisition period (10-14 March 2016) are being used to compute acoustic metrics including SPL_{rms}:

SPL_{rms}

The SPL_{rms} values were examined to assess the general trends in the acoustic characteristics of the study site. The entire data shows a significant variation in SPL_{rms} for the wideband, fish and shrimp bands signal, especially when the fish sounds were present (Fig. 7.1a). Box plots of the derived SPL_{rms} values for the wideband, fish bandand shrimp bands are also presented (Fig. 7.2 a)**.** The mean SPL_{rms} value of the wideband data is observed to be higher (117.70 dB re 1µPa) compared with the fish (113.50 dB re 1µPa) and shrimp (112.10 dB re 1µPa) bands.

Acoustic Entropy Index (H)

The H metrics derived from the soundscape are considered as a suitable proxy for estimating the biodiversity of a reef system (Sueur *et al*., 2008a; Harris et al., 2016). H metrics were calculated for wideband, fish and shrimp bands (Fig. 7.1b). The magnitude of the H values is higher for wideband sound followed by a shrimp band in comparison to the fish band due to the chosen bandwidth. The levels of the H values in the presence of fish sound are observed to be reduced for fish band as well as for wideband and shrimp band data (Fig. 7.1b). This is due to the harmonic nature of the fish vocalization as discussed in previous chapter (Bohnenstiehl *et al.*, 2018). Box plots show the mean H values of the wideband (0.840) and shrimp band (0.820) sounds during the entire data acquisition period (Fig. 7.2b). H values for fish band data showmuch-reduced values (0.530) in this location. The boxplot depicts much higher variations in the H-spreads for the wideband than the other two bands for entire data (Table 7.1a). Unlike the fish band, the shrimp and wideband data show non-normal distribution.

Acoustic Richness Index (AR)

The AR metric is derived based on the envelope complexity and intensity of the recorded data (Depratere *et al*., 2012). The AR values also show significant variation during the fish chorus for the wideband, fish and shrimp bands (Fig. 7.1c), which is in accordance with the SPL_{rms} (Fig. 7.1a) in the location studied here. The box plots of AR metric of the entire data show that the mean AR values of the wideband, fishand shrimp bands are 0.315, 0.312 and 0.311 respectively (Fig. 7.2c). The distributions of the AR metric for the three bands indicate negligible skewness, which indicates near-normal distribution except for the shrimp band data (Table 7.1a). Higher H-spread values are comparable for all the three frequency bands.

Acoustic Complexity Index (ACI)

The derived ACI metrics for the wideband, fish and shrimp band sounds are depicted in (Fig. 7.1d) (Farina, 2014; Pieretti *et al.*, 2011). The magnitude of ACI values is higher

for the wideband sound followed by shrimp band sounds. The magnitude of ACI values for the fish band sound is the lowest in comparison to the other two bands. Box plot (Fig. 7.2d) show mean ACI values are higher for the wideband sound (2.16x 10^4) and shrimp band (0.82x 10^4) in comparison to the fish band (0.07x 10^4). The skewness parameters of all the three bands indicate a normal distribution (Table 7.1a).

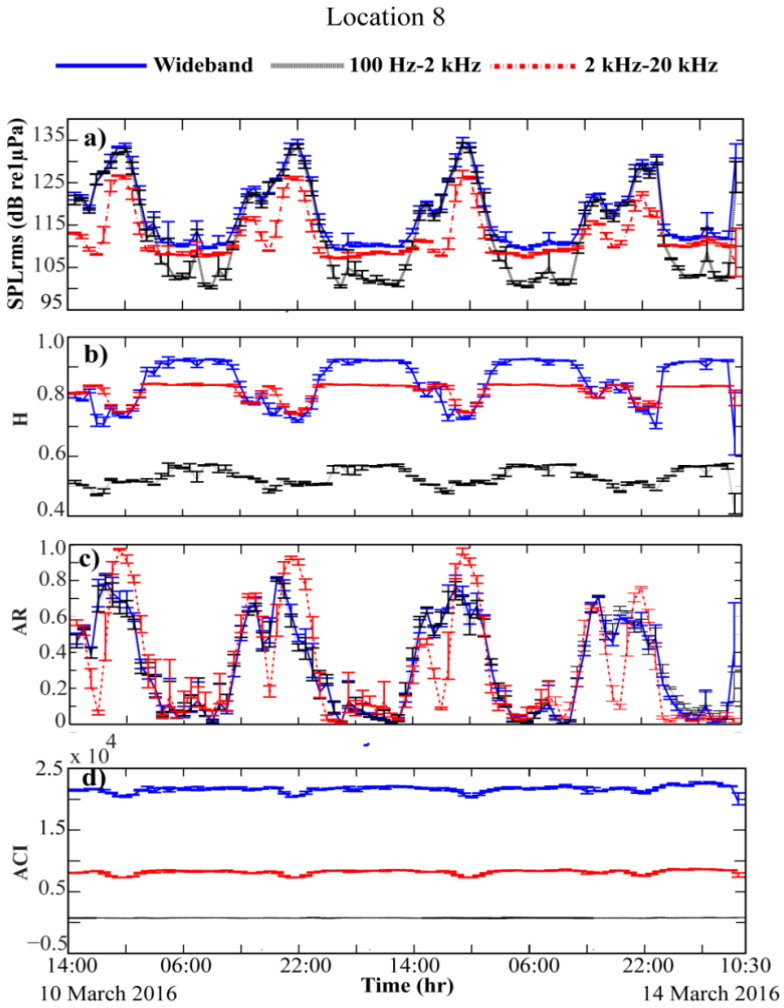

Fig. 7.1 a) SPL_{rms} (dB re 1µPa), (b) Acoustic entropy (H) (c) Acoustic richness (AR) (d) Acoustic complexity index (ACI) for wideband, fish and shrimp bands of the study location for entire data recorded from 14:00 hr of 10 March to 10:30 hr of 14 March 2016.

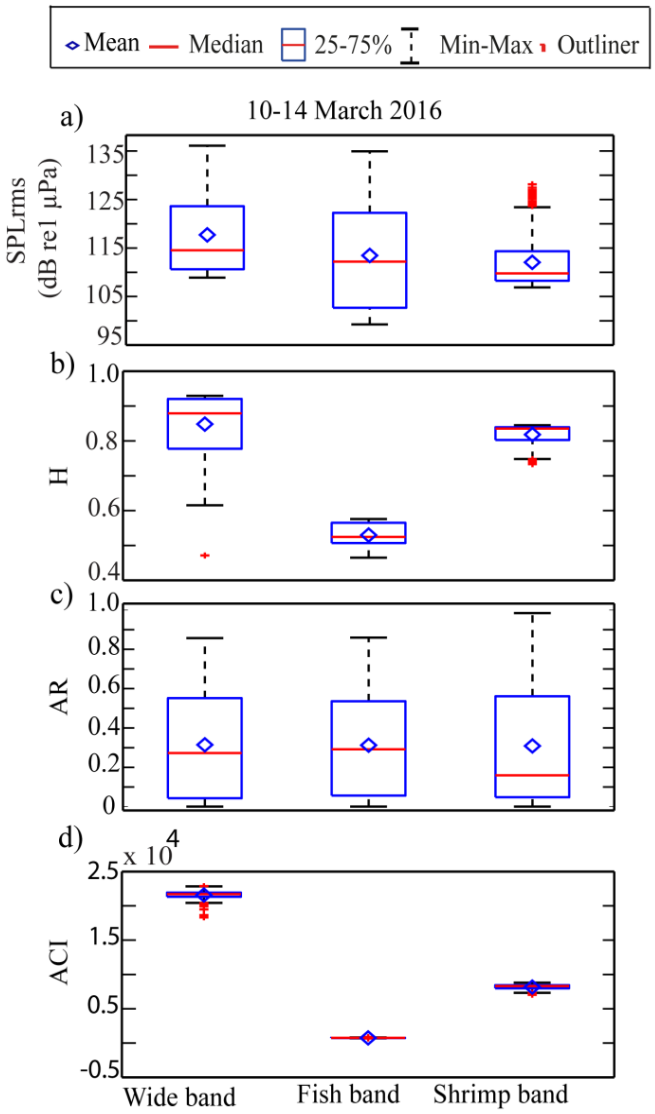

Fig. 7.2 Box plots of the derived metrics for wideband, fish band and shrimp bands: (a) SPL_{rms} (b) Acoustic entropy (H), (c) Acoustic richness (AR) and (d) Acoustic complexity index (ACI) for entire data recorded from 14:00 hr of 10 March to 10:30 hr of 14 March 2016.

Table 7.1a) Mean value of the acoustic metric and related H-spread and skewness values for location 8

Entire data (10-14 March 2016)	Frequency bands	Acoustic metric (Mean values)	H-spread	skewness
SPL_{rms} (dB re1 μPa)	Wideband	117.70	12.9861	3.1405
	Fish band	113.50	19.5812	1.3043
	Shrimp band	112.10	6.0690	2.3194
H (arbit. unit)	Wideband	0.840	0.1430	-0.0392
	Fish band	0.530	0.0581	0.0053
	Shrimp band	0.820	0.0365	-0.0172
AR (arbit. unit)	Wideband	0.315	0.5090	0.0420
	Fish band	0.312	0.4801	0.0207
	Shrimp band	0.311	0.5135	0.1494
ACI (arbit. unit)	Wideband	2.16×10^4	609.9586	-120.0626
	Fish band	0.07×10^4	36.5524	-0.1041
	Shrimp band	0.82×10^4	444.8156	-137.0013

Table 7.1 b) Mean value of the acoustic metric, and related H-spread and skewness values of fish families for Location 8

Metrics	Frequency bands	Sciaenidae			*Terapon theraps*			Grande Type A		
SPL_{rms} (dB re1 µPa)		Acoustic Metric (Mean)	H-spread	Skewness	Acoustic Metric (Mean)	H-spread	Skewness	Acoustic Metric (Mean)	H-spread	Skewness
	Wideband	123.9	7.574	-2.087	128.0	9.630	-3.763	113.2	3.072	0.426
	Fish band	123.5	8.083	-2.366	126.5	9.228	-4.030	109.2	6.574	-0.882
	Shrimp band	109.6	1.508	1.019	120.8	11.073	-3.073	108.7	0.953	-0.630
H	Wideband	0.764	0.070	0.0000	0.751	0.033	0.008	0.906	0.037	-0.006
	Fish band	0.494	0.034	-0.002	0.507	0.010	0.001	0.536	0.0616	-0.004
	Shrimp band	0.817	0.032	-0.005	0.765	0.031	0.009	0.840	0.0027	-0.000
AR	Wideband	0.581	0.362	0.062	0.435	0.229	-0.046	0.124	0.216	-0.003
	Fish band	0.566	0.353	0.060	0.392	0.223	-0.038	0.133	0.219	-0.001
	Shrimp band	0.405	0.376	-0.016	0.729	0.314	-0.106	0.021	0.032	-0.013
ACI	Wideband	$2.18x10^4$	329.262	5.350	$2.10x10^4$	961.960	263.570	$2.17x10^4$	264.120	-10.0
	Fish band	$0.07x10^4$	5.564	3.059	$0.07x10^4$	66.390	23.680	$0.07x10^4$	98.370	-13.06
	Shrimp band	$0.81x10^4$	301.020	-55.320	$0.76x10^4$	755.800	273.230	$0.083 x10^4$	1.700	-47.8

7.2.2 Study of acoustic metrics including SPL_{rms} within the 'fish vocalization period'

In order to determine the acoustic metrics of individual fish sound, the 24-hr datasets are chosen out of the entire recorded data and the identified fish sounds are segmented based on the timings (Section 3.5.7; chapter 3). The presentation of box plots of acoustic metrics for fish sounds within the 'fish vocalization period' [14:00 hr (11 March 2016) - 03 hr (12 March 2016)] has been depicted in (Fig. 7.3) Three different fish sound types were identified within the (16:00 to 18:30 hr), (19:00 to 22:30 hr) and (00:30 to 02:30 hr) as Sciaenidae, *Terapon Threaps* and the unnamed fish assigned as 'Grande Type A' respectively. Given below, is a discussion on the box plot data:

SPL_{rms}

Box plots of the derived SPL_{rms} values for the wideband, fish bandand shrimp bands are depicted in the case of Sciaenidae in (Fig. 7.3a)**.** The mean SPL_{rms} value of the wideband, fish and shrimp band data are found to be (123.9 dB re 1µPa), (123.5 dB re 1µPa), and (109.60 dB re 1µPa). As mentioned in the case of *Terapon threaps*, the mean SPL_{rms} value is found to be (128.0 dB re 1µPa), (126.5 dB re 1µPa) and (120.8 dB re 1µPa) for wide, fish and shrimp bands respectively (Fig. 7.3b).The mean SPL_{rms} values for the wideband, fish bandand shrimp bands in the case of the Grande Type A (Fig. 7.3c) are found to be (113.2 dB re 1µPa), (109.2 dB re 1µPa), (108.7 dB re 1µPa) respectively. The higher H-spread and skew values of the SPL_{rms}fish calls in the case of Sciaenidae and*Terapon threaps* show higher SPL_{rms} variations and non-normal characteristics (except for shrimp band data of Sciaenidae fish call) (Table 7.1b).

Acoustic Entropy Index (H)

Box plots show the mean H values for Sciaenidae fish sound data of the wideband and shrimp band data are observed to be 0.764 and 0.817 respectively (Fig. 7.3d). H values for fish band data showmuch-reduced values (0.494).Similarly, in the case of *Terapon threaps* sounds, the mean H values are found to be 0.751, 0.508, and 0.766 for wide, fish and shrimp bands respectively (Fig. 7.3e). The mean H values are found to be 0.907,

0.536, and 0.841 for wide, fish and shrimp bands respectively for the Grande Type A fish sounds (Fig. 7.3f). In the case of the H index, the H-spread and skew values for Sciaenidae, *Terapon threaps* and the unnamed fish calls are found to be negligible in all the three frequency bands (Table 7.1b).

Acoustic Richness Index (AR)

The box plots indicate that the mean AR values in the case of Sciaenidae fish sound data of the wideband, fish and shrimp bands are observed to be 0.582, 0.567 and 0.405 respectively (Fig. 7.3g). Similarly, for *Terapon threaps* sounds, the mean AR values are found to be 0.435, 0.393, and 0.729 for wide, fish and shrimp bands respectively (Fig. 7.3h).The mean AR values are found to be 0.124, 0.133, and 0.022 for wide, fish and shrimp bands respectively for the Grande Type A fish sounds (Fig. 7.3i).Higher H-spread values indicate significant variability in the AR box plot parameters of the Sciaenidae, *Terapon threaps* and Grande Type A fish sounds (except for shrimp band) calls (Table 7.1b). Skew values show non-normal data distribution especially for Sciaenidae, *Terapon threaps* fish calls in all the three frequency bands.

Acoustic Complexity Index (ACI)

The mean ACI values of the Sciaenidae fish sound data in the wideband, fish and shrimp bands are observed to be $2.18x10^4$, $0.07x10^4$, and $0.81x10^4$respectively (Fig. 7.3j). Similarly, for the *Terapon threaps* sounds, the mean ACI values are found to be $2.10x10^4$, $0.07x10^4$, and $0.76x10^4$ in the wide, fish and shrimp bands respectively (Fig. 7.3k). The mean ACI values are found to be $2.17x10^4$, $0.07x10^4$, and $0.84x10^4$ for the wide, fish and shrimp bands respectively in the case of the Grande Type A fish sounds (Fig. 7.3l).Negligible H-spread and skew values are observed here in all the three fish frequency call at all the three frequency bands for ACI box plot parameters (Table 7.1b).

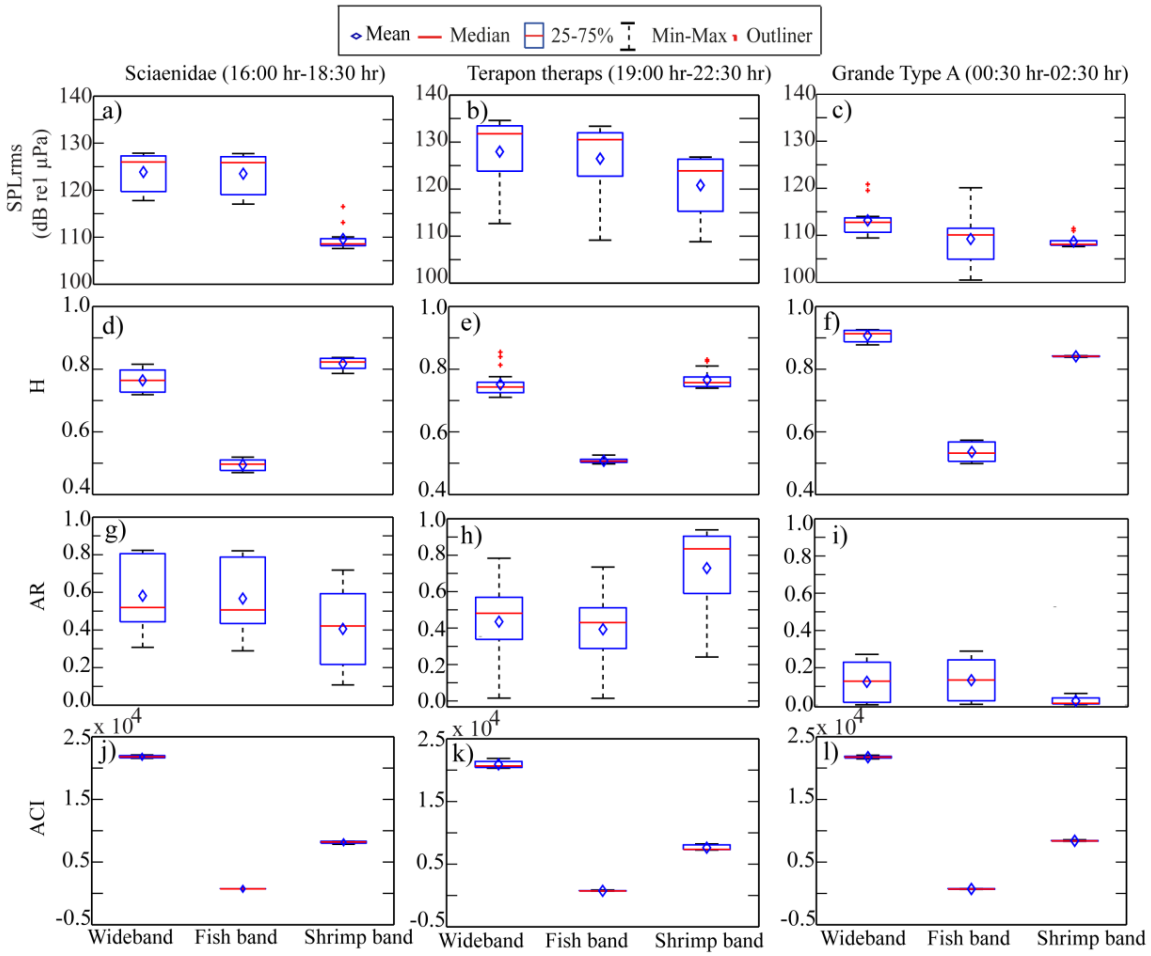

Fig. 7.3 Box plots of the derived metrics of the Sciaenidae fish sound for wideband, fish bands and shrimp bands: (a) SPL_{rms} (d) Acoustic entropy (H), (g) Acoustic richness (AR) and (j) Acoustic complexity index (ACI) from 16:00 – 18:30 hr of 11 March 2016. Box plots of the derived metrics of the *Terapon threaps* for wideband, fish bands and shrimp bands: (b) SPL_{rms} (e) Acoustic entropy (H), (h) Acoustic richness (AR) and (i) Acoustic complexity index (ACI) from 19:00-22:30 hr of 11 March 2016. Box plots of the derived metrics of the unnamed fish for wideband, fish bands and shrimp bands: (c) SPL_{rms} (f) Acoustic entropy (H), (i) Acoustic richness (AR) and (k) Acoustic complexity index (ACI) (l) from 00:00-02:30 hr of 12 March 2016.

7.2.3 Influence of environmental parameters on acoustic metrics for twenty-four-hour datasets

In the present study, principal component analyses (PCA) is applied to the passive acoustic data (Nedelec *et al*., 2015) to compare the effect of environmental parameters over the performance of the acoustic metrics. The present investigation involves 24-hr wideband (i.e., unfiltered data), fish and shrimp band data sets from 14:00 hr (11 March 2016) to 14:00 hr (12 March 2016). Seven parameters such as SPL_{rms} and three other acoustic metrics (H, AR, and ACI) along with environmental data: wind, current speed, and water temperature are used here.

The computation of the Pearsoncorrelation coefficients of the measured passive acoustic parameters and environmental data for three frequency bands of 24-hr data is carried out before PCA (Hristian *et al*., 2017) is performed. The clustering of thevariables is shown as a biplot of PCA in a three-dimensional view (Fig. 7.4a) for wide-band data. A correlation matrix of the wideband 24-hr datasets are generated, and the observation suggests correlation coefficients (0.810; $p<2.8077e^{-23}$)between (SPL_{rms}; AR). Elements of the correlation coefficient matrix having < 0.50 or negative values are not discussed in the text, though, they are employed for PCA. After performing PCA, it was observed that the first three principal components (PC1, PC2, and PC3) together explain 86.88% of the total variance in the data. For wideband sound data, the PCA based scatter plot between the PC1, PC2, and PC3 suggest that the parameters viz., SPL_{rms} and AR form a cluster along with the current speed (Fig. 7.4a) where moderate correlation coefficients are also found between the (SPL_{rms}; current speed) as well as between the (AR; current speed). Moderate correlation coefficients are observed, (0.661; $p<2.3203\ e^{-13}$) between (H; temperature), (0.569; $p<1.3730e^{-09}$) between (H; ACI), (0.500; $p<2.2869e^{-07}$) between (ACI; wind speed) and (0.640; $p<2.5568e^{-12}$) between (wind speed; temperature) indicating another cluster of H, ACI, temperature and wind speed parameters (Fig. 7.4a). The clustering patterns are also provided in the dendrogram (Fig. 7.4b), which also support the relationship between the parameters.A dendrogram for 7 variables delineated two main clusters from the study area. A dendrogram consists of many U-shaped lines

connecting variables in ahierarchical tree. The height of each 'U' represents the distancebetween the two objects being connected. Observations that are joined together below the line are in clusters. It is also evident from (Fig. 7.4b), cluster 1 consists of SPL_{rms}, AR and current speed, and cluster 2 is characterized by H, ACI, temperature and wind speed for wideband passive acoustic data.

Observation for fish band data of 24-hr shows that the first three principal components (PC1, PC2, and PC3) together explain 84.05% of the total variance in the data. For fish band data, the PCA based scatter plot between the PC1, PC2, and PC3 (Fig**.** 7.4c) suggest that the parameters viz., (SPL_{rms}; AR) show the highest influence 0.800, and they form a cluster along with the current speed where correlation coefficients are found to be (0.616; $p<2.2652e^{-11}$) between the (SPL_{rms}; current speed). The moderate correlation coefficients (0.610; $p<4.0247e^{-11}$) and (0.600; $p<2.3132e^{-10}$) between the parameter (H; temperature) as well as (H; wind speed) are observed respectively. Two clustering groups are also depicted in the dendrogram plot (Fig. 7.4d). Clustering between the SPL_{rms}, AR and the current speed is observed for fish band data, whereas the relationship within the H, temperature and wind speed forms another cluster where distant involvement with ACI is also seen.

The highest correlation coefficient (0.930; $p<5.8368e^{-4}$)is observed between the SPL_{rms} and AR for 24-hr data of high-frequency shrimp band. The moderate correlation coefficient (0.553; $p<4.8770e^{-09}$) between the ($SPL_{rms;}$ current speed) is seen. The similar correlation coefficient 0.514; $p<8.6428e^{-08}$ between the (AR; current speed) suggest a clustering group among the SPLrms, AR and current speed (Fig. 7.4e and f). A close examination of correlation coefficients between the (H; ACI) show the highest values 0.905; $p<8.9358e^{-37}$ for shrimp band data. Temperature and wind speed show a moderate 0.640; $p<2.5568e^{-12}$ correlation coefficient. Moderate correlation coefficients between the H and other two parameters (wind speed and temperature), and similar situation for ACI with the wind speed and temperature do not prevent to form clustering of H, ACI, wind speed and temperature for high-frequency shrimp band data from Grande Island data. For

shrimp band data, the first three principal components (PC1, PC2, and PC3) together explain 92.41% of the total variance in the data.

Fig**.** 7.5 (a-c) shows variations in wind speed, current speed and temperature data of the entire acquisition period. The PCA of the 24-hr data (from 14:00 hr of 11 March to 14:00 hr of 14:00 hr of 12 March 2016) has been carried out. From the PCA analyses, two clusters for 24-hr wideband, fish band and shrimp band passive acoustics data is seen. In cluster 1 for wideband data, the existence of SPL_{rms} and AR in the same cluster can be understood through the mathematical expressions utilized to compute both the parameters in the temporal scale. SPL_{rms} (computed using equation 5.1) is an RMS pressure level, and AR (computed using equations 6.3) is a product of the Hilbert transform, and median of the acoustic envelope as well as the inverse square of the number of recordings. AR metrics are designed for bird sound recording in temperate regions where background sound is dominant in comparison with sound due to acoustic activity. In Grande Island, the intensity of fish chorus is much higher in comparison to the background sound, especially during the fish chorus time. Under such conditions, the performance of AR and SPL_{rms} is observed to be similar as depicted in [Fig**. 7.1** (a and c)] and observed in time-series data

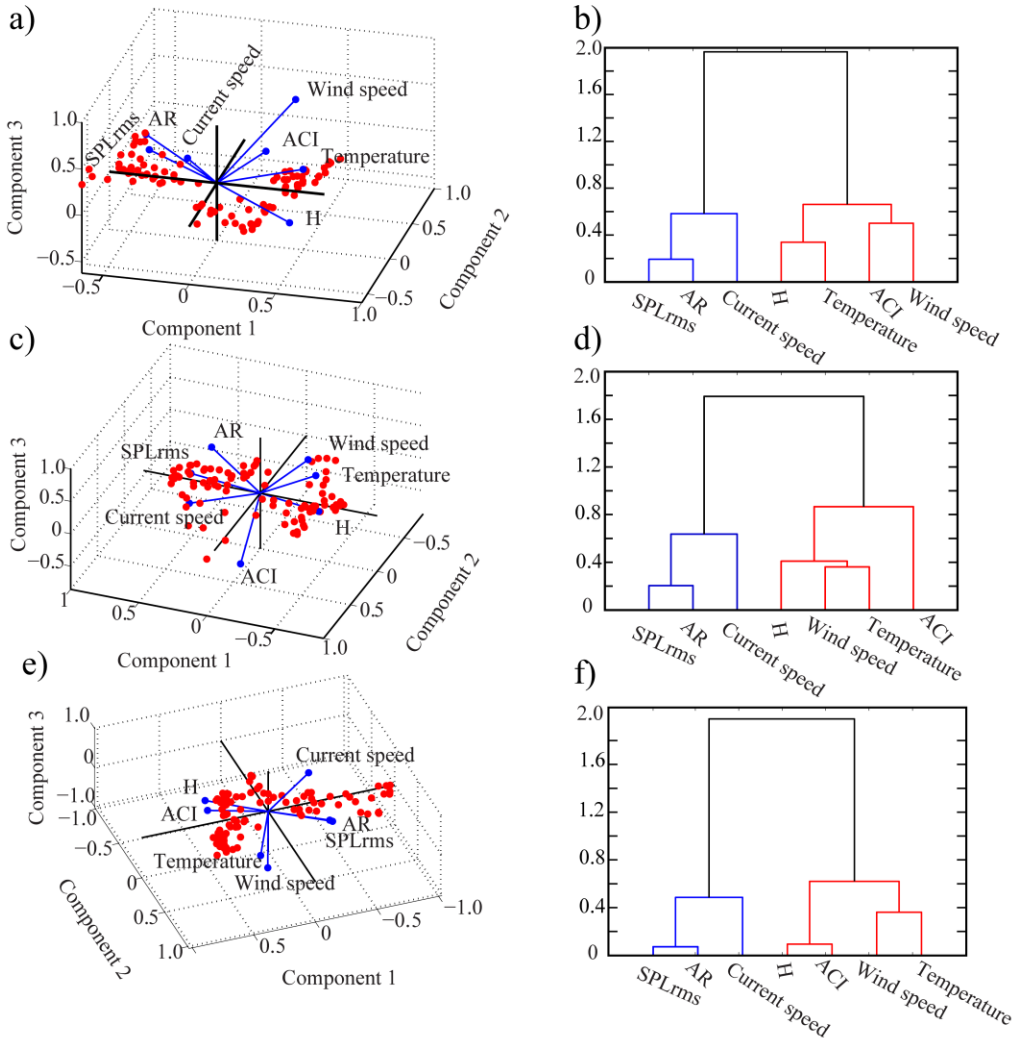

Fig. 7.4*(*a) represents a clustering of the seven variables including three environmental and SPL_{rms}, H, AR, and ACI computed parameters using 'wideband' passive acoustics data in three-dimensional views, (b) represents dendrogram for the clustering of seven variables for wideband. (c) represents a clustering of the above mentioned seven variables for 'fish band' data, (d) represents a dendrogram for the clustering of seven variables for 'fish band' (e) represents clustering of the above mentioned seven variables for 'shrimp band', (f) represents dendrogram for the clustering of seven variables for 'shrimp band'.

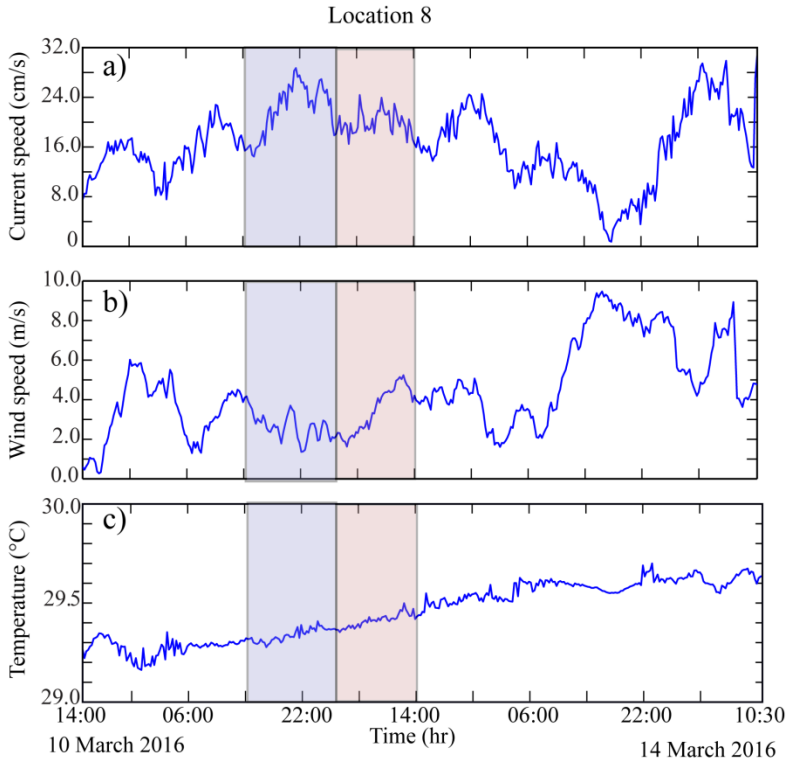

Fig. 7.5(a) measured current speed, (b) wind speed and (c) temperature data. Shaded part show i) 24-hr data from 14:00 hr of 11 March 2016 to 14:00 hr 12 March 2016, ii) 'Fish vocalization period' from 14:00 hr of 11 March 2016 to 03:00 hr 12 March 2016, and iii) 'No vocalization period' from 03:00 hr to 11:00 hr of 12 March 2016. Light gray and purple color combined bands are marked for twenty-four hr measured data whereas light gray band indicate 'fish vocalization period' within the twenty-four hr data.

7.2.4 Influence of environmental parameters on acoustic metrics within the 'fish vocalization period'

To compare the effect of the environmental parameters over the performance of the acoustic metrics data of the identified fish call timings, principal component analyses (PCA) is carried out. Once again, this investigation involves three different fish sound types, which are found within the recording period (16:00 to 18:30 hr), (19:00 to 22:30 hr) and (00:30 to 02:30 hr) as Sciaenidae, *Terapon threaps* and unnamed fish (Grande Type A) respectively within the 'fish vocalization period' [14:00 hr (11 March 2016) - 03

hr (12 March 2016)] from the Grande Island location. Acoustic metrics of different fish sounds are presented in section 7.2.2. Seven of the parameters are also considered here for similar studies described in previous sections.

Correlation coefficients computation and subsequent PCA based clustering for Sciaenidae fish family with the (16:00 to 18:30 hrs data) for the three frequency bands reveal interesting results. The highest correlation coefficients: (0.905 $p<5.1241e^{-05}$), (0.845 $p<5.3388e^{-04}$) and (0.702; $p<0.0109$) between the SPL_{rms} with respect to the wind, current speed, and AR respectively is observed for wideband passive acoustic data. AR also shows higher correlation coefficient (0.816; $p<0.0012$) with wind speed. The correlation coefficient between the two environmental parameters (wind; current speed) show (0.822; $p<0.0010$). PCA reveal clustering between the SPL_{rms}, AR, wind, and current speed along with another cluster involving H and temperature for wideband data (Fig. 7.6a). Similarly for fish band passive acoustic data, SPL_{rms} show correlation coefficients: (0.847; $p<4.9555e^{-04}$), (0.898; $p<7.2614e^{-05}$), (0.660 $p<0.0194$) between the current and wind speed and AR respectively. AR shows higher correlation coefficient: (0.808; $p<0.0015$) with the wind speed, and the correlation coefficient between the (wind; current speed) show (0.822; $p<0.0010$). The clustering between SPL_{rms}, AR, wind, and the current speed is observed along with another cluster linking the H and temperature (Fig. 7.6b). For shrimp band data involving Sciaenidae sound, SPL_{rms} shows correlation coefficients: (0.505; $p<0.0933$), (0.761; $p<0.0040$) between the wind speed and AR respectively. The correlation coefficient between the (wind; current speed) show(0.822; $p<0.0010$) and the correlation between the other two acoustic metrics (ACI; H) show higher value (0.926; $p<1.4887e^{-05}$). PCA based clustering reveal two broad-based clusterings between the SPL_{rms}, AR, wind and current speed, and another cluster between the ACI and H (Fig. 7.6c).

Correlation coefficients and PCA based clustering for *Terapon threaps* fish species within the (19:00 to 23: 30 hrs data) of the three frequency bands are covered here. For wideband data for *Terapon threaps*sound, SPL_{rms} show correlation coefficients: (0.867; $p<1.5189e^{-06}$), (0.704; $p<7.5885e^{-04}$) and (0.844; $p<5.5508e^{-06}$) between the current and

wind speed and AR respectively. The correlation coefficient between the (wind; current speed) show (0.504; $p<0.0277$), and the correlation coefficient between the other two acoustic metrics (H; ACI) show (0.609; $p<0.0057$), whereas the correlation coefficient between the (AR; current speed) is found to be (0.889; $p<3.4991e^{-07}$). PCA based clustering reveal two broad-based clusterings between the SPL_{rms}, AR, wind, and current speed and another cluster between the ACI and H (Fig. 7.6d). The highest correlation coefficients: (0.874 $p<1.0073e^{-06}$), (0.687; $p<0.0012$ and (0.811; $p<2.5352e^{-05}$) are found between the SPL_{rms} with respect to the current, wind speed and AR respectively for fish band acoustic data. AR also shows a higher correlation coefficient (0.873; $p<1.0608e^{-06}$) with the current speed. The correlation coefficient between the two environmental parameters (wind; current speed) show (0.504; $p<0.0277$). The correlation coefficient between the (H and temperature) show (0.542; $p<0.0164$). PCA based clustering show clustering between the SPL_{rms}, AR, wind and current speed along with another cluster linking H and ACI for fish band data (Fig. 7.6e). Similarly for shrimp band passive acoustic data of *Terapon threaps*, SPL_{rms} show correlation coefficients: (0.845; $p<5.1291e^{-06}$), (0.730 $p<3.8775e^{-04}$), (0.985; $p<1.7007e^{-14}$) between the current and wind speed and AR respectively. AR shows higher correlation coefficient (0.876; $p<8.6612e^{-07}$) with the current speed, and (0.687; $p<0.0011$) with the wind speed. The correlation coefficient between the (wind; current speed) show (0.504; $p<0.0277$). The correlation coefficient between the two acoustic metrics (H; ACI) is found to be (0.898; $p<1.7088e^{-07}$). PCA based clustering between SPL_{rms}, AR, wind, and the current speed is observed along with another cluster linking H and ACI for shrimp band data (Fig. 7.6f).

The correlation coefficients and PCA clustering for the Grande Type A fish within the (00:30 to 02:30hr) for wide frequency bands is determined. Moderate correlation coefficients: (0.740; $p<0.0060$), (0.526; $p<0.0793$) between the current speed with respect to H, and ACI respectively for wideband data is noted. AR show moderate correlation coefficient (0.632; $p<0.0274$) with wind speed. The higher correlation coefficient between the two acoustic metrics (H; ACI) is found to be (0.820 $p<0.0011$). PCA based clustering show three prominent clusters, between i) SPL_{rms} and temperature is observed

along with the two other clusters ii) AR, wind speed and iii) H, ACI and current speed for shrimp band data (Fig. 7.6g). The correlation coefficients of current speed are found to be (0.814; $p<0.0013$) and(0.806; $p<0.0015$) with respect to H and ACI for fish band data for Grande Type A fish. The higher correlation coefficient (0.984; $p<7.1028e^{-09}$) is found between (H and ACI). The moderate correlation coefficient (0.635; $p<0.0263$) between the (wind speed and AR) is noted. Two clustering patterns are visible in (Fig. 7.6h) i) ACI, H and current speed and ii) SPL_{rms}, AR, wind speed and temperature. For shrimp band data for unnamed fish, no significant correlation coefficients are obtained. The moderate correlation coefficient (0.503; $p< 0.0667$) is seen between the (temperature and SPL_{rms}). PCA based clustering show three clusters i) current and AR, ii) wind speed and H, and iii) SPLrms, temperature, and ACI.

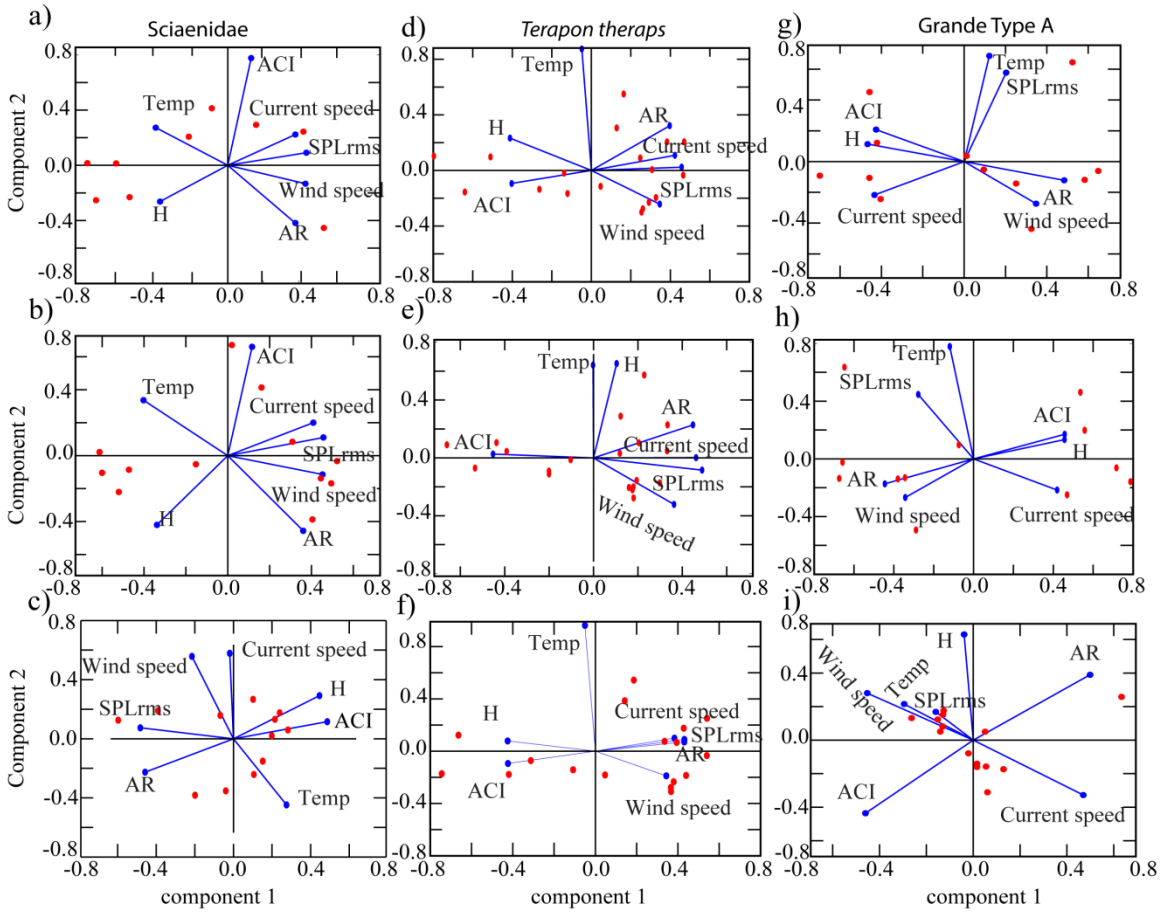

Fig. 7.6(a-c) represents a clustering of the seven variables including three environmental and SPL_{rms}, H, AR, and ACI of Sciaenidae fish sound computed using (a) wideband (b) fish band and (c) shrimp band passive acoustics data in two-dimensional views,(d-f) represents a clustering of the seven variables including three environmental and SPL_{rms}, H, AR, and ACI of Terapon theraps fish sound computed using (d) wideband (e) fish band and (f) shrimp band passive acoustics data in two-dimensional views, (g-i) represents a clustering of the seven variables including three environmental and SPL_{rms}, H, AR, and ACI of Unnamed fish sound computed using (g) wideband (h) fish band and (i) shrimp band passive acoustics data in two-dimensional view.

7.3 Discussions

The association between the environmental parameters and the acoustic metrics from the 24-hr data is evident**.** The recorded current speed is also found to be a component of cluster 1 (Fig. 7.4). The ambient sound due to current flow is normal, however, isolating the sound component due to flow from the recorded sound data is multifarious. An effort to record current flow-sound resulting from a turbulent oceanic environment is being made (Bassett *et al*., 2014). The pressure spectral density attributed to the current flow sound is studied using data-model comparison up to 500 Hz, indicating that the flow noise exceeds mean slack noise levels by more than the 50 dB at 20 Hz. Moreover, under strong flow condition, sediment generated sound is also reported (Bassett *et al*., 2013), which is frequency-dependent up to 1-30 kHz, especially having a significant effect within the 1-4 kHz. This suggests the importance of the flow sound level and scale. Along with the biophony i.e. fish sound, the extent of sound generated due to flow is also a function of bottom type. McWilliam and Hawkins (2013) and Bertucci *et al*. (2016), have observed that the acoustic characteristics (SPL_{rms}) of a habitat patch (clayey silty in present study location) are greatly influenced by extraneous sound i.e. fish sound. Similar conditions are also observed in the present study location. The measured current speed variations show (16 cm/sec to 28 cm/sec) within the 24-hr duration (Fig.7.5a). The moderate correlation coefficient between the time series of the flow data with AR and SPL_{rms} suggest the influence of flow noise as depicted in cluster 1 (Fig.7.4 a-e) for three frequency bands. In the case of current speed, moderate correlation coefficients with SPL_{rms} are found to be within the (0.640; $p<2.5568e^{-12}$) to (0.554; $p<4.8770e^{-09}$) even for the three frequency bands as observed through correlation coefficients as well as PCA and dendrogram based clustering for twenty-four-hour datasets. The variability of the SPL_{rms} along with the acoustic metric AR shows higher values of the correlation coefficients (0.930; $p<5.8368e^{-4}$) among the three frequency bands. Therefore, AR could be a proxy for the geophonies. However a similar relationship is absent for the other two

metrics (ACI and H) with respect to the geophonies, except for a high correlation coefficient (0.905; $p<8.9358e^{-37}$) among H and ACI for shrimp band data.

Acoustic metrics such as H, ACI and measured parameters such as temperature and wind speed form cluster 2. It has been reported that the wind affects the performance of ACI and H parameters due to their intermittent activities in the terrestrial environment (Sueur *et al*., 2008a; Depraetere *et al*., 2012). The same is found to occur in the underwater environment too. The wind-generated sound largely results in bubbles through the process of wave-breaking. At lower frequency (<500 Hz), it is the oscillation of bubble clouds themselves that are considered to be the source of the sound, while at higher frequencies the excitation of resonant oscillation by individual bubbles is the source of sound (Dahl *et al*., 2007). Therefore, the relationship between the ACI and H with respect to the wind speed is apparent in cluster 2. The measured wind speed is varying between 2 to 6 m/sec (Fig**.** 7.5b), which suggests that the sea state of 2 to3 i.e., smooth to a gentle breeze. Apart from that, the relationship between temperature and wind speed cannot be said to be unknown. An increase in water temperature (Fig**.** 7.5c) in the present study location has been observed.The intensification of a sound generation with the increase in water temperature influences the behavioral activity of the marine animal. Temperature affects animal sound characteristics in both stridulationand drumming sounds. Sound frequencies of both sound types shift to higherfrequencies with the rising temperature, and the effects of temperature on sound production and auditory abilities in the Catfish (family Doradidae) has been investigated (Papes and Ladich, 2011). It has also been demonstrated that the sound signal parameters (frequency and intensity) of the Terapontidae fish species (*Terapon Jarbua*) are related to the temperature variations (Amron *et al*., 2017). The mathematical expressions containing H and ACI involve frequency components. The efficiency of H metrics depends on the spectral component (H_f) to be flat or multi-peak for its effective use. Therefore, the change in water temperature affects the frequency of the fish sound generated which ultimately has an effect on the spectral component of H and ACI parameters. This

phenomena directly relates water temperature with H and ACI as seen in the cluster diagrams.

The relationship between the environmental parameters and acoustic metrics of fish calls in the case of Sciaenidae sound show good correlation (0.702; $p<0.0109$ - 0.660; $p<0.0194$) between SPL_{rms} and AR, for all the three frequency bands. A significant correlation coefficient values (0.810; $p<2.8077e^{-23}$) between SPL_{rms} and AR is also observed in the case of *Terapon Threaps* for the entire three frequency band. There is poor correlation coefficient between the SPL_{rms} and AR for the Grande Type A fish sound. For Scieanidae sound, AR shows good correlation (0.808; $p<2.8077e^{-23}$– 0.816; $p<0.0012$) with wind speed for the wide and fish band. For *Terapon theraps*, AR shows good correlation (0.889; $p<3.4991e^{-07}$– 0.873; $p<1.0608e^{-06}$) with current speed for all three bands whereas the correlation of AR with wind speed is moderate (0.687; $p<0.0012$) for shrimp band alone. For *Terapon threaps*, correlation of AR with wind speed for wide and fish bands are not significant. Moderate correlation coefficients are observed between the AR and wind for wide and fish band data of the Grande Type A fish sound. Besides, the SPL_{rms} shows significant correlations (0.905; $p<8.9358e^{-37}$ and 0.845 $p<5.3388e^{-04}$) with wind and current speed within the for wideband and fish band frequencies for Scieanidae sound. For *Terapon theraps* sound, SPL_{rms} shows a higher correlation coefficient (0.874; $p<1.0073e^{-06}$ and 0.687; $p<0.0011$) with respect to the wind and current speed for all the three frequency bands. In the absence of visual data as ground truth, SPL_{rms} and PSD of the fish sound can be considered as a ground truth. Here, correlation coefficients between the SPL_{rms} with the ACI and H (as already mentioned) are found to be poor. Though ACI and H do not show a relation with the geophonies, a moderate relationship is observed with temperature data for *Terapon Threaps* sound at fish band frequency range. *Terapon threaps* sounds are recorded during the (19:00 - 22:30 hrs period). Yet again, the Grande Type A fish sounds show a moderate relationship with the temperature which is recorded from 00:30 – 02:00 hrs. Relationship between the temperature parameter and fish sounds during the given time

allows understanding the fact that the temperature parameter regulates the activity of prey and predator species, which may cause diurnal change**.**

7.4 Conclusions

Underwater passive acoustic data analyses were carried out for soundscape monitoring in order to understand the biodiversity of the ecologically important Grande Island region, off Goa. Here, biological sounds were identified, which discerned theTerapontidae (*Terapontheraps)* and Sciaenidae family, and indicated the widespread presence of another fish community whose family/species could not be categorized (referred in the text as Grande Type A) (chapter 3).

Three eco-acoustic indices namely H, AR, and ACI along with SPL_{rms} were computed for three frequency bands viz., wideband, fish, and shrimp band. SPL_{rms} and the AR time series data helped reveal similar characteristics. At the peak vocalization level of the fish chorus, the SPL_{rms} and AR levels also show higher values for the three frequency bands (Fig. 7.1a, c). Besides, there is a similarity in the consistency of H and ACI metrics (Fig. 7.1b, d). Box plot values of the H and ACI show a reduction in mean values (H= 0.533 and ACI=$0.07x10^4$) for fish band data in comparison to the wideband (H=0.840 and ACI=$2.16x10^4$) and shrimp band (H=0.820 and ACI=$0.82x10^4$) data. However, the time-series data of H (Fig. 7.1b) show a reduction at the peak level of the fish chorus (Fig. 3.12c in Chapter 3), even for the three bands. The ACI time series data for three bands do not show any fluctuation (Fig. 7.1d). There is a minor drop in ACI for wideband and shrimp band data when the fish chorus level is high, but such reduction is found to be absent for the fish band data. Box plot-based statistical parameters highlight the performance of acoustic metrics more clearly indicating an H-spread (data range) and skewness (data distribution). In general, H-spread of the H and ACI metrics are significantly low in comparison to AR and SPL_{rms}.

To understand the effect of the environmental parameters over the performance of the acoustic metrics, the principal component analyses (PCA) is employed involving 24-hr

wideband data of 14:00 hr (11 March 2016) to 14:00 hr (12 March 2016) from Grande Island study location as a representative data. Seven parameters such as SPL_{rms} and three acoustic metrics (H, AR, and ACI) along with three other (elements of) environmental data (wind, current speed, and water temperature) form two clusters even for the three bands. Clustering among water flow, AR and SPL_{rms}suggest the importance of the flow noise along with with with the biophony i.e. dominant fish sound. The contribution of acoustic metrics H, ACI and the measured parameters such as temperature and windspeed forms the second cluster. It has been reported that the wind affects the performance of ACI and H parameters during their intermittent activities which lead to the generation of sound due to the bubbles in a shallow water environment. The intensification of the sound generation along with the increase in water temperature influences the behavioral activity of the marine animal. The temperature affects the animal sound characteristics in both stridulationand frequency of the generated fish sound which ultimately has an effect on the performance of H and ACI parameters. This phenomena directly relates to water temperature with H and ACI. drumming sounds, including the sound frequencies of both sound types that shift to higherfrequencies with the rising temperatures. The computation of H and ACI metrics depends on the spectral component and the changes in water temperature affect the

Overall, the present study emphasizes the importance of biophony. Here, the correlation coefficients between the SPL_{rms} and AR with respect to geophonies are moderate, and the SPL_{rms} includes the sound components such as biophony as well as geophony from the Grande Island shallow water environment, off Goa. In the case of the present study location, the above can also be deduced for AR metric. In other words, AR and SPL_{rms} can be treated as a proxy for geophoney. Other sound metrics such as ACI and H use a kind of online filters [that reduces the interfering sound data from geophony] during the data recording. Therefore, geophonies are generally found to be absent in ACI and H as seen in this study.

Chapter 8

Ambient noise study using time series measurements off Grande Island

8.1 Introduction

Ambient noise in the ocean is usually generated due to various sources such as sea surface agitation, surface wave interaction, biological sources and ship traffic. In an underwater acoustic system, the wind-induced ambient noise is considered to be the primary contributor to the background sound within the operational limits. The spatial noise properties which include coherence and directionality are highly dependent on the ocean environment. The characteristics of wind-induced noise such as vertical directionality rely on bottom conditions and sound speed profiles (SSPs). Therefore, the wind-induced ambient noise sensed by a vertical array can be utilized to invert many ocean environmental parameters including SSP, sea surface roughness and sediment properties (Harrison and Simons, 2002). Spatial-temporal measurements of ambient noise can be used to predict noise properties such as coherence and directionality models. A significant amount of research has been done for the estimation of coherence and directionality of ambient noise induced by wind (Buckingham, 1980). Cron and Sherman

(1962), proposed an analytical model of wind-induced ambient noise based on the ray theory. The model considers noises generated from a surface sheet of noise sources with a dipole radiation pattern at the ocean surface. Assuming a stratified ocean environment, a normal mode model for surface generated noise was developed by (Kuperman and Ingenito, 1980). Ray based method for noise cross correlation between hydrophones developed by (Jenson *et al.,* 2011) which include noise source as a sum of plane waves. Later, Harrison (1997), extended the method for the coherence of range and azimuth dependent medium.

Surface generated noise field exhibits a notch in the noise vertical directionality distribution for a downward refractive sound-speed profile (Buckingham, 1980; Hamson, 1985). The resulting noise trough at relatively shallow angles is often called the ambient noise notch. Existence of a "notch" in the noise vertical directionality in shallow water with a downward refractive sound-speed profile is reported (Hamson, 1997; Wilson and Knipfer, 1995; Wei et al., 2004). Employing normal mode and ray theory, directionality can be modeled with reliability knowing environmental characteristics. In other words, using the normal mode approach, the noise field and the environmental conditions under which the noise directionality results in a notch have been analyzed (Yang and Yoo, 1996). In the South China Sea, using beamforming technique analyses of vertical directionality proved the existence of noise notch. Rouseff and Tang (2006) studied the ambient noise notch phenomenon under the International Acoustics Experiment (ASIAEX) experiments. Clark (2007) had investigated the character of vertical directionality of midfrequency (2–5 kHz) surface noise in the downward refracting environment and related mechanisms that form the noise distribution.

In regards to the noise notch, Ferat and Arvelo (2003) proposed a ray-based model to explore the sensitivity of wind wave-generated source directionality, and it is seen that when shipping is present the notch gets filled up. This noise notch can also be 'filled in' by scattering effects due to the ocean surface, volume, and bottom. The volume scattering by internal waves shows almost 7dB difference in the noise at 224 Hz between the 0º point and the peak at 22º (the bottom critical incidence angle) (Katsnelson et al.,

2012). In the context of biological sound, D'Spain and Batchelor (2006) had recorded fish chorus, which causes a complete reversal in the vertical directional characteristics of the mid-frequency ambient sound field between the days and night. The vertical structure during the day shows a notch in the horizontal direction with levels more than 10 dB below those at higher angles. The night time levels in the horizontal can exceed those at other vertical angles by more than 10 dB.

In recent years the measurement and characterization of ambient noise in shallow waters in the Indian Ocean have been reported (Ramji *et al*., 2008). Most recent studies focusing on seabed characterization and modeling of ambient noise induced by the wind along the Indian continental shelf were also reported (Sanjana *et al*., 2013; Najeem *et al*., 2015). Recently, Sanjana and Latha (2012) had investigated directionality pattern, and quantified noise notch width and notch depth at different frequencies. Moreover, relationships between the wind speed and noise notch parameters are also reported from the Bay of Bengal.

In this work, directionality pattern within the 0.5 - 4.0 kHz band is determined using short hydrophone array and associated super gain array processing techniques(Siderus, 2012) and evolution of short term directionality pattern have been investigated using time- series measurements from Grande Island location. Presence of notch in the directionality pattern has been observed and notch width and depth have been quantified for different frequencies, and the behavior of the notch for different wind speeds has been investigated. The present study also includes the determination of the noise notch parameters during the fish chorus period. Furthermore, modeling of ambient noise vertical directionality and its variation due to shallow water environments including fish chorus is presented.

8.2 Data

The study involves three important aspects of data collections: i) beamforming technique, ii) sound speed data, and iii) sediment data. Vertical linear C55 hydrophone

array was deployed for time series measurements in the shallow water of Grande Island at water depth 20 m from 22-24 May 2018, placing the hydrophone array at mid-depth of the water column. A total of 82 data sets were sampled at 48 kHz, for the duration of 60 s at every 30 minutes interval.

8.2.1 Beamforming technique

Omni-directional hydrophones in the array having the bandwidth (0.5–5 kHz) acquired noise data with simultaneous 48 kHz samplings for the duration of the 60s at every 30 minutes. The C55 hydrophone with 6 elements array at 0.15 m spacing, the total length of the array set to 0.075 m with Omni-directional hydrophone devised for measuring at the 5 kHz designated frequency and beam width is 17º. Beamforming technique has been employed to determine the directionality of the recorded signal acquired using passive hydrophone elements array. Using the beam-forming technique it is possible to direct the array elements to receive maximum signal energy from a specific angular direction. In the present study, the conventional time-delay beamformer is employed to receive the signals at the array elements from different angular direction (-90 to +90). The algorithm was developed utilizing Matlab (www. mathwork. com) computation platform. The signals are first converted from ADC bits to corresponding voltage values with the time vector. The signals are then passed through a filter having a bandwidth of 50Hz, within the frequencies ranging from 0.5 kHz to 5.0 kHz at an interval of 10Hz. In the beamforming technique, the beam pattern of a line of equally spaced, equally phased (un-steered) elements can be derived as follows. Let a plane sinusoidal wave be incident at an angle to a line of such elements. The output of the element relative to that of the zeroth element will be delayed by the amount of time necessary for sound to travel the distance:

$$l_m = md \sin\theta \qquad (8.1)$$

where d is the spacing between elements. The time delay is given as

$$t = \frac{l_m}{c} \tag{8.2}$$

where c is the sound speed in seawater. The corresponding phase delay for the sound of wavelength λ will be w = 2πf

$$U_m = \frac{2\pi f l_m}{c} = km\, d\sin\theta \tag{8.3}$$

where$k = \omega/cisthewavenumber$.

Let P_n represent the total time harmonic noise field measured on the nth element of a vertical array. Beamformer output function at angle θ is

$$BF(\theta) = \sum_{n=1}^{N} P_n e^{ikd\,(n-1)Sin\theta}\ . \tag{8.4}$$

The magnitude squared value of the beamformed data is taken and averaged over the time period. The spatially interpolated virtual elements can transform the existing 6-element array to 11 elements, and reduce the inter-element spacing to 0.075 m (Siderius, 2012). The performance of the array and the resulting beam patterns greatly improved (Fig. 8.1). The vertical directionality patterns (Fig. 8.1) were computed, which include the biological chorus (Fig. 8.1 b,d) during the evening time (dusk period) (arrow marked in Fig. 8.3) along with the analogous pattern generated in the absence of biological noise at 10:30 hr (Fig. 8.1a,c).

The array pattern degradations are not unknown primarily when limited array lengths are used. Therefore, spatial taper (Chakraborty, 1988) or adaptive beamforming techniques are preferred (Siderius, 2012). However, due to the extreme sensitivity of adaptive arrays towards random errors, the concept of the super-gain array has been employed in this study (Fernandes et al. 2015). In the present study, for improved beamforming through a spatially interpolated virtual element are introduced within the existing 6-element array through enhancing the element numbers (i.e., total eleven elements) by reducing the inter-element spacing. The spatially interpolated virtual elements transform the existing 6-element array to 11 elements (design frequency of

10,000 Hz as the inter-element distance is reduced to half of the six elements), i.e., reduction in inter-element spacing to 0.075m from 0.15m of 6 element array. Through spatially interpolated virtual 11 hydrophone elements (half-power beamwidth 9.24^{o}), the performance of the 11 element array is improved than conventional (delay and sum) six-element methods (half-power beamwidth 17^{o}). Shallow water is usually noisy, and the limits of passive acoustics are basically related with the signal-to-noise ratio (SNR), array aperture, and ocean environment are ongoing research issues (Kuperman and Lynch 2004). In this study we have enhanced the beampattern characteristics through introduction of spatially interpolated virtual element based on the signal received by the two nearby elements.

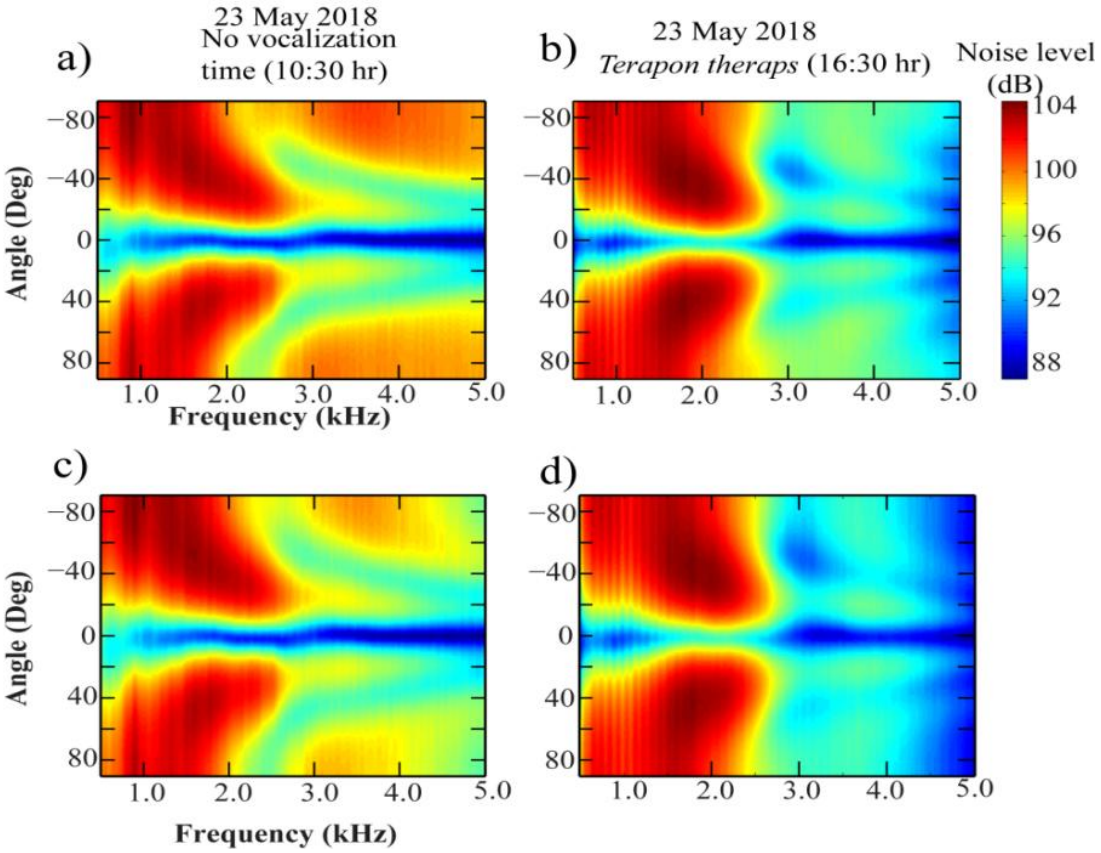

Fig. 8.1 Noise directionality from 0.5-5.0 kHz, a) without any fish vocalization, b) presence of fish vocalization for eleven elements and c) without any fish vocalization and d) presence of fish vocalization for six element array.

8.2.2 Sediment Grain Size:

The sediment collection was carried out using Van-veen Grab for grain-size analysis to comprehend the bottom reflectivity. The sediment samples collected at the sites were subjected to grain size analysis to estimate sound speed in the seabed. Grain size is determined in the laboratory using the methods given in section 2.5.4. The sediment samples from the site were found to be composed of sand, silt, and clay fractions (sand 95%, silt 3.93%, and clay 0.95%) i.e., Fine sand (Hamilton, 1980; Lurton, 2002) values for continental shelf and slope environment is used to arrive at the sound speed values.

Based on the sand data, the sound speed value at sea bed is considered to be 1725 m/s for Grande Island off Goa.

8.2.3 Sound Speed Profiles

Sound speed is seasonal and diurnal changes affect the oceanographic parameters in the upper ocean. The principal characteristic of shallow water propagation is that the sound speed profile is downward refracting or nearly constant over depth, meaning that long-range propagation takes place exclusively via bottom interacting paths (Najeem *et al.,* 2015). The important ray paths are either refracted bottom, reflected or surface reflected bottom. Typical shallow water environments are found on the reef system for water depths down to 20 m in Grande Island (Location 9). In shallow water, the surface, volume and the bottom properties are important and also the oceanographic parameter and had a certain role to play in shallow acoustic propagation. Sound speed profiles (SSP) (Fig. 8.2) were collected using Sound Velocity Profiler (SVP) (Section 2.5.3). The sound speed profiles measured at the site is given in (Fig. 8.2). The four profiles exhibit a structure i.e., a downward refracting profile off Grande Island off Goa. For evaluating the complex environment, the features in the SSP is investigated in terms of the value at the receiver (C_r), maximum value above the receiver (C_u), the maximum value in the entire water column (C_{max}), and sea bottom value(C_b) as per rule by (Harrision, 1996). These translate to angles,$(cos\,\theta_0 = C_r/C_u)$, $(\cos\,\theta_1 = C_r/C_{max})$, $(cos\theta_2 = C_r/C_c)$.If $C_u \geq C_r$ there is a possibility of noise notch in the directionality pattern, a range of angles that are surface noise free (Table 8.1). If $C_{max} > C_u$ there may be a surface duct (SD) with upward refraction. If $C_c > C_{max}$ there may be low loss surface and bottom reflected paths. Above $C_c$there may be direct paths and high bottom loss paths. The angles θ_0, θ_1 and θ_2 calculated from the sound speed in the water column and seabed are given in (Table 8.1) for the in Grande Islands (Location 9).

Table 8.1 Sound speed profile characteristics at the sites for four SSPs

Site	Sound speed in the water column (m/s)				Angles (degree)			
Grande Island	Receiver (C_r)	Top (C_u)	Botttom (C_b)	Maximum (C_{max})	θ_0	θ_1	θ_2	Wind speed (m/s)
Min	1548.400	1548.810	1548.590	1548.881	0.810	0.810	26.110	2.0
Max	1548.888	1549.400	1548.650	1549.400	1.811	1.811	26.150	8.0
Mean	1548.705	1549.125	1548.630	1549.125	1.356	1.356	26.122	5.1

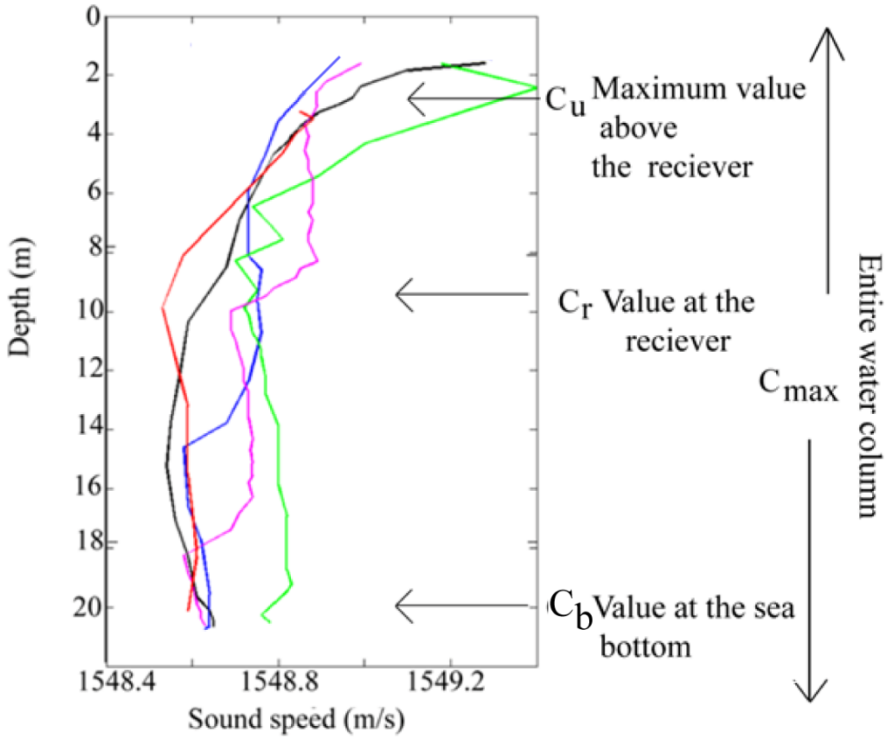

Fig. 8.2 Sound speed profiles were acquired at the site at three hr interval

8.2.4 Area soundscape

The concatenated Power Spectral Density (PSD) analysis time series data revealed the presence of fish choruses (Fig. 8.3). The functions, window length and Fourier parameters of PSD computation and single call power spectral density performed in Matlab are given (Table 3.1). The PSD peaks for the single call were generated with

frequencies: a) 1766 Hz at 114 dB re1µPa^2/Hz, b) 900 Hz at 123 dB re1µPa^2/Hz, c) 1766 Hz at 124 dB re1µPa^2/Hz and d) 900 Hz (Fig. 8.4). The analysis of peak frequency and sound pattern reveals the trumpet sound which can be identified as *Terapon theraps,* observed at 17:00 hr of 22 May 2018 (Fig. 8.3 and at 16:30 hr of 23 May 2018 (Fig. 8.4a,c). The family of the other fish sounds could not be verified. The fish sound recorded at 02:30 hr on 23-May 2018 and at 02:30 hrs on 24 May 2018 were matched as reported in Chapter 3 (Fig. 8.4 b and d). However, the family of the other fish sounds could not be verified, and the same was labeled as Grande Type A. Arrows 1 and 5 indicate *Terapon theraps,* Arrows 2 and 6indicate the mixed sounds of the fishes, and Arrow 3, 7 as Grande Type A respectively as shown in Fig. (8.3).

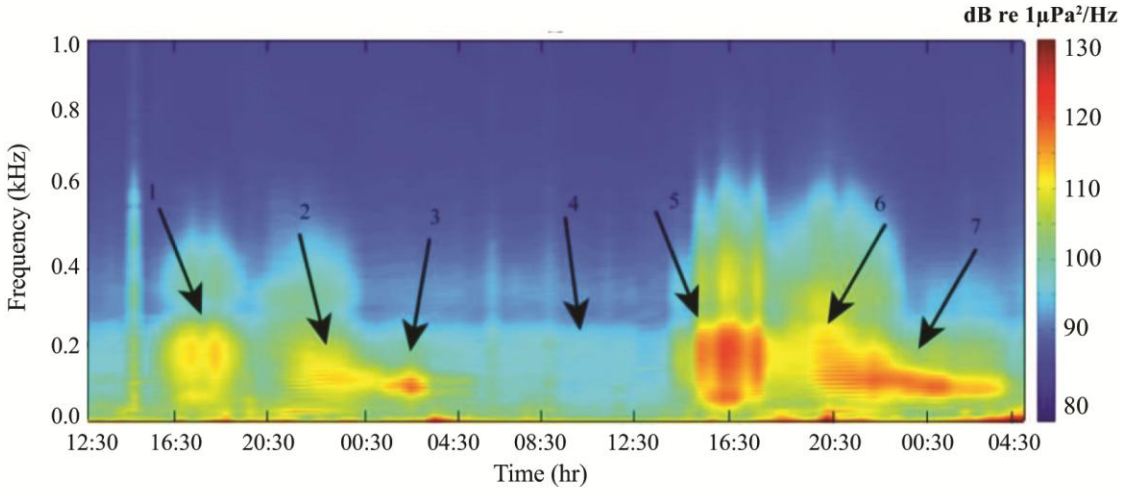

Fig. 8.3 Concatenated power spectral density (PSD) in dB re 1µPa^2/Hz concerning the time in 60 s at an interval of 30 min of 22-24 May 2018at location 9. Arrows 1 and 5 indicate *Terapon theraps,* Arrows 2 and 6 indicate the mixed sound, and Arrow 3, 7 Grande Type A respectively.

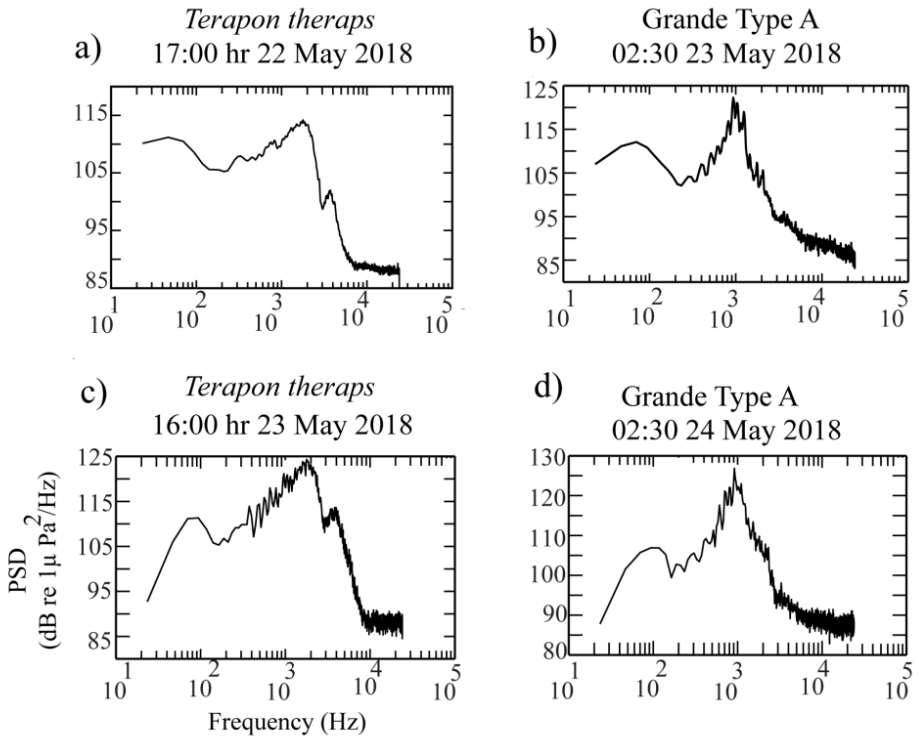

Fig. 8.4 Power spectral density in (dB re 1µPa^2/Hz for a) for a) *Terapon theraps*, (17:00 hr) b) Grande Type A fish (02:30 hr), c) *Terapon theraps,* (16:30 hr) and d) Grande Type A fish (02:30 hr).

8.3 Estimation of Geo-acoustic parameters

The seabed reflection coefficient (V) is given as (Brekhovskih and Lysanov, 1991),

$$V = \frac{mcos\theta - \sqrt{n^2 - sin^2\theta}}{mcos\theta + \sqrt{n^2 - sin^2\theta}} \qquad (8.5)$$

$\varphi$is a phase difference between reflected and incident wave,

$$\varphi = -2arctan\frac{\sqrt{Sin^2\theta - n^2}}{mcos\theta} \qquad (8.6)$$

where$n = c/c_1$ is the ratio of sound speed of water to sound speed of seabed determined from grain size analysis, and m= ρ_1/ρ where ρ density of water column and ρ_1 is

densitythe of the of seabed. These parameters are determined from grain size analysis. Computation of reflection coefficient using sound speed of water column 1548.88 m/s, density water column 1024 kg/m^3, sound speed of sea bed 1725 m/s, and density sea bed 1950 kg/m^3 has been taken from (Lurton, 2002; Hamilton, 1980) based on fine sand seabed sediment grain size data of the presently studied location. Surface/bottom reflections fall within ±26.19 (Fig. 8.5a). Beyond this, sound arrives as direct paths at the surface and high bottom loss path at the bottom.

Geo-acoustic properties can be inferred from the vertical directionality of AN derived from the hydrophones array. As the seabed reflection can cause variation in vertical directionality, the method involves beamforming and separating the up and down going beams (Harrison and Simons, 2002). RL can be derived from the ratio of upward-looking and downward-looking beams. The power reflection coefficient R_b =U/D, where U is upward flux and D is the downward flux, is considered as the ratio. U and D are measured using the receiver array deployed in an ocean wave guide and the R_b is worked out. At higher frequencies and in ray-based modeling, the RL estimate is considered more useful than conventional geo-acoustic properties utilizing a sound speed profile. Knowing the sound speed pro-file at the site, it is possible to map the beam ratio from the angle measured (by beam-forming at the receiver θ_r, to angle at the seabedθ_b) Based on the Snell's law:

$$\theta_b = \text{acos}((c_b / c_r)\cos(\theta_r)), \quad (8.7)$$

Reflection coefficient$R = \frac{1-\frac{\rho_c c_w \cos\theta_b}{\rho_b c_b \cos\theta_w}}{1+\frac{\rho_w c_w \cos\theta_b}{\rho_b c_b \cos\theta_w}}$. (8.8)

Knowing the reflection coefficient and water column sound speed, water column density, the sediment properties can be determined (Sanjana *et al*., 2013) such as seabed sound speed and sea bed density.

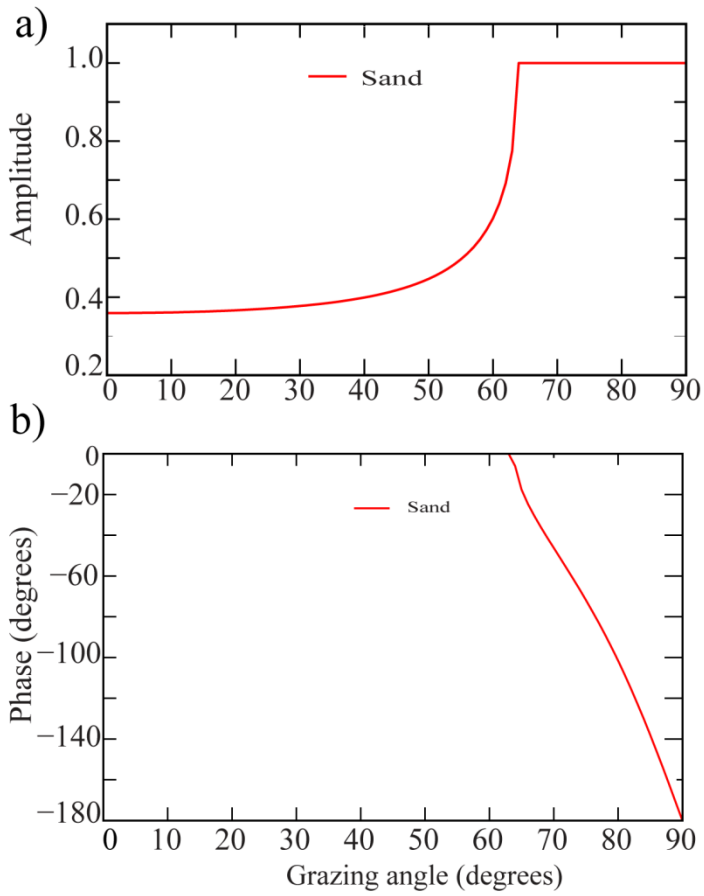

Fig. 8.5 Theoretical reflection coefficient for zero loss at Grande Island site

8.4 Acoustic Environment at Grande Island

The ambient noise study was carried out in a shallow water area near Grande Island, off Goa. The sound propagation in the shallow water environment is largely affected by the interaction with sea bottom. The bottom loss is a significant part of the total transmission loss, and the attenuation is less at low frequencies, a considerable amount of energy is transferred at the seabed (Ali *et al*., 1990). The frequency in the range of 0.5 to 4 kHz is of note here, and reflection is more predominant than bottom absorption. The sound propagation characteristics are determined by bottom material and the angle of incidence. The seabed of the present study area is found to be sandy in nature. The

reflection is dominant here as hard surface reflects most of the energy. The energy may propagate in two ways, as trapped discrete normal mode in the water column or form a part of the continuous spectrum at the bottom (Sanjana and Latha, 2012). The demarcation between discrete and continues modes depend on the critical angle $\theta_c = arccos\left(\frac{C_r}{C_s}\right)$ of the bottom, where C_s is the sound velocity estimated based on the seabed grain size. The critical angle depends on the compressional wave velocity in the water column and the wave velocity at the bottom (Buckingham and Jones, 1987). If the sediment composed mainly of fine sand based on the sediment data acquired from the study area i.e., (C_s =1725m/s) (Hamilton, 1980; Lurton, 2002). The critical angle at this location estimated from the water column and bottom properties is $\theta_c = arccos\left(\frac{1548.88}{1725}\right)$ = 26.11°. The propagation is characterized by normal modes corresponding to waves striking the bottom at grazing angles, lower than the critical angle. The width of the noise notch was found to be $2\theta_c$, roughly ~52.22°, which roughly matches with the theoretical value (Fig. 8.5). The noise sources due to local wind, wave actions and remote sources due to shipping are notable in the shallow waters. The noise from distant sources is most likely to travel in the form of discrete normal modes confined to a small angle about the horizontal direction. The energy propagating at steep angles will attenuate quickly due to repeated bottom and surface interactions over long ranges (Sanjana and Latha, 2012).

8.5 Vertical directionality using field measurements at Grande Island

Surface noise in downward refracting environments is vertically anisotropic, with varying complement from upward-looking beam angles, downward-looking beam angles, and near-horizontal angles (Clark, 2007). Thecompendium of noise arriving at the receiver along a direct path from the surface, besides noise reflected from the ocean bottom and a low angle notch through ray paths from the surface, are likely to have originated from a great distance, and hence would be significantly attenuated.

The hydrophone array is deployed midway in the water column and the central part of the array is aligned with the channel axis. The site away from the coral reef was monitored during which occasionally boat sounds were also observed in the soundscape data (Fig. 8.3). The vertical directionality pattern revealed notch noise in the frequency band of 1.0-1.5 kHz with no indication of biological sounds (Fig. 8.1a,c). In the presence of fish vocalization the noise notch varied between 1.0 kHz to 1.5 kHz (Fig. 8.1b, d). From the sound speed profiles obtained at the site, downward refracting negative gradient profiles were observed (Fig. 8.2). Wind speed was observed between 2 to 8 m/s (Fig. 8.7a). The ratio B_{up}/B_{down} canbe used to estimate the bottom reflectivity (Rouseff and Tang, 2006). The noise notch was well defined between 1 kHz and 3 kHz frequency where the beam width is narrow (Fig. 8.6 and Fig. 8.7d). The field measurements of the sea bottom properties indicated sandy bottom observed from sediment analysis. (Yang and Yoo, 1996; Ferat and Arvelo,2003; Clark, 2007; Sanjana and Latha, 2102). The present study indicates that the notch width decreases with increasing frequency (Fig. 8.6, Table 8.2). Based on the observations at every 30 minutes interval in the shallow water, the data indicates that the directionality pattern varies over time (Fig. 8.6).

The SPL_{rms} data shows higher values during fish vocalization (16:00-02:30 hr and 15:30-04:00 hr of 22-24 May 2018) as compared to no vocalization period (04:30-12:30 hr of 23-05-2018) (Figure 8.7b). The notch depth increases with increasing wind speed, ranging from 6 to 8 m/s in different frequency bands (Fig. 8.7c), but is more prominent in the bandwidth 1-2 kHz (Sanjana and Latha, 2012) (Table 8.1). The study reveals that notch depth variation is higher at lower frequency bands, 1.0 to 1.5 kHz, while the notch width decreases with increasing frequency that ranges from 2 to 4 kHz, during fish vocalization (Fig. 8.7d, Table 8.1).

The variation of notch depth with wind speed has been investigated (bandwidth 0.5 - 4.0 kHz) under three types of conditions *viz.* i) characteristics of notch depth with respect to wind speed for entire data, ii) notch depth versus wind speed during fish vocalization period and iii) notch depth versus wind speed in no vocalization period. For entire data, the notch depth showed an increase from frequency range 0.5 to 3.5 kHz frequency with

wind speed (6-8m/s) within the data collection period (Table 8.2 and Fig. 8.8). The analysis of vertical directionality pattern reveals a notch depth increase with increasing wind speed. In the presence of biological sounds, the data also revealed that the notch depth is higher, increasing from 0.5 to 3.5 kHz as shown (Table 8.2) (Sanjana and Latha, 2012). Under this condition, notch depth is found to be increasing with wind speed even in the presence of biological sound as it is observed (Table 8.2). The present study supports the fact that notch depth is functional of wind speed, and wind speed needs to be greater than 5 m/s. However, data presented for each frequency (Table 8.2) are averaged with respect to the time. A critical look at the data timings (20:30-00:30 hr of 22 May 2018) in Fig. 8.7, reveal the reciprocal relationship between the wind speed and notch depth when SPL_{rms} is higher and fish vocalization is present (Fig. 8.3). Similarly, a disturbance in noise notch is depicted in Fig. 8.1(b,d) during the presence of *Terapon theraps* vocalizations. More future research is needed to understand the notch filling phenomena due to biological sounds as predicted (D'Spain and Batchelor, 2006).

Table 8.2 Notch depth and notch width parameters with respect to different frequencies

Frequency (kHz)	Notch width (Degrees)	Notch depth (dB) of entire data	Notch depth (dB) Fish vocalization period 16:00-02:30 and 15:30-04:00 hr 22-24 May 2018	Notch depth (dB) No vocalization period 04:30-12:30 hr 23-05-2018
0.5	19.45±7.85	7.05±3.35	8.25± 3.34	4.51± 1.13
1.0	12.64±4.49	12.13±3.71	13.52±3.57	9.44±1.25
1.5	9.84±3.32	11.60±2.95	12.47±2.87	9.37±1.33
2.0	7.86± 2.84	10.86± 2.62	10.95±2.68	8.5± 1.64
2.5	6.71± 3.07	9.37±1.89	9.47±1.82	7.78± 1.20
3.0	12.26±5.22	8.12±1.20	8.35±0.99	7.66±0.51
3.5	7.83±3.38	9.45±1.48	9.21±1.03	9.06±0.79
4.0	7.59±2.36	8.53± 1.51	8.25±1.17	8.66± 0.72

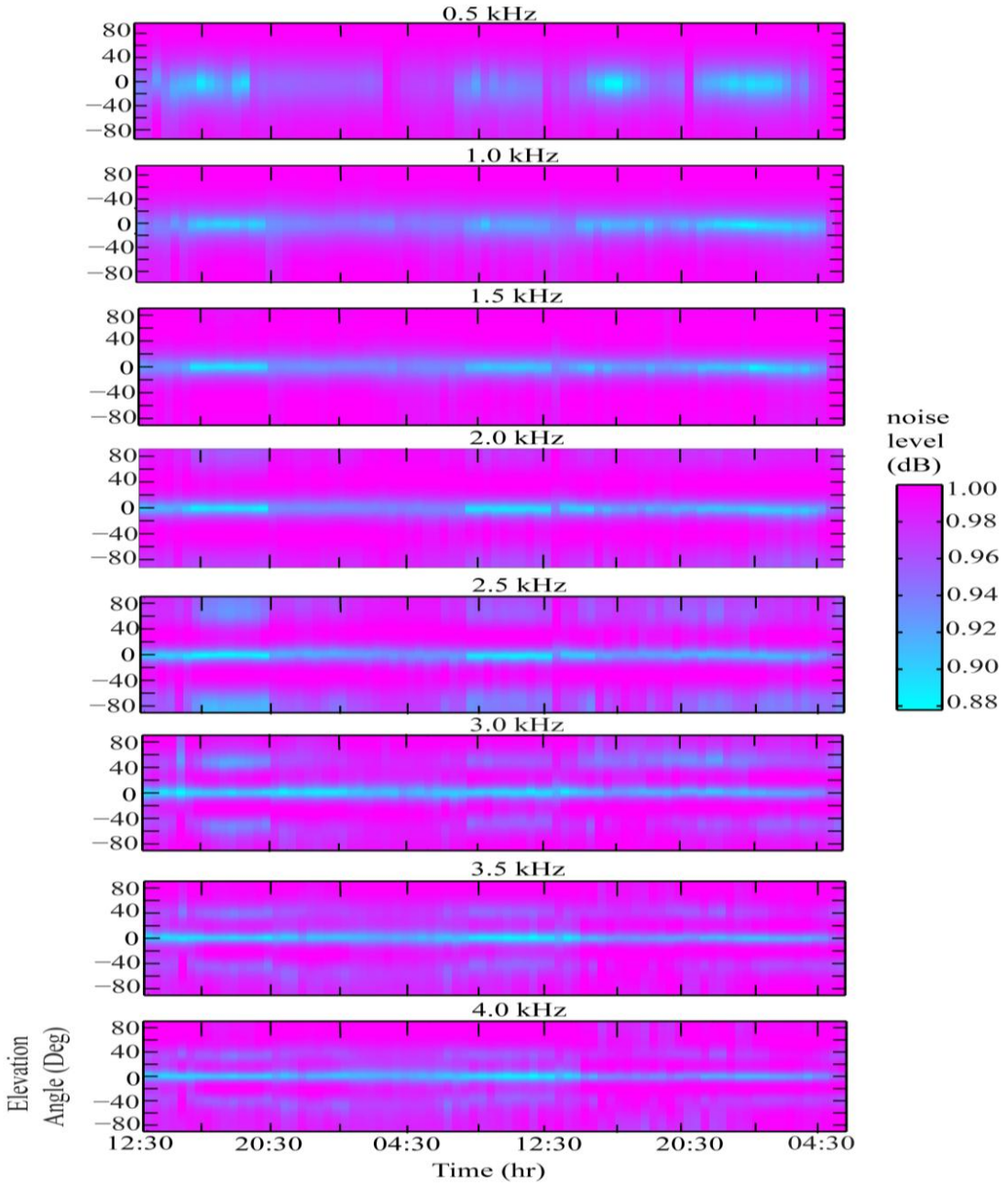

Fig. 8.6 Evolution of vertical directionality every half an hour during the entire period

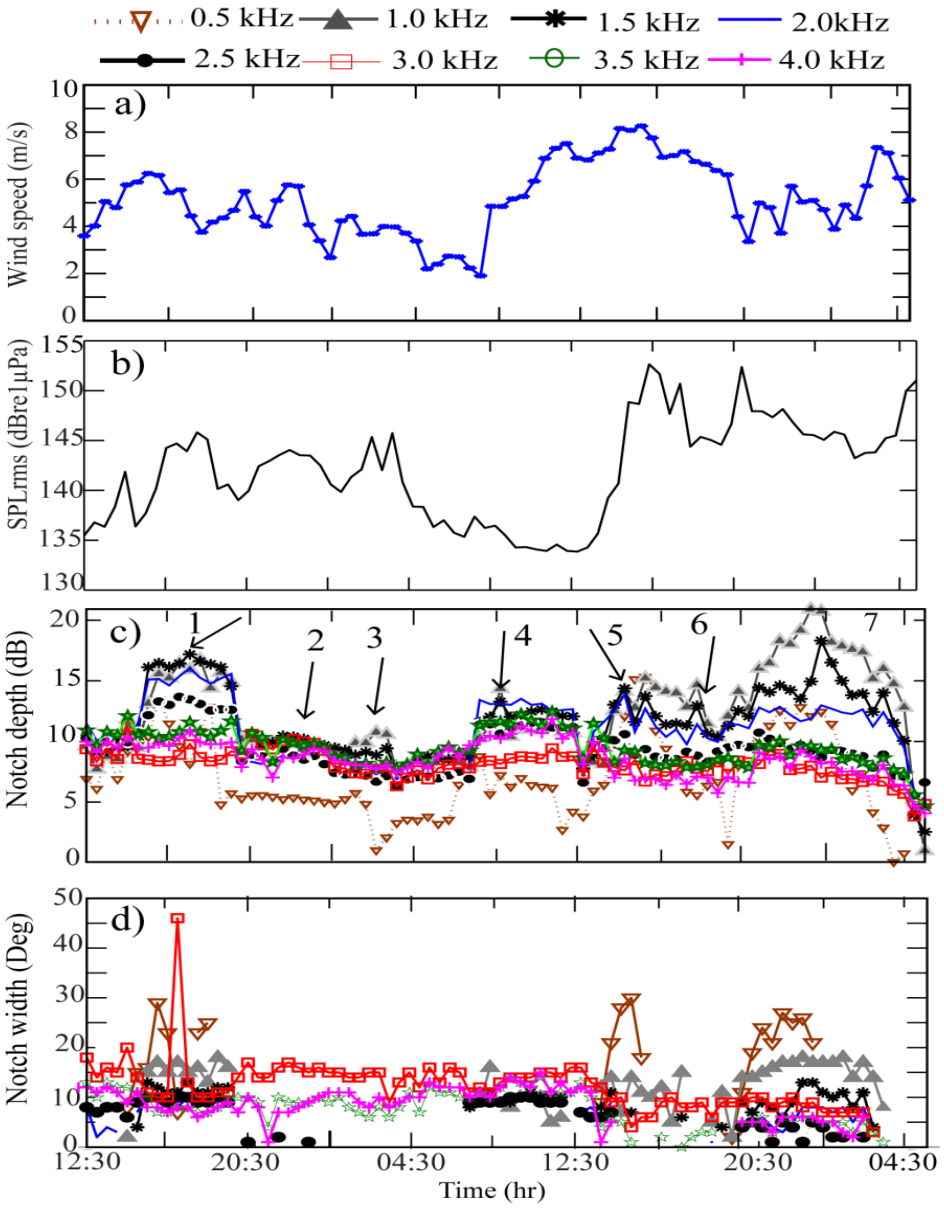

Fig. 8.7 Time series of ambient noise notch depth and notch width. In Fig.c) for arrows pl. see Fig. 8.3.

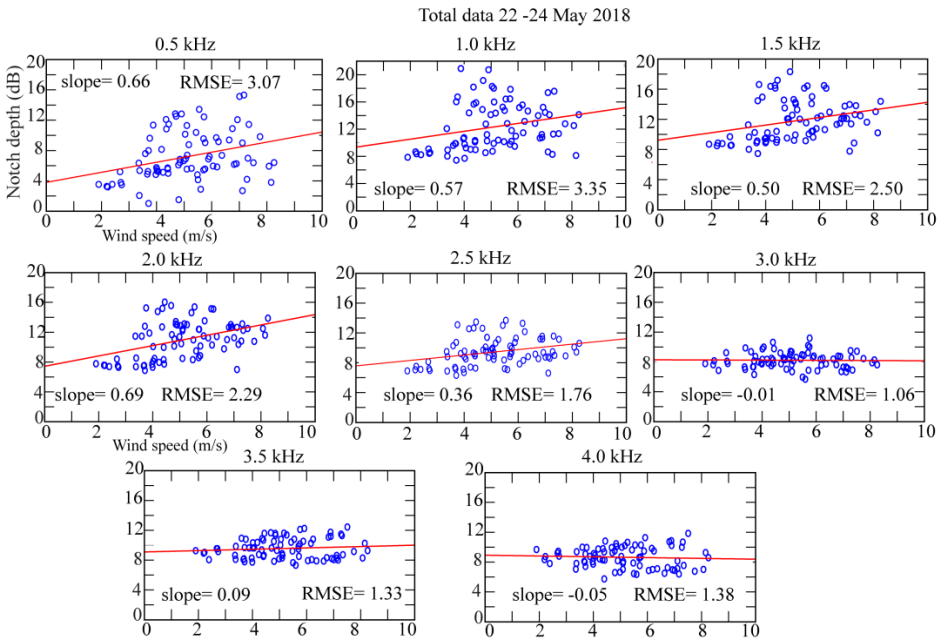

Fig. 8.8 Variation with notch depth and wind speed for 0.5-4 kHz for entire data

8.8 Conclusions

Ambient noise study is important to understand the shallow water environment. The vertical directionality pattern shows noise notch present in the frequency range of 0.5-3.5 kHz and the wind speed has a prominent role for the notch depth variation in the different frequency bands. The notch width decreases with increasing frequency which is evident from the negative gradient of sound speed refracting downward. The average notch width and notch depth arehigher in the frequency band of 0.5-3.5 kHz. Fish vocalization is not found to be prominent in this study. The field measurements of noise notch pattern and the downward refracting sound speed profile were seen in the shallow water environment. Critical angle obtained from theoretical expression is 26.11°. The noise notch width observed is $2\theta_c$, which is~52.22° and this is consistent with theoretical values. The vertical directionality of noise pattern is calculated from the field measurements.

Chapter 9

Summary

The thesis highlights a technological approach and the relevance of passive acoustic techniques to understand the shallow-water environments off Goa and Malvan areas of the West Coast of India (WCI). The soundscape of each of the eight experimental sites off Goa and Malvan, Maharashtra have been presented here. Besides soundscape, a semi-quantitative technique has been developed to segment the recorded fish calls used for identification of fish sound. The peak of power spectral density (PSD) of each of the fish calls recorded at the eight locations has been estimated. In addition, the temporal parameters of the fish calls were also determined. Scatter plots involving the temporal and spectral parameters of the call signals exhibit a pattern associated with fish calls. Chapter 3 covers fish identification and their characterization making use of the recorded fish calls from the eight locations off Goa and Malvan coast. Identification of Batrachoididae (common name: Toadfish) calls from the mangrove dominated Mandovi estuary was carried out at location 1. Terapontidae (species: *Terapon theraps*) fish sounds were reported from the Grande Island of Zuari estuary (Location 2) and Sal estuary (Location 3) near Betul. The short term data from these three locations also provide indication of ambient sound of wind, boat sound, water flow along with the reported biophonies.

Towards the deeper part of the Grande Island at 30 m water depth (Location 4), recording of "Barred Grunt" (*c.nobilis*) fish sound and its characteristics are presented. The fish sound recorded off Malvan, Maharastra (Location 5) revealed Terapontidae (*Terapon theraps*) fish chorus, producing a trumpet-like sound, as well as limited fish sound data of Carangidae fish family. At location 6 near Grande Island at 20 m water depth, data was recorded for nine days of March 2017. At another location near Grande Island (Location 8), two fish families, Teraontidae: *Terapon theraps* and Sciaenidae found at 20 m water depth were identified. Further, peak frequencies of the PSDs of a number of fish sounds were estimated. Despite that, identification of the fish family/species was not possible due to unavailability of the data archival.

Chapter 4 delves with the application of a nonlinear methods i.e., multifractal detrended fluctuation analysis (MFDFA), to describe fish sound data recorded from the open waters of two major estuarine systems. Applying MFDFA, the second-order Hurst exponent $h(q = 2)$ values are found to be 1.10±0.03 and 1.43±0.02 for the fish families Batrachoididae (common name: Toadfish) and Sciaenidae (common name: Croakers, drums) respectively. The results suggest that the Sciaenidae fish calls are smoother in comparison to that of Batrachoididae.

In chapter 5 passive acoustic data is utilized for quantitative characterization of the three shallow-water acoustic environments. To characterize the relative contributions of biophonies (fish), geophonies (windand flow, etc.) and anthrophony (boats, etc.), cluster analyses (principal component analysis) were carried out. In the Mandovi estuary, SPL_{rms} of Toadfish sound was observed to be a function of the water flow and temperature. In Zuari estuary, SPL_{rms} was a function of the water temperature and wind. In Sal estuary, it was the wind that mainly influenced the SPL_{rms}. The present study reveals relevant characterization of biotic and abiotic sound signals in the ecologically important region off Goa.

Underwater soundscape monitoring is an effective method to expand our knowledge and understanding of the biodiversity of the ecosystem. In chapter 6, three acoustic metrics such as Entropy (H), Acoustic richness (AR) and Acoustic complexity index

(ACI) of the passive acoustic data from Malvan, and the two locations one near Grande Island reef and the other away from reef in the West Coast of India (WCI), were computed using the recorded data of the dominant fish vocalizations. Present analysis based on the metrics along with the SPL_{rms} of the nine day data reveal the intricacies of the three locations.

In chapter 7, the soundscape characterization was carried out involving the computation of three acoustic metrics namely acoustic entropy (H), acoustic richness (AR), and acoustic complexity index (ACI) and SPL_{rms} (root-mean-square sound pressure level) of passive acoustic recordings and analyses, to understand the underwater environment. The box plot presentation of three acoustic metrics and SPL_{rms} reveal important statistical details. Here the SPL_{rms} along with the acoustic metric AR show higher correlation coefficients at three frequency bands. A clustering between the SPL_{rms}, AR and current speed in PCA and dendrogram suggest that the acoustic metric AR, as well as SPL_{rms}, could be proxy of geophonies (current speed). Interestingly, the other two metrics such as ACI and H do not show any relationship with SPL_{rms}, AR as well as any other physical parameters.

Chapter 8 covers ambient noise studies in the Grande Island at location 9 at 20 m water depth. The presence of a negative gradient of sound speed profiles indicates the presence of noise notch. The vertical directionality pattern shows noise notch present in the frequency range of 1.0-3.5 kHz, and the wind speed has a prominent role for the notch depth variation within the frequency range. The noise notch increases with wind speed beyond 5 m/s, and the investigation of fish vocalization effect on noise notch could not be established.

Though the influence on the measured parameters due to water depth limitations has not been addressed directly, howevour,the issue is taken care of in our analysis.We have computed correlation coefficients between the SPLrms versus water depth for nine locations from India's western continental shelf, which is week correlation i.e., 0.0104. Generally, in shallow water areas, recorded SPLrms is highly fluctuating. Moreover, it is difficult to get good relationships due to fluctuating environments, i.e., wind, bottom

material, and sound velocity. Because, these environmental parameters are temporally and spatially varying, which control recorded SPLrms besides water depth.

However, we have dealt with the SPLrms data from two different water depths within shallow water environments in chapters 5-7. Our analyses presented in chapter 5, where three locations having water depths 7, 20, and 11m, where the influence of environmental parameters on SPLrms is studied. In chapter 6 for locations 06 (off reef) and 07 (reef) having water depths 20m and 08m respectively. Eco-acoustics i.e., acoustic biodiversity parameters, are covered here. The present study allows us to understand the differences in estimated eco-acoustic parameters from the two sites having variable water depth. In chapter 7, environmental parameters and computed eco-acoustic parameters from these two locations are involved to understand the influence of environmental parameters on estimated eco-acoustic parameters of two locations (6 and 7). Furthermore, detailed fish sound characteristics are covered in section in chapter 3 (section 3.5.6) where soundscape differences due to water depth are demonstrated in concatenated PSDs, as given in Fig. 3.12 (a and b). On the whole, the variability in estimated acoustic parameters in shallow water environments where depth is one of the vital parameters is demonstrated in this thesis.

Overall the present study covers the extensive applications of the passive acoustic techniques for soundscape and fish sound identification using song meter system in the shallow water environments, and it is hoped that the present study would be of considerable relevance in the shallow water studies using passive acoustic methods. It must be stated that no claim for completeness is being made in the present research. But many aspects of the passive acoustics techniques are employed here, related to the acquired time-series datasets, using short hydrophone array system deployed in the Grande Island for investigating mid-frequency ambient noise notch.

There were several impediments while acquiring the target specimen to confirm the species identification caused by turbid waters, and also due to the non-avilability of specimen details. However, with the recorded fish sound temporal and spectral call parameters, it was possible to identify the fish family/species, which have been used in

this research. Estimating call by call temporal/spectral parameters is time-consuming and needs improvement. In the spectral method, power spectral density-based analysis shows multiple peaks, which are unsuitable for processing. The application of nonlinear signal processing techniques is useful to describe the complexities of animal vocalizations and have been hypothesized to play an essential role in individual species identification. Here, a non linear MFDFA (Multifractal Detrended Fluctuation Analysis) technique need extensive computation and incompatible for fish sound identification using an online recorder. Employing automatic techniques to recognize the fish species are useful for monitoring biodiversity in real-time. Eco acoustic parameters (ACI, H, and AR) applied to understand biodiversity used to identify the temporal and spatial complexity of a soundscape. The useful methods also remove background noise and identify fish zones in a complex habitat environment Acoustic richness shows higher biodiversity where the fishes are abundant. Eco-acoustic paprameters do not have standered proxies for biophony, as it depends on the environment. Likewise, eco-acoustic studies alone cannot be carried out to identify the species and needs validation based on temporal and spectral parameter estimation to identify the fish species, which has also been used successfully in this research. In chapter 8 of ambient noise study, use of short array hydrophone show limitations due to beam resolution as observed in estimated noise parameter statistics. However, future research is needed using long array hydrophone for improved noise parameter estimation. The techniques employed here would be useful for biodiversity measurements as well as modelling to fish sound propagation in order to characterize the shallow water environment.

Bibliography

Ali, H.B.: *The Role of the Seabed in Low-Frequency Shallow-Water Acoustic Propagation:Examplesfrom Measurements and Modelling*Atmos. Naval Oceanogr. Atmos. Res. Lab.,Tech. Note35, ADA223519, Jun.1990.

Ainslie, M.A.: Potential causes of increasing low frequency ocean noise levels. *Journal of the Acoustical Society of America.*, 129, 2497-2497, 2012.

Akamatsu, T., Okumura, T., Novarini, N., and Yan, H. Y.: Empirical refinements applicable to the recording of fish sounds in small tanks. *The Journal of the Acoustical Society of America.*, 112, 3073-3082, 2002.

Akamatsu, T., Wang, D., Nakamura, K., and Wang, K.: Echolocation range of captive and free-ranging baiji (Lipotes vexillifer), finless porpoise (Neophocaena phocaenoides), and bottlenose dolphin (Tursiops truncatus). *The Journal of the Acoustical Society of America.*, 104, 2511-2516, 1998.

Amorim, M. C. P.: Diversity of sound production in fish. *Communication in fishes, 1*, 71-104, 2006.

Amron, A., Hanafi, A. L., Jaya, I., Hestirianoto, T., and von Juterzenka, K.: Sound Characteristics of Terapon Jorbua as Representation to its Behavior. *Omni-akuatika*, 13, 34-42, 2017.

Anonymous Critical Habitat Information system of Malvan (Maharashtra India).Integrated Coastal and Marine Area Management, Project directorate, Chennai.Available at (www.icmam.gov.in/MAL.PDF) 2001.

APL-UW, A. P. L. U. W.: High-Frequency Ocean Environmental Acoustic Models Handbook. *Applied Physics Laboratory, University of Washington, US APL-UW*, 9407,1994.

Au, W. W., and Banks, K.: The acoustics of the snapping shrimp Synalpheus parneomeris in Kaneohe Bay. *The Journal of the Acoustical Society of America.*, 103, 41-47, 1998.

Au, W. W., and Hastings, M. C.: *Principles of marine bioacoustics*, Springer.New York, 121-174, 2008.

Au, W. W., and Lammers, M. O.: Introduction: Listening in the Ocean". In *Listening in the Ocean*, Springer, New York, 1-19, 2016.

Balk, H.: Development of hydroacoustic methods for fish detection in shallow water. Faculty of Mathematics and Natural Science, PhD thesis, University of Oslo, 2001.

Bardyshev, V. I.:.Underwater ambient noise in shallow-water areas of the Indian Ocean within the tropical zone. *Acoustical Physics,* 53, 167-171, 2007.

Brekhovskikh, L. M., Lysanov, Y. P.: *Fundamentals of ocean acoustics*,.3382-3383, 1991.

Bass, A. H., and Ladich, F.: Vocal–Acoustic Communication: From Neurons to Behavior. In *Fish bioacoustics*, edited by. J. F. Webb, R. R. Fay and A. N. Popper., Springer, New York, 253-278, 2008.

Bassett, C., Thomson, J., Dahl, P. H., & Polagye, B.: Flow-noise and turbulence in two tidal channels. *The Journal of the Acoustical Society of America.*, 135, 1764-1774, 2014.

Bassett, C., Thomson, J., Polagye, B.: Sediment Generated noise and bed stress in a tidal channel, J. *Geophysical Research Oceans.*, 118, 2249-226, 2013.

Bertucci, F., Parmentier, E., Lecellier, G., Hawkins, A. D., and Lecchini, D.: Acoustic indices provide information on the status of coral reefs: an example from Moorea Island in the South Pacific. *Scientific reports.*, 6, 33326, 2016.

Bohnenstiehl, D., Lyon, R., Caretti, O., Ricci, S., & Eggleston, D.: Investigating the utility of ecoacoustic metrics in marine soundscapes. *Journal of Ecoacoustics.*, *2*, R1156L, 2018.

Buckingham, M. J., and Jones, S. A.: A new shallow-ocean technique for determining the critical angle of the seabed from the vertical directionality of the ambient noise in the water column. *The Journal of the Acoustical Society of America*, 81, 938-946, 1987.

Buckingham, M. J.: A theoretical model of ambient noise in low loss shallow water channel, *J. Acoust. Scoc.Am*., 67,1186-1192, 1980.

Cato, D. H.: Private communication with Dr Bishwajit Chakraborty, Natonal Institute of Oceanography, Goa. February 2017. Subject: Conformation of *Terapon theraps* sound.

Chakraborty, B., Haris, K., Latha, G., Maslov, N., & Menezes, A.: Multifractal approach for seafloor characterization. *IEEE Geoscience and Remote Sensing Letters.*, 11, 54-58, 2014 b.

Chakraborty, B., Saran, A.K., Sinai D., Kuncolienker., Sreepadaa R. A., Haris K., and William Fernandes. A.: Characterization of Yellow Seahorse Hippocampus kuda feeding click sound signals in a laboratory environment: an application of probability density function and power spectral density analyses, *Bioacoustics.*, 23, 1–14, 2014 a.

Chakraborty, B., Vardhan, Y. V., Haris, K., Menezes, A., Karisiddaiah, S. M., Fernandes, W. A., & Kurian, J.: Multifractal Detrended Fluctuation Analysis to Compare Coral Bank and Seafloor Seepage Area-Related Characterization Along the Central Western Continental Margin of India. *IEEE Geoscience and Remote Sensing Letters.*, 13, 1542-1546, 2016.

Chakraborty, B.: Coaxial circular array: studies related to sidelobe suppressed beam patterns for underwater transducer application. *Proceedings of the IEEE.*, 76,1374-1376, 1988.

Clark, C. A.: Vertical directionality of midfrequency surface noise in downward-refracting environments. *IEEE Journal of Oceanic Engineering, 32*, 609-619, 2007.

Clarke, T. A., and Privitera, L. A.: Reproductive biology of two Hawaiian pelagic carangid fishes, the bigeye scad, Selar crumenophthalmus, and the round scad, Decapturus macarellus. *Bulletin of Marine Science.*, 56, 33-47, 1995.

Colson, D. J., Patek, S. N., Brainerd, E. L., and Lewis, S. M.: Sound production during feeding in Hippocampus seahorses (Syngnathidae). *Environmental Biology of Fishes.*, 51, 221-229, 1998.

Cron, B. F. and Sherman, C. H., Spatial correlation functions for various noise models, *J. Acoust. Scoc.Am.*, 34, 1732-1736, 1962.

D'spain, G. L., and Batchelor, H. H.: Observations of biological choruses in the Southern California Bight: A chorus at midfrequencies. *The Journal of the Acoustical Society of America.*, 120, 1942-1955, 2006.

Dahl, P. H., Miller, J. H., Cato, D. H., and Andrew, R. K.: Underwater ambient noise. *Acoustics Today.*, 3, 23-33,2007.

Demski, L. S., Gerald, J. W., and Popper, A. N.: Central and peripheral mechanisms of teleost sound production. *American Zoologist.*, 1141-1167, 1973.

Depraetere, M., Pavoine, S., Jiguet, F.,Gasc, A., Duvail, S,. & Sueur, J.: Monitoring animal diversity using acoustic indices: implementation in a temperate woodland, *Ecological Indicators.*, 13, 46-54, 2012.

Desjonqueres, C., Rybak, F., Depraetere, M., Gasc, A., Le Viol, I., Pavoine, S., & Sueur, J.: First description of underwater acoustic diversity in three temperate ponds.*PeerJ.*, 3, e1393, 2015.

Erbe, C., Verma A., McCauley, RD., Gavrilov, A., Parnum, I.: The marine soundscape of the Perth Canyon, *Progress in Oceanography.*,137, 38–51, 2015.

Erbe, C.: Underwater acoustics: noise and the effects on marine mammals. *Brisbane: JASCO Applied Sciences*, 2011.

Farina, A.: *Soundscape ecology: principles, patterns, methods and applications*, Springer-Verlag, New York, 2014.

Ferat, P. A., and Arvelo Jr, J. I.: Mid-to high-frequency ambient noise anisotropy and notch-filling mechanisms. *The Journal of the Acoustical Society of America.*, 114, 2462-2463, 2003.

Fernandes, B., Achuthankutty, CT. Seasonal variation in fishery diversity of some wetlands of the Salcete Taluka, Goa, India, *Indian Journal of Geo-Marine Sciences.*, 39, 238-247, 2010.

Fernandes, W. A., Agarvadekar, Y., Chakraborty, B., Haris, K., Vijayakumar, K., Sundar, D., Luis, R. R. A., Mahanty, M. M., and Latha G.: How biological (fish) noise affects the performance of shallow water passive array system. *IEEE Underwater Technology* (UT), 1-4, 2015.

Fernandes, W. A., Agarvadekar, Y., Chakraborty, B.: Developmentofmulti-channel data logger for passive acoustic measurements, *Journal of Acoustical society of India.*, 35-45, 2018.

Fine, M. L., and Parmentier, E.: Mechanisms of fish sound production. In *Sound communication in fishes* Springer, Vienna, 77-126, 2015.

Fish, M. P., Kelsey, A. S., and Mowbray, W. H.: *Studies on the production of underwater sound by North Atlantic coastal fishes*. Narragansett Marine Laboratory, University of Rhode Island, 1952.

Fish, M. P.: *The character and significance of sound production among fishes of the western North Atlantic* (Vol. 14). Bingham Oceanographic Laboratory. 1954.

Fish, M.P., and Mowbray,W.H.,: *Sounds of the western North Atlantic Fishes, A reference file of biological underwater sound,* rhode island univ kingston narragansett marine lab (Johns Hopkins Press. Baltimore MD),1970.

Gasc, A., Pavoine, S., Lellouch, L., Grandcollas, P., Sueur, J.: Acoustic Indices for Biodiversity assessment: Analyses on biased based on simulated bird assemblages and recommendations for field surveys. *Biological Conservation*, 191, 306-312, 2015.

Gervaise, C., S. Vallez, C. Ioana, Y. Stephan, and Y. Simard.: Passive acoustic tomography: New concepts and applications using marine mammals: A review. Journal of the Marine Biological Association of the United Kingdom 87:5-10, 2007.

Green, E., Hanan, W., and Heffernan, D.: The origins of multifractality in financial time series and the effect of extreme events. *The European Physical Journal B.*, 87, 129, 2014.

Greenfield, D. W.: Colletteichthys occidentalis, a new toadfish species from the Arabian Peninsula and northern Arabian Sea (Teleostei: Batrachoididae). *Zootaxa.*, 3165, 64-68, 2012.

Hamilton, E. D.: Geoacoustic modeling of the seafloor. *J. Acoust. Soc. Am.*, 68, 1313-1340, 1980.

Hamson, R. M.: Modeling of ambient noise due to shipping and wind noise in complex environments, *Appl. Acoust.*, 3, 251–287,1997.

Hamson, R. M.: The theoretical responses of vertical and horizontal line arrays to wind induced noise in shallowwater, *J. Acoust. Scoc.Am*., 78,1702-1712, 1985.

Haris, K., Chakraborty, B., Ingole, B., Menezes, A., and Srivastava, R.: Seabed habitat mapping employing single and multi-beam backscatter data: A case study from the western continental shelf of India. *Continental Shelf Research.*, 48, 40-49, 2012.

Haris, K., Chakraborty, B., Menezes, A., Sreepada, R. A., and Fernandes, W. A.: Multifractal detrended fluctuation analysis to characterize phase couplings in seahorse (Hippocampus kuda) feeding clicks. *The Journal of the Acoustical Society of America.*, 136, 1972-1981, 2014.

Harris, S. A., and Radford, C. A.: Marine soundscape ecology. In *INTER-NOISE and NOISE-CON Congress and Conference Proceedings,* .InstituteofNoise control Engineerin, 249, 5003-5011, 2014.

Harris, S. A., Shears, N. T., and Radford, C. A.: Ecoacoustic indices as proxies for biodiversity on temperate reefs, *Methods in Ecology and Evolution.*, 7, 713-724, 2016.

Harrison, C. H and Simons, D. G.: Geoacoustic inversion of ambient noise: A simple method, *J. Acoust. Scoc. Am*., 112 ,1377-1389, 2002.

Harrison,C.H.:Formulasforambientnoiseandcoherence, *J. Acoust. Scoc.Am*., 99, 2055-2066, 1996.

Harrison, C. H.: Noise directionality for surface sources in range-dependent environments, *J. Acoust. Scoc.Am.*, 102,2655-2662, 1997.

Hastings, M. C., Popper, A. N., Finneran, J. J., and Lanford, P. J.: Effects of low-frequency underwater sound on hair cells of the inner ear and lateral line of the teleost fish Astronotus ocellatus. *The Journal of the Acoustical Society of America.*, 99, 1759-1766, 1996.

Hawkins, A. D., and Popper, A. N.: A sound approach to assessing the impact of underwater noise on marine fishes and invertebrates. *ICES Journal of Marine Science.*, 74, 635-651, 2017.

Higuchi, T.: Relationship between the fractal dimension and the power law index for a time series: a numerical investigation. *Physica D: Nonlinear Phenomena.*, 46, 254-264, 1990.

Hill, P. S. M: "How do animals use substrate-borne vibrations as an information source?" *Naturwissenschaften*, 96, 1355-1371, 2009.

Hoppe, E., & Roan, M.: Principal component analysis for emergent acoustic signal detection with supporting simulation results. *The Journal of the Acoustical Society of America.*, 130, 1962-1973, 2011.

Hristian, L., Ostafe, M. M., Manea, L. R., and Apostol, L. L.: Experimental Researches on the Durability Indicators and the Physiological Comfort of Fabrics using the Principal Component Analysis (PCA) Method. In *IOP Conference Series: Materials Science and Engineering.*, 209, p. 012104, 2017.

Hughes, R. N., Hughes, D.J., Smith, I. P., Dale, A. C.: *Oceanography and Marine biology* An Annual Review 51:CRC Press, Boca Ranton, 2013.

Hussain, A., Thomas, L., Nagesh, R., Mote, S., Patil, A., Pujari, L., De, K., Ingole, B.: Coral Reef at Risk: Anthropogenic stressors in Grande Island, Goa. Proceeding of the National Seminar on Approaches to clean and sustainable development in coastal zones of India - Present status and future need. at CSIR-National Institute of Oceanography, Mumbai, 15 July, 2016.

Ihlen, E. A. F. E.: Introduction to multifractal detrended fluctuation analysis in matlab, *Frontiers in Physiol.*, 3, 97-114, 2012.

Ingole B. S.: Environmental Impact Assessment study for the desilting of a section of the river Sal between Khareband bridge and Talaulim-Varca new bridge, 2016.

Ingole, B. S., Rodrigues, N., and Ansari, Z. A.: Macrobenthic communities of the coastal waters of Dhabol, west coast of India, *Indian J. Mar. Sci*., 31, 93–99, 2002.

Ivanov, P. C., Amaral, L. A. N., Goldberger, A. L., Havlin, S., Rosenblum, M. G., Struzik, Z. R., and Stanley, H. E.: Multifractality in human heartbeat dynamics. *Nature.*, 399, 461, 1999.

Jensen, F. B., Kuperman, W. A., Porter, M. B, Schmidit, H.: *Computational Ocean Acoustics* 2nd Ed, Springer, New York, 15-60, 2011.

Kantelhardt, J. W., Zschiegner, S. A., Koscielny-Bunde, E., Havlin, S., Bunde, A., and Stanley, H. E.: "Multifractal detrended fluctuation analysis of nonstationary time series," *Physica A: Statistical Mechanics and its Applications., 316*, 87-114 2002.

Kaplan, M. B., Mooney, T. A., Partan, J., and Solow, A. R.: Coral reef species assemblages are associated with ambient soundscapes. *Marine Ecology Progress Series.*, 533, 93-107, 2015.

Kasumyan, A. O.: Sounds and sound production in fishes. *Journal of Ichthyology*, 48, 981-1030, 2008

Katsnelson, B., Petnikov, V., & Lynch, J. : *Fundamentals of shallow water acoustics*. Springer Science & Business Media, 2012.

Kranthi K. Chanda, Chakraborty , B., Vardhan Y. V., Gracias D., Mahanty M. M., Latha G., Fernandes W., and Chaubey A. K.: Passive acoustic metrics to understand shallow water biodiversity off Malvan area in the west coast of India, *Indian journal of Geo Marine Sciences*., 2019, (*in press*).

Kranthikumar. Chanda., Shubham, S., Chakraborty, B., Saran, AK., Fernandes, W.A., and Latha, G.: fish sound characterization using multifractal detrended fluctuation analysis, *Fluctuation and Noise Letters.*, 19, No. 1, 2020 (2050009) (DOI:10.1142/S0219477520500091).

Kuperman, W. A. and Ingenito, F.: Spatial correlation of surface generated noise in a stratified media, *J. Acoust. Scoc.Am*., 67,1988-1996, 1980.

Kuperman, W. A., and Lynch, J. F.: Shallow-water acoustics. *Physics Today*, *57*, 55-61, 2004.

Kuperman, W., and Philippe, R.: "Underwater acoustics." *Handbook of Acoustics*, Springer,149-204, 2007.

Ladich, F., and Bass, A. H.: Underwater sound generation and acoustic reception in fishes with some notes on frogs. In *Sensory Processing in Aquatic Environments* .Springer, New York, NY, 173-193, 2003.

Ladich, F., and Fine, M. L.: Localization of swimbladder and pectoral motoneurons involved in sound production in pimelodid catfish. *Brain, behavior and evolution.*, 44, 86-100, 1994.

Ladich, F., and Myrberg, A. A.: Agonistic behavior and acoustic communication. *Communication in fishes*, 1, 121-148, 2006.

Ladich, F.: *Sound communication in fishes*, Springer, New York, 4, 2015.

LammersM. O.,Au,W**.** *W. L.:* Listening in the Ocean. *Springer, New York, 2016.*

Lammers, M.O., Brainard, R. E., Au,W. W. L., Mooney, T.A. and Wong, K.B.: An ecological acoustic recorder (EAR) for long-term monitoring of biological and anthropogenic sounds on coral reef sand other habitats. *J. Acoust. Soc. Am.,123*, 1720-1728, 2008.

Levington, J. S.: *Marine Biology: Function, Biodiversity, ecology*, 420, New York: Oxford University Press, 1995.

Loutridis, S. J.: Quantifying sound-field diffuseness in small rooms using multifractals, *The Journal of the Acoustical Society of America.*, 125, 1498-1505, 2009.

Luczkovich J. J, Mann D. A, Rountree R. A.: Passive acoustics as a tool in fisheries science. *Transactions American Fisheries Society.*, 137**,** 533-541, 2008.

Lurton, X.: *An introduction to underwater acoustics: principles and applications*. Springer Science and Business Media, 2002.

Madhusudhana, S. K., Chakraborty, B., and Latha, G.: Humpback whale singing activity off the Goan coast in the Eastern Arabian Sea. *Bioacoustics.*, 28, 329-34, 2019.

Mahanty, M. M., Latha G, L., and Govindan, R.: Soundscapes in shallow water of the eastern Arabian Sea. *Progress in oceanography.*, 165, 158-167, 2018.

Mahanty, M. M., Kannan, R., Harikrishanan, C., and Latha, G.: Terapon Theraps chorus observed in shallow water environment in the southeastern Arabian sea, *Indian Journal of Geo Marine Sciences.,* 44,150-155, 2015.

Mahanty, MM., Latha, G., Ashokan, M.: Acoustic characteristics of soniferous fishes inshallow waters off Kochi, Proc. Acoustis2013NewDelhi: November 1015, 262-266, 2013.

Mandelbrot, B. B. Multifractal measures, especially for the geophysicist. In *Fractals in geophysics*, Birkhäuser, Basel,5-42, 1989.

Manikandan, B., Ravindran, J., Mohan, H., Periasamy, R., Murali, R. M., & Ingole, B. S.: Community structure and coral health status across the depth gradients of Grande Island, Central west coast of India. *Regional Studies in Marine Science.*, *7*, 150-158, 2016.

Mann, D. A., Hawkins, A. D., and Jech, J. M.: Active and passive acoustics to locate and study fish. In *Fish bioacoustics* Springer, New York, 279-309, 2008.

Mann, D. A., Locascio, J. V., Coleman, F. C., and Koenig, C. C.: Goliath grouper Epinephelus itajara sound production and movement patterns on aggregation sites. *Endangered Species Research.*, 7, 229-236, 2009.

Marmelat, V., Torre, K., and Delignières, D.: Relative roughness: an index for testing the suitability of the monofractal model. *Frontiers in physiology.*, *3*, 208, 2012.

McCauley, R. D., and Cato, D. H.: Patterns of fish calling in a nearshore environment in the Great Barrier Reef. *Philosophical Transactions of the Royal Society of London. Series B: Biological Sciences.*, 355, 1289-1293, 2000.

McCauley, R.: Fish choruses from the Kimberley, seasonal and lunar links as determined by long term sea noise monitoring. *Proceedings of the Acoustical Society of Australia.*,1-6, 2012.

McWilliam, J. M., Hawkins, A. D.: A comparison of inshore marine Soundscape: J *Experimental Marine Biology and Ecology.*, 446, 166-176, 2013.

Mehra, P., Tsimplis, M. N., Prabhudesai, R. G., Joseph, A., Shaw, A. G., Somayajulu, Y. K., and Cipollini, P.: Sea level changes induced by local winds on the west coast of India. *Ocean dynamics.*, 60, 819-833, 2010.

Mensinger, A. F.: Disruptive communication: stealth signaling in the toadfish. *Journal of Experimental Biology.*, 217, 344-350, 2014.

Moulton, J. M..: Swimming sounds and the schooling of fishes. *The Biological Bulletin.*, 119, 210-223, 1960.

Movahed, M. S., Jafari, G. R., Ghasemi, F., Rahvar, S., & Tabar, M. R. R.: Multifractal detrended fluctuation analysis of sunspot time series. *Journal of Statistical Mechanics: Theory and Experiment.*, 2006, P02003, 2006.

Najeem, S., Sanjana, M. C., Latha, G. and Edwards Durai, P.: Wind induced ambient noise modelling and comparison with field measurements in Arabian Sea, *Appl. Acous*., 89, 101-106, 2015.

Nedelec, S. L., Simpson, S. D., Holderied, M., Radford, A. N., Lecellier, G., Radford, C., and Lecchini, D.: Soundscapes and living communities in coral reefs: temporal and spatial variation. *Marine Ecology Progress Series.*, 524, 125-135, 2015.

Nystuen, J. A., Amitai, E., Anagnostou, E. N., and Anagnostou, M. N.: Spatial averaging of oceanic rainfall variability using underwater sound: Ionian sea rainfall experiment 2004. *The Journal of the Acoustical Society of America.*, 123, 1952-1962, 2008.

Pace, N. G., and Jensen, F. (Eds.).: *Impact of littoral environmental variability on acoustic predictions and sonar performance*. Springer Science and Business Media, 2002.

Padovese, L. R., Martin, N., & Millioz, F.: Time—frequency and time-scale analysis of Barkhausen noise signals. *Proceedings of the Institution of Mechanical Engineers, Part G: Journal of aerospace engineering.*, 223,, 577-588, 2009.

Papes, S., & Ladich, F.: Effects of temperature on sound production and auditory abilities in the striped Raphael catfish Platydoras armatulus (Family Doradidae). *PLoS One.*, 6, e26479, 2011.

Parmentier, E., and M.L. Fine.: Fish Sound Production: Insights, (Eidited by), R.A. Suthers, W.T. Fitch, R. R. Fay, and A.N. Popper, *Vertebrate Sound Production and Acoustic Communication*, Springer, Cham, 19-50, 2016.

Parvulescu, A.: ‘‘The acoustics of small tanks,’’ in *Marine BioAcoustics*, edited by W. N. Tavolga (Pergamon, Oxford) 2. 7–13, 1967.

Pieretti, N., Farina, A., &Morri, D.A.: A new methodology to infer the singing activity of an avian community: The acoustic complexity index (ACI), *Ecological Indicators.*, 11, 868-873, 2011.

Pijanowski, B. C., Villanueva-Rivera, L. J., Dumyahn, S. L., Farina, A., Krause, B. L., Napoletano, B. M., Stuart H. G and Pieretti, N.: Soundscape ecology: the science of sound in the landscape. *BioScience.*, 61, 203-216, 2011.

Politi, A., Ginelli, F., Yanchuk, S., and Maistrenko, Y.: From synchronization to Lyapunov exponents and back, *Physica D: Nonlinear Phenomena.*, 224, 90-101 2006.

Pombo, M., Denadai, M. R., Bessa, E., Santos, F. B., de Faria, V. H., and Turra, A.: The barred grunt Conodon nobilis (Perciformes: Haemulidae) in shallow areas of a tropical bight: spatial and temporal distribution, body growth and diet. *Helgoland marine research.*, 68, 271, 2014.

Popper, A. N., and Fay, R. R.: The auditory periphery in fishes. In *Comparative hearing: Fish and amphibians*, Springer, New York, 43.100, 1999.

Popper, A. N., and Hawkins, A. (Eds.). *The effects of noise on aquatic life II* (p. 1292). New York: Springer, 2012.

Putland, R. L., Constantine, R., and Radford, C. A.: Exploring spatial and temporal trends in the soundscape of an ecologically significant embayment. *Scientific reports.*, 7, 5713, 2017.

Ramcharitar, J., Gannon, D. P., & Popper, A. N.: Bioacoustics of fishes of the family Sciaenidae (croakers and drums). *Transactions of the American Fisheries Society.*, 135, 1409-1431, 2006.

Ramji, S., Latha, G., Rajendran, V. and Ramakrishnan, S.: Wind dependence of ambient noise in shallow waters of Bay of Bengal, *Appl. Acous.*, 69,1294-1298, 2008.

Rice, A. N., Land, B. R., and Bass, A. H.: Nonlinear acoustic complexity in a fish 'two-voice'system. *Proceedings of the Royal Society B: Biological Sciences.*, *278*, 3762-3768, 2011.

Rountree, R. A., Gilmore, R. G., Goudey, C. A., Hawkins, A. D., Luczkovich, J. J., and Mann, D. A.: Listening to fish: applications of passive acoustics to fisheries science, *Fisheries.*, 31, 433-446, 2006.

Rouseff, D., and Tang, D.: Ambient noise directivity in the East China Sea: Model/data comparison. *The Journal of the Acoustical Society of America.*, *119*, 3218-3218, 2006.

The R Devolpment core team,: R: A Language and Enivronment for Statistical Computing, 2010.

Sanjana, M. C., & Latha, G.: Midfrequency Ambient Noise Notch using Time-Series Measurements in Bay of Bengal. *IEEE Journal of Oceanic Engineering.*, *37*, 255-260, 2012

Sanjana, M. C., Latha, G., & Mahanty, M. M.: Seabed characteristics from ambient noise at three shallow water sites in Northern Indian Ocean. *The Journal of the Acoustical Society of America.EL.*134, 366-372, 2013.

Shabangu, F. W., Coetzee, J. C., Hampton, I., Kerwath, S. E., de Wet, W. M., and Lezama-Ochoa, A.: Hydro-acoustic technology and its application to marine science in South Africa. *Marine and Maritime Sectors.*, 122, 2014.

Siderius, M., and Harrison, C.: High-Frequency Geoacoustic Inversion of Ambient Noise Data Using Short Arrays. In *AIP Conference Proceedings*, 728, 22-31, 2004.

Siderius, M., Harrison, C. H., and Porter, M. B.: A passive fathometer technique for imaging seabed layering using ambient noise. *The Journal of the Acoustical Society of America.*, 120, 1315-1323, 2006.

Siderius, M.: Using practical supergain for passive imaging with noise. *The Journal of the Acoustical Society of America Express Letters.*, 131, 14-20, 2012.

Simpson, S. C.: Use of hydroacoustics to examine spatial and temporal patterns of Pacific salmon (Oncorhynchus spp.) behavior during spawning migrations in Nushagak River, Alaska (PhD thesis, Alaska Pacific University), 2014.

Singh, I. J., Singh, S. K., Kushwaha, S. P. S., Ashutosh, S., & Singh, R. K.: Assessment and monitoring of estuarine mangrove forests of Goa using satellite remote sensing. *Journal of the Indian Society of Remote Sensing.*, 32, 167-174, 2004.

Southall, B. L., Bowles, A. E., Ellison, W. T., Finneran, J. J., Gentry, R. L., Greene JR, C. R., Green, D., Kastak, D. R., Ketten, J.H., Miller, P.E., Nachtigall, W.L., Richardson, W. J., Thomas, J. R., andTyack, P. L.: Overview. *Aquatic mammals.*, 33, 411, 2007.

Sreekanth, G. B., Manju Lekshmi, N., and Singh, N. P.: Fisheries profile of Zuari estuary. *International J. Fish.Aquat.Stud.*, 3, 24-34, 2015.

Stanley, H. E., Buldyrev, S. V., Goldberger, A. L., Goldberger, Z. D., Havlin, S., Mantegna, R. N., Ossadnik, S.M., Peng, C.K., and Simons, M.: Statistical mechanics in biology: how ubiquitous are long-range correlations?. *Physica A: Statistical Mechanics and its Applications.*, 205, 214-253, 1994.

Sueur, J., Aubin, T., and Simonis, C.: Seewave, a free modular tool for sound analysis and synthesis, *Bioacoustics.*, 18, 213-226, 2008b.

Sueur, J., Gasc, A., Grandcolas, P., and Pavoine, S.: Global estimation of animal diversity using automatic acoustic sensors. *Sensors for ecology. Paris: CNRS*, 99-117, 2012.

Sueur, J., Farina, A., Gasc, A., Pieretti, N., & Pavoine, S.: Acoustic Indices for Biodiversity Assessment and Landscape Investigation, *Acta acustica united with acustica.*, 100, 772 – 781, 2014.

Sueur, J., Pavoine, S., Hamerlynck, O., & Duvail, S.: Rapid acoustic survey for biodiversity appraisal. *PloS one.*, 3, e4065, 2008a.

Sundar, D., Unnikrishnan, A. S., Michael, G. S., Kankonkar, A., Nidheesh, A. G., & Subeesh, M. P.: Observed variations in stratification and currents in the Zuari estuary, west coast of India. *Environmental Earth Sciences.*, 74, 6951-6965, 2015.

Theiler, J., Eubank, S., Longtin, A., Galdrikian, B., and Farmer, J. D.: Testing for nonlinearity in time series: the method of surrogate data. *Physica D: Nonlinear Phenomena.*, 58, 77-94, 1992.

Tokuda, I., Riede, T., Neubauer, J., Owren, M. J., and Herzel, H.: Nonlinear analysis of irregular animal vocalizations. *The Journal of the Acoustical Society of America.*, 111, 2908-2919, 2002.

Tower, R. W.: The production of sound in the drumfishes, the sea-robin and the toadfish. *Annals of the New York Academy of Sciences.*, 18, 149-180, 1908.

Towsey, M., Planitz, B., Nantes, A., Wimmer, J., and Roe, P.: A toolbox for animal call recognition. *Bioacoustics.*, 21, 107-125, 2012.

Tricas, T. C., and Boyle, K. S.: Acoustic behaviors in Hawaiian coral reef fish communities. *Marine Ecology Progress Series.*, 511, 1-16, 2014.

Tyack, P. L., Frisk, G., Boyd, I., Urban, E., and Seeyave, S.: International Quiet Ocean Experiment science plan, 2015.

Tyack, P. L.: Implications for marine mammals of large-scale changes in the marine acoustic environment. *Journal of Mammalogy.*, 89, 549-558, 2008.

Udaykumar, G. V., Sanitha., K. S., Ingole, B. S.: Effect of tropical rainfall in structuring the macrobenthic community of Mandovi Estuary**,** west coast of *India: Journal of Marine. Biological.Association.UK*, 93, 1727-1738, 2013.

Urick, R. j.: ambient noise in the sea, underseawarfare technology office naval sea systems command department of the navy washington, d.c. 20362, 1984**.**

Urick, R. J.: Principles of Underwater Sound, McGraw-Hill, New York, 1983.

Vasconcelos RO., Simoes JM., Almada VC., Fonseca PJ., Clara M.. and Amorim P.: Vocal Behavior During Territorial Intrusions in the LusitanianToadfish: Boatwhistles Also Function as Territorial'Keep-Out' Signals, *Ethology.*,116, 155–165, 2010.

Vijay Kumar.: Installation and Operation of Air-Sea Flux Measuring System on BoardIndian Research Ships. MS thesis, Centre for Atmospheric and Oceanic Sciences, Indian Institute of Science, Bangalore, 1-159, 2017.

Webb, J. F., Fay, R. R., and Popper, A. N.: (Eds.): *Fish bioacoustics* (Vol. 32). Springer Science and Business Media, 2008.

Wei, R. C., Chen, C. F., Newhall, A. E., Lynch, J. F., Duda, T. F., Liu, C. S., & Lin, P. C. : A preliminary examination of the low-frequency ambient noise field in the South China Sea during the 2001 ASIAEX experiment. *IEEE Journal of Oceanic Engineering.*, *29*, 1308-1315, 2004.

Weilgart, L. I. N. D. Y.: The impact of ocean noise pollution on fish and invertebrates. *Report for OceanCare, Switzerland. URL: https://www. oceancare.org/wpcontent/uploads/2017/10/OceanNoise_FishInvertebrates*_May 2018.

Welch, P.: The use of fast Fourier transform for the estimation of power spectra, A methodbased on time averaging over short, modified peridograms, *IEEE Transactions on Audio and Electroacoustics.,* 15, 70-73, 1967.

Wenz, G.M.: Acoustic ambient noise in the ocean: Spectra and sources. *Journal of the Acoustical Society of America.,* 34:1936-1956, 1962.

Wilden, I., Herzel, H., Peters, G., and Tembrock, G.: Subharmonics, biphonation, and deterministic chaos in mammal vocalization. *Bioacoustics.*, 9, 171-196, 1998.

Wilson,D.andKneipfer,R.: Preliminaryresultsofexperimenttomea- sure vertical directionality of ambient noise in shallow water, Naval UnderseaWarfareCntr.(NUWC),Washington,DC,Tech.Rep.,1995.

Wood H, Parrish BB.: Echo-sounding experiments on fishing gear in action. *ICESJournal of Marine Science.*, 17, 25-36, 1950.

Yang, J., Jackson, D. R., & Tang, D.: Mid-frequency geoacoustic inversion using bottom loss data from the Shallow Water 2006 Experiment. *The Journal of the Acoustical Society of America.*, 131, 1711-1721, 2012.

Yang, T. C., and Yoo, K.: Influence of acoustic environment on the vertical directionality of ambient noise in coastal water. In *OCEANS 96 MTS/IEEE Conference Proceedings. The Coastal Ocean-Prospects for the 21st Century* ,Volume 1, IEEE, 351-357, 1996.

Yang, T. C., and Yoo, K.: Modeling the environmental influence on the vertical directionality of ambient noise in shallow water. *The Journal of the Acoustical Society of America.*, 101, 2541-2554, 1997.

Yost, W. A., and Dye, R. H.: Fundamentals of directional hearing. In *Seminars in Hearing,* 18, 321-344, 1997.

Yu, Z., Yee, L., and Zu-Guo, Y.: Relationships of exponents in multifractal detrended fluctuation analysis and conventional multifractal analysis. *Chinese Physics B.*, 20, 090507, 2011.

Zimmer, W. M.: *Passive acoustic monitoring of cetaceans*. Cambridge University Press, 2011.

List of Publications from the thesis:

Kranthikumar.Chanda., Shubham Shet., Chakraborty Bishwajit., Arvind Saran, William Fernandes Latha G. Fish sound characterization using multifractal detrended fluctuation analysis, *Fluctuation and Noise Letter*, 19, No. 1, 2020 (2050009) (DOI:10.1142/S0219477520500091).

Kranthikumar. Chanda, Chakraborty B., Vardhan Y. V., Gracias D., Mahanty M. M., Latha G., Fernandes W., and Chaubey A. K. "Passive acoustic metrics to understand shallow water biodiversity offMalvan area in the west coast of India", *Indian Journal of Geo Marines Science 2019 (in press)*

Kranthikumar *et al*., Passive acoustics studies from shallow water locations off Goa, *Journal of acoustical socitiy of America* (Under review)

Kranthikumar Chanda., Bishwajit Chakraborty., Tomonari Akamatsu., Arvind Saran. A passive acoustic study from a coral reef system – Grande Island, central west coast of India.*Environmental Monitoring and Assessment*(Under review)

Other publications:

Chaitanya A.V.S, Lengaigne M, Vialard J., Gopalakrishna V.V., Durand F., **Kranthikumar C**, Amritash., Suneel V., Papa F., Ravichandran.M "Salinity measurements collected by fishermen reveal a "river in the sea" flowing along the eastern coast of India" *Bulletin of the American Meteorological Society*, 2014, 95(12), p.1897.

Chaitanya, Akurathi Venkata Sai, Fabien Durand, Simi Mathew, Vissa Venkata Gopalakrishna, Fabrice Papa, Matthieu Lengaigne, Jerome Vialard, **Chanda Kranthikumar,** and R. Venkatesan. "Observed year-to-year sea surface salinity variability in the Bay of Bengal during the 2009–2014 period." *Ocean Dynamics* 65, no. 2 (2015): 173-186.

Conferences attended in National & International

1. Presented paper on National Symposium (NSA 2016) on Acoustics for Engineering "Applications on 17-19 Nov **2016** at KIIT college of Engineering, Gurugram "**Underwater soundscape environmental characteristics off Goa-A study**" ***Kranthikumar Chanda and Bishwajit Chakraborty.***

2. Presented paper on International symposium on acoustics **NSA-2016** for Engineering "Applications on 17-19 Nov 2016 at KIIT college of Engineering, Gurugram**Seabed Characterization from underwater ambient noise: A case study off Goa coast** Vishal Gupta, William Fernades and**Chanda** K. K. et al

3. Presented poster in **IBAC 2017** on 8-13 October International conference at Haridwar "**Underwater soundscape analysis of Malvan a shallow water area of (WCI) West coast of India"*Kranthikumar Chanda, Bishwajit Chakraborty, G Latha A Chaube. AK***

4. Presented paper in National Symposium on acoustics on October 28-30(**NSA-2017**) (AMU) at Aligarh Muslim University. "**Characterization of Fish signals using Multifractal detrended fluctuation analysis in the shallow water area of Goa"*KranthiKumar Chanda, Bishwajit Chakraborty***

5. Presented poster in International conference on Sonar systems Sensors (**ICONS2018**) on held at **NPOL-DRDO** on February 22-24 in Kochi "**Applications of acoustics indices to characterize the shallow water soundscape Off Grande Island *Kranthikumar Chanda, Bishwajit Chakraborty***

6. Presented paper in Western Pacific Commission on an Acoustic Conference **(WESPAC-2018)** on held at **National Physical Laboratory** on November 11-15 in Delhi "Soundscape characteristics in the marine environmental area of Grande Island, off Goa**" (Best Presentation Award), Kranthikumar Chanda, Bishwajit Chakraborty.**